Chapter 3: Geological Survey

3-1 Overview of the Geology

3-1-1 Overview of the Geology in the Paraná Basin

(1) Overview of Paraná Basin

The Paraná Basin is located in the south-east of the South American Continent and covers Brazil, Uruguay, Argentina, and Paraguay (Fig. II-3-1-1). The total area of the Paraná Basin is approximately 1,600,000 km^2. The area of the basin in Brazil is approximately 1,000,000 km^2 in the N-W direction and covers from the south of Minas Gerais Province to Rio Grande do Sul Province.

The Paraná Basin was formed in the late Ordovician as a sedimentary basin in the continent. The shape reflects the basement structure and shows a NE-SW directional trend in concordance with the Brasiliano structure trend. The deepest part of the Paraná Basin reaches approximately 5,000 m under sea level. Within the Basin, marine siliceous sediments were deposited with an average thickness of 2,000 m in the Paleozoic, and continental sediments were deposited in the Mesozoic. Milani (1998) describes that the Paleozoic sediment was controlled by a large-scale rift with a NE-SW direction trend.

The basic to acid volcanic rocks (Paraná flood basalt and Etendeca flood basalt) with a maximum thickness of approximately 1,700 m extruded to deposit itself on the Paleozoic sediments. The basic rocks are composed of gabbro and basalt. The acid rocks consist of dacite and rhyolite.

(2) Arch Structure

The arch topography extending in the NW-SE direction is observed in the eastern and western end at the margin of the Paraná Basin. This part crosses the major structural trend with the NE-SW direction of the Basin (Fig. II-3-1-2, II-3-1-4). The Ponta Grossa Arch, Campo Grande Arch, and Rio Grande Arch are representative arches in the Basin. The tectonic movement from the Devonian to the Jurassic formed this arch structure (Fulfaro et al. 1982). The Ponta Grossa Arch, for example, is located within the Basin with a width of 600 km. The Arch has affected the sedimentation since the Devonian.

Many basic dykes aligned with the NW direction are observed in the arch structure. The direction corresponds to part of the volcanic feeder of the Paraná Basin and the magnetic anomaly trend in the NW - SE direction. (e.g., Ferreira et al., 1982: Guapiara, São Gerônimo, Rio Alonzo, et al.).

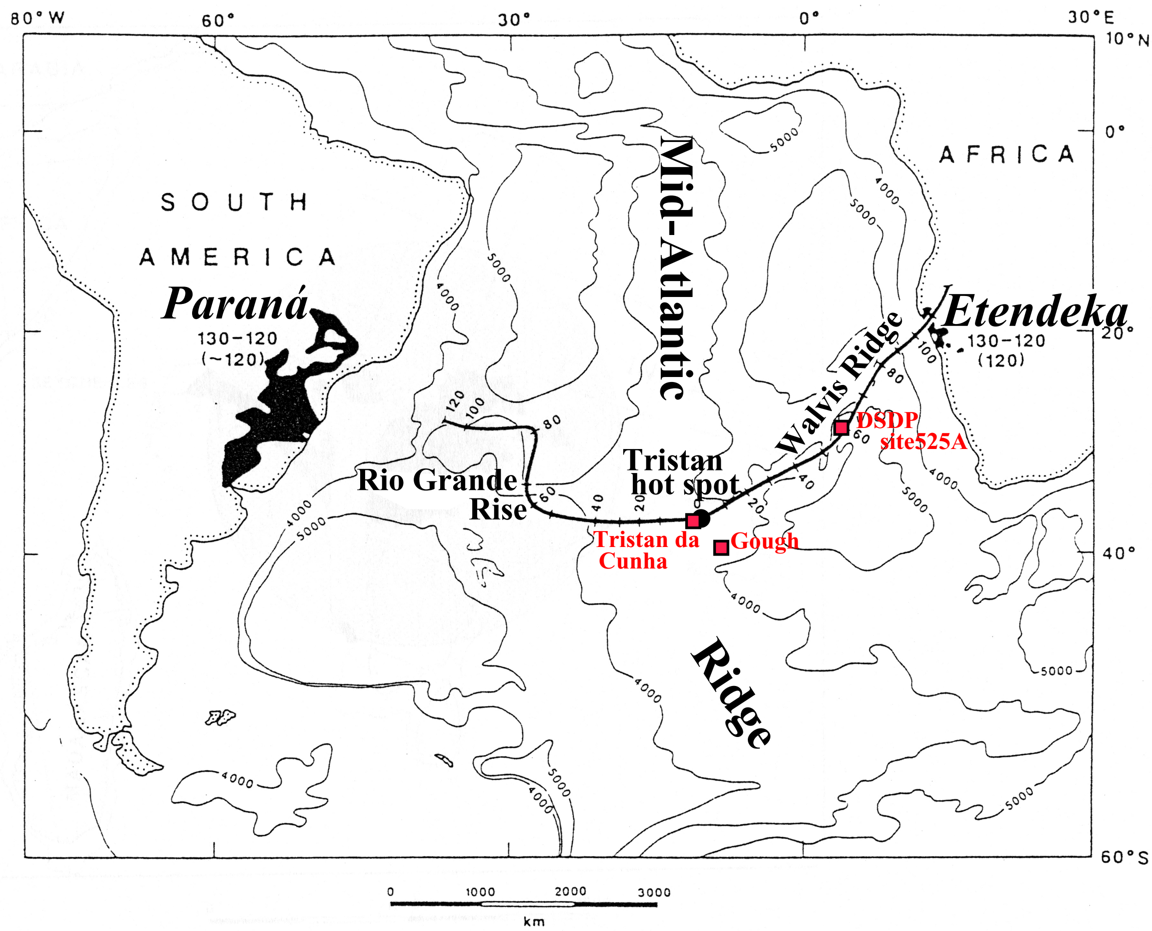

Fig. 16. Present configuration of the South Atlantic showing the thick volcanic ridges of the Rio Grande Rise and the Walvis Ridge produced above the mantle plume as the ocean opened. Hot-spot track is from *Duncan* [1984].

(from White and McKenzie, 1989)

Fig. II-3-1-1 Presence configuration around the Parana flood basalt (after White and McKenzie,1989)

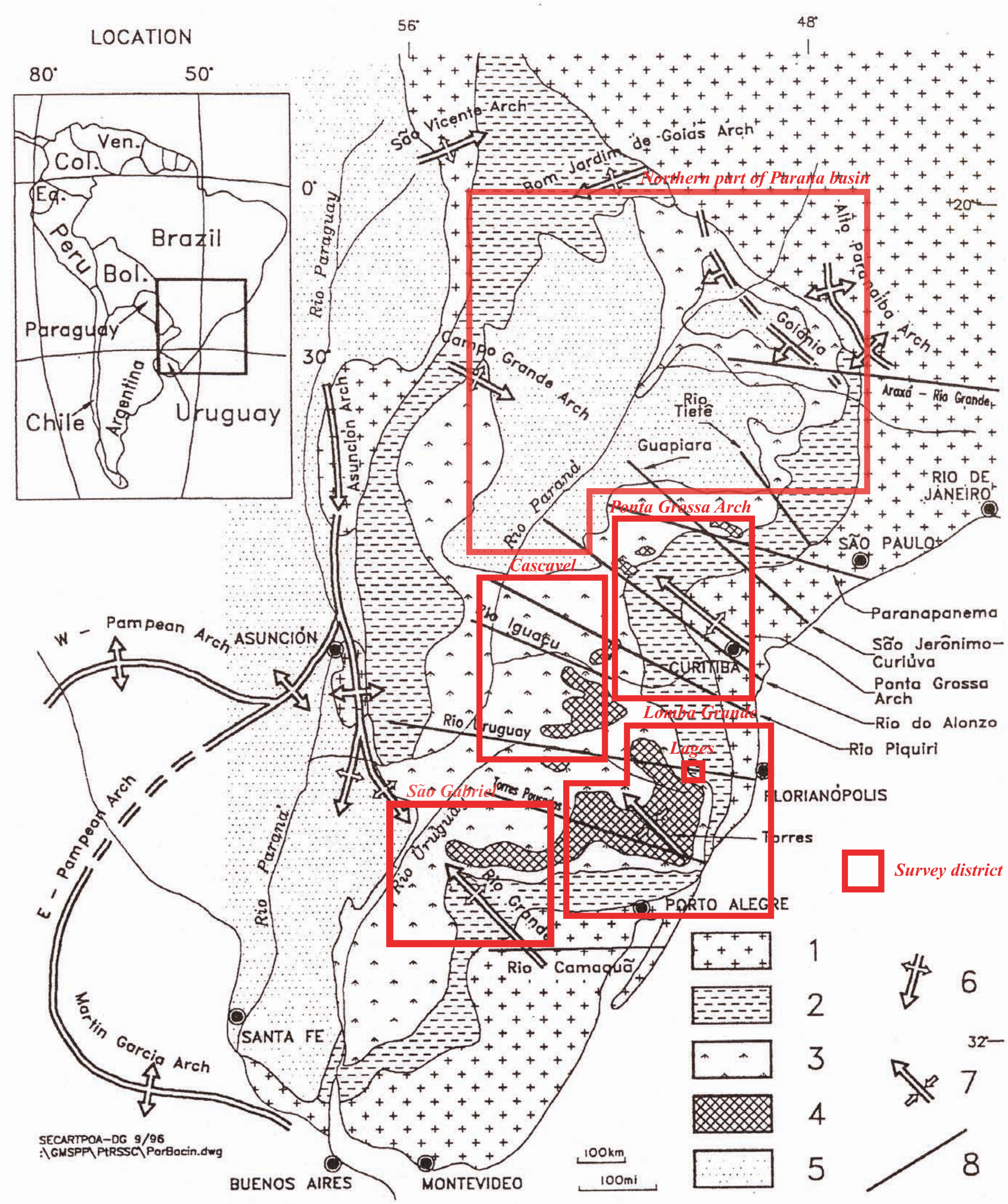

– Generalized geological sketch map of Paraná Basin (Melfi et al, 1988)

1. Pre-Devonian crystalline basement; 2. Pre-volcanic sediments (mainly Paleozoic); 3. Basic to intermediate flood volcanics (Serra Geral Formation: Lower Cretaceous); 4. Acid stratoid lava flows (Serra Geral Formation); 5. Post-volcanic sediments (mainly Upper Cretaceous); 6. Arch-type structure; 7. Syncline-type structure; 8. Tectonic and/or magnetic lineament.

Fig. II-3-1-2 Generalized geological sketch map of the Paraná basin (Melfi et al, 1988)

(3) Development of the Paraná Basin

The Paraná Basin was formed on the craton. The Paraná Basin, surrounded by a collision belt and the Foreland basin, accelerated the subsidence speed in the early formation stage from the effect of the structural pressure releasing along the weak line within the plate (Milani and Ramos, 1998). Over 50 % of the subsidence of the whole Basin, however, is from the isostatic load of the sedimentary and the volcanic rocks. Although the Ponta Grossa Arch did not ascend, for example, the hinge zone of the Arch located in the center of the Basin subsided from the effect of the isostasy (Oliviera, 1989).

There are four stages in the Paraná Basin development. The earlier two stages were composed of double cycles of the tectonic movement and sedimentation that occurred during the subsidence of synform basin. The later two stages consisted of the elevation of the Paraná Basin, the extrusion of large quantities of tholeiitic basalt lavas (Paraná and Etendeca flood basalt), and intrusion with relationship to the extrusion. The schematic section of the Paraná Basin is shown in Fig. II-3-1-3.

The first stage occurred from the Devonian to early Carbonatite to form the thick marine sediment called the Paraná Group. The Ponta Grossa Arch and the Asuncion Arch began to ascend from the late Silurian to the early Devonian and affected the sedimentation process. This stage ended with the epeirogeny and the fault movement. The movements caused the erosion that created the distinct stratigraphic discontinuity of the Paraná Basin.

The second stage occurred from the early Carboniferous to the late Permian with active epeirogeny. The epeirogeny continued during sedimentation, and the marine and continental sedimentation continued during the glacial climate. It can be observed in the Itarare Formation of the Tubarao Group.

The third stage occurred from the late Paleozoic to Jurassic with the erosion due to the upheaval of the whole area. The NW-SE arch rose up to the highest position in this stage. The continental sedimentation in this stage shows the nature of river deposits. The sedimentation was performed in a comparatively stable environment as observed in the Piramboia Formation. Then, the desertification gradually progressed in the South American Continent, and formed the Botucatu Formation expanding in all over the Basin that is composed of aeolian sandstones.

The fourth stage occurred from the late Jurassic to early Cretaceous with the development of the marked tension structure from the mantle plume and tholeiitic igneous activity. The structure of the Paraná Basin shifted to an anti-form structure. The progress of desertification continuing from the third stage formed the Botucatu Formation that consists of the frequently alternating beds of old basalt lavas and sandstones.

The tectonic movement in this stage finished in the last rifting with a vertical upheaval of 700m. In the middle of the Cretaceous, the Caiua Formation consisted of aeolian sandstone

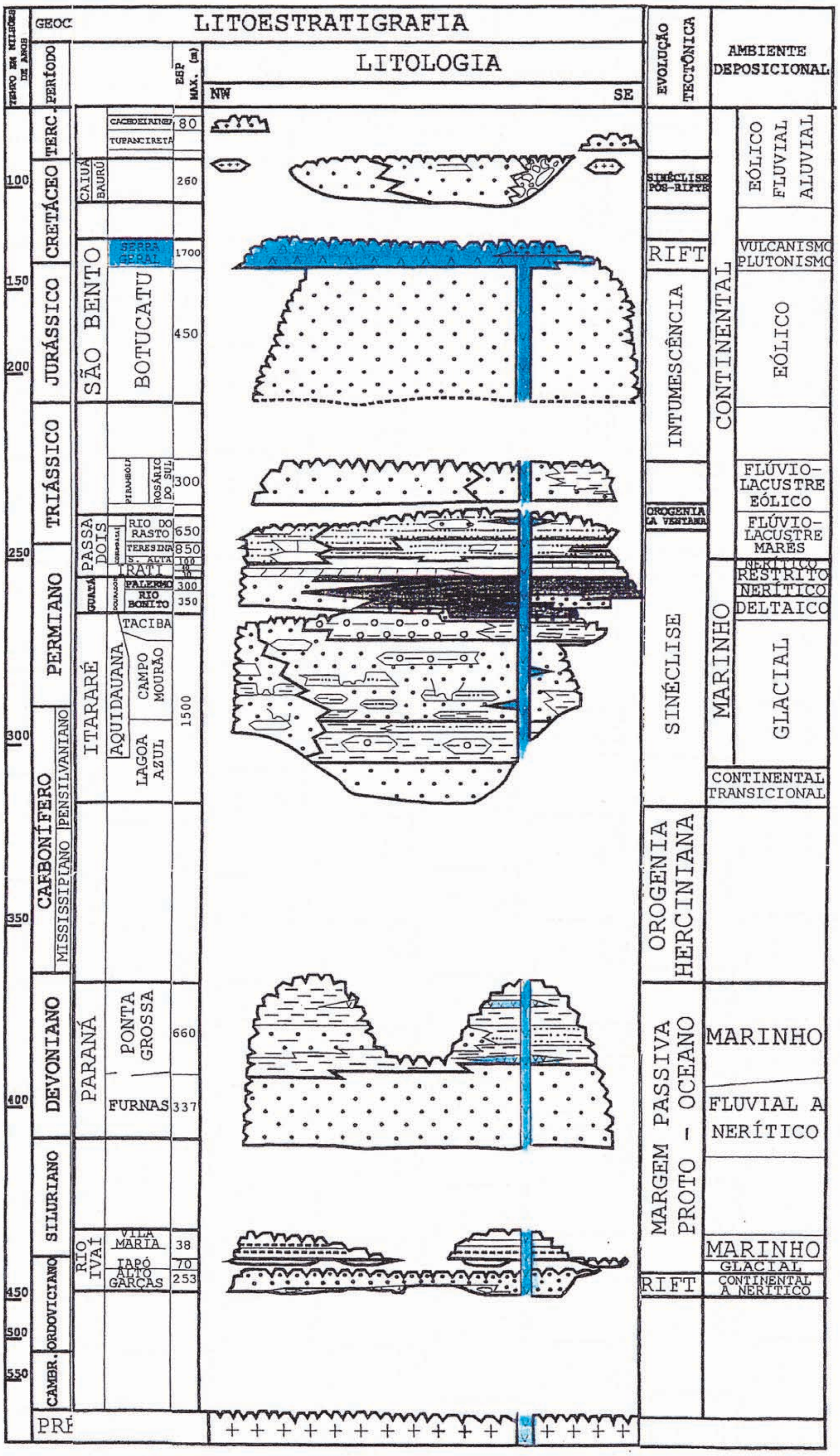

Fig. II-3-1-3 Sequence-stratigraphic chart for the Paraná basin (simplified from Milani et al., 1974)

and red sandstone with cross-bedding deposited because of the climactic change from a desert climate to an alluvial/delta environment (Fúlfaro and Barcelos, 1993). Paraná flood basalt is covered by the Caiura Formation, which is mainly composed of aeolian sandstone (Rocha-Campos et al., 1988). Therefore, the climate in the active period of Paraná flood basalt was mostly a desert climate from the beginning to the end. Columnar joints of Paraná flood basalt suggest the desert climate at the period of basalt eruption. The columnar joints in the Paraná flood basalt lava indicates that it had been a desert climate at the time of eruption. The columnar joints means that water including precipitation did not penetrate into the lava when the basalt erupted (Long and Wood, 1986). This is the same mode of occurrence with Columbia River Basalt which erupted in the similar environment.

3-1-2 Paraná Flood Basalts

(1) Paraná Flood Basalt Outline

The Paraná Flood Basalt distributed in the south east of the South American Continent formed a large igneous province from only one igneous activity with the separation of the Gondwana continent and the spreading of the South Atlantic Ocean. The Etendeka Flood Basalt is distributed in Namibia on the African Continent as the same igneous province (Erlank et al., 1984; Bellieni et al., 1984).

It is thought that the mantle plume participated in forming Paraná/Etendeka flood basalts (e.g., Morgan, 1981: White and McKenzie, 1989; Peate et al., 1990). The Tristan hot spot is now located in the vicinity of the Mid-Atlantic Ridge between the Paraná Flood Basalt and the Etendeka Flood Basalt. The Rio Grande Rise and the Walvis Ridge distributed on the ocean floor from the South American to African Continents, both the track of the Tristan hot spot (Fig. II-3-1-1). The present igneous activity of the Tristan plume is observed in Tristan de Cunha Island and Gough Island (O'Conner and Duncan, 1990; Gallagher and Hawkesworth,1994).

The Paraná Flood Basalt is a part of the Gondwana III super-sequence named the Serra Geral Volcanism (Formation) (Almeida, 1964; Zalan et al., 1988; Fig. II-3-1-3).

The distribution of the Paraná Flood Basalt and the Etendeka Flood Basalt is defined by a drilling survey (Fig. II-3-1-4, II-3-1-5). The distribution area of the Paraná Flood Basalt is 1.2 x 10^6 km^2 (Cordani and Vandoros, 1967) and that of Etendeka Flood Basalt is 0.8 x 10^5 km^2 (Erlank et al., 1984). The original areas of both basalts were estimated as 2.0 x 10^6 km^2, and the maximum eroded thickness was calculated at 3 km (Gallagher et al., 1994). The present thickness of the Paraná Flood Basalt is 0.7 km in average (Leinz et al., 1968).

The lava thickness reflects the Paraná Basin structure in general. The thickest part of the lava corresponds to the deepest part of the Basin, the lava thickness is over 1 km. The

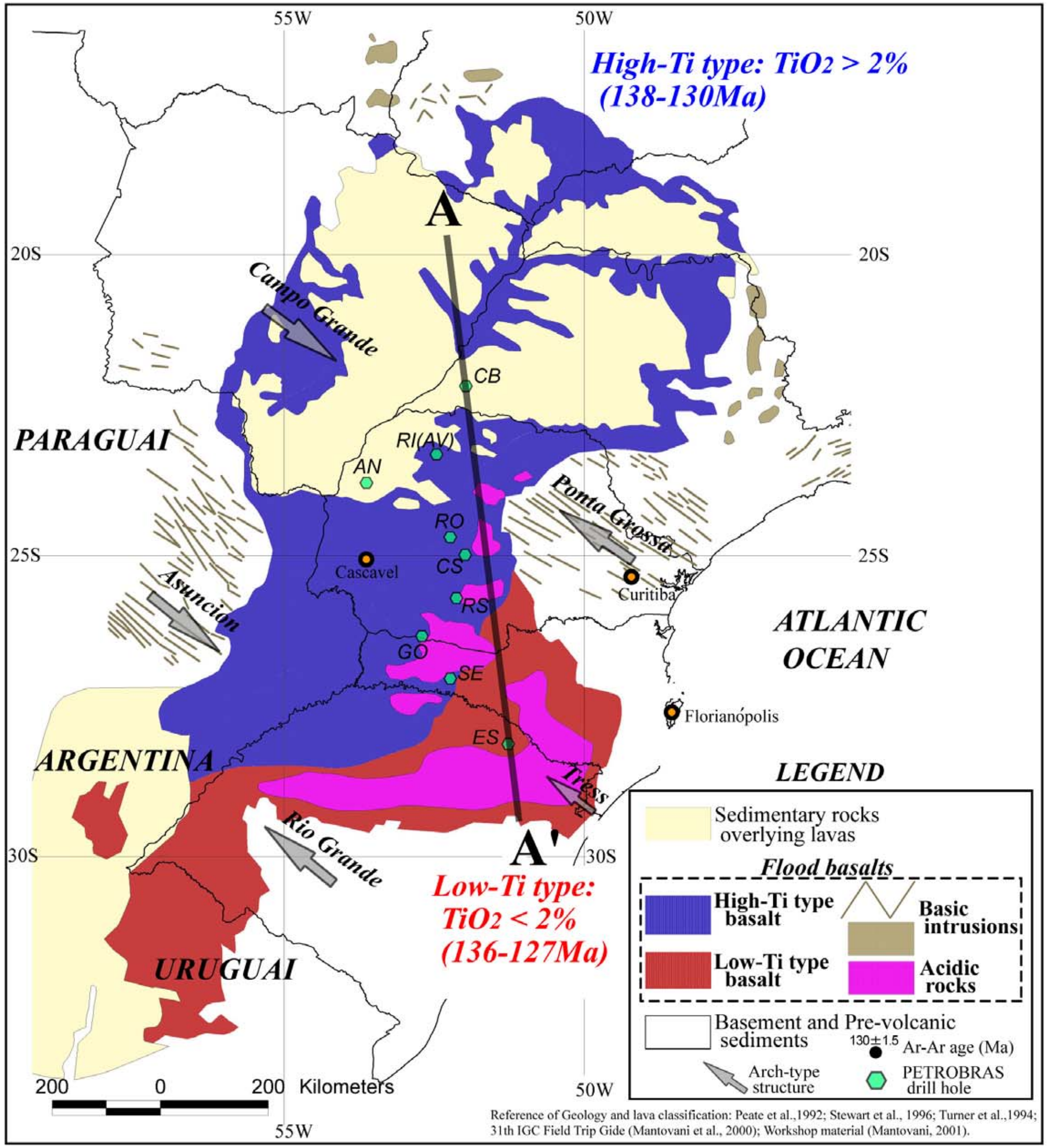

Lava	
Distribution	Paraná: 1,200,000 km^2; Etendeka: 80,000 km^2
Thickness	Paraná: Max 1,700 m (northern part of Paraná basin), ave 660 m; Etendeka: max 900 m
Rock types	tholeiitic basalt and basaltic andesite (90 vol%), alkalic basalt+acidic rocks (10 vol%)
Phenocrysts	CPX, plagioclase, olivine (rare), OPX (rare)
Microscopic texture	Aphyric
Magma types	high-Ti type (TiO_2>2 wt%) and low-Ti type (TiO_2<2 wt%); subdivided into 6 magma types
Duration time of volcanism	138-127 Ma (Duration time: 10-15 Ma; peak: 134-129 Ma)
Melt generation rate	high-Ti type: max 0.15 km^3/yr; low-Ti type: max 0.4 km^3/yr

Intrusion (dyke and sill)	
Trend of direction	NW-SE trend (Ponta Grossa, Uruguai), N-S trend (coast-parallel)
Extension	dyke: max 200 km (Ponta Grossa); sill: max 120 km^2
Thickness	dyke: max 600 m (Ponta Grossa); sill: max 100 m
Rock types	tholeiitic dolerite and gabbro, picritic gabbro (Lomba Grande district: very small volume)
Duration time of genelation	NW-SE trend dyke and sill: 137-130 Ma; coast-parallel dykes: 133-129 Ma

Fig. II-3-1-4 Overview of the Paraná flood basalts

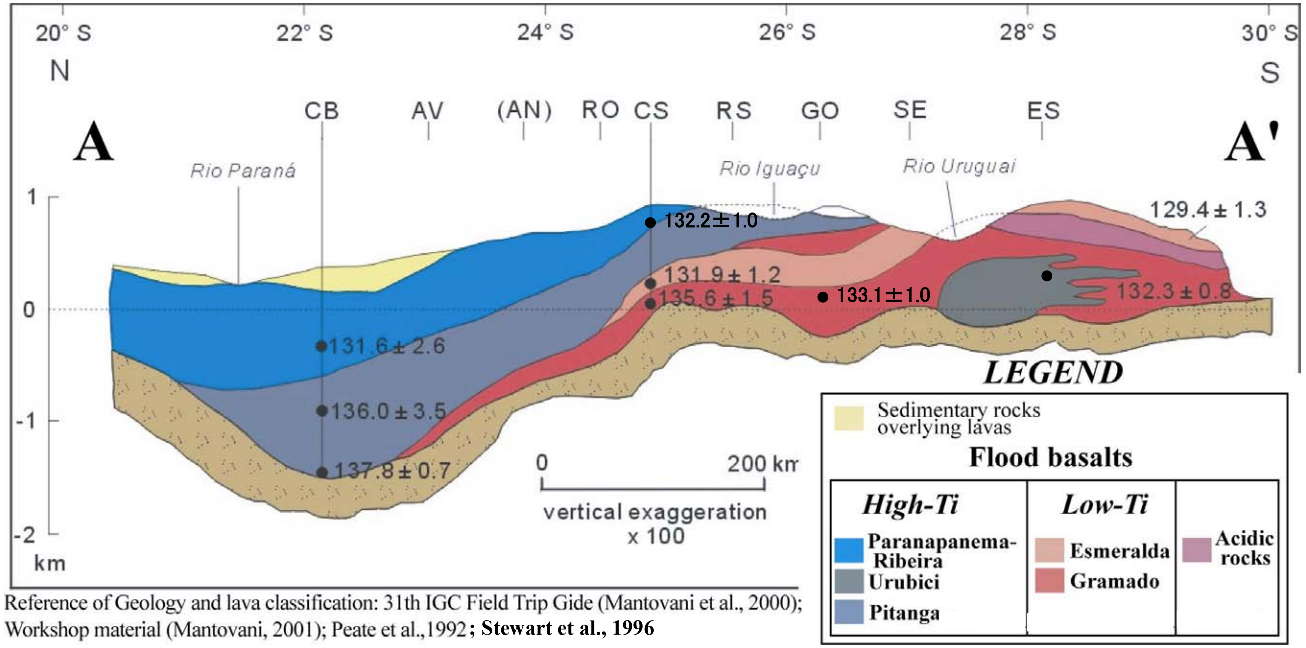

Reference of Geology and lava classification: 31th IGC Field Trip Gide (Mantovani et al., 2000); Workshop material (Mantovani, 2001); Peate et al.,1992; **Stewart et al., 1996**

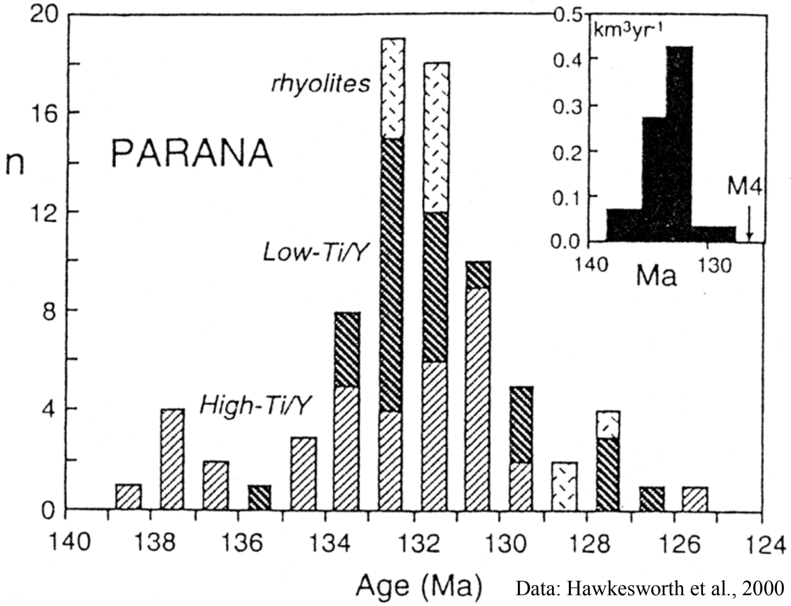

Data: Hawkesworth et al., 2000

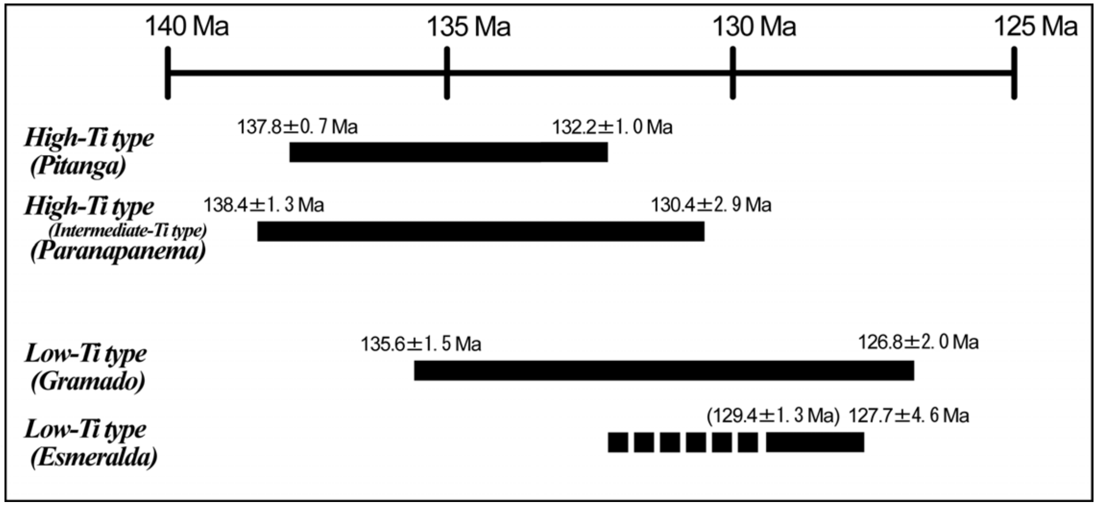

Data: Turner et al., 1994; Stewart et al., 1996; Hawkesworth et al., 2000

Fig. II-3-1-5 Duration time of activity and eruption rate for the Paraná flood basalts

thickness increases toward the center. For example, the lava thickness exceeds 1,500 m in Pontal of Paranapanema in the west of São Paulo Province according to the drilling data of the 1-CB-2-5P hole by PETROBRAS (Fig. II-3-1-4, II-3-1-5). The thickness there exceeds 1,700 m including the intrusive rocks in the sedimentary rocks (Paulipetro, 1982; Zalan et al., 1988). The thickness of the sedimentary rocks in this area is 6,500 m. The maximum thickness of the Etendeka Flood Basalt, the counterpart of the Paraná Flood Basalts, is 900m in the Tafelberg field (Erlank et al., 1984). The scale of the distribution area and thickness is very small compared to the Paraná Flood Basalt.

The lava of a member of the flood basalt is distributed in the basin in the ocean off Brazil (Chang et al., 1992). Lava of 600 m thick with an area of 10^5 km^2 was observed by drilling carried out at 200 km east of Rio de Janeiro. The chemical composition of this lava has a closer resemblance to that of the Paraná Flood Basalt than that of MORB (Mizusaki et al., 1992). The basalt whose chemical composition is a close resemblance to the Paraná Flood Basalt has been reported from the Espirito Santo Basin located 500 km north east of Rio de Janeiro, 150 km away from coast (Fodor and Vetter, 1984).

(2) Igneous Activity of the Paraná Flood Basalts

Tholeiitic basalt and andesite occupy approximately 90 % of the Paraná Flood Basalt (Fig. II-3-1-4). The distinct bimodal igneous activity is observed both in the Paraná and Etendeka Flood basalts. The activity is divided into basalt and acid rocks (dacite to rhyolite) by the SiO_2 gap of 60 to 64 wt% (Fig. II-3-1-6 (a)). The acid rocks occupy approximately 4 % of the Paraná Flood Basalt and the maximum thickness is 400 m.

The basic rocks which compose Paraná Flood Basalt are gabbro, alkaline basalt, tholeiitic basalt, andesitic basalt, and andesite. The acid rocks are dacite and Hawaiitic rhyolite.

The characteristics of the major elements of the Paraná Flood Basalt show a different source from the ocean floor basalt. Since the Paraná Flood Basalt was formed by igneous activity that occurred in a vast area, a different participation of the mantle source is thought to have occurred.

The basalt lavas are divided into a high-Ti type (Pitanga, Paranapanema, and Urubicí) and low-Ti type (Ribeira, Gramado, and Esmeralda). Except for the Urubicí lava, the high-Ti type lavas are distributed in the north of the Paraná Basin. The low-Ti type lavas are distributed from the central to the south east of the Basin (Fig. II-3-1-4). Both types of lavas were affected by fractional crystallization shown as low MgO content (3 ~ 7 wt%). The low-Ti type lavas were markedly affected by crustal contamination.

The acid rocks are also divided into two types by the TiO_2 content. Though the distribution of the acid rocks is limited to the margin of the Paraná Flood Basalt, the basalt is closely involved in the distribution of acid rock. The high-Ti type acid rocks are distributed in

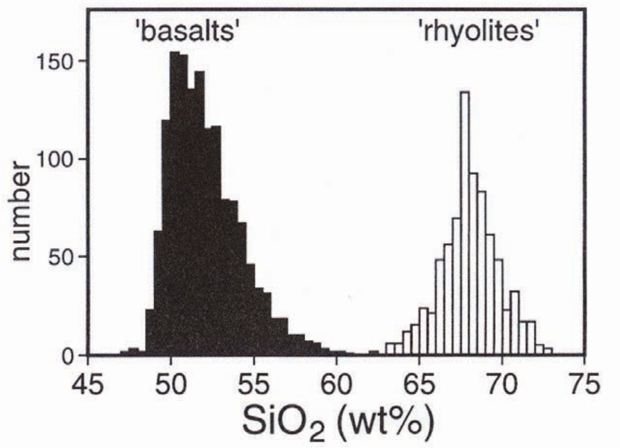

(a) SiO_2 histogram illustrating the bimodal composition of the Paraná-Etendeka lavas. The silica gap between 61 and 63 wt% forms a natural division into 'basalts' (black shading) and 'rhyolites' (white shading). The histogram distribution does not reflect the relative erupted volumes of basalt and rhyolite magma due to the bias of sampling towards the coastal margins where rhyolites are more common. Terminology for the silicic rocks is complicated because their compositions straddle the boundaries of several fields on many classification diagrams. As a simplification, *Erlank et al.* [1984] used the term 'quartz latites' for all the Etendeka silicic rocks, whereas *Bellieni et al.* [1986] preferred the term 'rhyolite' to encompass all the compositions of the Paraná silicic rocks.

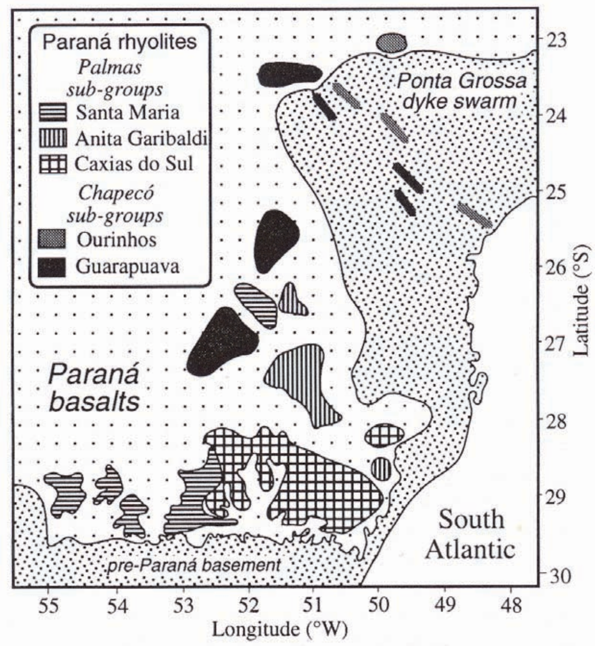

(b) Distribution of rhyolite subgroups within the Paraná province [*Peate et al.*, 1992; *Garland et al.*, 1995].

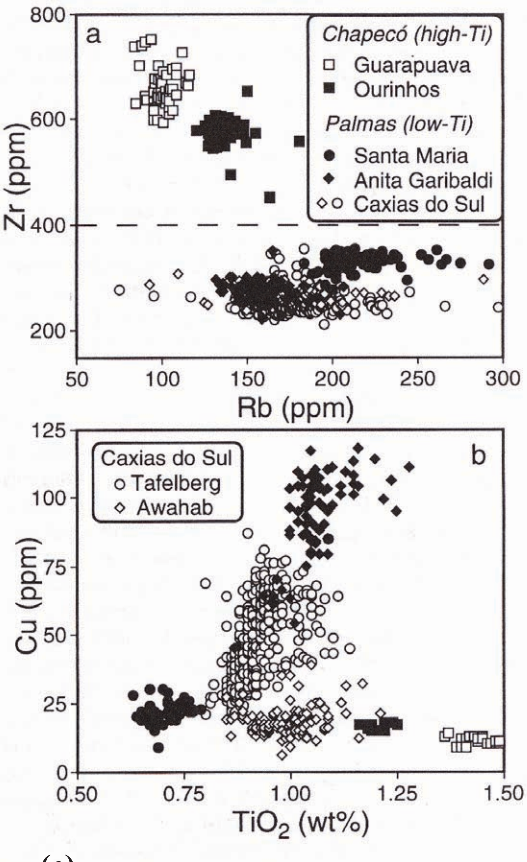

(c) (a) Rb vs. Zr: 400 ppm Zr discriminates between high-Ti Chapecó and low-Ti Palmas rhyolite types, and the Chapecó subgroups are resolved by different Rb/Zr (Ourinhos >0.2; Guarapuava <0.2), (b) TiO_2 vs. Cu, illustrating compositional differences between the low-Ti rhyolite subgroups. The Caxias do Sul subgroup is divided into the Tafelberg and Awahab magma systems which lie, respectively, above and below an erosional disconformity in the field [*Milner et al.*, 1995b]. Data from *Hawkesworth et al.* [1988], *Peate* [1990], *Mantovani and Hawkesworth* [1990], *Whittingham* [1991], *Garland et al.* [1995], and S.C. Milner and A.R. Duncan (unpubl. data).

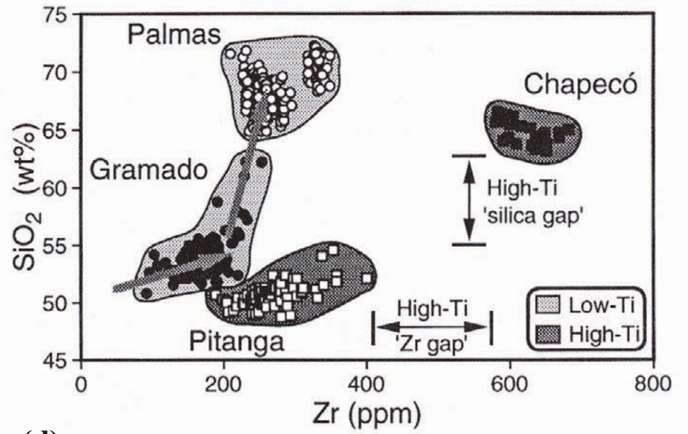

(d) Zr vs. SiO_2 diagram highlighting the different petrogenetic origins of the high- and low-Ti rhyolites. Data sources as in Figure 16.

Fig. II-3-1-6 Chalacteristics of the acidic rocks concerned with the Parana flooḋ basalts

the north of the Basin and the low-Ti type rocks are distributed in the south of the Basin.

(3) Intrusive Rocks (Sill)

The distribution of the intrusive rocks concerned with the activity of the Paraná Flood Basalt is shown in Fig. II-3-1-7.

Various kind of sills with 200 m in thickness that were accompanied by the activity of the Paraná Flood Basalt were obtained in sedimentary rocks especially in Irati Formation and Itarare Group of Paleozoic from the PETROBRAS drilling (Zalan et al., 1986; Piccirillo, 1988). The sill with a markedly larger scale is observed in the northern center of the Paraná Basin where the thick lava is distributed (Fig. II-3-1-7). The sills are also observed in the Paraná Flood Basalt (Melfi and Girargi, 1983; Marini et al., 1967; Davino et al., 1982). The thickness of these sills is from 2 to 200 m and they intruded upon each other (e.g., Piracicaba - Limeira sills etc). A comparatively big outcrop of the sill is known in the north west of São Paulo. The total thickness of the sills distributed in the north of the Paraná Basin exceeds 1000 m (Bellieni et al., 1984b).

Almost all the sills range from doleritic basalt to gabbro in the tholeiite series and the chemical composition are similar to those of the lavas (Regelous, 1993). The sill of picritic gabbro observed in Lomba Grande district is an exception. Peate et al (1990) pointed out that the chemical composition of the sill is similar to that of the lava distributed around the sill.

(4) Intrusive Rocks (Dykes)

(i) Ponta Grossa Dykes

The dykes with the NW-SE strike are distributed in the Pre-Cambrian basement and sedimentary rocks of the Paraná Basin in Ponta Grossa Arch (Fig. II-3-1-4). A few dykes intruded into lavas (Piccirillo et al., 1990). The width of the dykes ranges from several to 500 m. The extension of some dykes reaches several kilometers. There are some extensions of the Ponta Grossa Dykes in southern Angola on the African Continent. Their existence means that the activity of the dykes occurred before the separation of the continent (Piccirillo et al., 1990). Almost all these dykes are dolerite. Their chemical compositions are similar to those of Paranapanema lavas. The chemical composition of part of the dykes is a similar to that of the Pitanga lava.

Piccirillo et al. (1990) propose that the dykes of Ponta Grossa Arch are the feeders of the lava eruption. Turner et al. (1994) and Renne et al. (1996) concluded that the dykes of Ponta Grossa Arch were the feeders for the lavas in the north of the Paraná Basin, because they obtained a similar ^{40}Ar-^{39}Ar age to vicinal lava for their dating of the dykes.

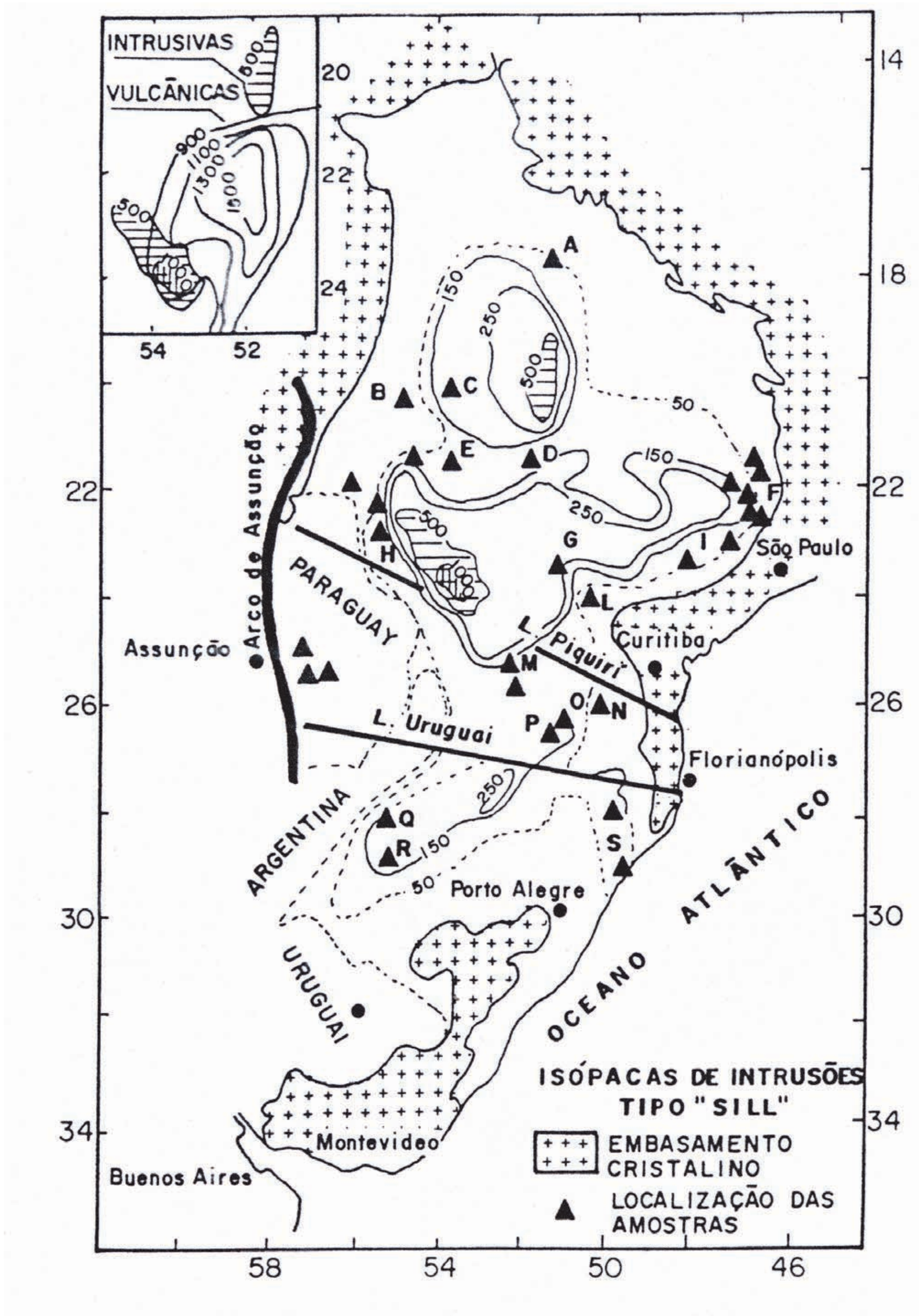

Fig. II-3-1-7 Isopachs of combined sill thicknesses with Paraná basin sediments (Bellieni et al, 1984)

(ii) Dykes Distributed Along Coast from São Paulo to Rio de Janeiro

Many dykes with the NE-SW direction intruded into the Pre-Cambrian basement distributed along the coast from Sao Paulo to Rio de Janeiro (Fig. II-3-1-4). Their chemical composition is the high-Ti type (Ti/Y>310: Comin-Chiaramonti et al., 1983).

The dykes are divided into two types, the Paraiba type (SiO_2: 50~53 wt%, TiO_2: 3.2~4.1 wt%) and the Ubatuba type (SiO_2: 54~58 wt%, TiO_2: 2.2~2.6 wt%). Since the relationship between these two types cannot be explained with the simple genetic process, their activities are considered different magma activities (Hawkesworth et al., 1992). Regelous et al. (1993) pointed out that it is not possible to explain the activities of the relationship between the Paraná Flood Basalt and both dykes. The age 133 to 129 Ma was obtained by age determination with the ^{40}Ar-^{39}Ar method. This age covers the generation age of the Paraná Flood Basalt in Ponta Grossa and in the north of the Basin (Turner et al., 1994). A new results (125 to 120 Ma: Peate, 1997), however, has recently been obtained, and a conclusion has not been obtained.

(iii) Other Intrusive Rocks

The NW-SE direction dykes were confirmed from the east of Paraguay to the west of the Paraná Flood Basalt by airborne geomagnetic prospecting (Druecker and Gay, 1987; Fig. II-3-1-4). The chemical compositions of these dykes have a close resemblance to those of the Pitanga and the Paranapanema lavas. The age 137 Ma was obtained from a dyke sample using ^{40}Ar-^{39}Ar dating. This age is close to the age of lava distributed in the west of Paraná Flood Basalt.

In the south of the Paraná Basin, there are few intrusive rocks related to the Paraná Flood Basalt. The confirmed dykes and sills are distributed within the cliff of the Flood Basalt lava in Serra Geral or along the coast, and show a parallel strike to the coastal line. Though the chemical compositions of the dykes and sills are the Gramado or Urubicí type, the intrusive rocks along the coast show a similar chemical composition to the Urubicí lava (Peate, 1996).

There are some places on the basalt lava cliff of Serra Geral where many sills intruded into lava are observed. In the vicinity there, dykes 100 m wide intruded into the sedimentary rocks of the Basin. The compositions of all these dykes show the Esmeralda type composition ($_{\varepsilon}Nd_i$: ~ +0.5; $^{87}Sr/^{86}Sr$: 0.7059, $(Ce/Sm)_N$: ~1.3; Peate and Hawkesworth, 1996).

(5) Alkaline Rock Activity

The activities of alkaline rock existed on the margin of the Paraná Basin as same period magma activity of the Paraná Flood Basalt activity (Fig. II-3-1-8). The chemical compositions of the alkaline rocks vary widely. The alkaline gabbro, phonolite, alkaline syenite, and alkaline granite are observed (Milner et al., 1995). Alkaline composite rock body with a comparatively large scale is particularly distributed in Ponta Grossa.

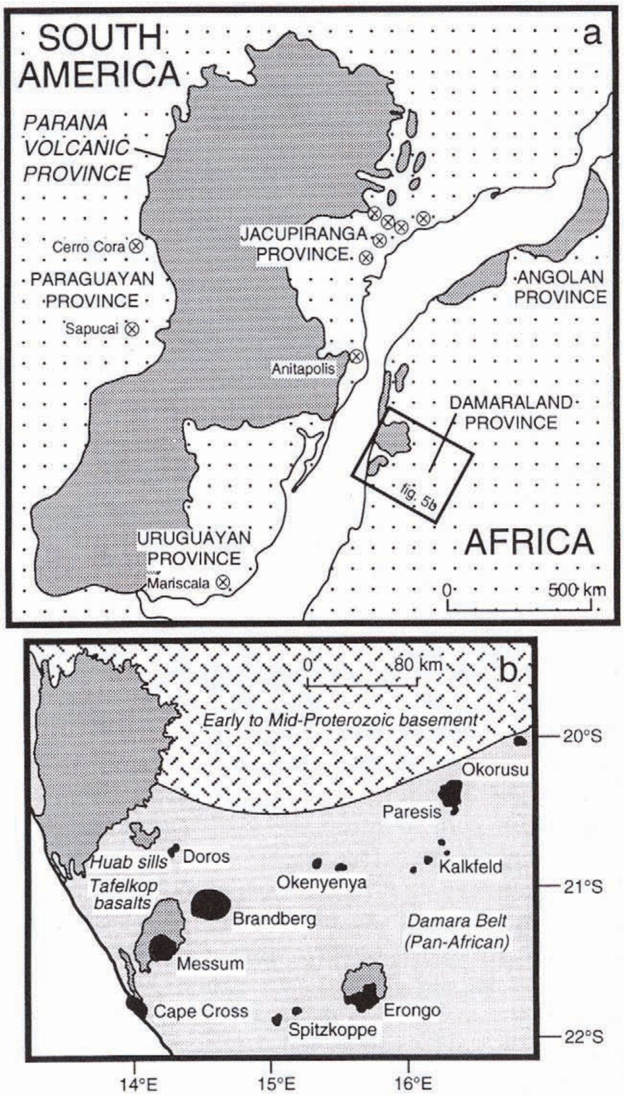

(a) Location of alkalic magmatism (circles with crosses) contemporaneous with the Paraná-Etendeka flood volcanism (dark grey shading); (b) detailed map of the Damaraland complexes (black shading) in relation to the Etendeka lava field (dark grey shading) and basement rocks (Early to Mid-Proterozoic; speckled shading: Pan-African; light grey shading) [from *Milner et al.*, 1995a].

Fig. II-3-1-8 Activity of alkalic magmatism contemporaneous with the Parana flood basalts (Peate, 1997)

The age of the igneous activity of the alkaline rocks is 132 Ma in the Jacupiranga carbonatite in the west of São Paulo from ^{40}Ar-^{39}Ar dating (Renne et al., 1993). The age of 127 Ma from a sample in the east of Paraguay (Renne et al., 1993), 131 Ma from a sample in the vicinity of Anitapolis, in south east Brazil, and 133 Ma (Stewart et al., 1996) from a sample in the vicinity of Mariscala, in south east Uruguay, were obtained as ages of the other alkaline composite rock bodies.

The activity of the alkaline rocks in the Etendeka Flood Basalt continued for a comparatively long period in the Etendeka Flood Basalt. The activity period in Messum is 132 to 127 Ma and 129 to 123 Ma in Okenyenya (Milner et al., 1995; Renne et al., 1995: both ages were obtained using ^{40}Ar-^{39}Ar dating). This means that the activity of the alkaline rocks occurred before the activity of the Etendeka Flood Basalt.

Milner et al. (1995a) think that the period of the activity of the alkaline rocks was the same period as the Flood Basalt activity, and they also point out the same relationship in Deccan and Siberian Trap.

(6) Mineralization and Geochemical Anomaly within the Paraná Flood Basalt

There have not been any reports about the metallic ore deposits and the indications of mineralization related to the Paraná Flood Basalt. There are, however, some descriptions about native copper and sulfide (pyrite) that fill the gas cavities and cracks of lavas, sills, and dykes as faint indications of mineralization. The geochemical anomalies of Cu, Ni, Cr, Pt, Pd, and others were extracted in the distribution area of the Paraná Flood Basalt of the south west of Paraná Province from the geochemical prospecting of river sand carried out in Paraná Province by MINEROPAR.

(7) Formation Period, Activity Time, and Extrusion Rate of Paraná Flood Basalt

Renne et al. (1992) concluded the following about the Paraná Flood Basalt in the south of Brazil from the ^{40}Ar-^{39}Ar dating: Igneous activity commenced in 133 ± 1 Ma and ended within 1 m.y. The effusion rate was estimated at <1.5 Km^3. This rate is almost similar to that of the Deccan Flood Basalt. Later, Renne et al. (1996) obtained the ^{40}Ar-^{39}Ar age of 131.4 ± 0.4 Ma to 129.2 ± 0.4 Ma from the sample dyke (dolerite) distributed in Ponta Grossa Arch. In addition, the age of approximately 120 Ma was obtained from a few samples. Based on this data, they amended the age of the peak igneous activity by approximately 3 m.y.

Turner et al. (1994), however, calculated based on the ^{40}Ar-^{39}Ar dating that the time of the Paraná Flood Basalt activity was 137 Ma to 127 Ma (10 m.y.), and the extrusion rate was <0.1 km^3.

Stewart et al. (1996) suggested the extrusion rate increased with time. They estimated 138 to 133 Ma was the time with less extrusion rate, and the main extrusive time was 133 to 129

Ma. Therefore, the whole activity time of the Paraná Flood Basalt was concluded within 10 Ma.

Milner et al. (1995b) clarified that at least ten different geomagnetic reversals occurred within 135 to 130 Ma by using the rhyolite lava units of Paraná Flood Basalt. The time for the geomagnetic reversals occurring was 0.24 m.y. on average. Based on this result, the time necessary to erupt the lava with 1 km in thickness was calculated to be 2.4 m.y. The time calculated from the ^{40}Ar-^{39}Ar dating was <1 m.y. (Renne et al., 1996) and < 3 m.y. (Stewart et al., 1996).

As the result, the time of the igneous activity within the continent by the rift formation of the early stage of the Paraná Flood Basalt activity is 138 to 135 Ma (Turner et al., 1994; Stewart et al., 1996). The time of the major igneous activity occurred accompanied with the separation of the Gondwana Continent toward the north. The time was 134 to 129 Ma (Turner et al., 1994; Stewart et al., 1996). The peak of the quantities of extrusion is thought to be in 135 to 132 Ma.

The dykes that are observed along the coast are thought to intrude in the age of 128 to 120 Ma (Turner et al., 1992; Renne et al., 1996; Stewart et al., 1996), as the latest igneous activity at the surface.

(8) Relationship between Rifting during Gondwana Break-up and Igneous Activity of the Paraná Flood Basalt

(i) Process of Spreading of the South Atlantic Ocean and Rift Formation

Austin and Uchupi (1982) thought that the seafloor spreading in the South Atlantic Ocean obviously commenced from the south to the north. The oldest seafloor is located near Cape Town in South Africa. The age of 137 Ma or 130 Ma is obtained by geomagnetic anomaly. Yet, the age calculated by geomagnetic anomaly of the seafloor located at a similar latitude of the distribution area of the Paraná/Etendeka Flood Basalt did not exceed 127 Ma according to reference of Renne et al. (1992).

In addition, Light et al. (1992) pointed out that the commencement of the rifting in southern Argentina was 220 to 200 Ma and the commencement of the rifting in northern Argentina did not exceed 170 Ma. Then, Chang et al., (1992) pointed out that the commencement of the seafloor spreading at the margin of Brazil did not exceed 140 Ma.

According to these results, it is obvious the forming of the rift and the spreading of the South Atlantic Ocean commenced from the south.

(ii) Relationship between Tristan Plume and the Paraná Flood Basalts

O'Connor and Duncan (1990) insisted that the distribution of the Paraná Flood Basalt has a relationship to the Tristan plume location at the activity of the Paraná Flood Basalt. They estimated that the Tristan plume in 130 Ma was located below the present distribution area of the Paraná Flood Basalt. Similarly, Tomson and Gibson (1991) suggested that the relationship of the locations between the plume and the bottom of the lithosphere had important roles in the igneous activity distribution of flood basalt. Nonetheless, the radial dykes presumed on the Tristan plume reaching the upper mantle are not observed. The NW-SE direction dykes in the east of Uruguay and in Ponta Grossa Arch reflect Proterozoic basement structure. Since the strike of dykes is determined by the direction of large-scale stress fields, it may suggest tectonic structure due to the plume, nonetheless the deformation in the Paraná-Chaco Basin and the Colorado Basin in northern Argentina also show the NW-SE direction. This suggests deformation with a clockwise sense was dominant in the stage of continent separation (Nürnberg and Müller, 1991; Turner et al, 1994), so the structure of the NW-SE direction does not always mean plume activity.

VanDecar et al. (1995) found the low-density anomaly within the lithosphere mantle in the north east of the Paraná Flood Basalt distribution area, and thought the anomaly to be the plume fossil. This low-density anomaly area is a cylindrical shape 200 to 600 km in depth and 300 km in diameter.

(iii) Transition of Igneous Activity for the Paraná Flood Basalts

Peate et al. (1990) pointed out that the rift zone developed toward the north in the early time of the South Atlantic Ocean spreading and, as the result, the upper lavas were piled up toward the north. Peate et al. (1992) also showed that each unit of the Paraná Flood Basalt was piled up with the inclination toward the north from it's geochemical stratigraphy. This means that the magma activity moved toward the north. Renne et al. (1992, 1996) also thought that the lavas of the south of the Paraná Basin extruded in 133 to 132 Ma, and the lavas of the north of the Basin extruded in 131 to 129 Ma from the results of ^{40}Ar-^{39}Ar dating. Turner et al. (1994), however, thought that the magma activity of the initial stage occurred within the continent, and the lavas extruded from the west and north of the Paraná Basin. Then, the magma activity moved to the north end of the Atlantic Rift.

The Paraná Flood Basalt age from ^{40}Ar-^{39}Ar dating by Turner et al. (1994) and Stewart et al. (1996) suggests that different types of magmas extruded in different places at the same time. During 133 to 132 Ma, the Paranapanema lavas of the north Paraná Basin extruded at the same time with the Gramado and Urubicí lavas (Fig. II-3-1-5). Since the intrusive rocks and lavas classified in the same magma type are distributed in approximately the same place in the Paraná Flood Basalt, the lavas are considered to extrude at the present place. Based on these characteristics, the original magma of the Paraná Flood Basalt was not generated as different types of magma by fractionation from the single mantle source, but was generated by different sources or different magmatism. Moreover, it is suggested that the magma was generated in a wider area than that of the distribution area of lavas.

The fact that an older age is not obtained in the dykes distributed along the coast of Brazil suggests that the generation of the magma and lava eruption occurred in a remote place from the rift for at least the initial atage of the Atlantic Rift. The different types of magma were generated by mutual reaction between the plume and lithosphere, and the lithosphere spreading. Then, finally, they are thought to have erupted in different locations.

3-2 Contents of the Survey

3-2-1 Sampling

The positions of the samples from the outcrops are shown in Fig. II-3-2-1. The positions of the drilling holes where the core samples were collected are shown in Fig. II-3-2-2. The above samples are described in the data in Appendix 4 at the back of this report.

(1) Sampling of Rocks

The observation of the occurrence and sampling for analysis specimen was carried out in the distribution area of the Paraná Flood Basalts.

(2) Sampling of Drill Cores and Cuttings

CPRM carried out the drilling survey for coal prospecting along the eastern margin of the Paraná Flood Basalts. Confirmation of the distribution of sills by the drilling sections was carried out, and the main sills were collected in this survey (Fig. II-3-2-2). Also, we collected drill cuttings from drill holes for water resource.

(3) Sampling of Stream Sediments and Stream Water

Sampling of stream sediments and stream water was carried out in the sill distribution area of picritic basalt ~ gabbro. Sampling of stream sand was also carried out in São Gabriel Arch and Ponta Grossa Arch. The collected sand was prepared as less than 80 mesh in the Porto Alegre Branch of the CPRM to analyze.

3-2-2 Laboratory Test

The analysis items, numbers, and content are listed in the following. The results of the laboratory test are described in the text and in the data at the back of this report.

- Thin section:
  125 samples
- Polished thin section:
  55 samples
- Polished ore:
  5 samples
- Whole rock analysis (ICP):
  642 samples for 61 elements

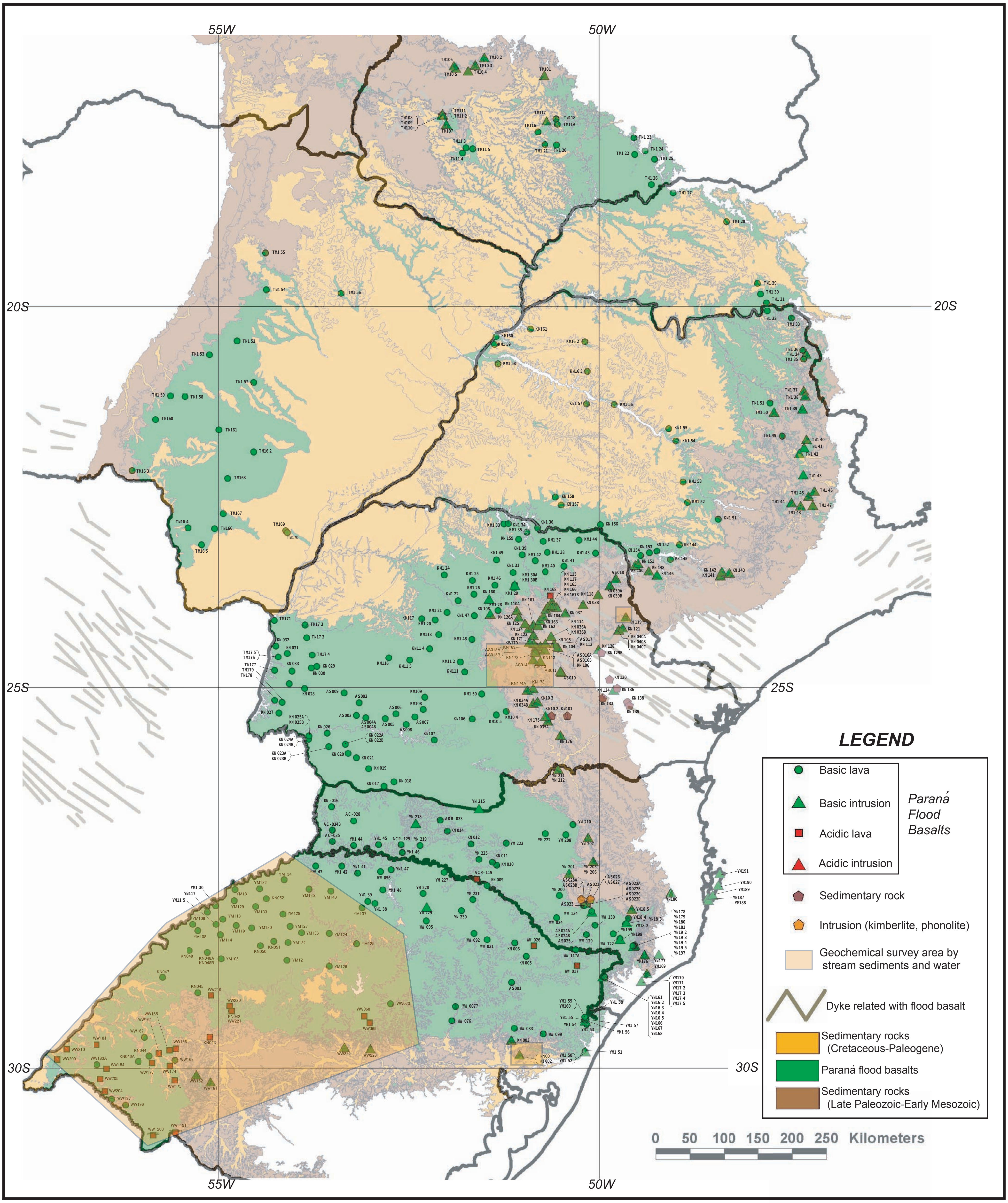

Fig. II-3-2-1 Distribution of collected samples in the survey area

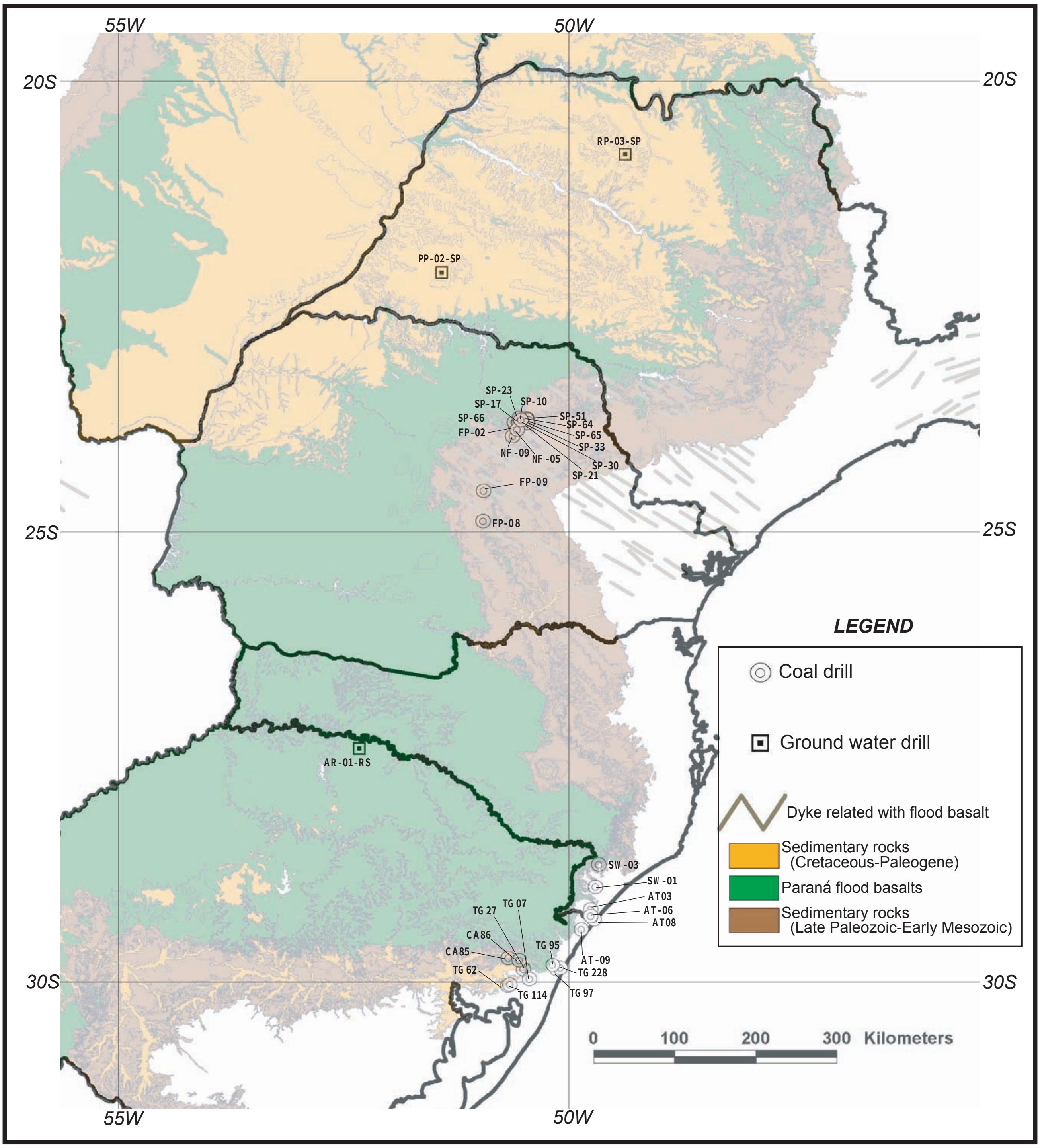

Fig. II-3-2-2 Drill location of collected core and cuttings samples in the survey area

(Major elements: SiO_2, TiO_2, Al_2O_3, Fe_2O_3, MnO, MgO, CaO, Na_2O, K_2O, P_2O_5. Trace elements: Ag, As, Au, Ba, Be, Bi, Br, Cd, Co, Cr, Cs, Cu, Hf, Ir, Mo, Nb, Ni, Pb, Rb, S, Sb, Sc, Se, Sn, Sr, Ta, Tl, V, W, Y, Zn, Zr, La, Ce, Pr, Nd, Sm, Eu, Gd, Tb, Dy, Ho, Er, Tm, Yb, Lu, U, Th. Platinum group elements: Pt,Pd,Au.)

- Analysis of platinum group elements (Ir,Rh,Re):
  34 samples
- Sr and Nd isotopic ratio:
  70 samples
- ^{40}Ar-^{39}Ar dating:
  16 samples
- EPMA:
  10 samples (quantitative analysis)
- X-ray diffraction:
  4 samples
- $\delta^{34}S$ isotopic ratio:
  12 samples
- Panning conc. analysis:
  5 samples, 11 elements (Ag, Cd, Cu, Mn, Mo, Ni, Pb, Zn, S, Pd, Pt)
- Stream sediments (ICP):
  598 samples, 30 elements
  (Ag, Cu, Cd, Mn, Mo, Pb, Ni, Zn, S, As, Ba, Sb, W, Al, Be, Bi, Ca, Co, Cr, Fe, K, Mg, Na, P, Sc, Sn, Ti, V, Y, Zr)
- Stream water (ICP):
  182 samples, 69 elements (Li, B, Be, Na, Mg, Al, Si, K, Ca, Sc, Ti, V, Cr, Mn, Fe, Co, Ni, Cu, Zn, Ga, Ge, As, Se, Br, Rb, Sr, Y, Zr, Nb, Mo, Ru, Pd, Ag, Cd, In, Sn, Sb, Te, I, Cs, Ba, La, Ce, Pr, Nd, Sm, Eu, Gd, Tb, Dy, Ho, Er, Tm, Yb, Lu, Hf, Ta, W, Re, Os, Au, Pt, Hg, Tl, Pb, Bi, Th, U (Sulphate ion)

3-2-3 Occurrences of the Paraná Flood Basalts

The sampling and observation of outcrops were limited to quarries and crosscut for the road because of poor rock exposure in the survey area.

(1) Lava

Basalt lava is dark green to green. Most of it is aphyric. The phenocrysts that can be observed when a lens is used are mainly plagioclase, and CPX. Sometimes olivine can be recognized. Dacite to rhyolite lava is gray to dark black and the texture varies from aphyric to porphyritic.

The thickness of one lava flow was described as from several meters to several hundred meters in the existing reports (Pacca and Ernesto, 1982; Bellieni et al., 1983; Montes-Lauar et al., 1987; Ernesto and Pacca, 1988). Although lava flow can be observed from the bottom to the top as one flow in some quarries, the thickness of the lava flow is approximately 10 to 15 meters. Sandstone or mudstone layer is often observed at the bottom of the lava, which means that there was a time interval after the lava eruption. The sandstone or mudstone is black to yellowish gray or reddish gray, and was altered by heat to become enriched silica.

The foaming traces are often recognized in both the upper and lower parts of lava flows. The middle parts of the lava flows are comparatively massive. The vertical joints are generally developed. Remarkable foaming traces are observed in the lava in the south of Cascavel in the center of the survey area (Fig. II-3-2-3:①). There, black glasses like bubbles less than 0.5 centimeters in diameter are observed (Fig. II-3-2-3:②). Moreover, in the middle of the lava flow, a coarse grained flow of a doleritic to gabbro pegmatite part that occurs as a lenticular shape is sometimes observed (Fig. II-3-2-3:②).

Native copper like flake is observed along the joints or in vesicle of lava as a characteristic occurrence (Fig. II-3-2-3:③). This occurrence is marked in the lava that is distributed around Cascavel in the center of the survey area. The volatile component rich magma is considered to be active in the center of the distribution area of Paraná flood basalt compared to the other area.

(2) Intrusive Rock

Intrusive rocks are from coarse dolerite to gabbro with dark gray to dark green. The major phenocrysts are monoclinic pyroxene, plagioclase, and olivine. Picritic gabbro sill with large amounts of olivine is only distributed in the quarry of the Lomba Grande region.

The occurrence of intrusive rocks is observed to be particularly marked in the quarries of Lomba Grande and Ponta Grossa Arch as well as in the cutting for the road and the distribution area of sedimentary rocks in south east of survey area near Sera Geral. The identification of the difference between lava and intrusive rock is difficult in the distribution area of lavas because lava and intrusive rock are the same kind of rocks and the outcrop condition is bad for observation. In the part where sill has been intruded into the sedimentary rocks, the sedimentary rocks contacting of the upper part of the sill have changed to hornfels from the heat at the intrusion (Fig. II-3-2-4:①). The sulfides mineralization (mainly pyrite) are often observed as the secondary mineral in sills and dykes that differ from those in lavas (Fig.II-3-2-4: ②). They are markedly observed along the joints and child margins.

There are often coarse grained parts like pegmatite with lenticular occurrence in the center of sills that are similar to lava (Fig. II-3-2-4:③).

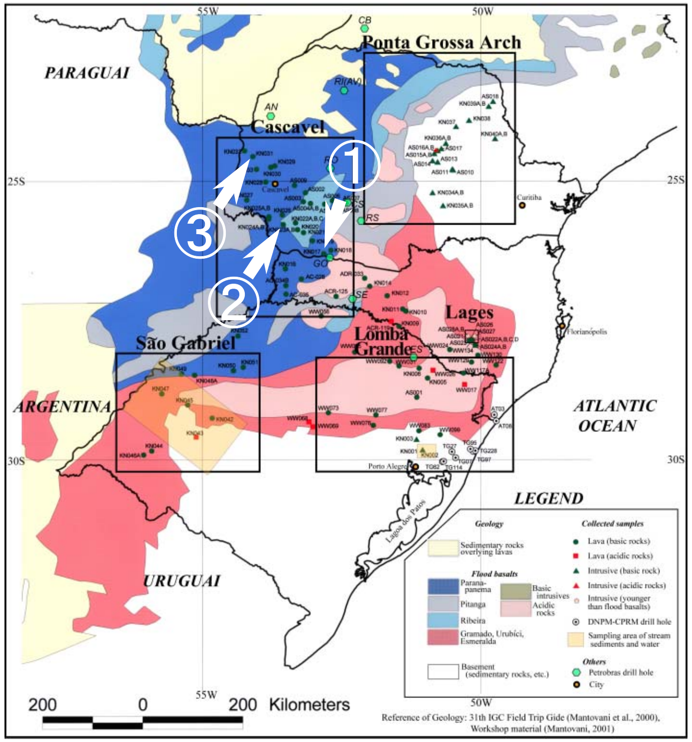

Investigated district	Lava: Lomba Grande	Lava: Cascavel	Lava: São Gabriel	Intrusion (dyke and sill): Lomba Grande	Intrusion (dyke and sill): Ponta Grossa Arch
Rock type	Tholeiitic basalt			Tholeiitic dolerite-gabbro, (rarely Picritic gabbro)	Tholeiitic dolerite-gabbro
Phenocrysts	Plagioclase, CPX, Olivine (rare), OPX (rare)			Plagioclase, CPX, Olivine (rare), OPX (rare)	
Remarkable occurrences of outcrops	Massive (relatively)	Amygdaroidal texture (common); with spheric black glass (rare); with gabbroic part (partly)	Massive (with gabbroic part)	Massive (with gabbroic part)	
Microscopic texture	Aphyric	Aphyric (partly porphyritic)		Porphyritic	
Sulphide	—	Pyrite, Pyrrhotite (dissemination)		Pyrite, Pyrrhotite, Chalcopyrite	Pyrite, Pyrrhotite, Chalcopyrite, Galena, Sphalerite
Mineral-ization	Native copper	Native copper (abundance)	Native copper	Native copper	

Fig. II-3-2-3 Occurrences of lava in the central part of Paraná flood basalts

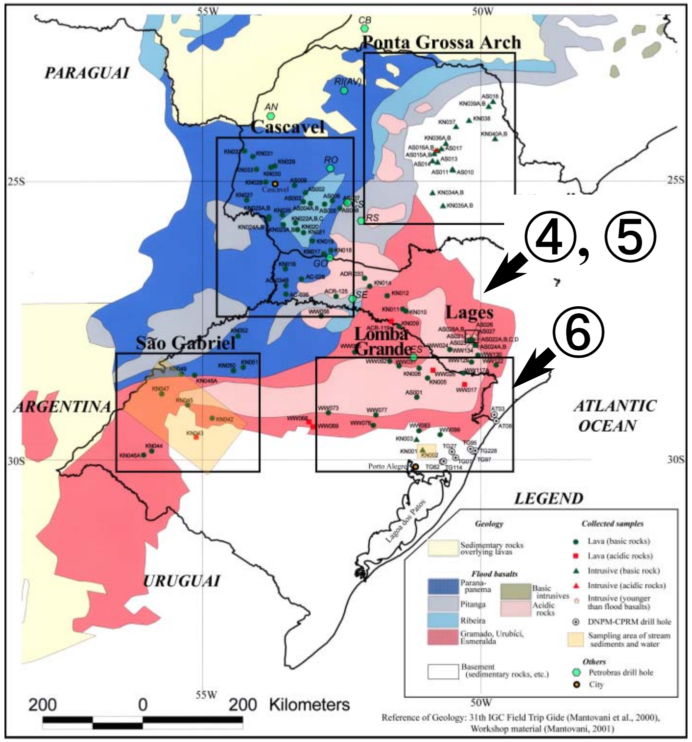

	Lava			Intrusion (dyke and sill)	
Investigated district	Lomba Grande	Cascavel	São Gabriel	Lomba Grande	Ponta Grossa Arch
Rock type	Tholeiitic basalt			Tholeiitic dolerite-gabbro, (rarely Picritic gabbro)	Tholeiitic dolerite-gabbro
Phenocrysts	Plagioclase, CPX, Olivine (rare), OPX (rare)			Plagioclase, CPX, Olivine (rare), OPX (rare)	
Remarkable occurrences of outcrops	Massive (relatively)	Amygdaroidal texture (common); with spheric black glass (rare); with gabbroic part (partly)	Massive (with gabbroic part)	Massive (with gabbroic part)	
Microscopic texture	Aphyric	Aphyric (partly porphyritic)		Porphyritic	
Sulphide	—	Pyrite, Pyrrhotite (dissemination)		Pyrite, Pyrrhotite, Chalcopyrite	Pyrite, Pyrrhotite, Chalcopyrite, Galena, Sphalerite
Mineral-ization	Native copper	Native copper (abundance)	Native copper	Native copper	

Fig. II-3-2-4 Occurrences of sills around the southeastern Paraná basin

3-2-4 Microscopic Observation of the Paraná Flood Basaltic Lava and Intrusion

Microscopic observation of the lavas and intrusive rocks is shown in Table II-3-2-1.

(1) Lava

The maximum size of phenocryst is approximately 0.5 millimeters. The rock shows aphyric to fine grained porphyritic. The phenocrysts are mainly plagioclase and CPX. Phenocrysts of olivine and OPX are sometimes observed. The groundmass is composed of fine-grained plagioclase, CPX, and glass. Magnetite and ilmenite are observed in the groundmass, but part of them were altered to hematite and limonite.

As mentioned later (Section 3-3, Chapter 3, Part II), although the magma that generated the lavas and the intrusive rocks is classified by geochemical characteristics, the marked difference of the phenocryst and the texture is not observed in spite of the different magma type lava.

The quantities of olivine and OPX are generally limited. The Gramado, the low-Ti type, includes relatively more olivine phenocryst than the high-Ti type or the intermediate-Ti type lavas.

(2) Intrusive rock

The rock is coarse grained porphyritic to equi-granular compared to lavas. The mineral composition and the quantities are the same as lavas.

The only sample of sill that was collected in the quarry of the Lomba Grande region is picritic gabbro with large quantities of olivine. The feeder dyke (fine grained basalt) that was sampled in the other quarry near the above quarry includes large quantities of olivine phenocryst.

The intrusive rocks are accompanied by sulfide minerals. Almost all the sulfide minerals are pyrite.

Table II-3-2-1 Microscopic observation of the Paraná flood basalts

Magma Type		Rock type	Mineral Assemblage	
				Accessary Mineral
Low-Ti type	Gramado	lava	Pl > CPX >> Ol > OPX	Mt, Sul, native copper
		intrusion	Pl > CPX >> Ol > OPX	Mt, Sul, native copper
	Esmeralda	lava	Pl > CPX >> Ol > OPX	Mt, Sul, native copper
		intrusion	Pl > CPX >> Ol > OPX	Mt, Sul, native copper
Intermediate-Ti type	Paranapanema-Ribeira	lava	Pl > CPX >>> Ol > OPX	Mt, Sul, native copper
		intrusion	Pl > CPX >>> Ol > OPX	Mt, Sul, native copper
High-Ti type	Pitanga	lava	Pl > CPX >>> Ol > OPX	Mt, Sul
		intrusion	Pl > CPX >>> Ol > OPX	Mt, Sul
	Urubici	lava	Pl > CPX >>> Ol > OPX	Mt, Sul
		intrusion	Pl > CPX >>> Ol > OPX	Mt, Sul

pl: plagioclase, opx: ortho pyroxene, cpx: clino pyroxene, ol: olivine
mt: magnetite, sul: sulfide

3-3 Geochemical Feature and Volcanism of the Paraná Flood Basalts

3-3-1 Review of Geochemical Feature of the Paraná Flood Basalts

The geochemical characteristics and the generation model of Paraná Flood Basalts in the existing documents and papers are described in the following.

(1) Geochemical Characteristics of the Paraná Flood Basalts

(i) Classification of Basalts

Basalt to andesite of the tholeiite series occupies more than 90 vol% of all the Paraná flood basalt. The above basalt to andesite was roughly divided into two magma groups by the classification in the early day's. One is the high content of TiO_2 lavas in the north of the Paraná Basin. The other is the low content of TiO_2 lavas in the south of the Basin (Bellieni et al., 1984a; Mantovani et al., 1985). Moreover, the origins of the two magma groups were considered to be different (Atalla et al., 1982; Bellieni et al., 1984; Mantovani et al., 1985).

The two magma groups that are divided by TiO_2 content are commonly recognized in each LIP that was accompanied by the activity at the period of the Gondwana break-up like the Karoo flood basalt in African Continent (Erlanket et al., 1986). In addition to the above classification, the characteristics of trace elements and isotopes that are commonly recognized in the ocean islands in the South Atlantic Ocean were specified as the Dupal anomaly by Hart (1984).

Later, the unreasonableness of the classification using only TiO_2 content was corrected. Then, classification by using several elements was established (Peate et al., 1988). The elements that were used in the classification are Ti, Zr, and Y of HFS elements and Sr and Ba of LIL elements. Since these incompatible elements have a tendency to concentrate in the liquid phase, they probably reflect the composition of magma that was not fractionated. Moreover, the chemical differences of magma types can be further pointed out by proportion of these elements.

Peate et al. (1992) compiled over 2000 analysis results of samples. They classified the magma types into 6 groups by the major elements, trace elements, and isotope compositions. According to the classification, the Pitanga, Paranapanema, and Ribeira of the high-Ti type are distributed in the north of the Basin. The Gramado and the Esmeralda of the low-Ti type, and the Urubicí of the high-Ti type, are distributed in the south of the Basin.

(ii) Geochemical Characteristics and Distribution of low-Ti Type Magma

Characteristics

The Gramado and the Esmeralda classified as the low-Ti type contain equal to less Ti than MORB (<310 ppm) (Hergt et al., 1991).

As the characteristics of trace elements, the Gramado and the Esmeralda that are rich in LIL elements, HFS elements, and light rare earth elements show a low ratio of Ti/Zr (<60) (Fig.II-3-3-1(A)). They both contain less Nb and Ta compared to their La contents (Nb/La: 0.5 ~ 0.8).

As the characteristics of isotope compositions, the Gramado shows a high $^{87}Sr/^{86}Sr$ ratio (0.7075 ~ 0.7167) and low εNd_i (-8 ~ -3). To the contrary, the Esmeralda magma shows a low $^{87}Sr/^{86}Sr$ ratio (0.7046 ~ 0.7086) and high εNd_i (-4 ~ +3) (Fig.II-3-3-1(C)). Both types show a high $^{206}Pb/^{204}Pb$ ratio ($^{206}Pb/^{204}Pb$>18.2) compared to the high Ti type. Yet, the $^{206}Pb/^{204}Pb$ ratio of the Esmeralda magma concentrates in a narrow range (Esmeralda: $^{206}Pb/^{204}Pb$ = 18.6 ~ 18.8; Gramado: $^{206}Pb/^{204}Pb$=18.4 ~ 19.1: Fig. II-3-3-1(D)) compared to the Gramado magma.

Distribution

The Gramado lavas are widely distributed from the southwest to the southeast of the Paraná Basin. The distribution is particularly well known in the lava cliffs of Serra Geral along the coastal line of the southeast of Brazil. The Esmeralda lavas are distributed in a comparatively narrow area of the southeast of the Paraná Basin, and they cover the Gramado lavas like a cap. This relationship is clearly observed on the inland area of the Paraná Basin. The Esmeralda lavas are identified as the upper unit of the Gramado lavas by above occurrence (Peate et al., 1992).

Only the Gramado lavas of the low-Ti type are characteristically distributed on the surface in Argentina and Uruguay in the southwest to the south of Paraná Basin.

The Gramado occupies approximate 5 ~ 10 vol% of all the Paraná flood basalt, and the erupted quantity ranks No.3 in individual magma type.

(iii) Geochemical Characteristics and Distribution of High-Ti Type Magma

Characteristics

The Pitanga, Urubicí, Paranapanema, and Ribeira are all classified as high-Ti types. The TiO_2 content of the Pitanga, Paranapanema, and Ribeira vary in a wide range (1.5 ~ 4.1 wt%) and their element contents resemble each other in many ways. The only difference is the enrichment rate of each element. For example, the Ti/Y of the Ribeira is <360, that of the Paranapanema is <410, and that of the Pitanga is <530 (Fig. II-3-3-1(A)).

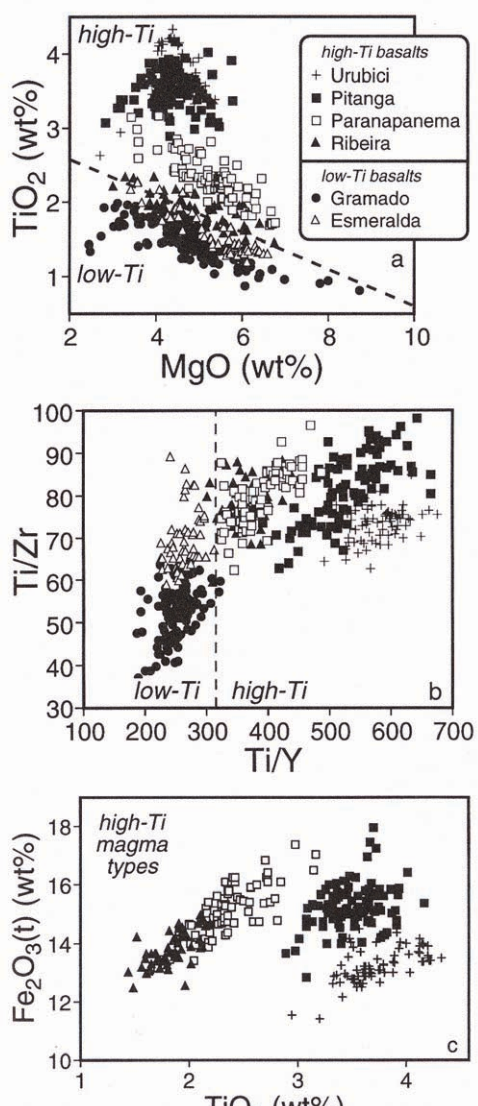

(A) (a) MgO vs. TiO_2: this shows the evolved nature and compositional variety of the Paraná basalts. The dashed line marks the approximate division between low-Ti and high-Ti magma types. (b) Ti/Y vs. Ti/Zr: low-Ti magma types (Gramado, Esmeralda) are distinguished from high-Ti magma types (Urubici, Pitanga, Paranapanema, Ribeira) by low Ti/Y (<310). Esmeralda magmas have higher Ti/Zr (>60) than Gramado magmas. (c) TiO_2 vs. total Fe (Fe_2O_3(t)), showing the different high-Ti basalt magma types. Data sources: *Petrini et al.* [1987], *Hawkesworth et al.* [1988], *Mantovani and Hawkesworth* [1990], *Peate* [1990], *Peate and Hawkesworth* [1996].

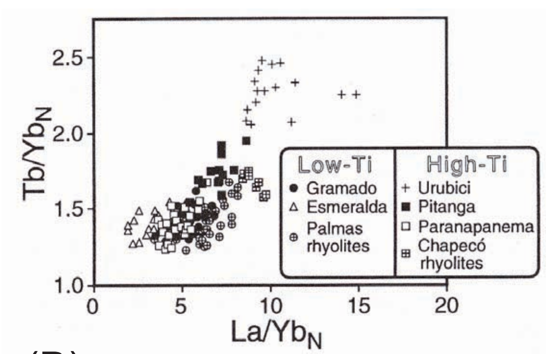

(B) Tb/Yb_N vs La/Yb_N for Paraná basalts and rhyolites (N denotes chondrite-normalised). For the low-Ti magmas, Tb/Yb_N remains fairly constant over a range in La/Yb_N from 1 to 8. For the high-Ti basalt magma types, the Paranapanema magmas overlap with the low-Ti Gramado magmas, whereas the Pitanga and Urubici magmas are displaced to successively higher Tb/Yb_N and La/Yb_N. Data sources for Paraná lavas as for Figure 9.

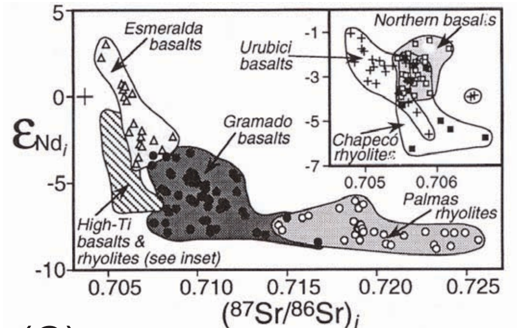

(C) Initial Sr- and Nd-isotopic composition of Paraná magmas (at 130 Ma). Data for the low-Ti magmas are plotted on the main diagram, and the inset is an expanded view to highlight features of the high-Ti magmas that have a more limited isotopic variation. 'Northern Basalts' group combines the Pitanga, Paranapanema and Ribeira magma types. Cross marks bulk Earth estimate. Data sources: *Cordani et al.* [1988], *Mantovani and Hawkesworth* [1990], *Peate* [1990], *Peate and Hawkesworth* [1996].

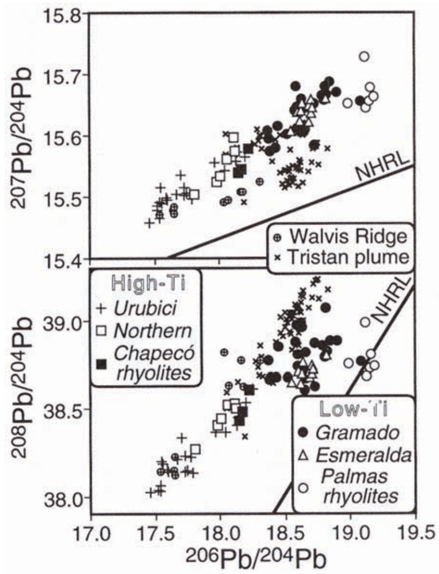

(D) Variation in present-day Pb isotope ratios for Paraná basalts and rhyolites. Data for samples of recent Tristan plume activity (Tristan da Cunha, Gough, Inaccessible) and from the Walvis Ridge plume trace are plotted for reference [*Sun*, 1980; *Richardson et al.*, 1982; *le Roex et al.*, 1990; *Cliff et al.*, 1991]. Symbols and data sources for Paraná lavas as for Figure 9.

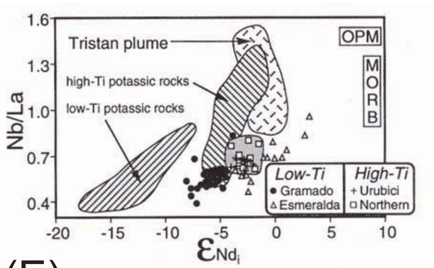

(E) εNd_i vs. Nb/La diagram to illustrate the low εNd_i and Nb/La characteristics of the Paraná basalts, which are distinct from the present-day Tristan plume and MORB compositions. The positive correlation of εNd_i and Nb/La for the Esmeralda magma type indicates the addition of a MORB-like component. Data on Brazilian mafic potassic magmas which represent small-degree lithospheric mantle melts are also plotted to assess their potential role in Paraná magmatism [*Gibson et al.*, 1996]. The minor Tafelkop basalts in Etendeka are compositionally similar to the Tristan plume [*Milner and le Roex*, 1996]. Symbols and data sources for Paraná lavas as for Figure 7. Tristan plume data from *le Roex et al.* [1990] and *Cliff et al.* [1991]. OPM - average oceanic plume magma [*Gibson et al.*, 1996].

Fig. II-3-3-1 Geochemical chalacteristics of the Paraná Flood Basalts

The Ti content of the Paranapanema and Ribeira are intermediate. Although the range of the contents covers that of the low-Ti magma type, they show a high Ti/Y ratio (>310). Since the composition of the other elements is similar to the high-Ti type, they are classified as the high Ti type (Peate et al., 1992). The Ti content of the Ribeira is low, and the MgO content is the same as of the Gramado and the Esmeralda. The Ribeira, however, is classified as the high-Ti type because of the higher Ti/Y ratio and Zr/Y ratio than those of the low-Ti type magma. The spatial distribution of the Ribeira lavas having a close relationship to the distribution of the Paranapanema and Pitanga is one of reason it is classified as the high-Ti type. The Ribeira and Paranapanema are divided by their TiO_2 contents.

The Sr isotope initial ratio of the basalts that was generated from high-Ti type magma distributed in the north of the Paraná Basin is 0.7055 ~ 0.7060 (Fig. II-3-3-1(C)). The juvenile Sr isotope ratio of the Urubicí, the same high-Ti type, shows the tendency of a little higher ratio (Mantovani et al., 1985; Peate et al.,1988; Cordani et al., 1989).

The Pitanga, Paranapanema, and Ribeira, the high-Ti type, that are distributed in the north of the Paraná Basin show the characteristics of less enrichment of Nd and Sr isotope compositions. They show the lower content of Nb and Ta for the content of La and K compared to the ocean floor basalt. These characteristics suggest that they were separately generated from the mantle source that was located under the continent in the early stage of activity (Peate, 1997).

The magma that generated the Urubicí has a resemblance to the Pitanga of the high Ti magma that is distributed in the north, but the distribution area of Urubicí lava is markedly definite.

The Urubicí shows high TiO_2 content (TiO_2>3 %) the same as the Pitanga, and it is more enrich in the incompatible element than the Pitanga. For example, there is a high content of Sr (>550 ppm), low content of total Fe_2O_3 (<14.5 wt%), and low content of heavy rare earth elements (Tb/Yb: Urubicí~0.58, Pitanga~0.38; See Figs. II-3-3-1(A), (B)). Although the isotope copositions of Sr, Nd, and Pb of the Urubicí partly cover those of the magma type that is distributed in the north of the Basin, the range of the ratios is wider than that of the magma ($^{87}Sr/^{86}Sr$ = 0.7048 ~ 0.7065, $^{206}Pb/^{204}Pb$ = 17.46 ~ 18.25; Fig. II-3-3-1 (C), (D)). The Urubicí also shows a low $^{206}Pb/^{204}Pb$ ratio, high $^{207}Pb/^{204}Pb$ ration $^{208}Pb/^{204}Pb$ ratio, and that is the Dupal anomaly (Hawkesworth et al., 1986; Peate, 1990; Milner and le Roex, 1996). The low $^{206}Pb/^{204}Pb$ ratio is the characteristic of the lithosphere mantle.

The Urubicí is known to have been generated under the low oxygen partial pressure compared to the Paranapanema and Pitanga magma from the analysis of Titan-magnetite and ilmenite (Peate, 1997).

Distribution

The Paranapanema lava is most widely distributed in the north of the Paraná Basin. The Pitanga lava is mainly distributed in the northeast and the east in the Paraná Basin. The Paranapanema is the upper layer of the Pitanga from observing the drilling cores.

The Ribeira shows the same horizontal distribution of the Paranapanema (Peate et al., 1987). The distribution of the Ribeira is confirmed in the underneath the Paranapanema and Pitanga by the drilling survey that was carried out in the center of the Paraná Basin (Peate et al., 1992).

The distribution of the Paranapanema under the Gramado of the low-Ti type is confirmed by the drilling survey in Uruguay (Stewart et al., 1996).

The erupted quantities of the Pitanga and Paranapanema are approximately the same. They consist of approximately 20 vol% of all the Paraná Flood Basalts. The Ribeira consists of approximately 5 vol%.

The surface distribution of the Urubicí is markedly definite. It covers approximately 100 x 350 kilometers in the southeast of the distribution area of Paraná Flood Basalts. In this area, alternating beds of Gramado and Urubicí type lavas are distributed (Peate et al., 1992). The Urubicí type magma is often recognized in the bottom of the drilling holes that are located in the center of the Paraná Basin (Peate et al., 1992).

There is a description about Khumib magma that is the same type as the Urubicí magma in the Etendeka flood basalt distribution area (Duncan et al., 1988). The distribution means that they were formed by the same igneous activity before the separation of the Gondwana break-up.

The quantity of the eruption of the Urubicí is approximately 5 vol% of all the Paraná flood basalt.

(iv) Classification of Acid Rock

A large quantity of acid rocks are observed in the upper horizon of the igneous activity in the vicinity of the margin of the distribution area of Paraná flood basalt in the southeast of Paraná Basin (Fig. II-3-3-2). The rock is classified according to the SiO_2 content. If the SiO_2 content exceeds 64 %, then the rock is rhyolite. If the SiO_2 content is less than 60 wt%, then the rock is basalt (Fig. II-3-1-6 (a)). The existence of the acid rock is distinct in Serra Gaucha in the southeast of the Paraná Basin. The quantity of the acid rocks decreases toward the north.

The rhyolite is divided into two groups according to the Ti content like the basalt (Bellieni et al., 1986; Harris et al., 1990; Fig. II-3-1-6 (c)). The rhyolite of the high-Ti type is called Chapeco rhyolite, and the plagioclase phenocryst is characteristic. The characteristics of geochemical compositions are being rich in incompatible elements (Zr: >500 ppm), having low

$\delta^{18}O$ (pyroxene: ~ +6.5), and the same $^{87}Sr/^{86}Sr$ ratio of the high-Ti type basalt (0.705 ~ 0.708; Fig. II-3-1-6 (c) (d)).

The rhyolite of the low-Ti type is called Palmas rhyolite, and it is aphyric. The characteristics of geochemical compositions are being poor in incompatible elements, having high $\delta^{18}O$ (pyroxene: ~ +10‰), and the same $^{87}Sr/^{86}Sr$ ratio of low-Ti type basalt (0.714 ~ 0.727; See Fig. II-3-1-6 (b) (c) (d)).

Since the activity of the rhyolite magma is definite in the margin of the continent, the rhyolite is thought to have been generated in the late stage of the activity of the Paraná/Etendeka flood basalt. Since the distribution of the rhyolite was limited by the Ti content as is the case of basalt, the rhyolite had a close relationship to the basalt and the marked fractional crystallization, contamination of the crust materials, and re-melting of the basalt are all thought to have been it's genesis (Bellieni et al., 1986; Garland et al., 1995).

(2) Magma Source of the Paraná Flood Basalt

The upper mantle that is rich in incompatible elements is considered to be the source of the Pitanga, Paranapanema, and Ribeira of the high-Ti type, and the Gramado (Garland et al., 1996; Peate, 1997).

The characteristics of the isotope ratio (high Rb/Sr ratio and low U/Pb ratio) of the basalt generated from low-Ti type magma are enrichment. This is thought to be from the effect of the contamination of the crust material (Hawkesworth et al., 1992).

The Esmeralda was formed in a later period than the rhyolite in the south of the Paraná Basin. Since the incompatible elements are exhausted in the Esmeralda, the Esmeralda has the characteristics of the oceanic crust, and the participation of the asthenosphere materials is thought to have taken place in the generation.

(3) Effect of Fractional Crystallization of the Paraná Flood Basalts

Both Paraná and Etendeka flood basalts show low MgO contents (3.0 ~ 6.5 wt%) and incompatible elements (Ni:<100 ppm). The lavas that are more basic show high MgO content (6.5 ~ 9.0 wt%), but they occupy less than 2 % of all the lavas. These characteristics show that the magma was widely affected by the fractional crystallization, and it means that the eruption location is very far from the location of the melt generation (e.g. Cox, 1980).

Therefore, since almost all the Paraná flood basalt was controlled by the fractional crystallization of gabbroic minerals (olivine + CPX + plagioclase ± magnetite - ilmenite), the final stage of the fractional crystallization was at least conducted within the magma chamber near the surface under low pressure that was probably 1 atm (Peate, 1997).

(4) Effect of Assimilation of the Crust Material in Paraná Flood Basalts

The low-Ti type basalt shows high Sr, Nd, Pb, and O isotope ratios, and a high incompatible elements ratio. For example, the $\delta^{18}O$ value of the sample of Paraná Flood Basalts after separating the minerals shows a higher value (+6.3‰ ~ +8.3‰) than that of the typical mantle (<+5.5‰) by crust material assimilation (Harris et al., 1989). These characteristics suggest that magma activity in an open system in the shallow area of the crust (Erlank et al., 1984; Mantovani et al., 1985; Fodor et al., 1985; Mantvani and Hawkesworth, 1990; Peate and Hawkesworth, 1996). The increase in the $^{87}Sr/^{86}Sr$ ratio according to the increase of SiO_2 content in the Gramado type magma is evidence of the effect of assimilation of the upper crust material and fractional crystallization.

There is an idea that the magma sources were the same for the Esmeralda of the low-Ti type and the Gramado, and the Esmeralda was generated by the temporary decrease of the quantity of crust contamination (Petrini et al., 1987). The Gramado magma has a correlation to an $^{87}Sr/^{86}Sr$ ratio that corresponds to the contamination quantity of the crust material and the Th/Ta ratio. Yet, the Esmeralda has the same Th/Ta ratio as the Gramado, and the $^{87}Sr/^{86}Sr$ ratio of the Esmeralda is low. From this fact, Peate and Hawkesworth (1996) thought the Gramado magma and the Esmeralda magma have been generated from different magma sources. They suggested that it was generated by fractional crystallization after the contamination of the crust material, and the Gramado magma being mixed in a relatively shallow part of the under ground.

The $\delta^{18}O$ value of the Khumib type basalt of the high-Ti type magma (corresponds to the Urubicí of Paraná Flood BasaltS) in Etendeka Flood Basalt is ~+5.9‰. This value shows the small contamination rate of the crust materials (Harris et al., 1989), but the Urubicí shows the high content of incompatible elements and the narrow range of the $^{87}Sr/^{86}Sr$ ratio. The Urubicí also correlates to the high content of SiO_2 (50 ~ 60 wt%) and the high Th/Ta ratio (2.1 ~ 4.0). The characteristic is thought to be the effect of the assimilation and fractional crystallization (Peate et al., 1999).

The high-Ti type magma (Pitanga, Paranapanema, and Ribeira) distributed in the north of the Paraná Basin is thought to have had little contamination effect of the crust material because of the definite ranges of Sr, Nd, and Pb compositions.

(5) Participation of Mantle Plume for Magmatism of the Paraná Flood Basalts

A large-scale temperature anomaly must occur within the mantle to erupt large quantities of basalt lava like flood basalts. Mantle plume is considered to be necessary for this to take place (Morgan, 1981 and others). There is a relationship in space and time between the distribution of the flood basalt and the trace of the hot spot in the ocean basin. The flood basalt magma was generated by melting with rapid decompression of the plume mantle in most generation model. There are several ideas about melting with decompression as follows; the expansion and thinning of the lithosphere (White and McKenzie, 1989), the temperature anomaly and thinning of the lithosphere (Yuen and Fleitout, 1985), and rapid contact of the huge plume head with the lithosphere in the earliest stage of mantle plume activity (Richards et al., 1989). These melting models with decompression can be applied to some flood basalts. For example, Deccan Flood Basalt has a great eruption rate (<1 km^3/year), and the characteristics of the trace element contents and isotope ratios of the basalt samples that mean relatively less contamination of the crust materials are similar to the present volcanic rocks from the Réunion plume. The characteristics of trace element content show the high Fe and the low Si contents that reflect the melting of enriched peridotite from the depth (Peng and Mahoney, 1995; Turner et al., 1996).

Still, it is difficult to explain the generation model of Paraná flood basalt with only melting with decompression (Turner et al., 1996). The high-Ti type magma that was not affected by contamination of the crust shows a low Nb/La ratio (<0.8) and low $_{\varepsilon}$Ndi (<0) that differs from MORB and basalt of the ocean islands. At the same time, the characteristics of major elements suggest a different mantle source from oceanic basalt (Hergt et al., 1991; Hawkesworth et al., 1992; Turner and Hawkesworth, 1996).

The eruption rate of Paraná flood basalt is less than that of Deccan Flood Basalt (Turner et al., 1994). The difference between Paraná flood basalt and Deccan flood basalt is the participation of the lithosphere above the mantle plume. The question remains, however, of the possibility of explaining magma with large scale that generates flood basalt only with the lithospheric mantle.

There is less chemical composition similarity between the Paraná and Etendeka flood basalts and the magma activity of Tristan plume. The content of the incompatible elements and isotope compositions of Paraná Flood Basalts are similar to Tristan plume related lavas of Tristan de Cunha Island and Gough Island (Fig. II-3-1-1).

The Esmeralda, however, that was generated in the latest stage, only shows the characteristic asthenospheric composition within Paraná flood basalt. The erupted quantity of the Esmeralda is very small, and the quantity therefore rarely has significant meaning (Peate and Hawkesworth, 1996). Within Esmeralda lavas, $_{\varepsilon}Nd_i$ correlates with Nd/La ratio and Sm/Ce ratio, but those values do not resemble those of the present Tristan plume magma. They actually resemble the values of MORB ($(Ce/Sm)_N$:<1, Nb/La:>0.9, $_{\varepsilon}Nd_i$ >+4; Peate and Hawkesworth, 1996).

(6) Generation of Paraná Flood Basalt Magma by Melting of Lithospheric Mantle

Presently the geochemical evidence shows that the lithosphere mantle materials participated in generating several flood basalts. The model of melting with decompression in the plume for flood basalt generation anticipated that the volume of melt generation in the early stage of magma generation within the lithosphere mantle was a small quantity (less than 5 %). This model is not proper to apply to several flood basalts because it supposes large eruption rates (White and McKenzie, 1989 and others).

The generation of melt within the lithosphere mantle is promoted by the existence of $H_2O \pm CO_2$ (0.3 wt%). The solidus rich in volatile components melts at low temperatures (Gallagher and Hawkesworth, 1992). Turner et al. (1996) considered the Heat Conduction Model where the melting take place within the lithosphere mantle. The mechanism is that the heat conducts from the mantle plume sustained under the lithospheric cap to the lithospheric mantle (Saunders et al., 1992).

The important variables in this model are the potential temperature of the plume, the thickness of the mechanical boundary layer, and the term of the conduction continuation. These variables are important because the heat movement occurs during a long time scale by conduction. In this model, the magma generation is long term and the mantle melting widely occurs within the lithosphere mantle on a scale of 10 m.y. Without the melt that directly caused by the plume, a lava eruption with a thickness of 1 ~ 3 kilometers occurs. In this model, the thickness of the lithosphere is anticipated as under 100 kilometers.

When the thickness of the lithosphere becomes under 100 kilometers due to expansion of lithosphere and corrosion with heat, melting with decompression begins within the plume, and magma with characteristics of both the asthenosphere composition and the lithosphere composition is thought to erupt.

Turner et al. (1994) thought that asthenosphere melting with decompression did not occur because thinning of the lithosphere by tension was too small considering the term of the activities of Paraná/Entedeka Flood Basalts. According to this, the thickness of the lithosphere was at least 150 kilometers.

According to the above model, the conclusion is as follows.

The Tristan plume that participated in the generation of the Paraná/Entedeka flood basalts caused only the melting of the lithosphere due to heat conduction. That is the difference from the Siberian Trap and Deccan flood basalt (Turner et al., 1996). Therefore, the participation of the Tristan plume and the materials of the asthenosphere like MORB were limited in Paraná and Etedeka flood basalts. The origin of the basalts was the continental lithospheric mantle that was exhausted in Fe (Hergt et al., 1991; Turner and Hawkesworth, 1995).

The Pitanga, Paranapanema, and Ribeira distributed in the north of the Paraná Basin were generated in shallow part from the same mantle source by successive but different rates of partial melting (Garland et al., 1996). Melt generated from melting asthenosphere participated only for the Esmeralda type magma, activated in the latest stage of Paraná flood basalt. This is thought to occur from the progress of the thinning of the lithosphere and the melting with the decompression of the asthenosphere in the late stage of the igneous activity.

3-3-2 Geochemical Characteristics of the Paraná flood basalts

(1) Application of classification method by Peate et al. (1992) to the Paraná flood basalt

Peate et al. (1992) classified magma that formed lava into six types, by major element content, HFS element content and LIL element content, and HFS/LIL element ratio. For examining the analytic values in this survey, sampled basalt lava was classified according to the classification by Peate et al. (1992). Fig. II-3-3-2 shows the classification by Peate et al. (1992) while Table II-3-3-1 shows the result of the analysis under this survey. In the classification, samples whose loss of ignition (L.O.I.) exceeded 2.5% were excluded because they were assumed to have been subjected to weathering, following the procedure taken by Peate et al. (1992). Actually, in the samples showing high L.O.I. were observed seladonite and hematite under microscope. Magnesium number (Mg#) was calculated according to (Mg number: 100 Mg/(Mg+Fe_{total}), Fe^{2+}/Fe^{3+} = 0.85).

Pitanga and Urubicí were classified into high-Ti type magma while Gramado and Esmeralda into low-Ti type. In addition to the high-Ti and the low-Ti types, "Intermediate-Ti type" was allocated as a magma type showing an intermediate Ti content, to Paranapanema and Ribeira which were distinctly identified (Fig. II-3-3-5).

Significant difference was not recognized between Paranapanema and Ribeira in element contents and element ratios except a small difference in Ti quantity. Consequently, these two were handled as one type named Paranapanema-Ribeira.

As a general geochemical characteristic trend, high-Ti type magma is rich in HFS/LIL elements while low-Ti type magma is poor in these elements (Fig. II-3-3-2).

(2) Spatial Distribution of Magma Types

Fig. II-3-3-3 shows the spatial distribution of Paraná flood basalts lava and intrusive rocks classified according to Peate et al. (1992).

The distribution of magma types classified as a result of the present survey agrees roughly with that indicated by Peate et al. (1992).

Individual magma types are found in different limited distribution ranges in the Basin. In the northern to northeast part of Paraná Basin are distributed high-Ti type Pitanga lava and intrusive rocks. In the central to quasi-southern part of Paraná basin are distributed high-Ti type Pitanga and intermediate-Ti type Paranapanema-Ribeira lava and intrusive rocks. In the

Geochemical classification for the Paraná flood basalts (from Peate et al., 1992)

	"High-Ti"				"Low-Ti"	
Peat et al., 1992	*Urubicí*	*Pitanga*	*Paranapanema*	*Ribeira*	*Esmeralda*	*Gramado*
This survey	*High-Ti*		*Intermediate-Ti*		*Low-Ti*	
SiO_2	> 49	> 47	48 - 53	49 - 52	48 - 55	49 - 60
TiO_2	> 3.3	> 2.8	1.7 - 3.2	1.5 - 2.3	1.1 - 2	0.7 - 2.0
P_2O_5	> 0.45	> 0.35	0.2 - 0.8	0.15- 0.50	0.15 - 0.50	0.05 - 0.40
Fe_2O_3 total	< 14.5	12.5-18	12.5 - 17	12 - 16	12 - 17	9 - 16
Sr	>550	>350	200 - 450	200 - 375	<250	140 - 400
Ba	>500	>200	200 - 650	200 - 600	90 - 400	100 - 700
Zr	>250	>200	120 - 250	100 - 200	65 - 210	65 - 275
Ti/Zr	> 57	> 60	> 65	>65	>60	
Ti/Y	>500	>350	>350	>300	<330	<330
Zr/Y	> 6.5	> 5.5	4.0 - 7	3.5 - 7.0	2.0 - 5.0	3.5 - 6.5
Sr/Y	> 14	> 8	4.5 - 15	5 - 17	< 9	<13
Ba/Y	> 14	> 9	5 - 19	6 - 19	< 12	<19
Content of HFS elements	*High* ———					*Low*
Content of LIL elements	*High* ———					*Low*

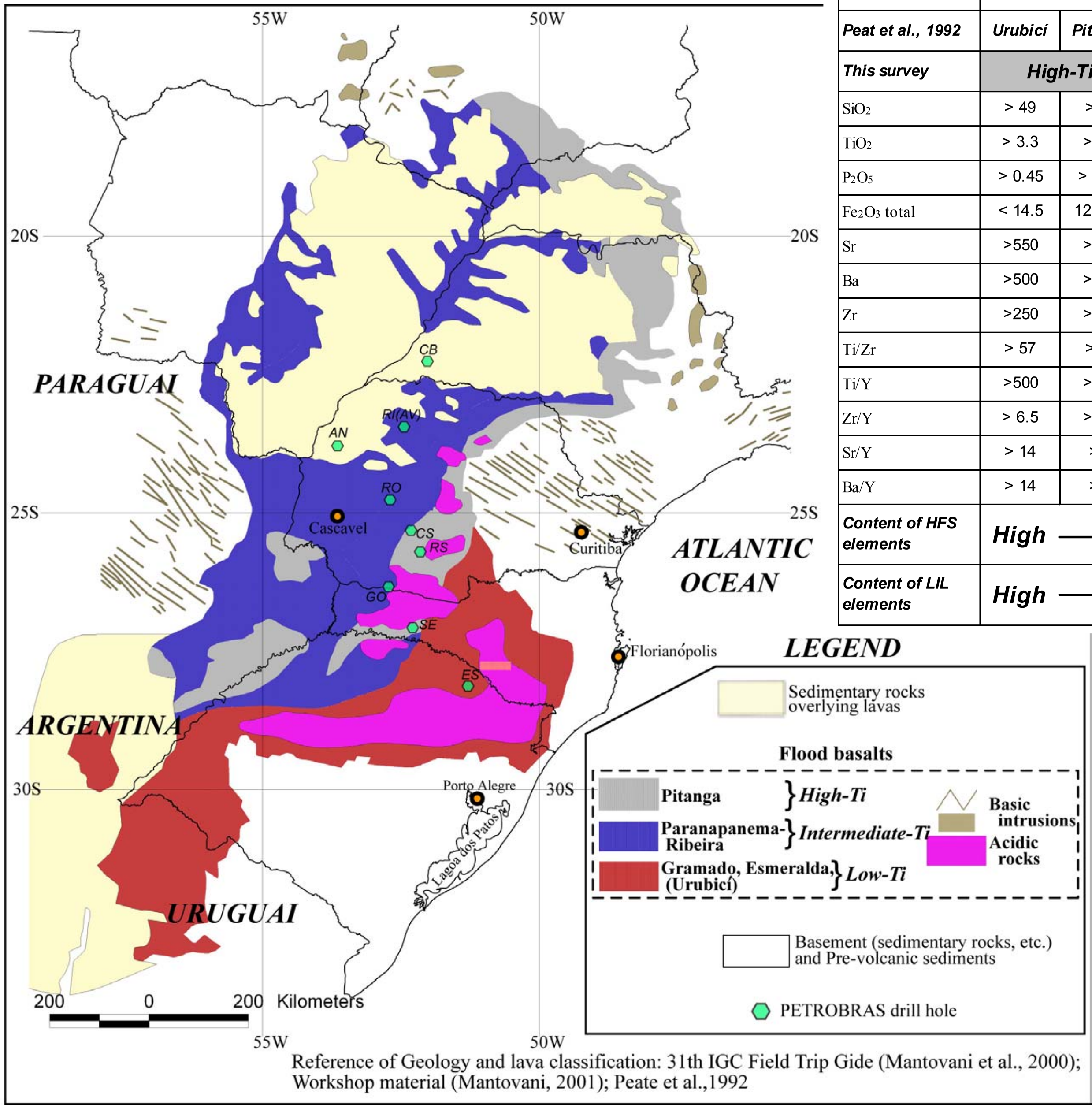

Fig. II-3-3-2 Geochemical classification for the Paraná flood basalts (after Peate et al., 1992)

Table II-3-3-1 Analytical results of major, trace and metal elements for the Paraná flood basalts in this survey

Lava type	Low-Ti				Intermediate-Ti		High-Ti			
	Gramado		Esmeralda		Paranapanema-Ribeira		Pitanga		Urubicí	
Number of samples	44		25		133		80		8	
	Avarage	Range	Avarage	Range	Avarage	Range	Avarage	Range	Avarage	Range
Major elements (wt%)										
SiO_2	54.52	51.65–57.70	52.48	50.14–56.30	51.16	49.65–53.90	51.34	48.57–55.10	51.76	50.50–53.70
Al_2O_3	13.89	12.67–15.80	13.46	12.28–14.90	13.03	11.87–14.00	12.58	10.46–13.30	13.17	12.88–13.40
Fe_2O_3	12.33	9.77–14.40	13.79	11.18–16.10	14.73	11.22–16.30	15.08	12.36–17.90	13.29	12.05–14.20
MnO	0.18	0.15–0.20	0.21	0.17–0.30	0.21	0.16–0.30	0.21	0.16–0.30	0.17	0.15–0.20
MgO	4.89	2.26–8.30	5.27	3.06–7.20	5.31	3.64–6.6	4.30	2.86–6.80	4.53	4.15–5.40
CaO	8.43	5.96–11.70	9.46	6.84–11.80	9.36	7.47–10.80	8.11	5.70–9.60	7.97	7.46–8.20
Na_2O	2.65	2.08–3.40	2.59	2.28–3.00	2.55	2.25–3.40	2.79	2.33–3.40	2.83	2.56–3.70
K_2O	1.55	0.61–2.80	1.04	0.34–2.40	1.10	0.47–2.00	1.51	0.72–3.30	1.94	1.65–2.60
TiO	1.36	0.79–1.90	1.49	1.03–2.00	2.26	1.65–3.50	3.56	2.69–4.10	3.82	3.35–4.20
P_2O_5	0.20	0.09–0.30	0.18	0.12–0.30	0.28	0.18–0.90	0.52	0.32–0.80	0.52	6.46–0.60
Mg #	64.0	43.4–79.8	63.3	48.3–74.9	62.5	51.3–70.5	56.9	47.3–66.7	61.3	58.4–66.3
Trace elements (ppm)										
Ba	369	146–717	232	114–355	332	233–682	521	378–1020	636	561–720
Sr	219	126–349	175	140–216	302	218–520	464	317–676	700	571–837
Y	32	17–53	32	21–43	35	24–62	39	29–54	35	33–39
Zr	153	70–245	124	80–172	162	113–239	256	191–378	291	257–340
Nb	12	7–18	9	5–13	14	10–23	24	18–31	27	22–31
Ti/Zr	54	39–71	74	63–102	84	71–106	85	43–118	79	72–92
Ti/Y	261	167–314	278	254–324	397	217–592	549	302–714	654	535–757
Zr/Y	5	4–6	4	3–5	5	2–6	7	5–8	8	7–9
Sr/Y	7	3–11	6	4–9	9	4–17	12	7–20	20	16–25
Ba/Y	12	8–20	7	4–11	10	6–17	13	11–27	18	16–20
Cu	126.00	58–295	177	132–251	218	78–711	57	47–67	157	128–226
Ni	66.00	<1–400	75	<1–361	43	14–87	155	26–1315	151	40–225
Pd (ppb)	6.50	0.2–33.4	10.1	<0.2–18.8	14.3	<0.2–41.3	4.5	<0.2–28.4	6.0	<0.1–8.6
Pt (ppb)	5.50	0.4–14.7	7.1	2.3–15.2	7.9	<0.2–22.8	2.2	<0.2–11.2	4.7	<0.1–7.3
Au (ppb)	5.00	<2.0–69.0	3.0	<2.0–18.0	4.0	<2.0–22.0	2.0	<2.0–13.0	3.0	<2.0–5.0
Isotope										
$^{143}Nd/^{144}Nd$	0.51219	0.51213–0.51226	0.51229	0.51220–0.51241	0.51228	0.51224–0.51235	0.51231	0.51225–0.51281	0.51230	0.51228–0.51232
$^{87}Sr/^{86}Sr$	0.70947	0.70857–0.71022	0.70709	0.70619–0.70903	0.70581	0.70560–0.70603	0.70586	0.70548–0.70654	0.70519	0.70512–0.70526
ε Nd	−8.7	−9.8 – −7.5	−6.8	−8.5 – −4.4	−7.1	−7.7 – −5.6	−6.4	−7.7 – 3.4	−6.5	−6.9 – −6.2
ε Sr	70.5	57.8 – 81.2	36.7	23.9 – 64.4	18.6	15.6 – 21.7	19.3	13.9 – 29.0	9.8	8.8 – 10.8

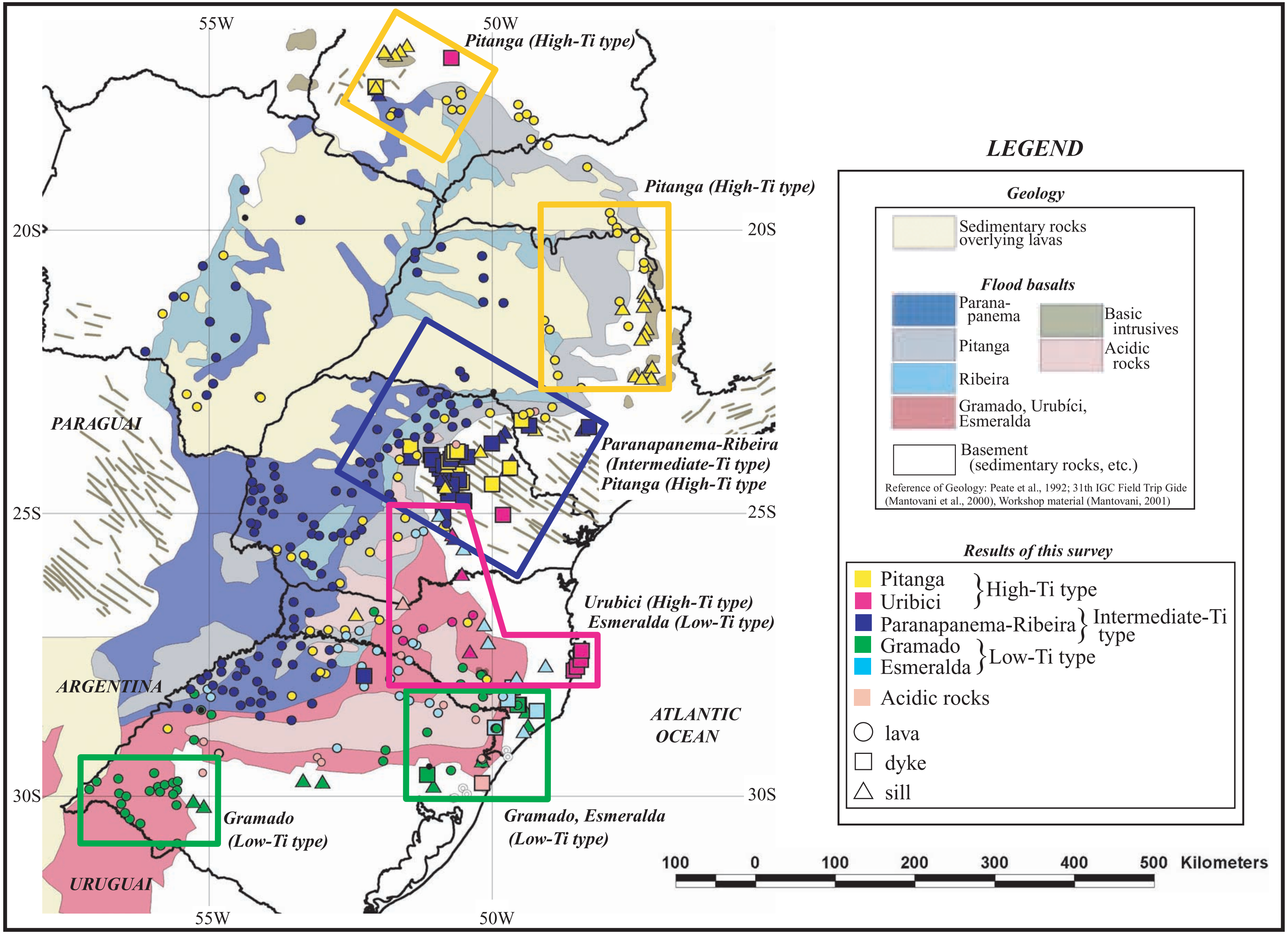

Fig. II-3-3-3 Disribution of geochemical classified lava and intrusion in the Paraná flood basalts

southern part of Paraná basin are low-Ti type Gramado lava and intrusive rocks. In the southeastern part of Paraná basin are high-Ti type Urubicí and low-Ti type Esmeralda. In short, as a trend of magma type distribution, high-Ti, intermediate-Ti, and low-Ti types are distributed, in the descending order, from north to south.

Distribution boundaries of magma types include neighboring lava of different magma types overlapping (mingling). For example, in Ponta Grossa Arch, lava and dyke activities of both high-Ti type Pitanga and intermediate-Ti type Paranapanema-Ribeira are recognized. In central to southern part of the survey area, Paranapanema-Ribeira as well as Gramado and Esmeralda are distributed over the same place.

Since activities of different magma types are recognized in the same place, it can be said that different magma formations occurred gradually and simultaneously.

Sill and dyke are, in terms of chemical composition, the same as lava distributed over the same place (for example, Ponta Grossa Arch). This means that the same magma was active at the same place, and suggests that magma groups which are different in geochemical characteristics were formed over different places. It is considered, therefore, that lava and intrusive rocks have locally characteristic geochemical features. Accordingly it is unreasonable to discuss the differentiation of magma formed from a single mantle source or to discuss the generation of Paraná Flood Basalts from the same magma formation mechanism.

(3) Characteristics of Major Elements

Fig. II-3-3-4 shows the AFM diagram and a SiO_2-Alkali diagram of Paraná flood basalts lava. The Paraná flood basalts lava can be classified into non-alkali rock (Fig. II-3-3-4 (B)), belonging to the series of tholeiite (Fig. II-3-3-4 (A)). Most basalt samples are classified into basalt to andesite while acid rock into dacite to rhyolite (Fig. II-3-3-4 C)).

Figures II-3-3-5 to II-3-3-7 are diagrams, whose horizontal axis is Mg# and vertical axis shows the major elements: SiO_2, TiO_2, P_2O_5, Al_2O_3, Fe_2O_3, MgO, CaO, Na_2O_3, and K_2O. All the diagrams show a clear trend by crystallization differentiation.

Low-Ti type magma shows high Mg# values in a wide range (Gramado up to 79.8). High-Ti type magma shows lower value than those of low-Ti type magma (Pitanga up to 66.7, Urubicí up to 66.3) in a narrower range. This may indicate that high-Ti type magma has been subjected to more crystallization differentiation.

Low-Ti type magma contains much SiO_2. In particular, Gramado shows the highest SiO_2 quantity (SiO_2: maximum 57.7 %), and large fluctuations in content irrespective of the degree of differentiation. Gramado also shows large fluctuations in quantity of major elements.

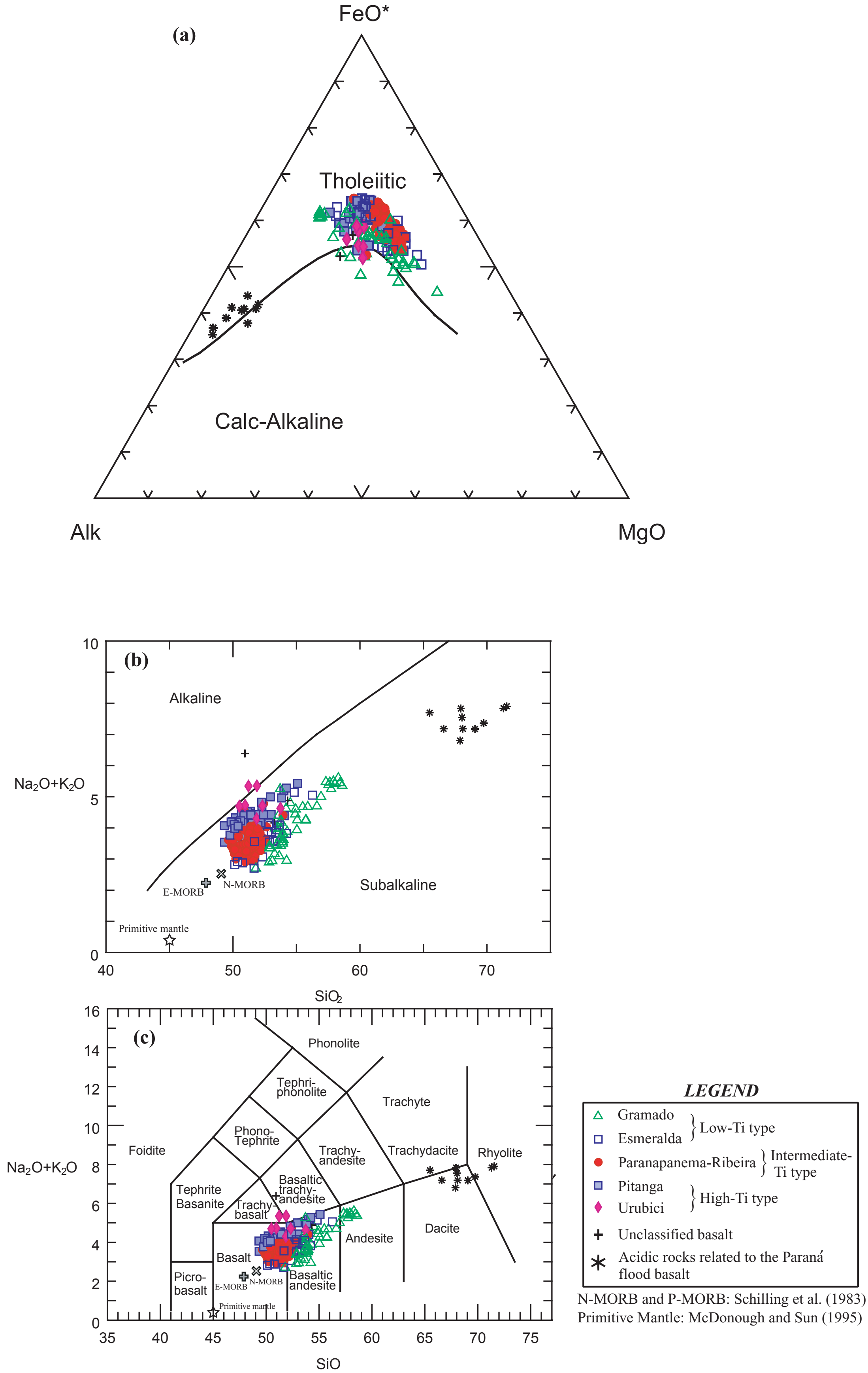

Fig. II-3-3-4 AFM diagram and SiO2 vs. alkali diagram for the Paraná flood basalts

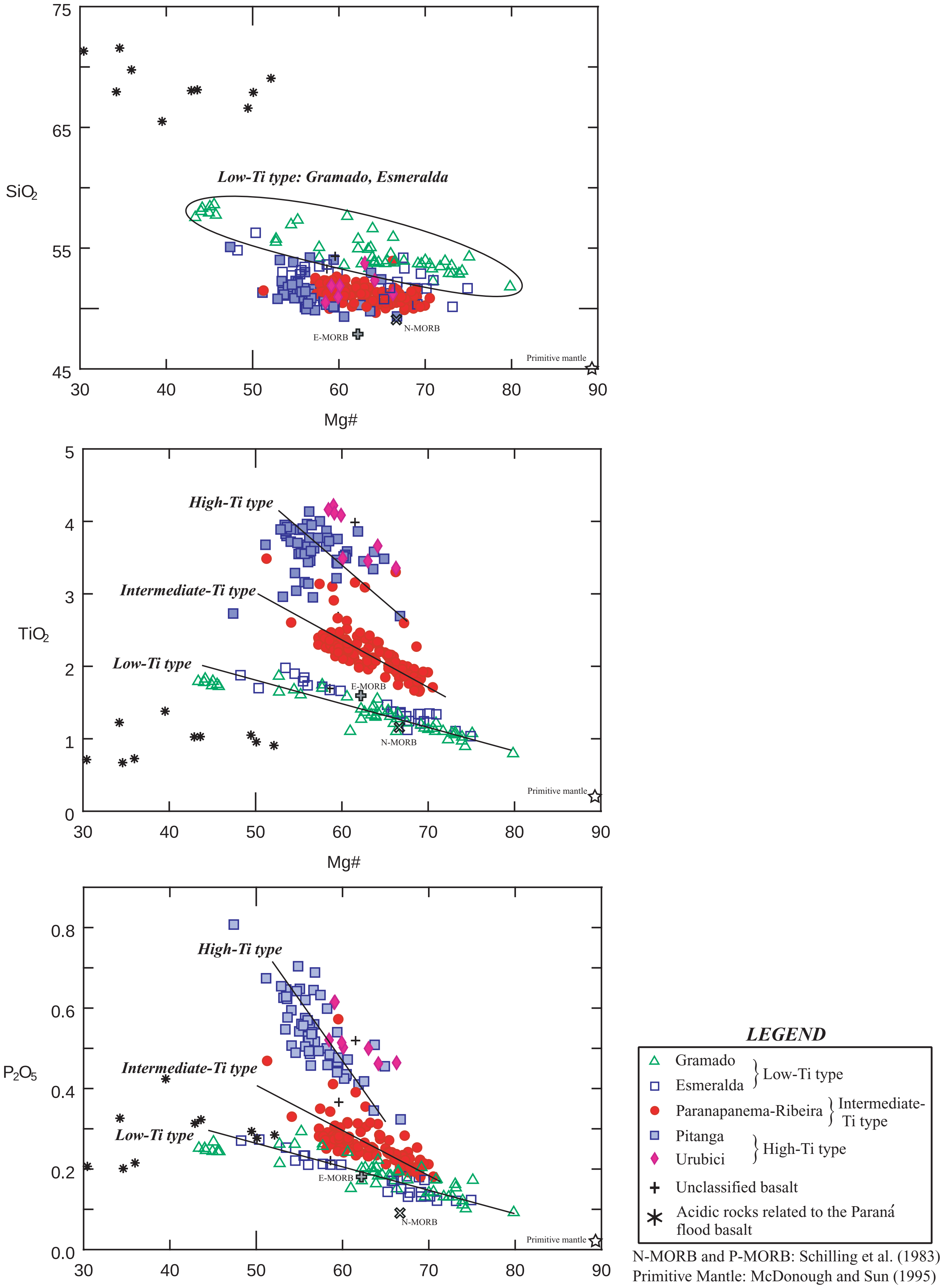

Fig. II-3-3-5 Mg number vs. SiO_2, TiO_2 and P_2O_5 diagrams for lava samples

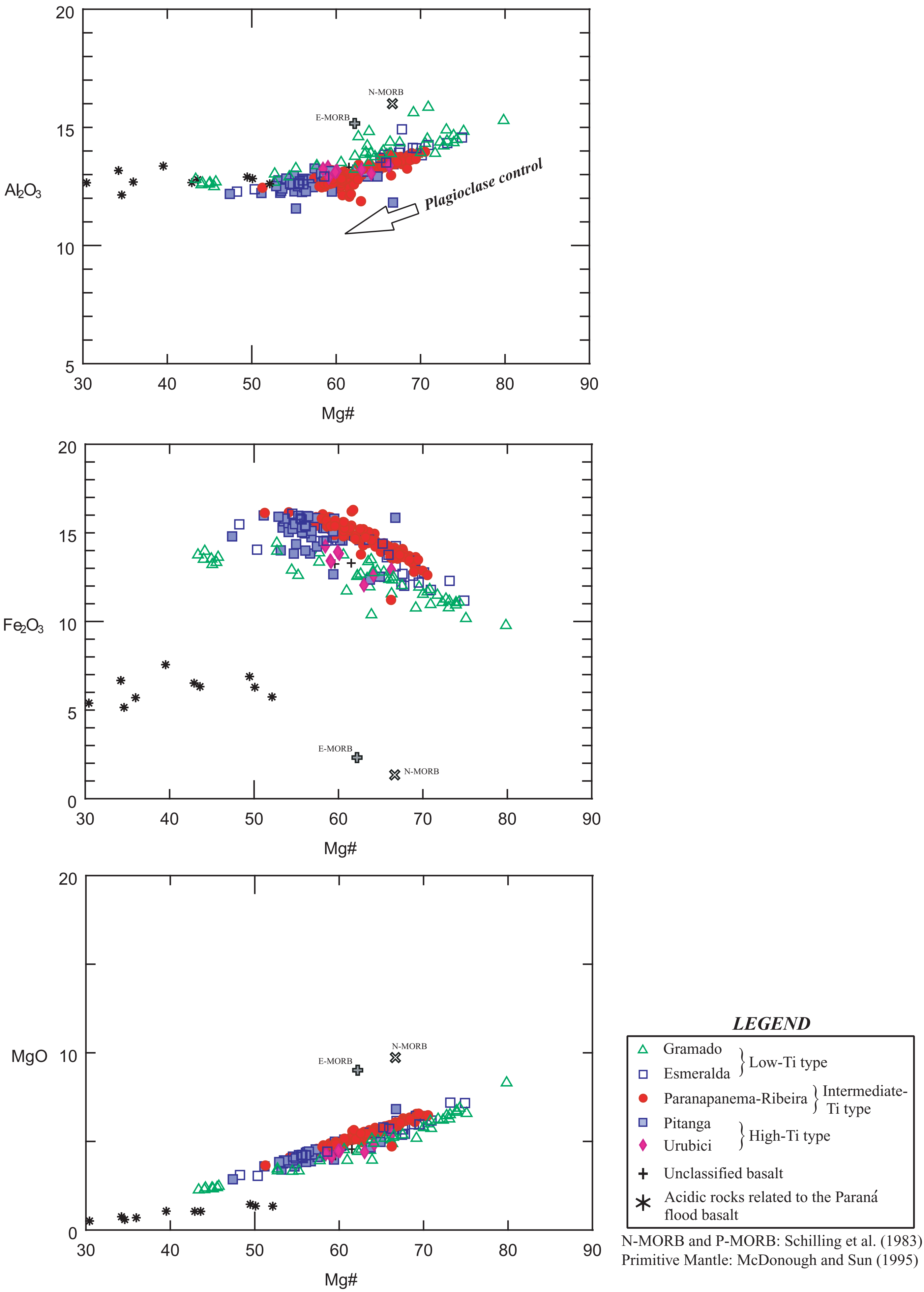

Fig. II-3-3-6 Mg number vs. Al_2O_3, Fe_2O_3 and MgO diagrams for lava samples

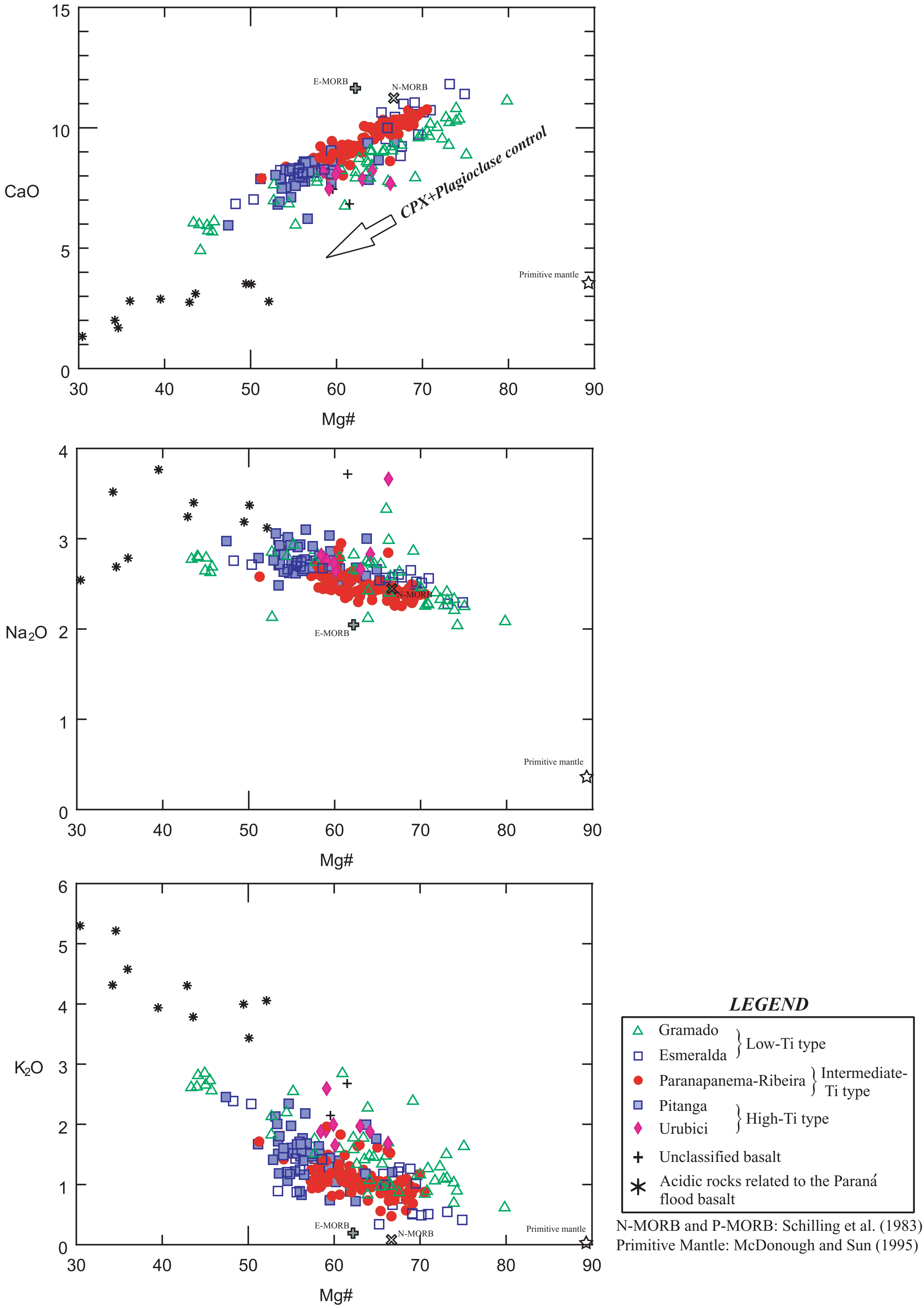

Fig. II-3-3-7 Mg number vs. CaO, Na_2O and K_2O diagrams for lava samples

The high-Ti type, the intermediate-Ti type and the low-Ti type are divided distinctly by the quantities of TiO_2 and P_2O_5, and these types show different differentiation trend. This shows that they are from different magma types. It is difficult to consider that they have been formed by crystallization differentiation from the same magma.

The trend that the quantities of Al_2O_3 and CaO decrease with the decrease of Mg#, that is, with the progress of differentiation, is considered to have been affected by the influence of the crystallization of CPX + plagioclase, from the combination of phenocrysts assemblage under microscope.

(4) Characteristics of Trace Elements (HFS, LIL Elements)

Fig. II-3-3-8 to II-3-3-10 are diagrams, whose horizontal axis is Mg# and vertical axis shows Nb, Zr, Y, Rb, Sr, Ba, Th, U, and La. All the trace elements in the diagrams have high liquid phase concentrations and, except for Sr, show the trend toward higher concentration as differentiation develops.

In particular, Nb, Zr, and Y, which are HFS elements, show this trend remarkably. Esmeralda, which is of low-Ti type magma, is lowest while Pitanga and Urubicí, which are high-Ti type magma, are higher in the quantities of Nb and Zr. Nb and Zr are plotted in areas, in which the three magma types (high-Ti type, intermediate-Ti type, and low-Ti type) show different fractionation trends (Fig. II-3-3-8). This, as well as the differetiation trends of TiO_2 and P_2O_5 of major elements, may suggest that they belong to different magma types.

Rb, Sr, and Ba, which are LIL elements, do not show a clear differentiation trend as the HFS elements do. However, Pitanga and Urubicí, which are high-Ti type magma, tend to show high values of these elements as well as the HFS elements. This may reflect characteristics of sources which have been enriched with incompatible elements.

Gramado, low-Ti type, is rich with trace elements compared it with other magma types. This magma shows trace element quantities in a wide range. In particular, the quantities of Rb, Th, and U vary remarkably. This may have been affected by the contamination of upper earth crust consisting of the granite, containing lots of Rb, Th, and U.

(5) Characteristics of Trace Elements (Siderophile Elements and Chalcophile Elements)

Fig. II-3-3-11 and II-3-3-12 are diagrams, whose horizontal axis is Mg# and vertical axis shows Cu, Ni, Au, Pt, and Pt+Pd.

The Ni quantity change trend shows that separation of olivine, which is distributed by Ni, took place at the early stage of differentiation (up to Mg#=70) , and then crystallization of CPX + plagioclase took place (Fig.II-3-3-11).

Paranapanema-Ribeira, intermediate-Ti type magma, shows high Cu, Pt, and Pd values (Cu:711 ppm maximum; Pt: 22.8 ppb maximum; Pd:41.3 ppb maximum). These Pt and Pd values are

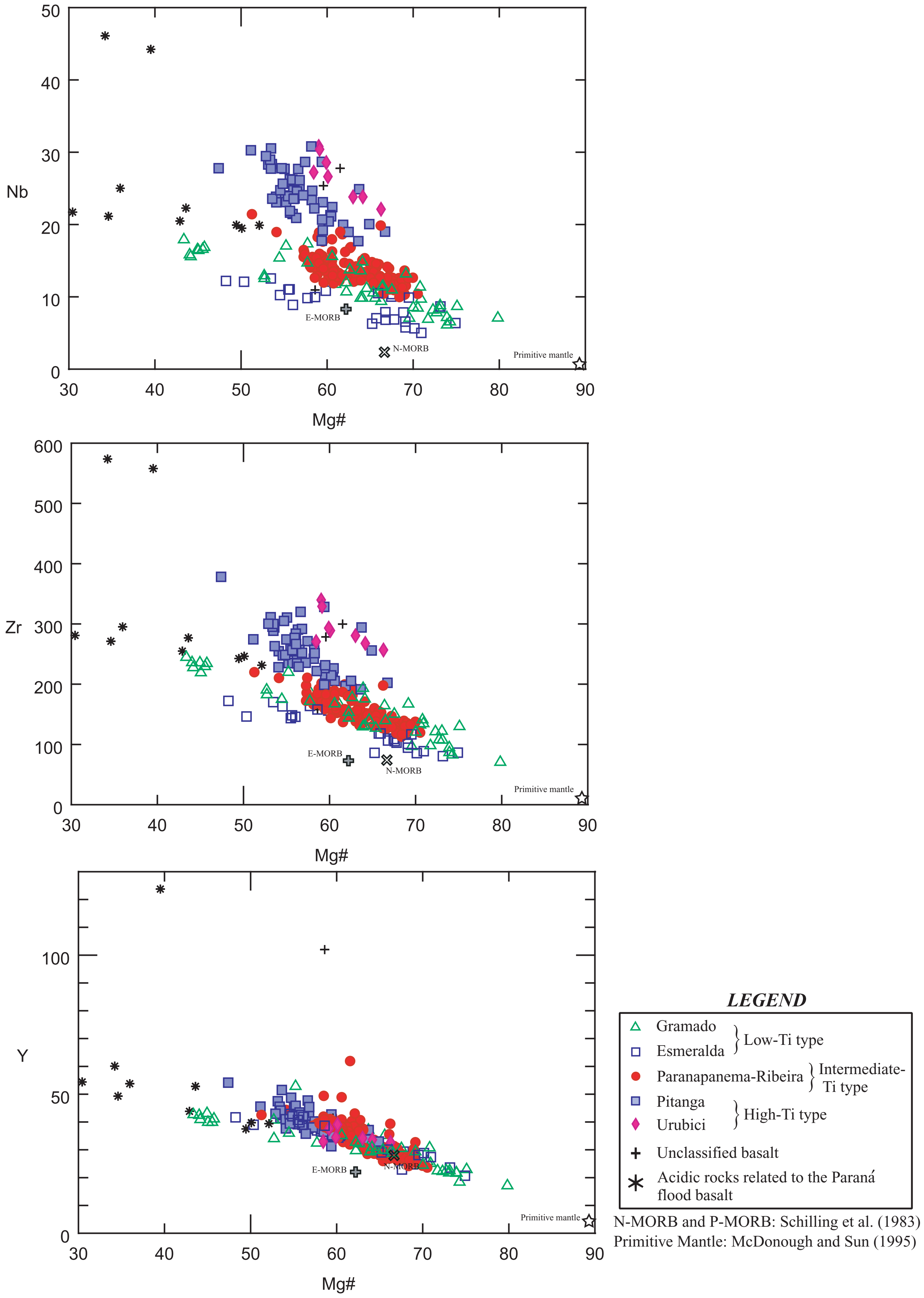

Fig. II-3-3-8 Mg number vs. Nb, Zr and Y diagrams for lava samples

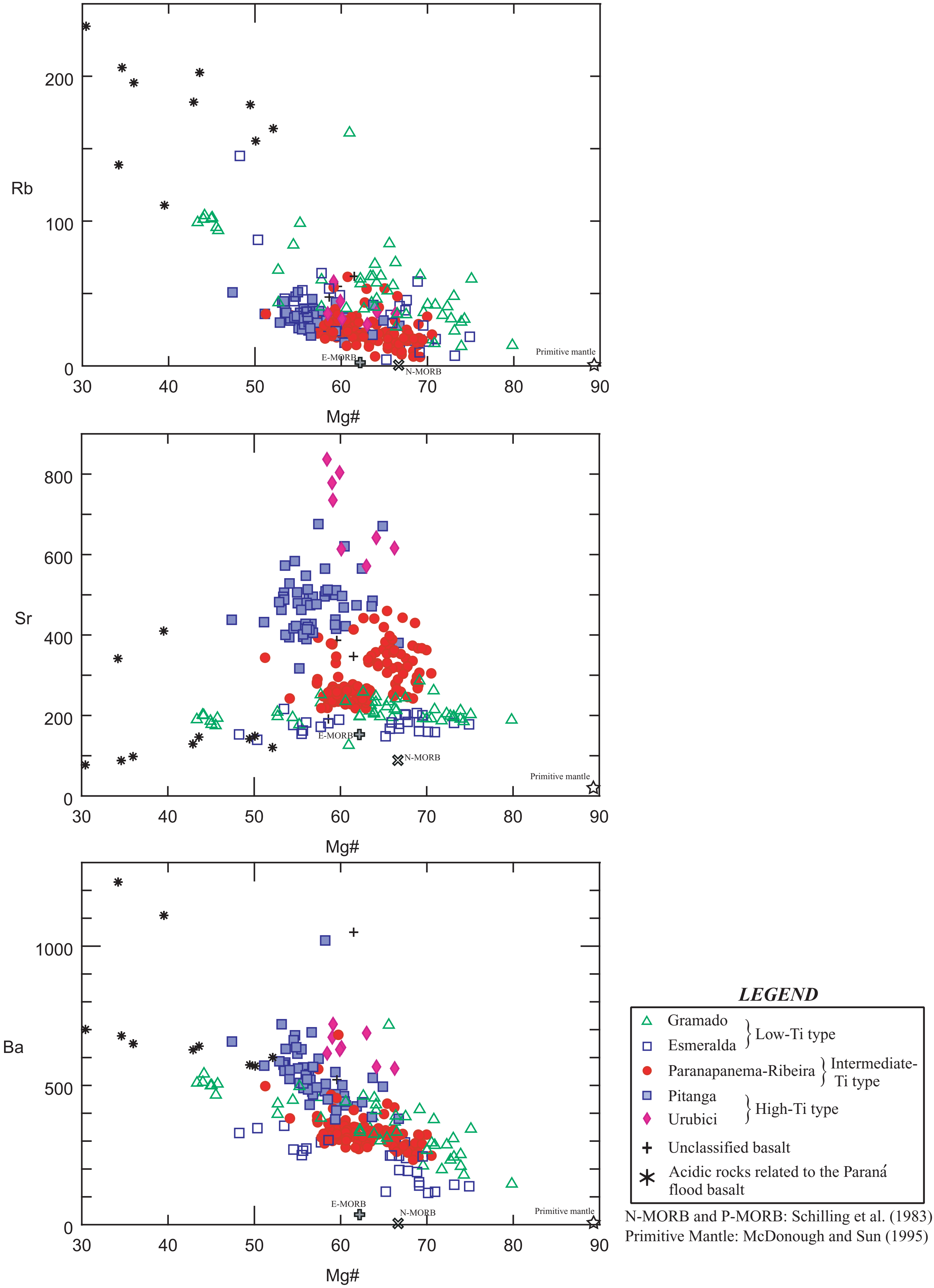

Fig. II-3-3-9 Mg number vs.Rb, Sr and Ba diagrams for lava samples

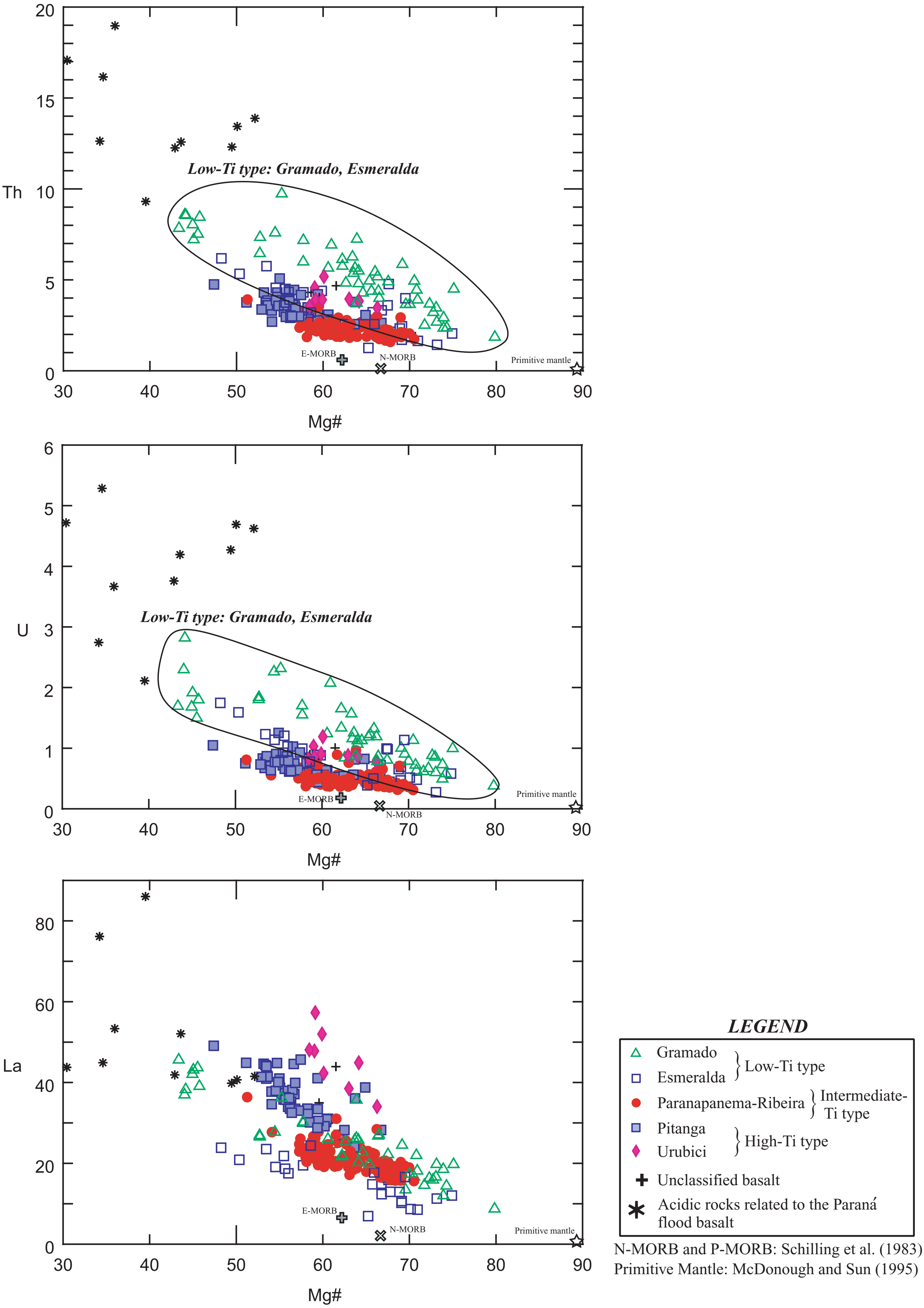

Fig. II-3-3-10 Mg number vs.Th, U and La diagrams for lava samples

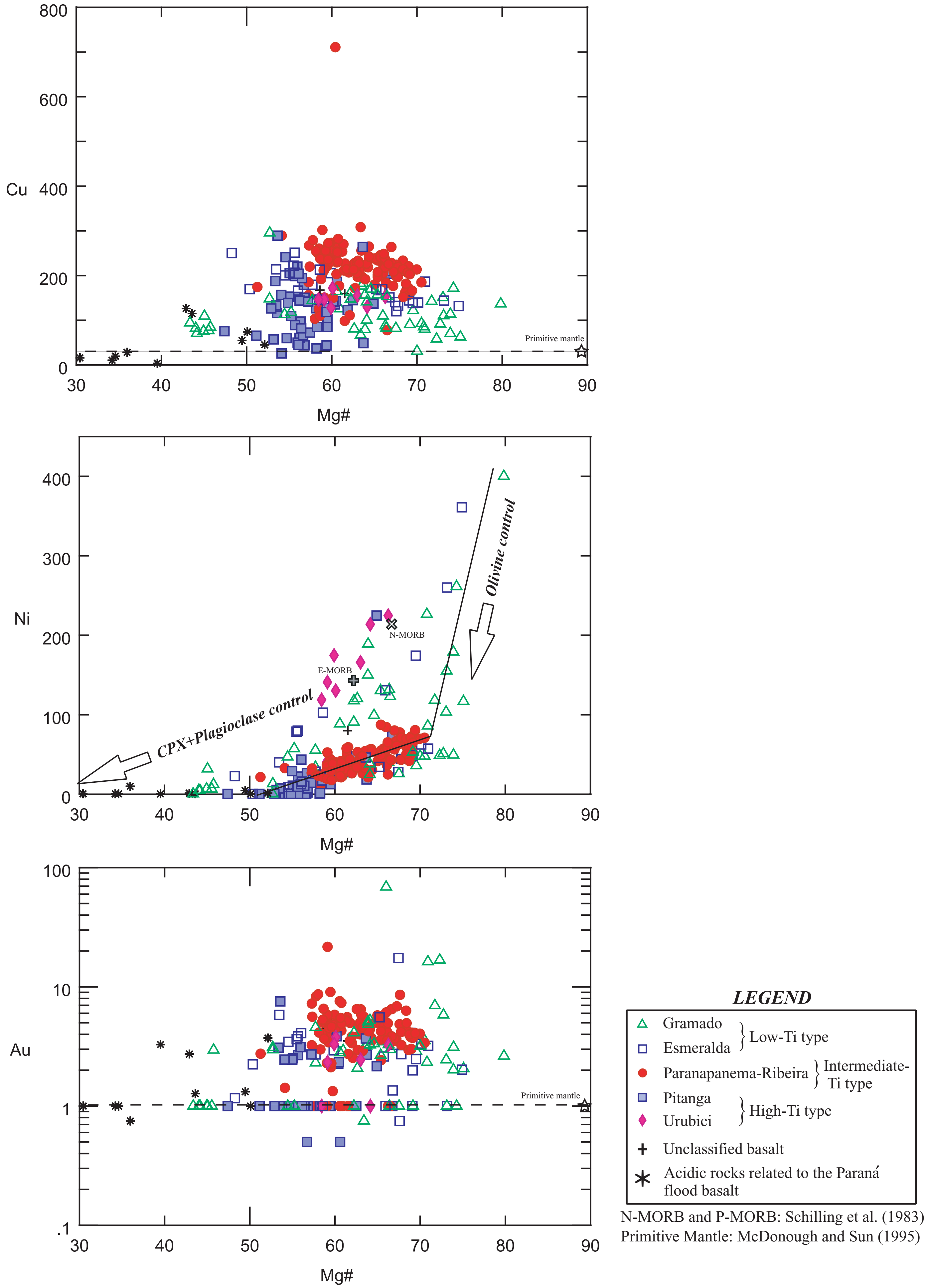

Fig. II-3-3-11 Mg number vs. Cu, Ni and Au diagrams for lava samples

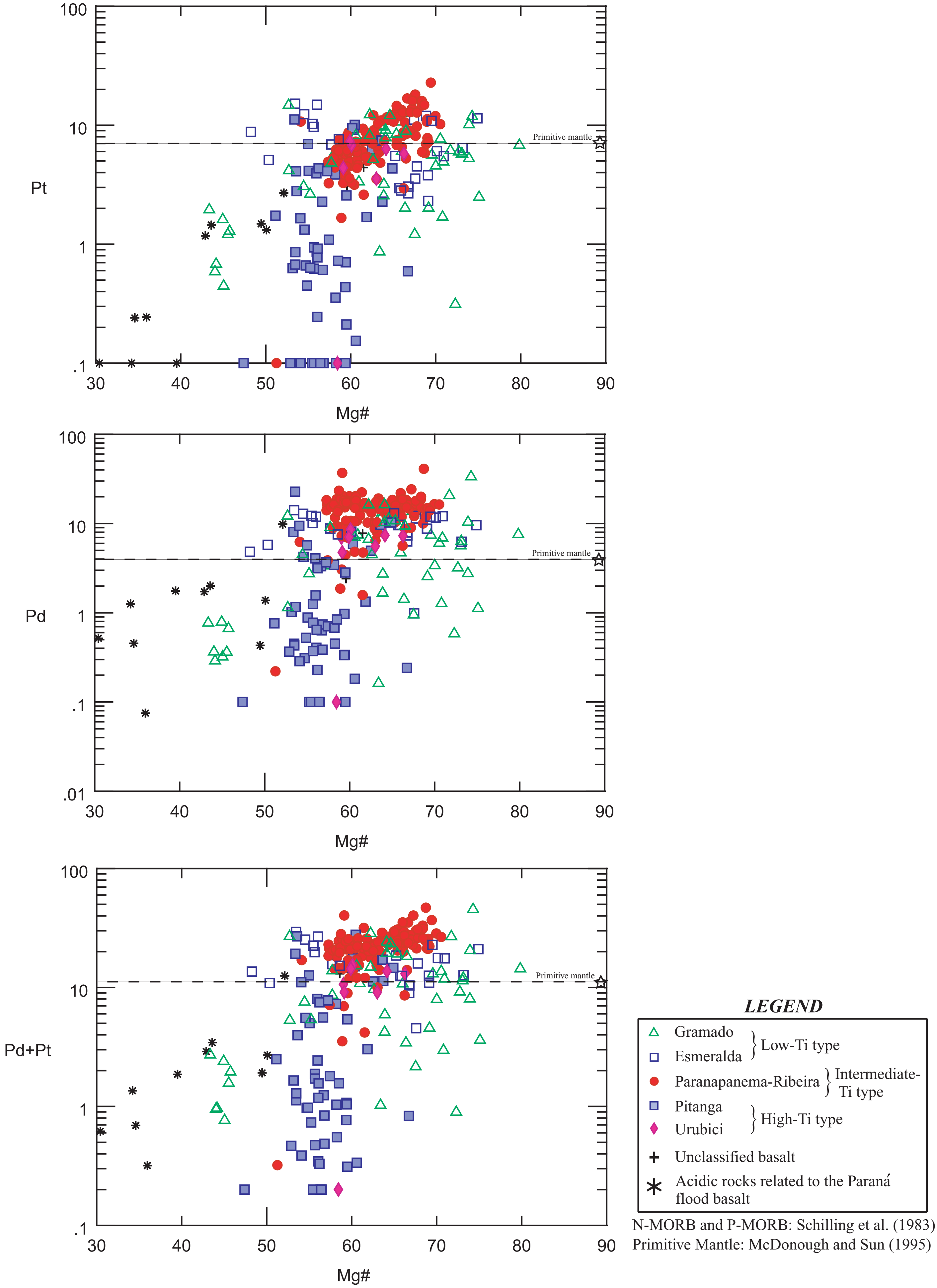

Fig. II-3-3-12 Mg number vs.Pt, Pd and Pt+Pd diagrams for lava samples

as high as or even higher than those in the lava distributed around Noril'sk deposit outskirts (Brugman et al.,1993; Tuklonsky Pt: 9.0-13.0 ppb, Pd: 9.0-13.0 ppb). Meantime, Paranapanema-Ribeira shows the trend that the quantity of Pt decreases by the progress of differentiation.

Low-Ti type Esmeralda and high-Ti type Urubicí show comparatively high Cu, Pt, Pd values, which are, however, lower than those contained in Paranapanema-Ribeira.

Pitanga, high-Ti type magma, and Gramado, low-Ti type magma, show Rb, Pt, and Pd values in a wide range of fluctuations irrespective of differentiation; some samples show little Cu, Pt, and Pd while other samples are rich with them in the same manner as Paranapanema-Ribeira.

(6) Spacial Distribution of Trace Elements (Siderophile Elements and Chalcophile Elements)

Spacial distribution of quantities of Cu, Au, Pt, and Pd which are contained in lava and intrusive rock samples were studied. Threshold values used for plotting on drawings were determined from the histogram of the elements (Fig. II-3-3-13) and the accumulative frequency distribution curve (Fig. II-3-3-14).

Characteristics of Cu (Fig. II-3-3-15)

Samples containing much Cu (200-350 ppm) were found in Paranapanema-Ribeira of intermediate-Ti type magma in the central area of Paraná basin. Samples of more than 350 ppm were collected from Ponta Grossa Arch dyke and lava in the center of Paraná basin.

Characteristics of Au (Fig. II-3-3-16)

Samples in general showed low Au content. There was no group which showed apparently anomaly values. Samples showing more than 18 ppb were collected from sill in the northeast part of Paraná basin, dyke in Ponta Grossa Arch, and lava in the central part and southeastern part of Paraná basin.

Characteristics of Pt (Fig. II-3-3-17)

Samples showing more than 7.5 ppb are scattering in whole Paraná basin areas where all the magma types are distributed. Samples showing more than 13 ppb are concentrated around the dyke in Ponta Grossa Arch, and the central part of Paraná basin. High Pt content is observed in Paranapanema-Ribeira of intermediate-Ti type. Samples exceeding 13 ppb were also collected from Pitanga, high-Ti type, and Gramado, low-Ti type.

Characteristics of Pd (Fig. II-3-3-18)

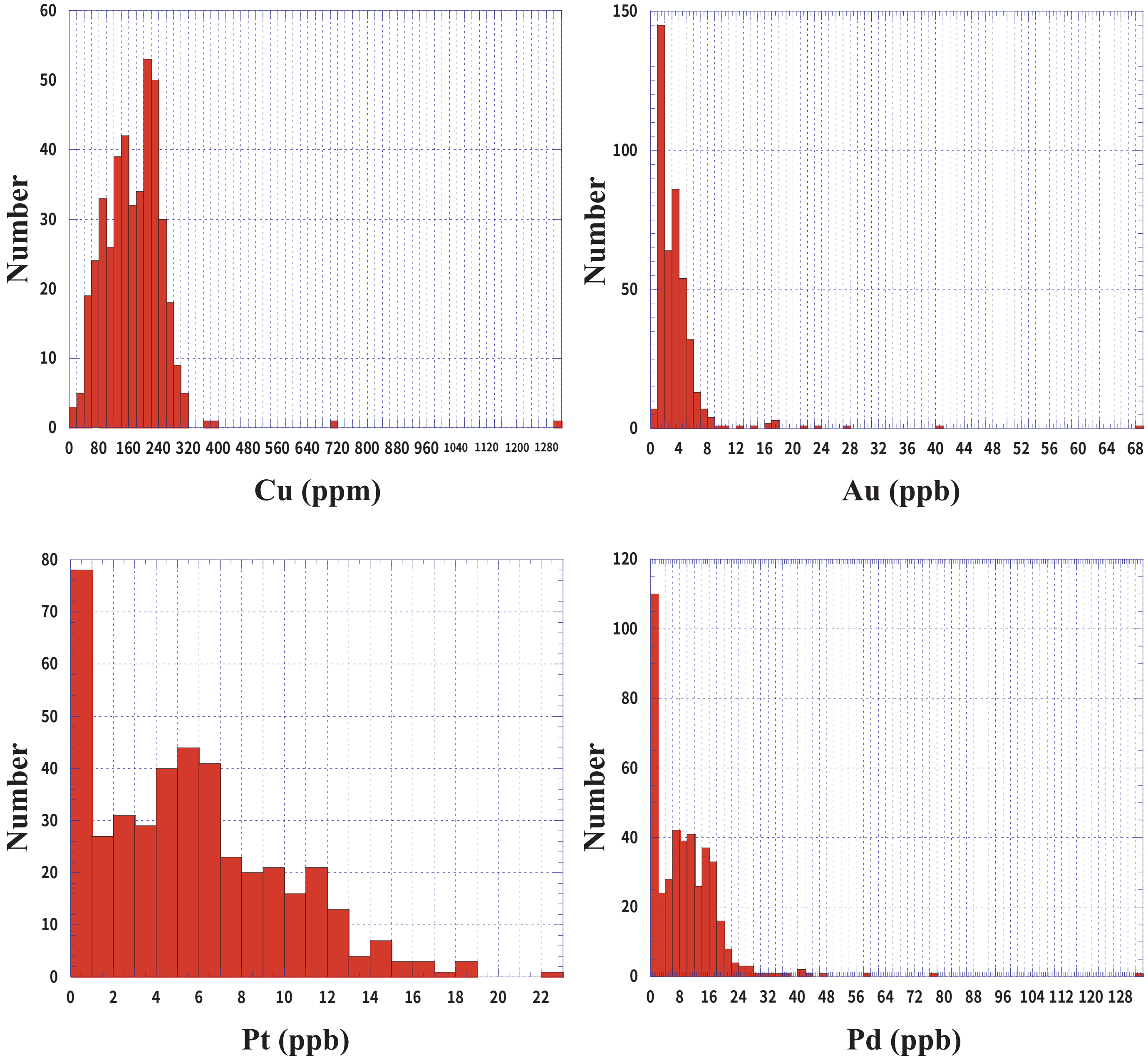

Fig. II-3-3-13 Histograms of Cu, Au, Pt and Pd contents for lava and intrusion of Parana flood basalt

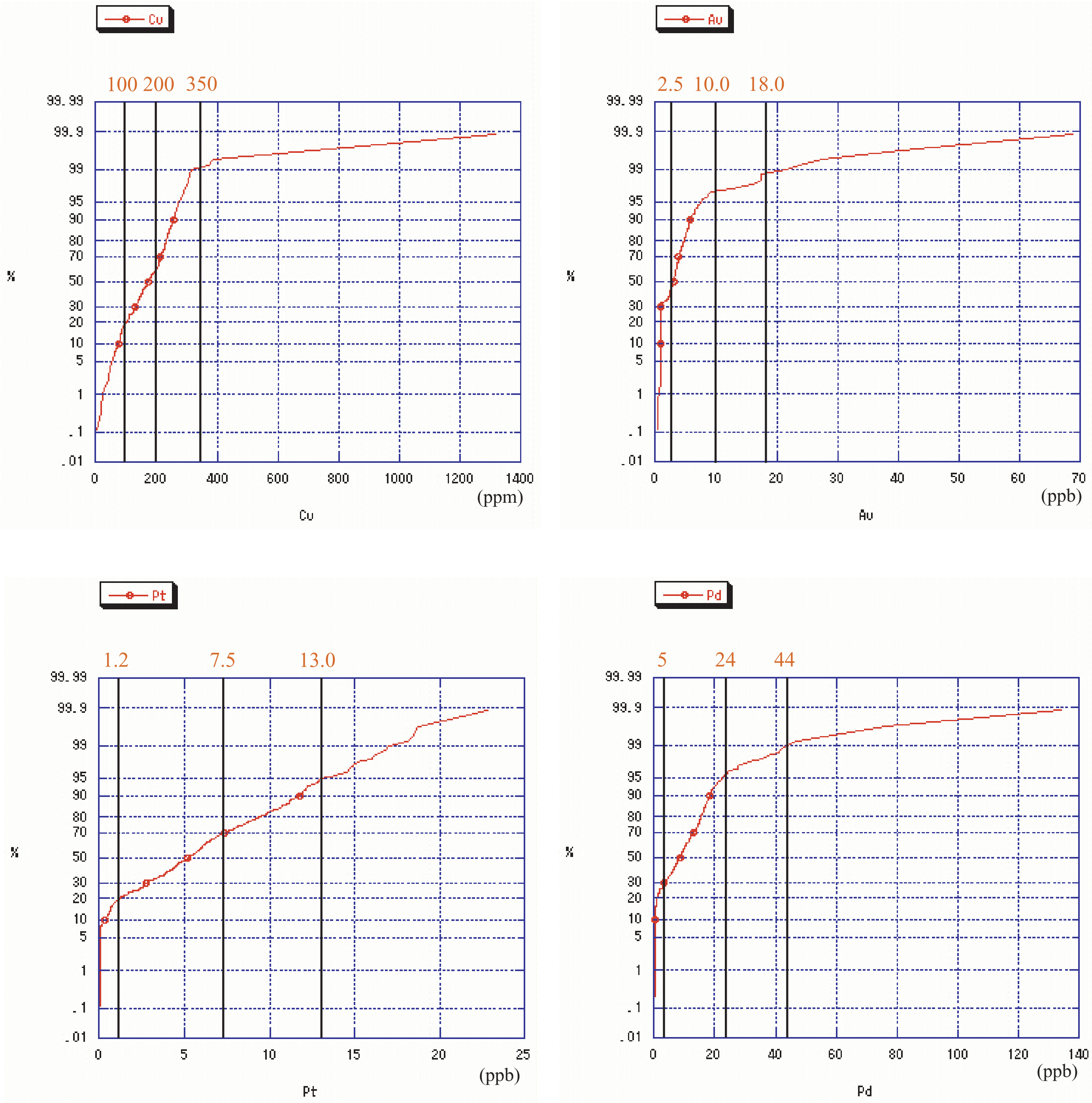

Fig. II-3-3-14 Decision of thresholds by accumulation frequency curve of transition and noble elements for lava and intrusion

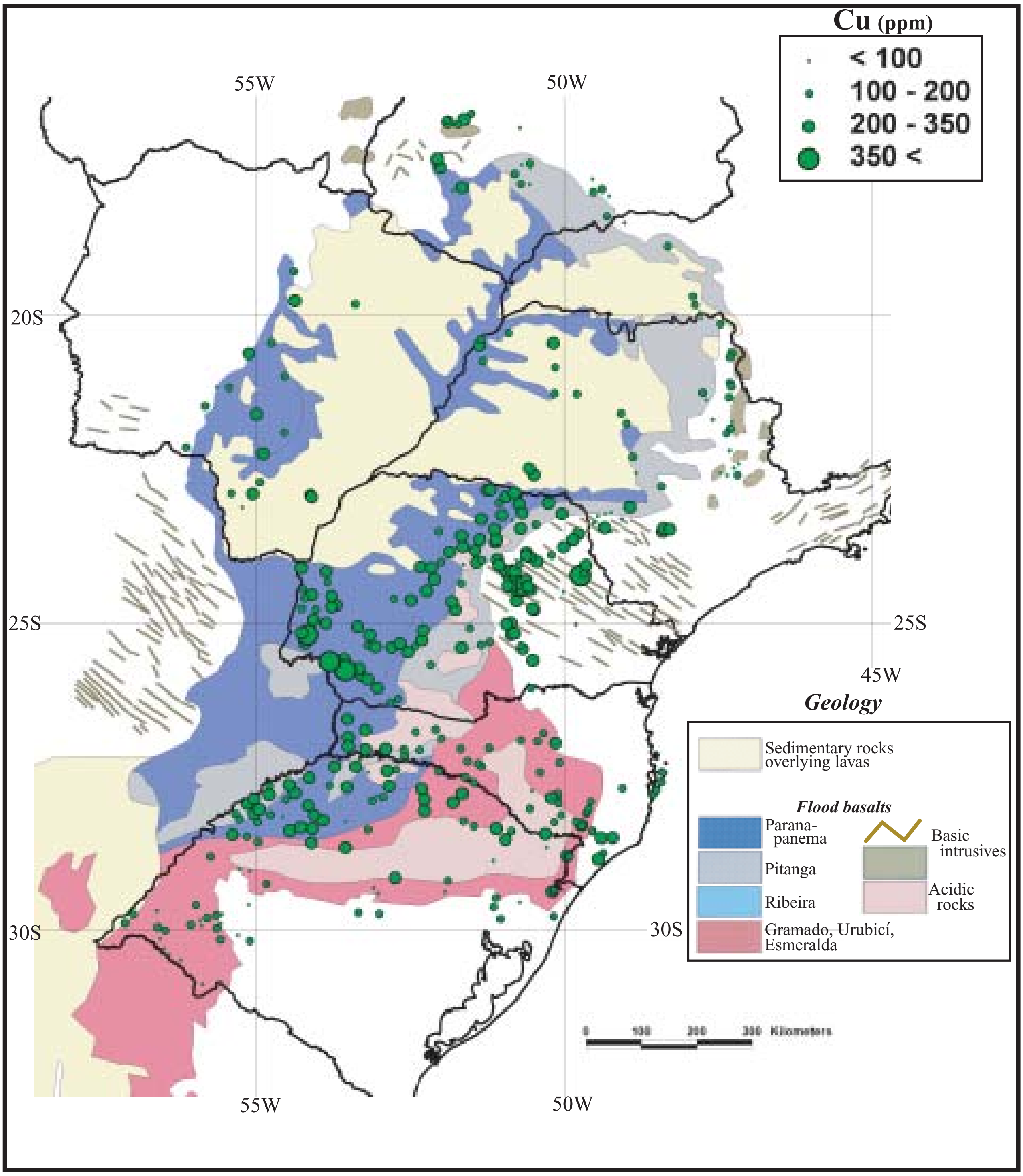

Fig. II-3-3-15 Distribution map of Cu contents of lava and intrusion samples in the Parana flood basalts

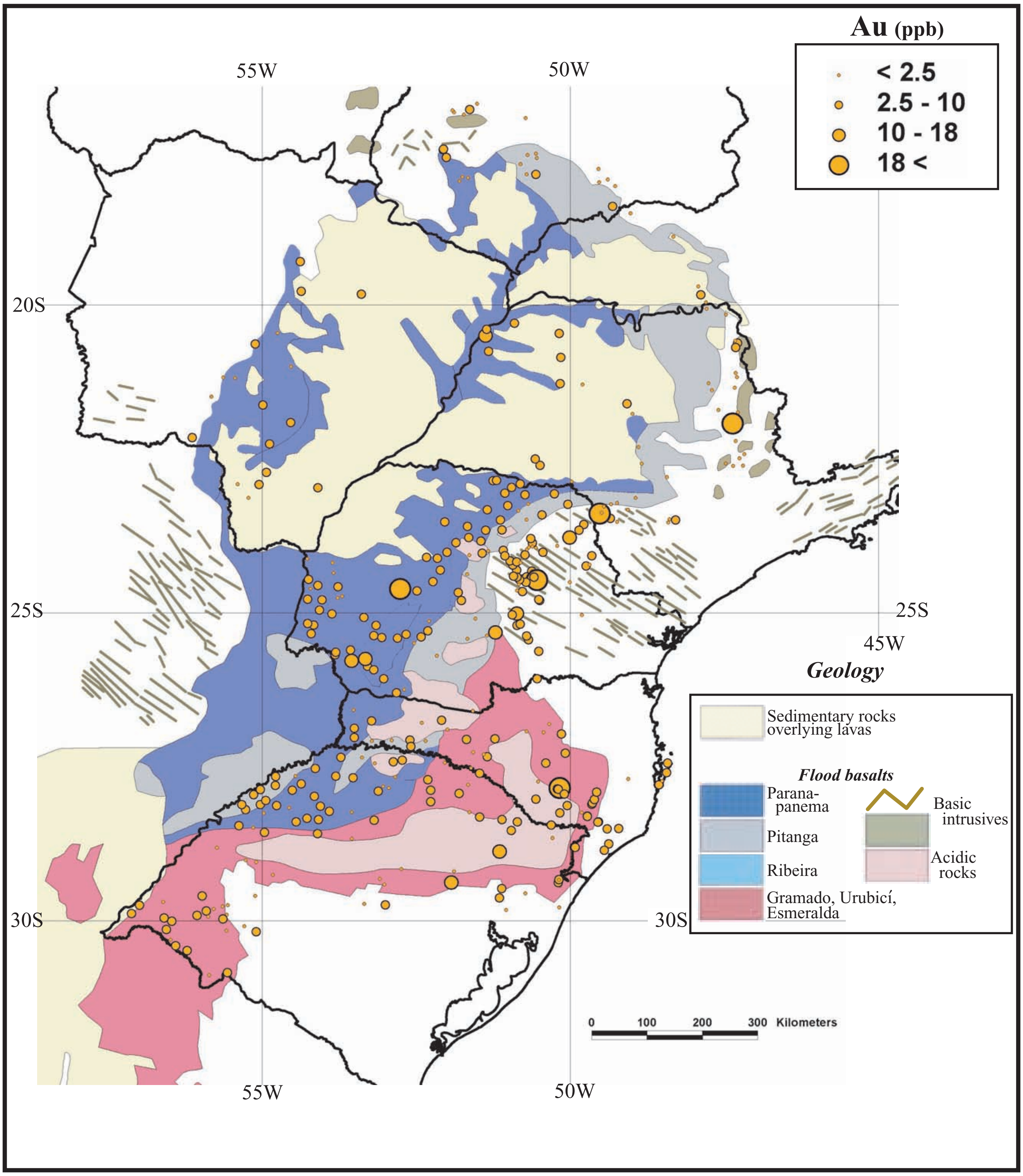

Fig. II-3-3-16 Distribution map of Au contents of lava and intrusion samples in the Parana flood basalts

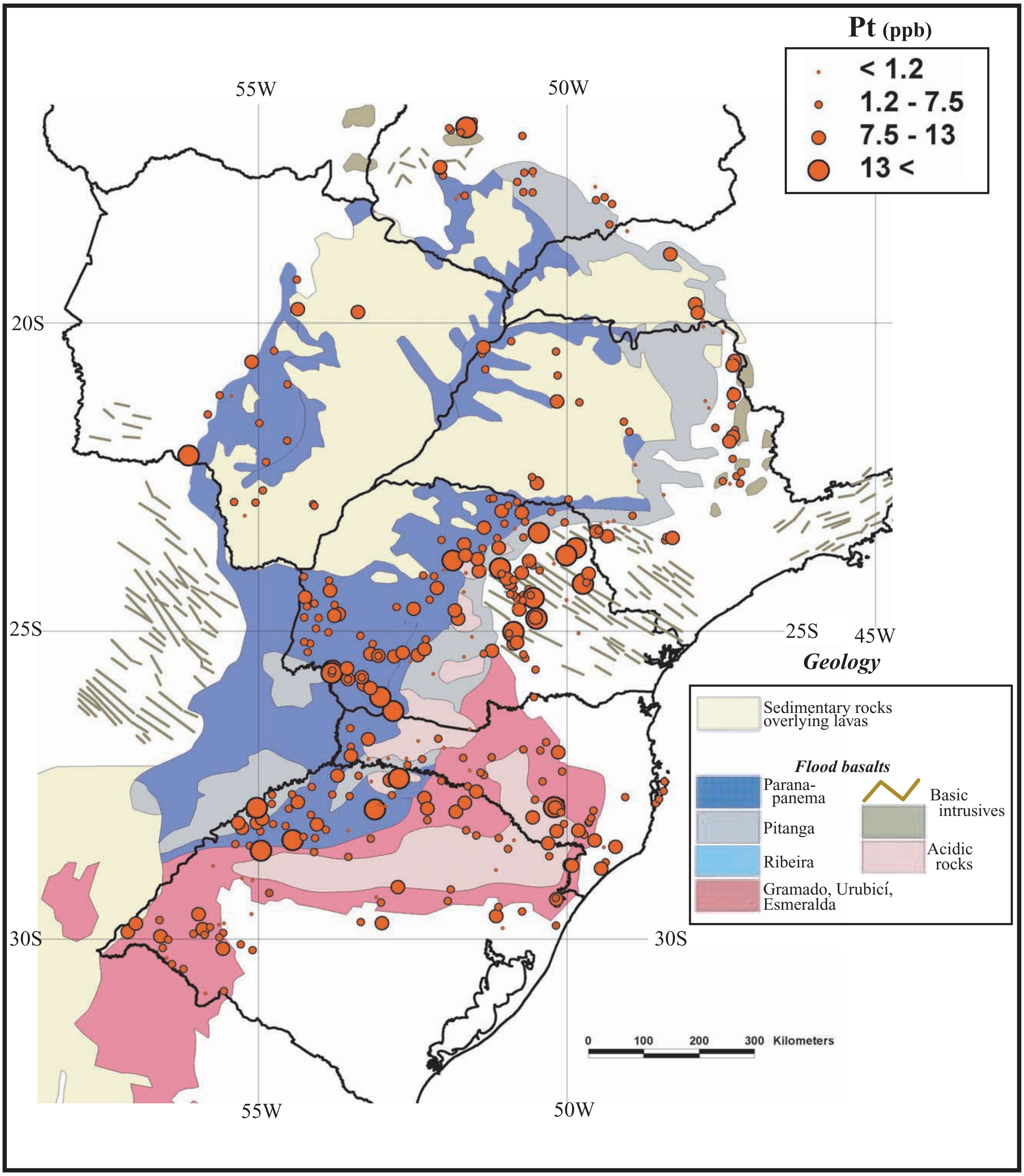

Fig. II-3-3-17 Distribution map of Pt contents of lava and intrusion samples in the Paraná flood basalts

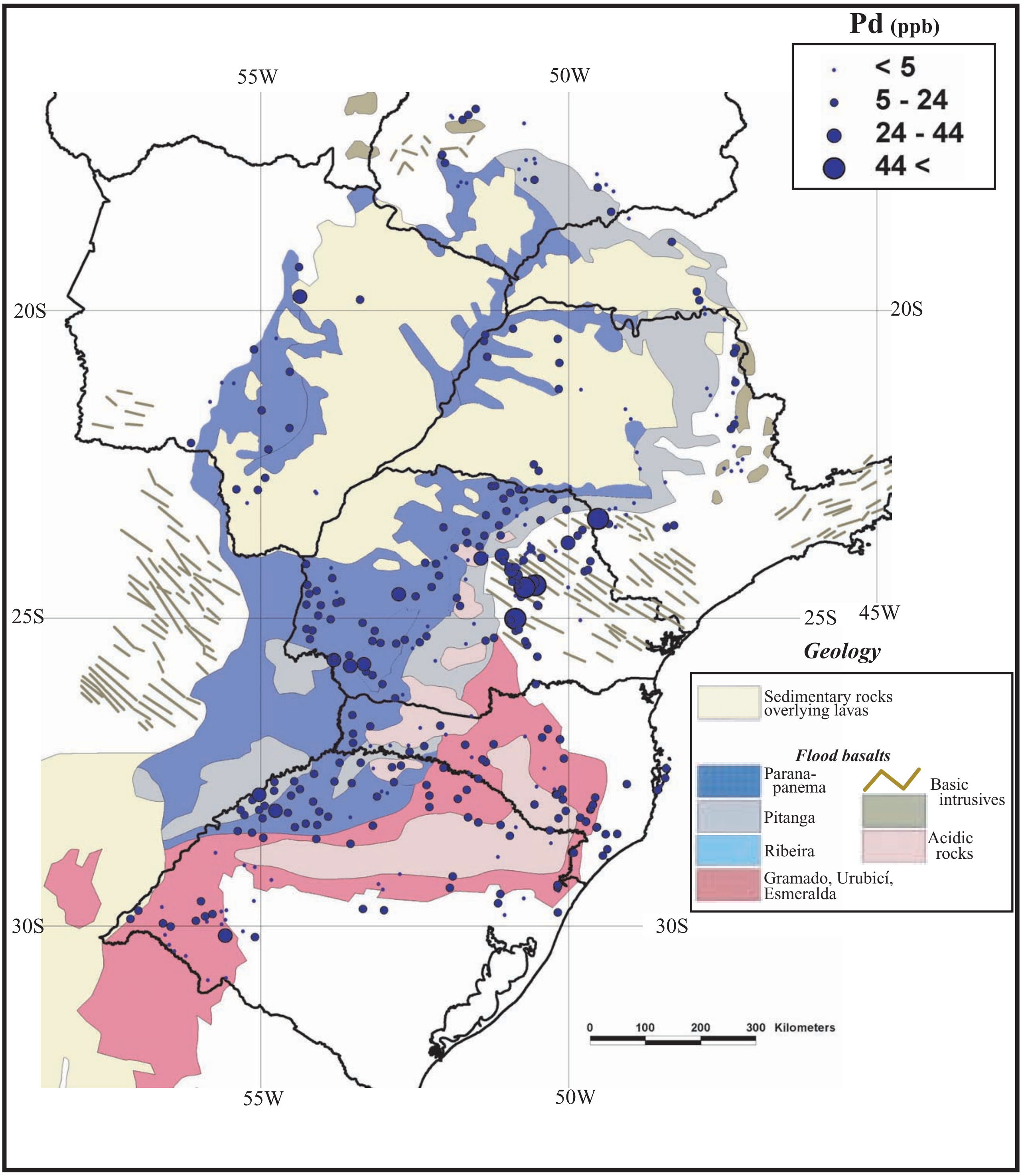

Fig. II-3-3-18 Distribution map of Pd contents of lava and intrusion samples in the Paraná flood basalts

Samples showing more than 24 ppb are distributed in the dyke in Ponta Grossa Arch, the central part and southwestern part of Paraná Basin. This distribution agrees with that of Paranapanema-Ribeira of intermediate-Ti type magma. Particularly, samples exceeding 44 ppb were gathered from dyke in Ponta Grossa Arch.

Distribution of the samples showing high Cu, Au, Pt, and Pd values concord with that of Paranapanema-Ribeira of intermediate-Ti type magma. Particularly high values are observed in dyke group area in Ponta Grossa Arch and the central part of Paraná basin.

(7) Features of Rare Earth Elements

Samples having content values closest to the average content value of the elements are chosen for each magma types. The resulting values of analysis are standardized by chondrite, undifferentiated mantle, N-MORB and E-MORB, and spider diagrams were drawn (Fig.II-3-3-19).

In all spider diagrams, magma of high, intermediate and low-Ti types were clearly divided into three different categories classified by standardized values. Urubicí of high Ti type is the richest and Esmeralda of low-Ti type the poorest in trace elements. All magma types show curves each trending downward on the right side. The contents of HREE (heavy rare earth elements: Dy, Ho, Er, Tm, Y, Yb, Lu) are nearly the same in all magma types. Urubicí tends to decrease largely in standardized values of HREE. On the LREE (light rare earth elements) side, on the other hand, the standardized values vary widely among magma types. This feature is important characteristics of melt by partial melting occurring with garnet existing as residue. Consequently, the difference in LREE contents may reflect a difference in the degree to which such partial melting takes place.

In spider diagrams drawn with incompatible elements standardized by primitive mantle, N-MORB and E-MORB, a negative anomaly of Nb was seen in all magma types. This shows the fact that Paraná Flood Basalt was formed from sources more exhausted of Nb than in the case of oceanic basalt like MORB. From this it will be seen that the place where magma was formed is obviously different than in the case of oceanic basalt. In Pitanga and Urubicí of high-Ti type magma, a positive anomaly of Ba was observed. As in the case of Nb this fact may suggest a different source contributing than in the case of intermediate or low-Ti type magma.

In magma types other than those of Intermediate-Ti type, a positive anomaly of Pb was observed. Particularly low-Ti type magma Gramado shows a Pb value remarkably higher than other magma types. This fact reflects some features of the source and suggests that an influence was exercised by the assimilation of materials like granite constituting the upper crust.

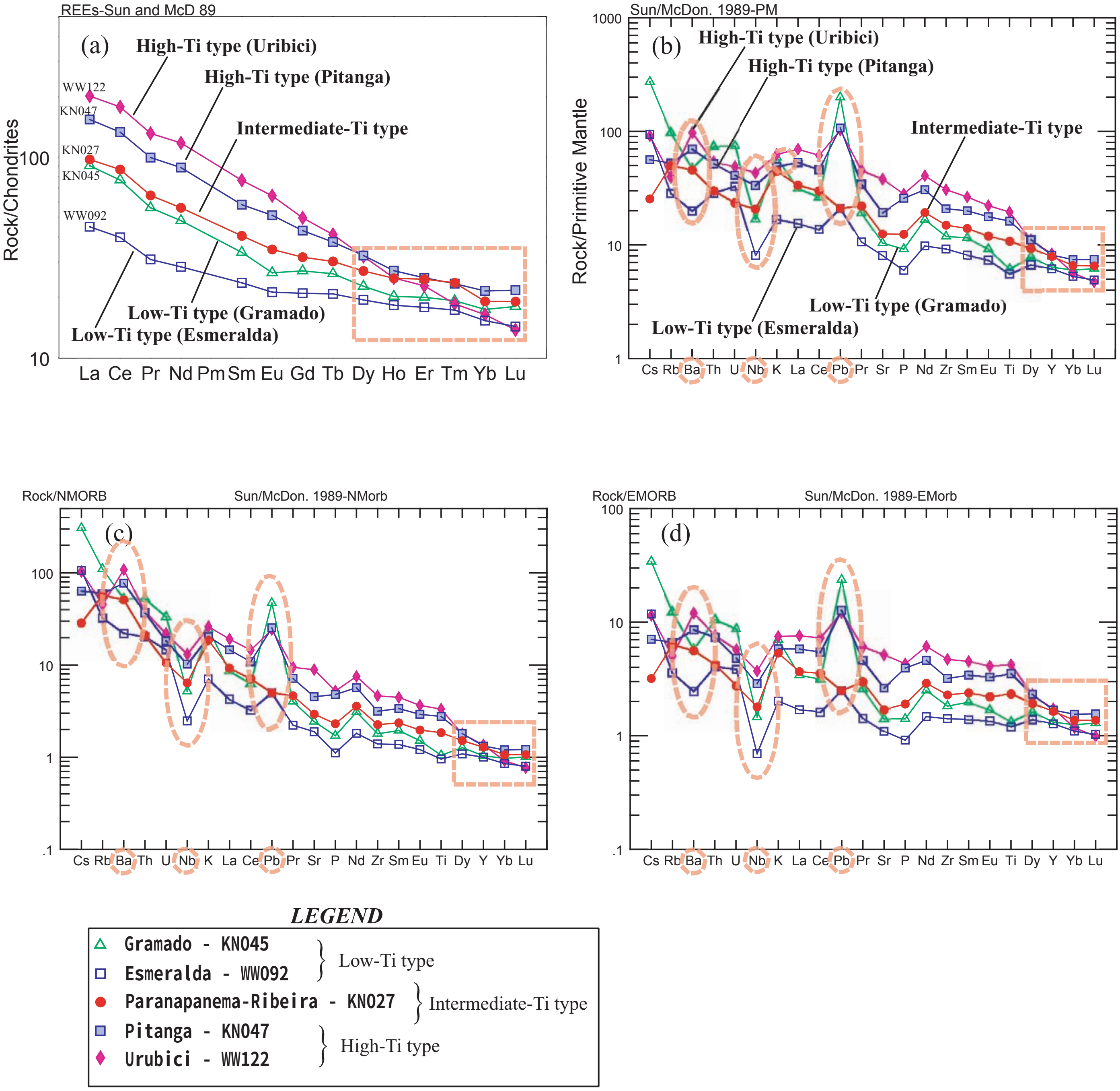

(a) chondrites-nomalized rare earth elements; (b) primitive mantle-nomalized trace elemens; (c) N-MORB-normalised trace elements, (d) E-MORB-normalized trace elements.

Fig.II-3-3-19 Spider diagrams of trace elements for lava samples

(8) Features of Isotopic Ratio

$^{87}Sr/^{86}Sr$ ratio, $^{143}Nd/^{144}Nd$ ratio, Mg# and $^{87}Sr/^{86}Sr$ ratio and $^{143}Nd/^{144}Nd$ ratio are plotted in a diagram (Fig.II-3-3-20) and the results of calculation for isotope ratios of Sr and Nd are given at Appendix.

One sample of the low Ti type magma Pitanga, which shows an abnormally high $^{143}Nd/^{144}Nd$ ratio and is excluded from discussion.

On the diagram, magma types are roughly divided into two groups, one with a relatively low $^{87}Sr/^{86}Sr$ ratio and with a little high $^{143}Nd/^{144}Nd$ ratio and the other with a relatively high $^{87}Sr/^{86}Sr$ ratio and with a little low $^{143}Nd/^{144}Nd$ ratio. The former are high-Ti type magma Urubicí and Pitanga, Intermediate-Ti type magma Paranapanema-Ribeira and a part of low-Ti type magma Esmeralda. The latter is the part of the low-Ti type magma Esmeralda and Gramado.

It is thought that the difference in $^{87}Sr/^{86}Sr$ ratio has been caused by the effect of contamination of crust materials like sedimentary rocks abounding in Rb. It may be said that such contamination of the crust exercises a greater influence on the low-Ti type magma than on other magma types. Gramado in particular shows a high $^{87}Sr/^{86}Sr$ ratio in all samples, from which one may deduce a large contamination of the crust material.

Pitanga and Urubicí of high-Ti type and Paranapanema-Ribeira of Intermediate-Ti type show $^{143}Nd/^{144}Nd$ ratio similar to each other, indicating a high probability that they might have been formed from one and the same source. Esmeralda of low-Ti type, however, shows a high $^{143}Nd/^{144}Nd$ compared with other magma types, presenting features close to those of oceanic basalt.

(9) Vertical Geochemical Variations for the Lava Samples

Peate et al. (1992) drew vertical profiles of some magma types, using samples taken during the drilling conducted by PETROBRAS (See Fig.II-3-1-5). In the present survey, cuttings were taken during drilling for underground water and, in analogy with Peate et al. (1992), an attempt was made to grasp vertical distributions of magma types and vertical variations in content of various elements. The locations of the drilling sites used for sampling are shown in Fig.II-3-2-2.

(i) RP-3 hole (Fig.II-3-3-21 – II-3-3-24)

<u>Location</u>

The drilling site is located in the north of Paraná Basin and is surrounded by widely distributed sedimentary rocks produced after the activities of Paraná Flood Basalts and the like.

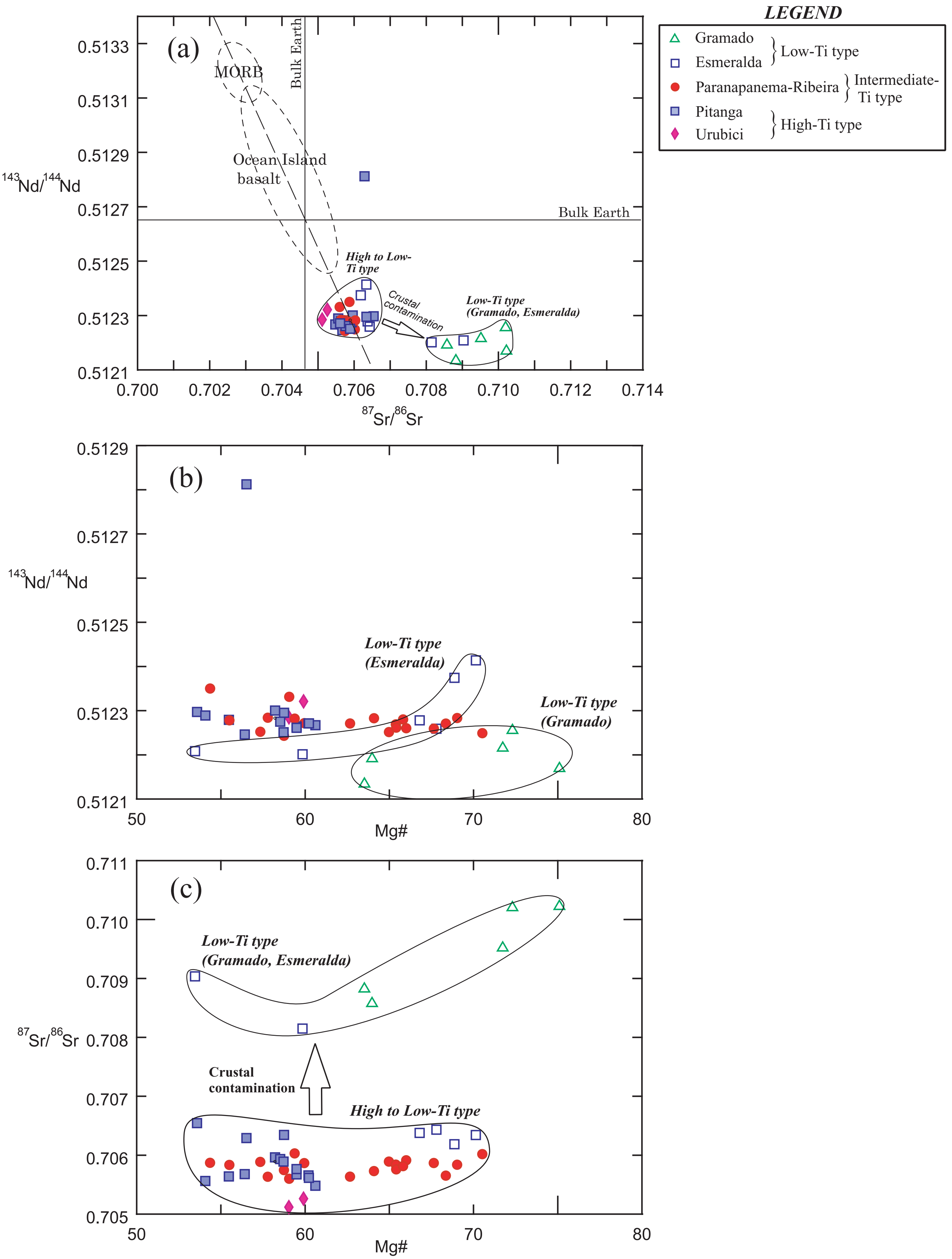

Fig. II-3-3-20 Plots of $^{87}Sr/^{86}Sr$ ratio and $^{143}Nd/^{144}Nd$ ratio for lava samples

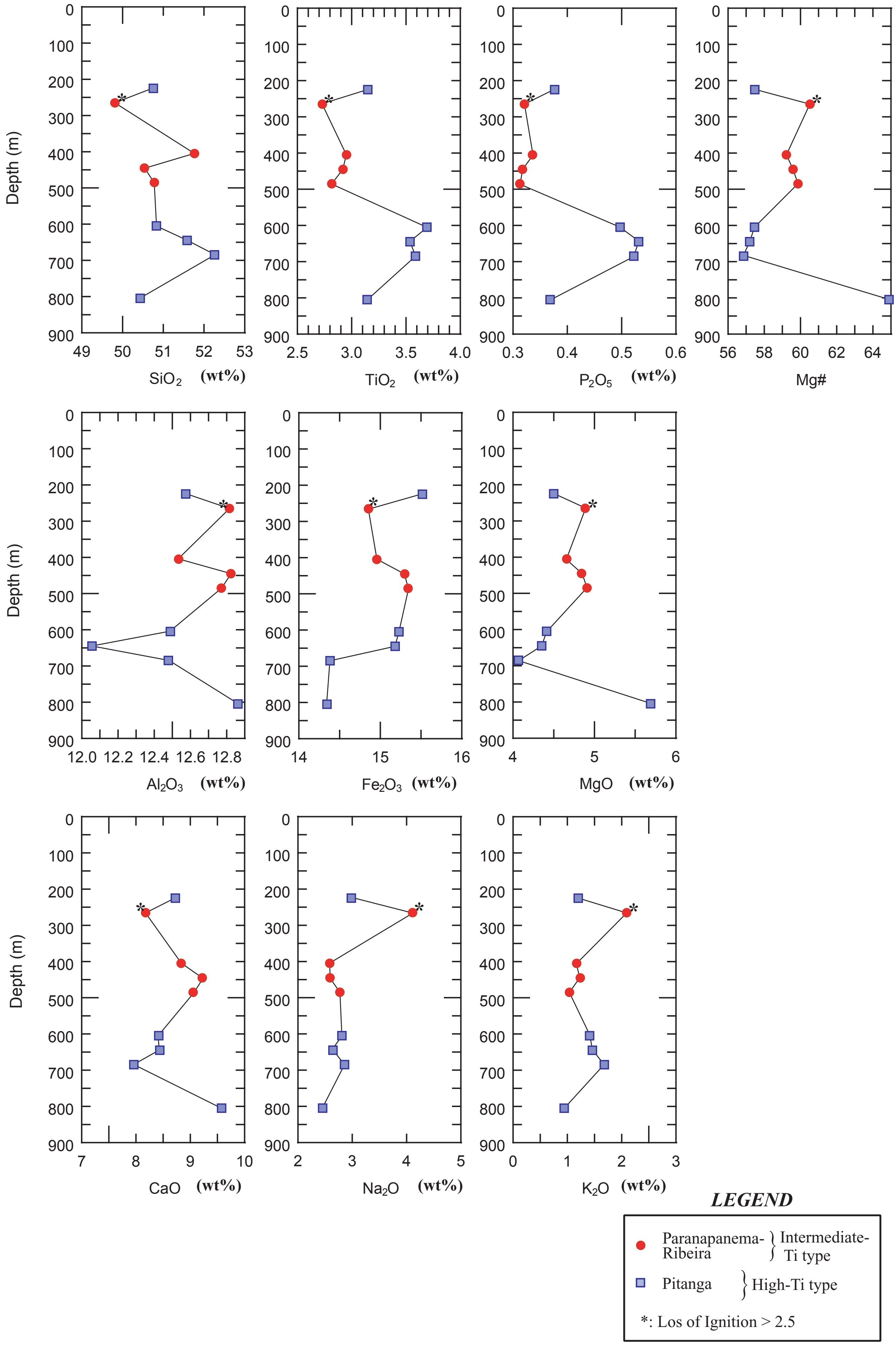

Fig. II-3-3-21 Vertical variations of major elements in lava samples (drill hole: RP-3)

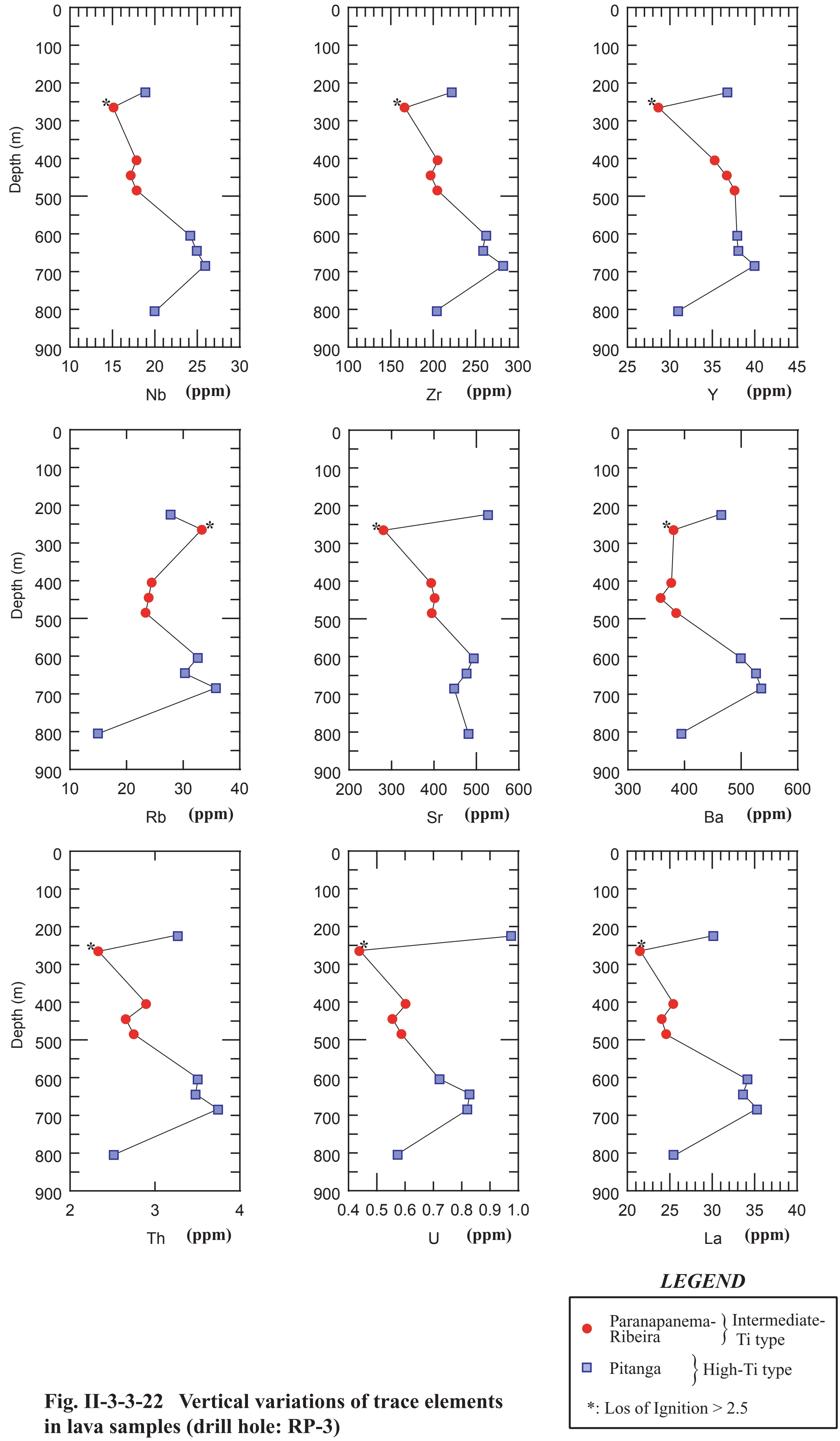

Fig. II-3-3-22 Vertical variations of trace elements in lava samples (drill hole: RP-3)

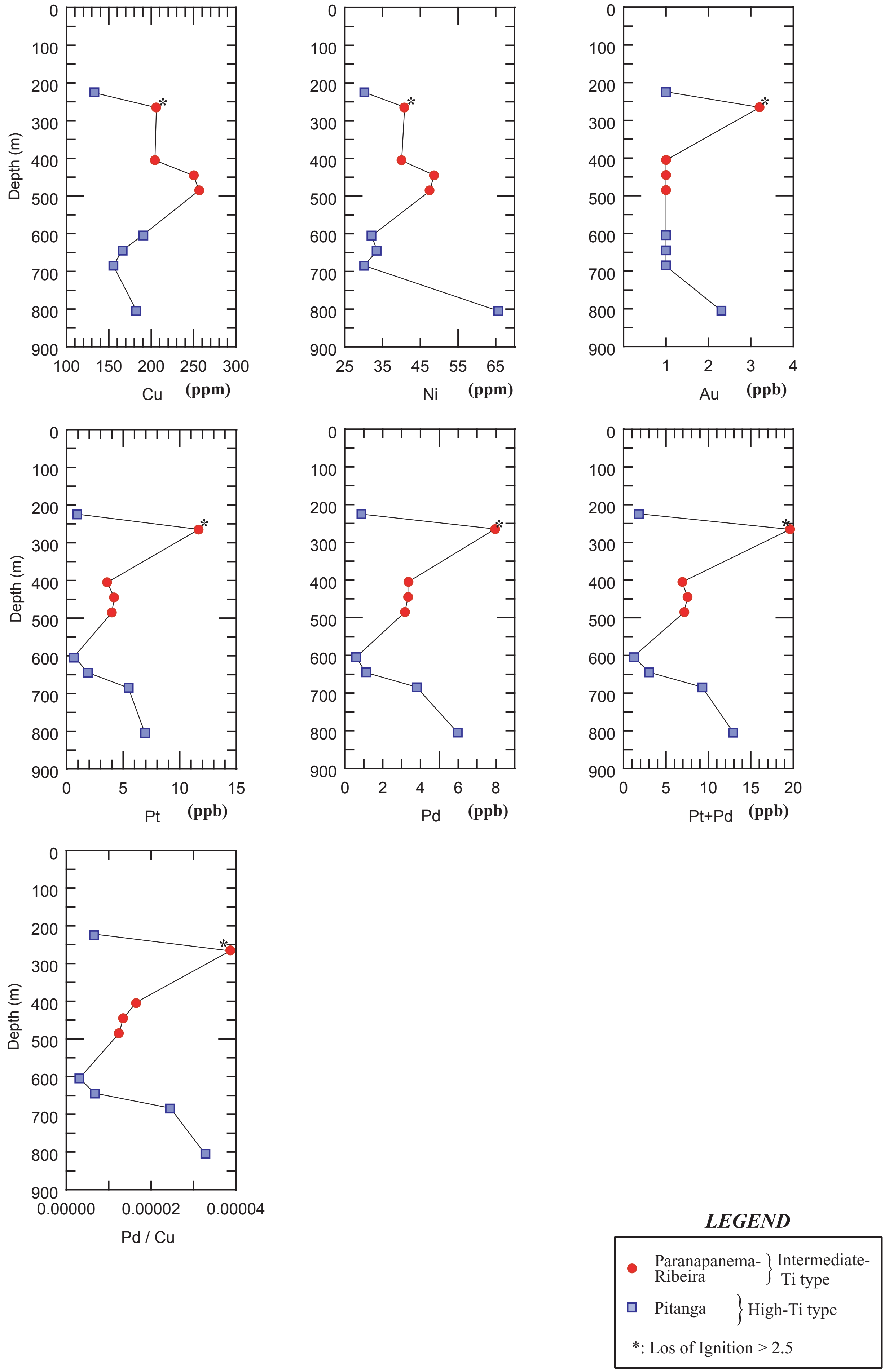

Fig. II-3-3-23 Vertical variations of transition and noble elements in lava samples (drill hole: RP-3)

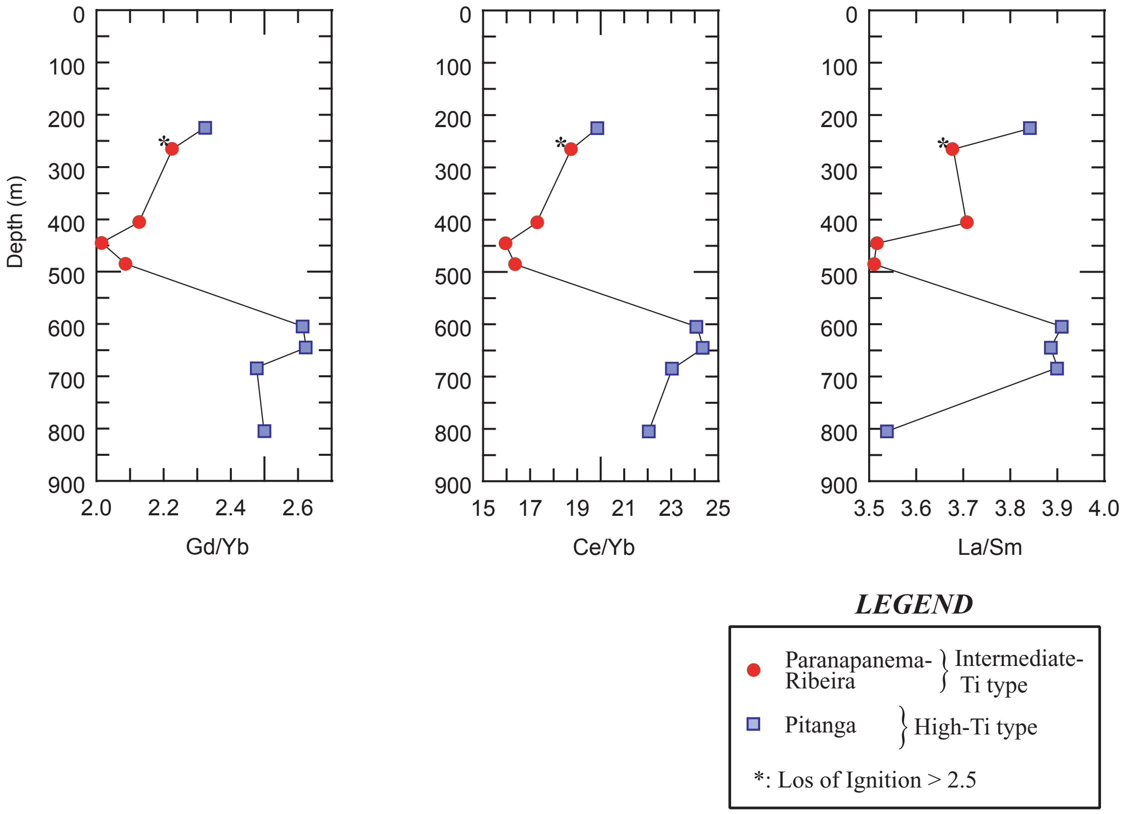

Fig. II-3-3-24 Vertical variations of the ratios of selected trace elements in lava samples (drill hole: RP-3)

The lava distributed on the surface is Paranapanema-Ribeira of Intermediate-Ti type.

Lava stratigraphy by geochemical classification

The depth of lava at the drilling site is about 800 m. The magma types distributed from bottom to top are high-Ti type magma Pitanga (stratum of about 250 m thick), Intermediate-Ti type magma Paranapanema-Ribeira (stratum of about 300 m thick), and high-Ti type magma Pitanga (stratum of less than about 25 m thick). Apparently the Intermediate-Ti type magma Paranapanema-Ribeira is existed between two layers of Pitanga lava, a high-Ti type magma. This is thought to be due to the fact that in the north of Paraná Basin, there were activities of Pitanga and Paranapanema-Ribeira during nearly the same period.

Variations in chemical composition

The Pitanga lava at the bottom, compared with the one above it (about 700 m underground), shows high Mg# and Ni values (Fig.II-3-3-21, II-3-3-23). It is characterized by a low SiO_2・TiO_2 content, a high Mg# content and scarcity of incompatible elements like Nb, Zr, Y, Th and U. This may indicate the fact that during the initial phase of its activity there was an eruption of undifferentiated magma at first.

In the Pitanga lava 800 to 600 m depth, Pt and Pd contents tend to decrease as it is closer to the ground surface.

(ii) PP-2 hole (Fig.II-3-3-25 – II-3-3-28)

Location

The drilling site is located in the north and the central part of Paraná Basin where the lava layer is the thickest, surrounded by widely distributed sedimentary rocks produced after the activities of Paraná flood basalt and the like. The lava distributed on the surface is Paranapanema-Ribeira of Intermediate-Ti type.

Lava stratigraphy by geochemical classification

The lava is about 1600 m thick at the drilling point. The magma types distributed from bottom to top are low-Ti type magma Gramado (about 25 m), high-Ti type magma Pitanga (about 75 m), Intermediate-Ti type magma Paranapanema-Ribeira (about 75 m), high-Ti type magma Pitanga (about 250 m), and Intermediate-Ti type magma Paranapanema-Ribeira (less than about 575 m or so).

At the bottom of the lava, as reported by Peate et al. (1992), there is a distribution of a thin layer of lava of low-Ti type. Located above it are Pitanga of high-Ti type and Paranapanema-Ribeira of Intermediate-Ti type.

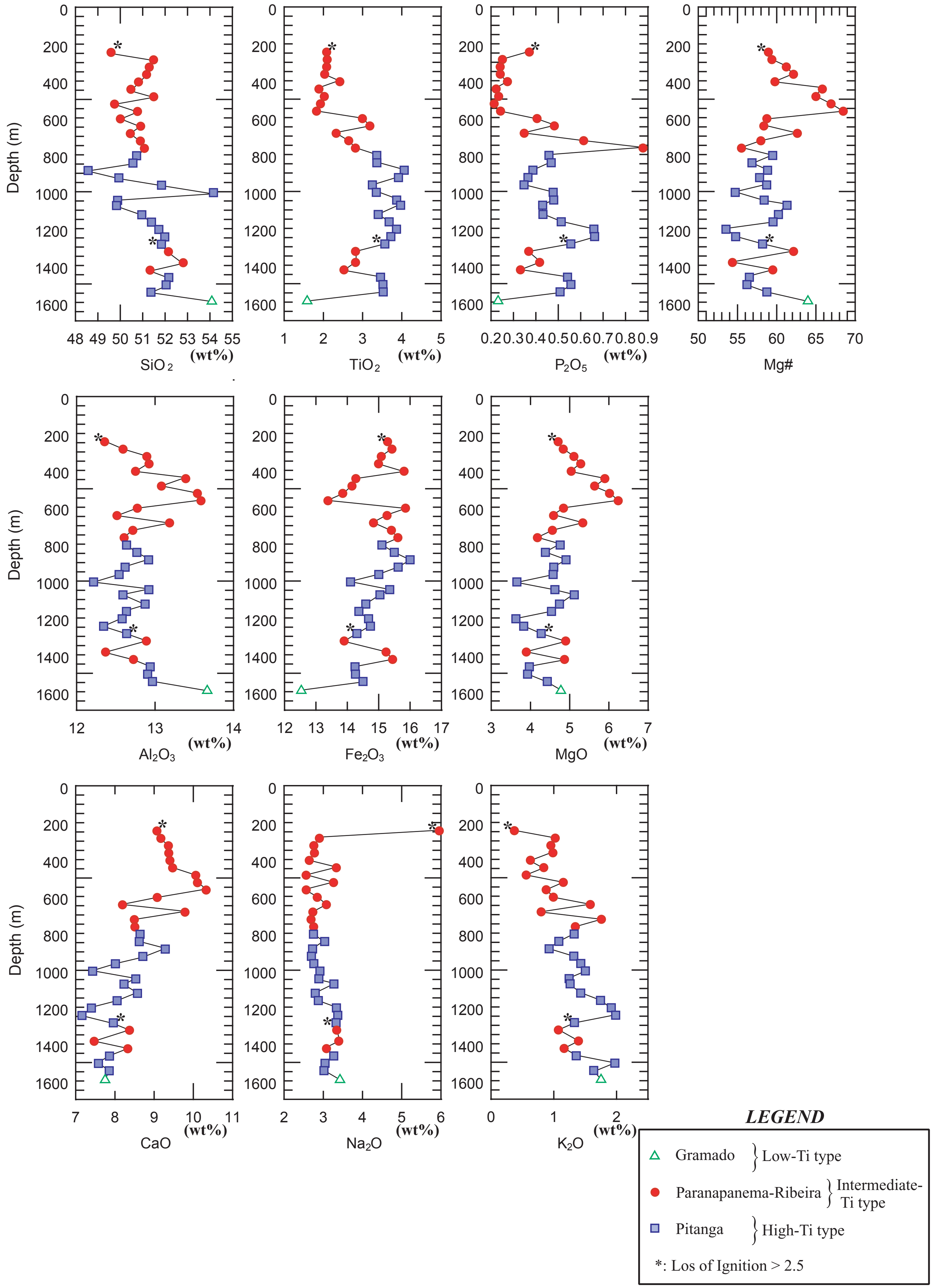

Fig. II-3-3-25 Vertical variations of major elements in lava samples (drill hole: PP-2)

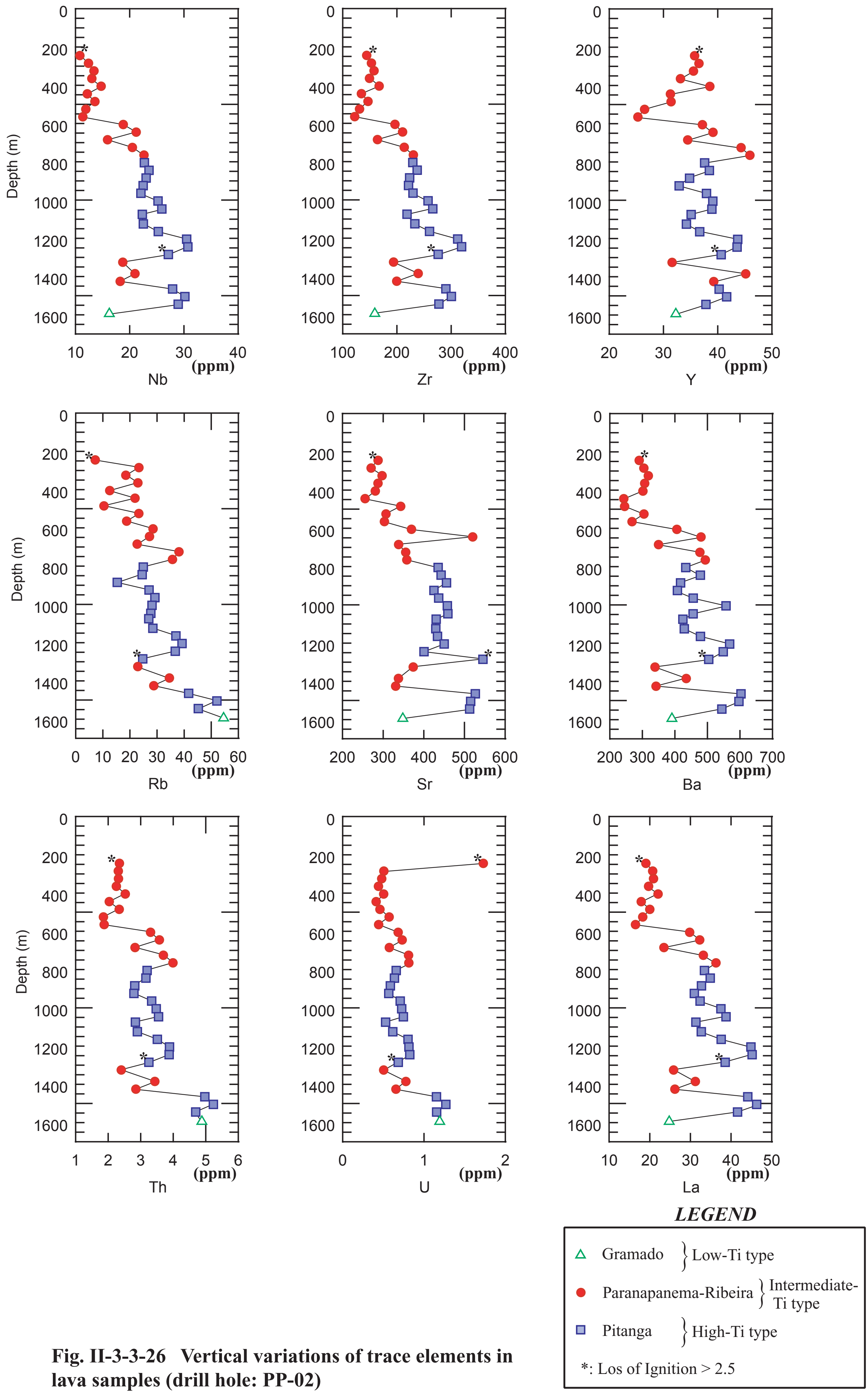

Fig. II-3-3-26 Vertical variations of trace elements in lava samples (drill hole: PP-02)

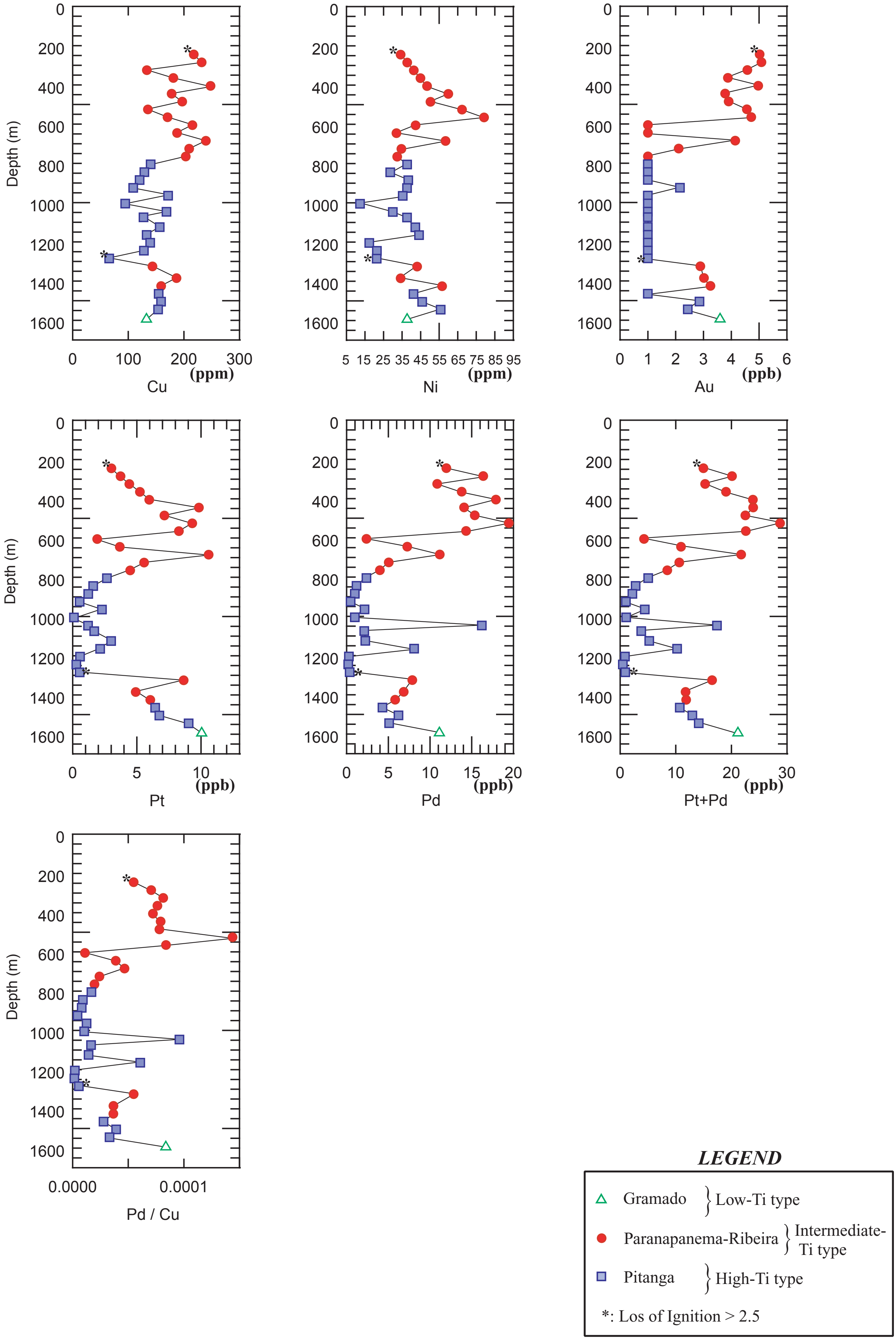

Fig. II-3-3-27 Vertical variations of transition and noble elements in lava samples (drill hole: PP-2)

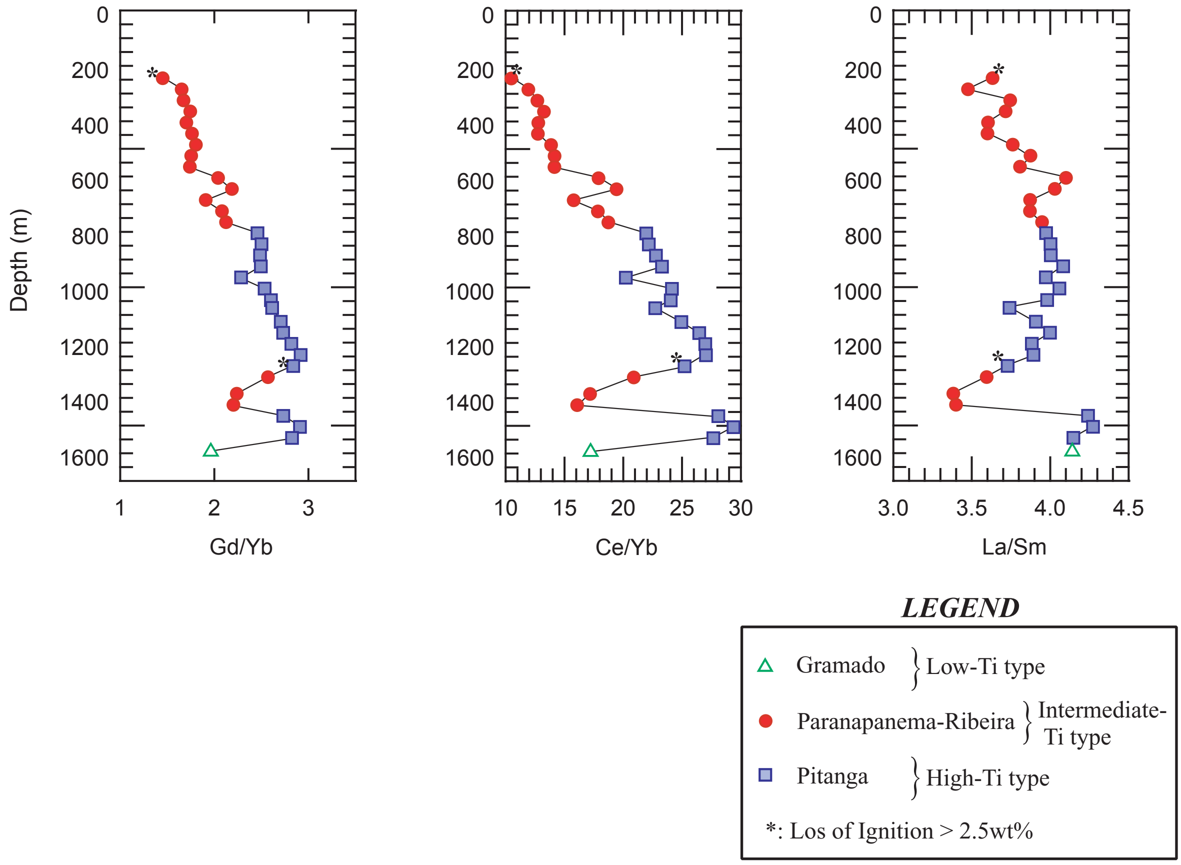

Fig. II-3-3-28 Vertical variations of the ratios of selected trace elements in lava samples (drill hole: PP-2)

Variations in chemical composition

An influence of crystallization-differentiation is clearly observed in the Intermediate-Ti type magma Parapanema-Ribeira located shallower than some 600 m underground where Mg# decreases continuously, which shows a progress of differentiation. A decrease in Al_2O_3 may indicate discrimination of plagioclase. Yet it is interesting that there is no change in the quantity of TiO_2 or P_2O_3, which should normally increase as the differentiation progresses. The quantities of Zr and Y tend to increase while there is not much change observed in Nb. A decrease in Ni is thought to indicate a differentiation of olivine. Pt and Pd show a trend to decrease continuously and it was confirmed that they are discriminated by crystallization-differentiation.

Gramado at the bottom and Pitanga above it tend to abound in Th and U. It is thought that they have been affected by a contamination of the crust material.

Apparently Paranapanema-Ribeira, a thin layer of Intermediate-Ti type, is existed between two layers of Pitanga lava, a high-Ti type magma. But there is no large difference in geochemical features.

With the elevation increasing from bottom to top the whole drilling site shows a trend to decrease in HFS elements like Nb and Zr, LIL elements like Rb, Sr, Ba as well as in Th, U, La. This trend, which is also observed in RP-03, may not reflect the characteristics of the magma types but rather represent the trend of the magmatic evolution of Paraná Flood Basalts and the like as a whole. That is, it is likely to reflect the general changes produced in the source and the difference existing in the degree of partial melting.

(iii) AR-1 hole (Fig.II-3-3-29 - II-3-3-32)

Location

The drilling site is located a little way to the south of the center of Paraná Basin. Distributed on the surface is Gramado of low Ti type.

Lava stratigraphy by geochemical classification

The lava at the drilling site is about 400 m thick. The magma type distributed from bottom to surface is all low-Ti type magma Gramado.

Variations in chemical composition

All lava in AR-1 hole was classified as low-Ti type Gramado regardless of depth. But, a reference to Mg# makes it possible to divide it into three different units at 200 m and 125 m depth.

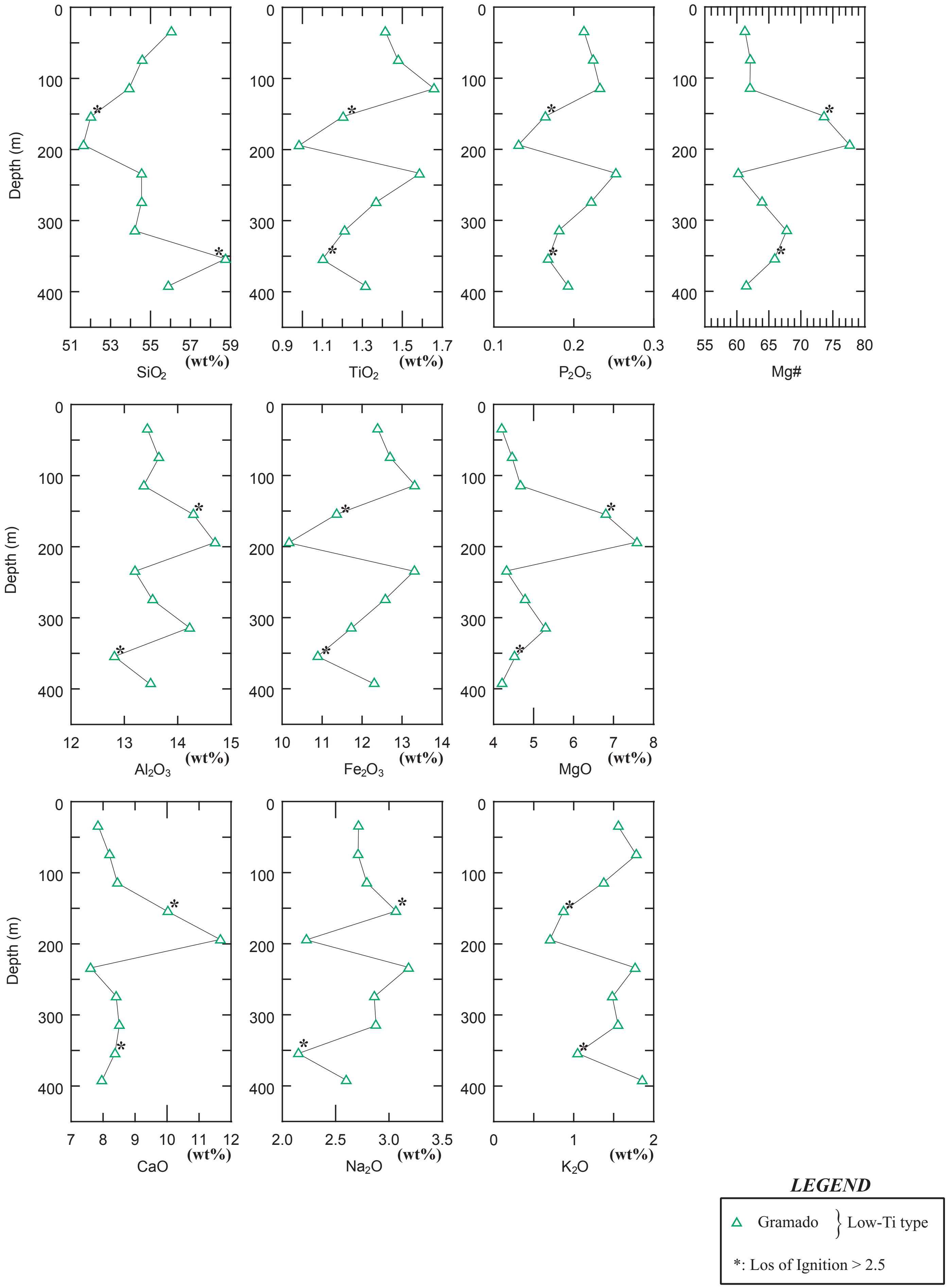

Fig. II-3-3-29 Vertical variations of major elements in lava samples (drill hole: AR-1)

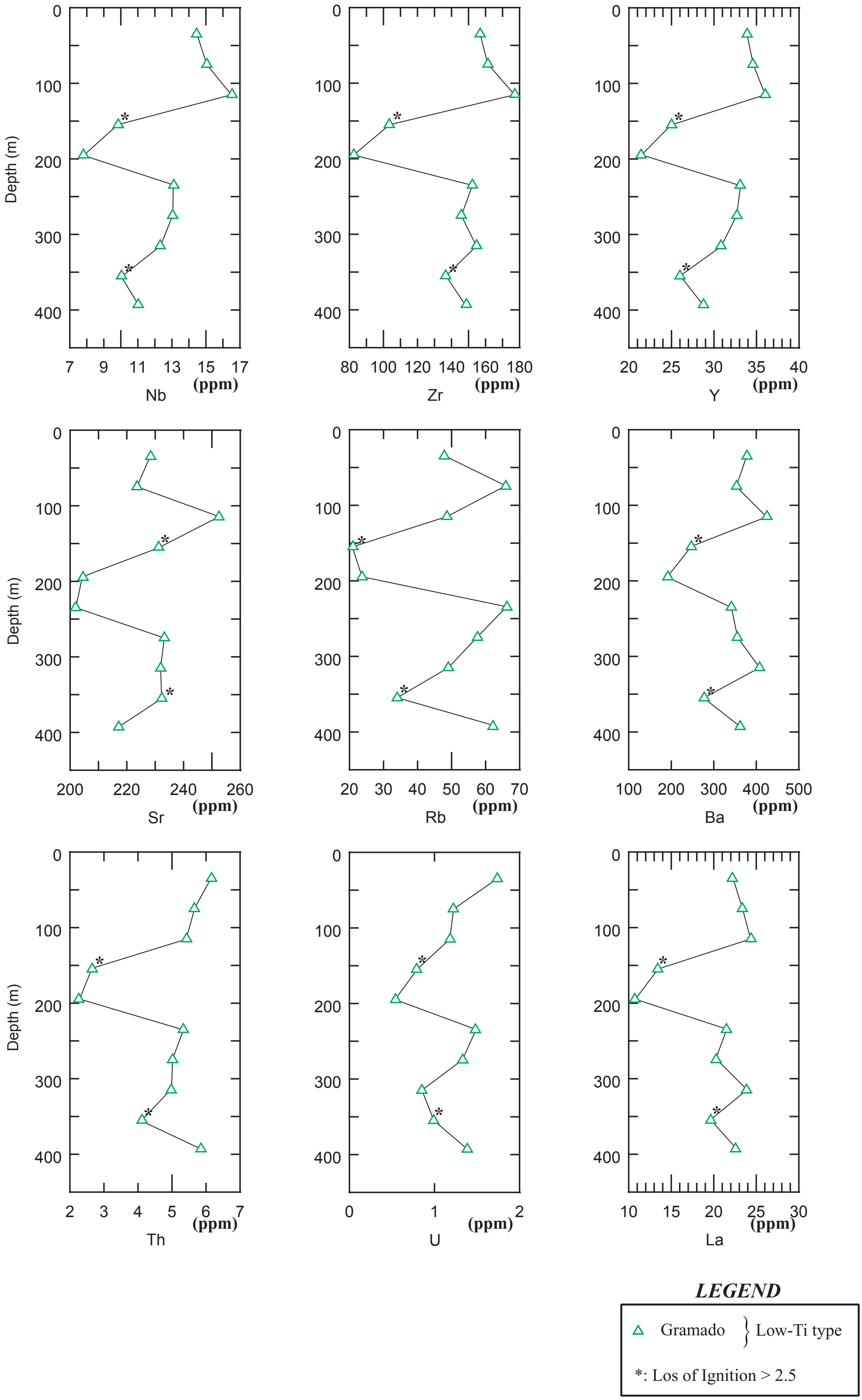

Fig. II-3-3-30 Vertical variations of trace elements in lava samples (drill hole: AR-1)

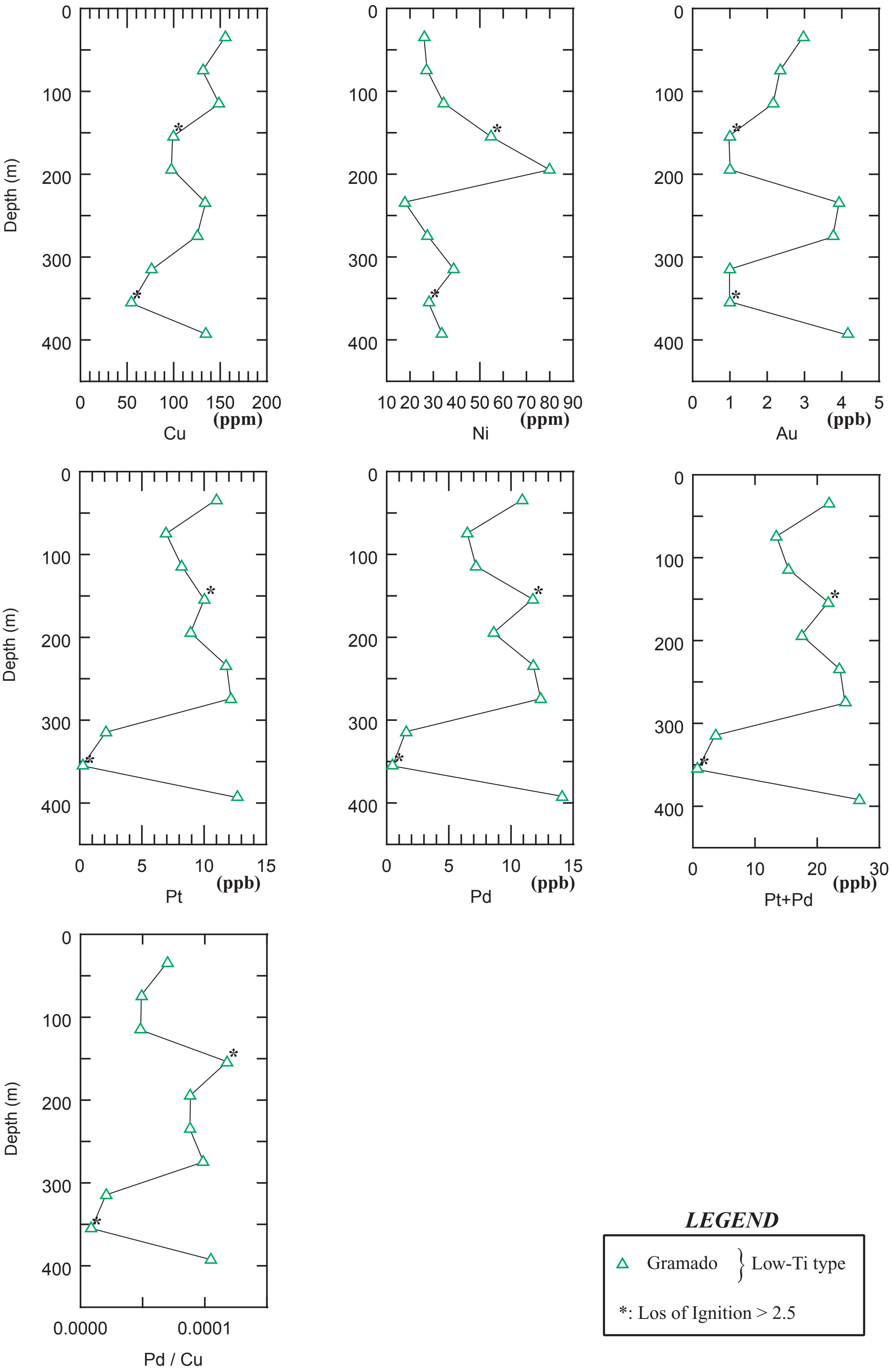

Fig. II-3-3-31 Vertical variations of transition and noble elements in lava samples (drill holl: AR-1)

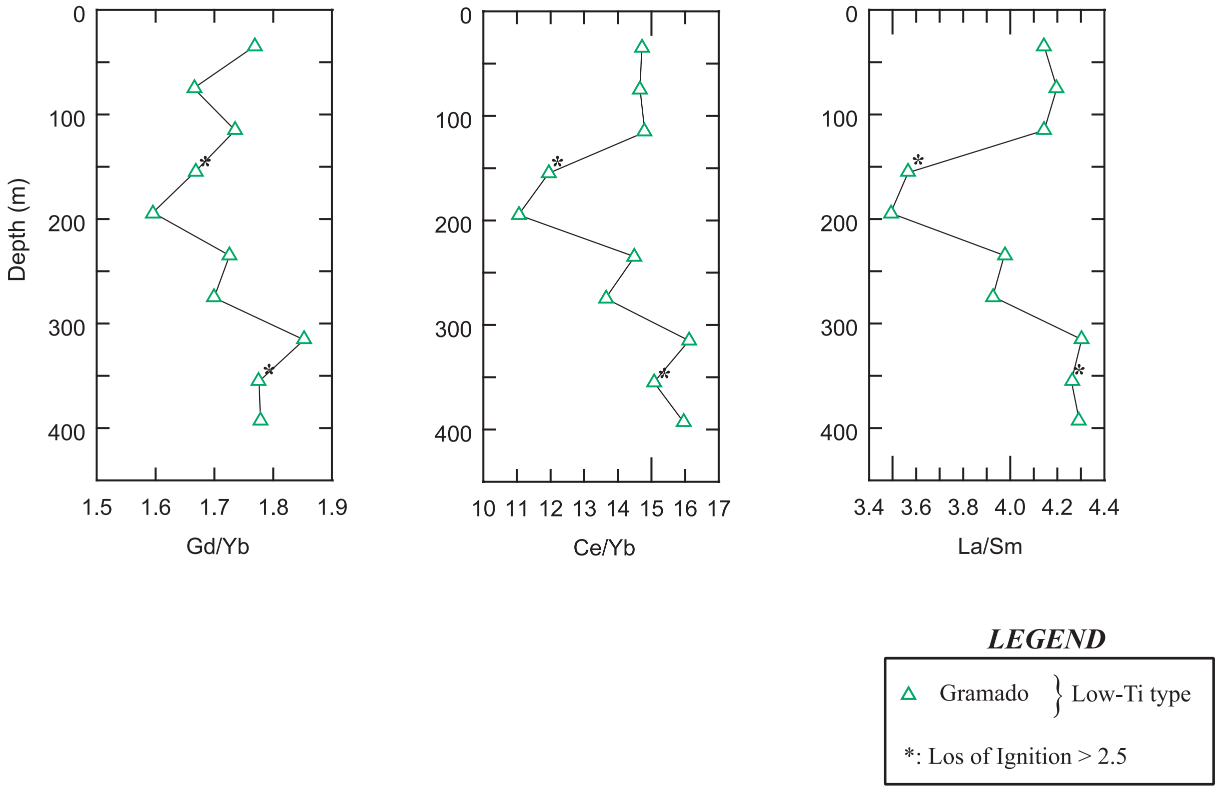

Fig. II-3-3-32 Vertical variations of the ratios of selected trace elements in lava samples (drill hole: AR-1

The bottom and top units show a trend for TiO_2 and P_2O_5 to increase with the progress of differentiation. The middle unit, on the other hand, shows features poor in incompatible elements.

Ni is observed decreasing in all the units due to fractionation of olivine.
Pt and Pd remarkably decrease in the bottom unit at 350 to 300 m depth. They tend to continue decreasing with the depth decreasing starting from 300 m depth.

(10) Comparison of Source Mantle

Fig.II-3-3-33 is a diagram showing the result of a study made on the features of original materials of the magma types deduced from Ta/Yb ratio and Th/Yb ratio as well as from Zr/Nb ratio and Y/Nb ratio using trace elements Y, Zr, Th, Ta, which are normally used to estimate a tectonic field because they are not easily affected by any difference in degree of partial melting. Features of enriched original materials are presented by Pitanga and Urubicí of high-Ti type and Paranapanema-Ribeira of Intermediate-Ti type while features of most exhausted original materials are presented by Esmeralda of low-Ti type. (Fig.II-3-3-33 (a) (b)).

Low-Ti type magma Gramado, compared with other magma types, has high Th/Yb ratio, which greatly fluctuates. From this it is gathered that it suffered a greatest contamination of crust materials. For that reason, low-Ti type Gramado shows indistinctly similar characteristics of original material with Intermediate-Ti type Paranapanema-Ribeira (Fig.II-3-3-33 (b)).

High-Ti type magma abounds in rare earth elements, unlike oceanic basalt, is also thought to indicate features of enriched original materials. Unlike the other magma types, low-Ti type magma Esmeralda presented features of exhausted original materials as features of the Nd isotope ratio. Consequently Esmeralda might have been influenced by a melt produced from original materials different from those of the other magma types.

(11) Comparison of Degree of Partial Melting

Degree of partial melting was compared among the different magma types by using a ratio of trace elements of mantle and the basalt magma which differ in distribution coefficient.

Fig.II-3-3-34 is a diagram (Onuma and Mantoya, 1984) showing a degree of partial melting deduced from Ba/Ca ratio and Sr/Ca ratio.

This diagram divides magma into three groups from high-Ti through low-Ti. The greatest degree of partial melting is observed in the low-Ti type and the smallest in Pitanga of high-Ti type. Paranapanema-Ribeira of Intermediate-Ti type fell out with a degree of partial melting which is somewhere between the above two types. However, each one of the magma types deviated from a reference line under the effect of crystallization-differentiation in progress and contamination of crust materials, so that it is impossible to find an exact degree of partial

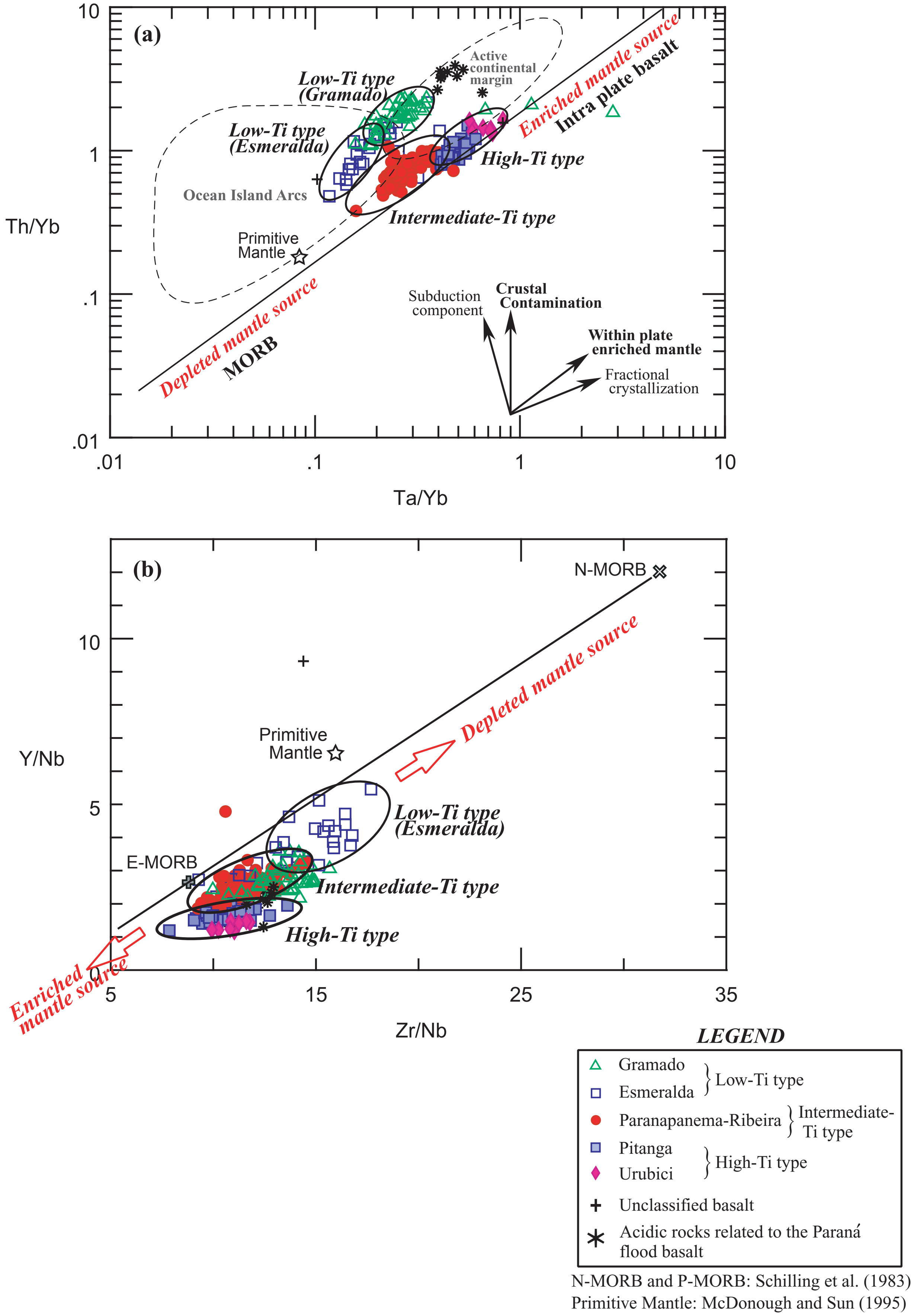

Fig. II-3-3-33 (a) Ta/Nb vs. Y/Nb diagram for lava samples; (b) Zr/Nb vs. Y/Nb diagram for lava samples

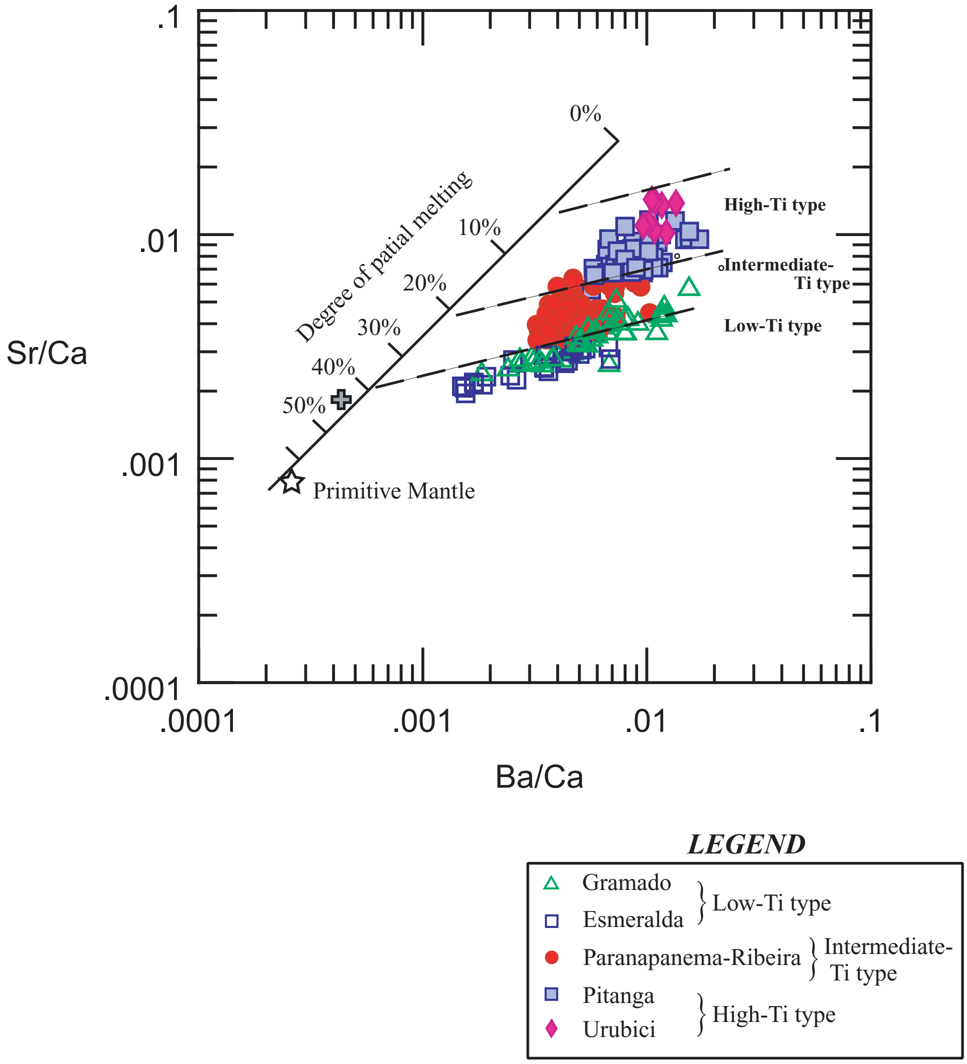

N-MORB and P-MORB: Schilling et al. (1983)
Primitive Mantle: McDonough and Sun (1995)
Reference line of patial melting: Onuma and Montoya, 1984)

Fig. II-3-3-34 Discriminant diagram to examine degree of partial melting for the Paraná flood basalts
Plots of Ba/Ca vs. Sr/Ca for lava samples

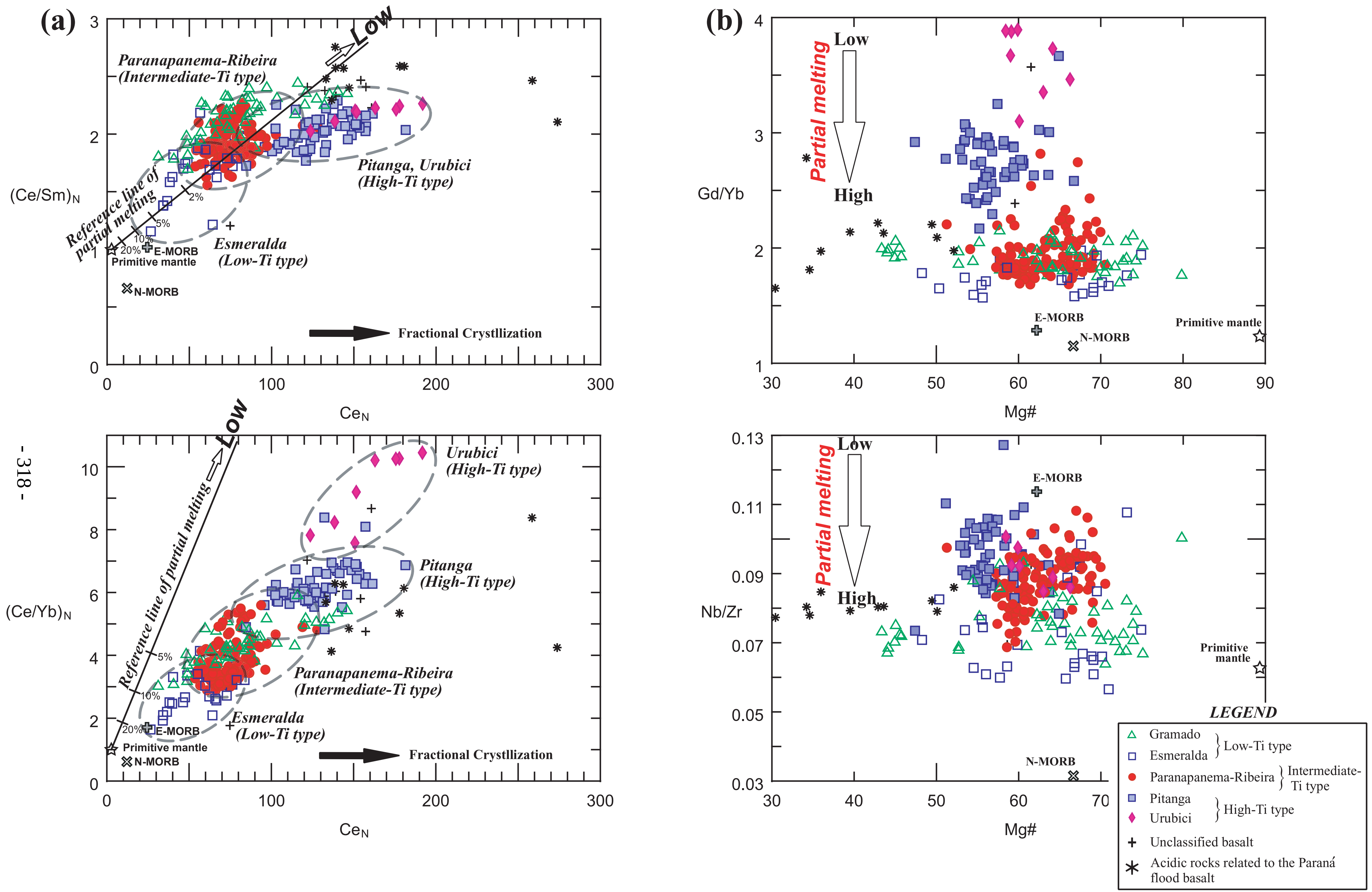

Fig. II-3-3-35 Discriminant diagrams to examine degree of partial melting for the Paraná flood basalts

melting.

Fig.II-3-3-35 (a) is a diagram drawn with Ce value normalized by chondrite as abscissa and Ce/Sm, Ce/Yb values likewise normalized as ordinate.

Like Fig.II-3-3-34, this diagram, too, divides magma into three groups from high-Ti through low-Ti. Here the greatest degree of partial melting is observed in Esmeralda, magma of low-Ti type and the smallest degree of partial melting in Pitanga and Urubicí, magma of high-Ti type. Paranapanema-Ribeira, a magma of Intermediate-Ti type shows a degree of partial melting plotting somewhere between the low-Ti type and High-Ti type.

Fig.II-3-3-35(b) is a diagram drawn to express HREE with Mg# as abscissa and Gd/Yb ratio and Nb/Zr ratio as ordinate.

The diagram of Gd/Yb ratio shows that the degree of concentration of HREE is distinctly different among the different magma types. High-Ti type magma generally tend to be rich in HREE and thus might have suffered a partial melting to a lesser degree than low-Ti type magma.

Nb and Zr differ in distribution coefficient between the mantle and the basalt magma while the Nb/Zr ratio, although it does reflect a degree of partial melting, tends to behave similarly.

As can be seen from the above, the study done on a diagram-by-diagram basis reveals the fact that the degree of partial melting diminishes in the order from low-Ti type, Intermediate-Ti type, to high-Ti type. A trend towards the greatest degree of partial melting was seen in Esmeralda above all.

(12) Study of Crystallization Differentiation

The effect of crystallization-differentiation contributing toward the formation of Paraná Flood Basalt and the like was studied on the basis of a diagrams (Fig.II-3-3-36) shown with incompatible element Zr as abscissa and TiO_2, Ni, Yb as ordinate.

The diagram is shown with incompatible elements TiO_2 and Yb as ordinate indicates a differentiation, which tends to differ from one type of magma to another and by which magma can be divided into three groups from high-Ti type, Intermediate-Ti type to low-Ti type. It shows a differentiation trend of each magma and different fields without continuity, so that it is difficult to explain the formation of the magma types supposedly taking place by crystallization-differentiation from one and the same magma. The low-Ti type magma Gramado affected by contamination of crust materials, on the other hand, shows sporadic differentiation trends.

A diagram is shown with Ni as ordinate indicates that Gramado and Esmeralda both low-Ti type have differentiation trend due to discrimination of olivine.

A greatest influence of crystallization differentiation is seen exerted mostly on Paranapanema and Pitanga but there is no effect of assimilation to be seen. This probably goes

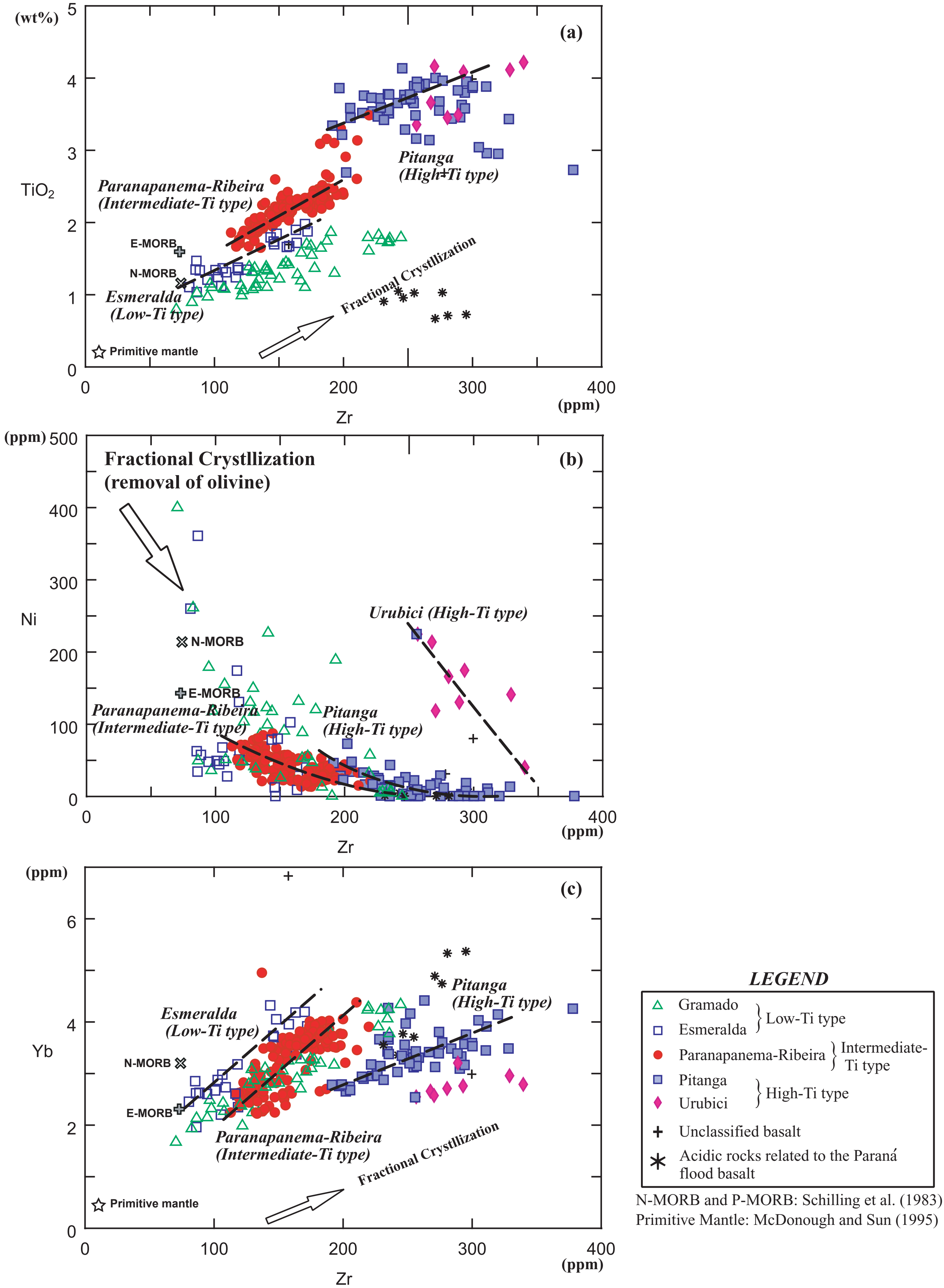

Fig. II-3-3-36 Selected diagrams to examine influence of fractional crystallization

to show that the location of a magma chamber or so was located deeper than the low-Ti type magma.

(13) Study of Assimilation of Crust Materials

An influence exerted by a contamination of crust materials is reported in connection with such kinds of flood basalt as may be active in the continent. The $^{87}Sr/^{86}Sr$ ratio is an effective index showing an influence of the contamination of crust materials. Hence the influence of the contamination of crust materials was studied with the help of diagrams drawn with $^{87}Sr/^{86}Sr$ ratio as abscissa and SiO_2, Th, U, La/Sm, Th/Yb as ordinate, which supposed to be contained in granite, which constitutes the upper crust (Fig.II-3-3-37). Consequently, each one of these diagrams shows a positive correlation of $^{87}Sr/^{86}Sr$ ratio, elements and ratio of elements in the samples from the low-Ti type magma Gramado and in a part of the samples from Esmeralda.

Fig. II-3-3-38 shows a diagram verified in Fig. II-3-3-37 with La/Sm ratio and Th/Yb in ordinate and Mg# in abscissa. This diagram shows that the low-Ti type magma Gramado, compared with the other magma types presents the highest values of La/Sm and Th/Y varying most widely. This proves that Gramado was strongly influenced by a contamination of crust materials. The low-Ti type magma Esmeralda, too, showed a trend similar to that of Gramado, from which fact it may be deduced that crust materials behaved a greater role than in the other magma types.

(14) Chemical Composition of Olivine in Basalt Lava and Intrusion

As mentioned earlier, it is obvious that the Paraná Flood Basalts is affected with crystallization-differentiation. So, lava and intrusive rocks with olivine considered to be relatively primitive were examined and the composition of primitive magma, the degree of differentiation and the effect of fractional crystallization were studied by analysis result of olivine.

Samples with high Mg# were chosen from among the samples of lava and intrusive rocks to analyze the composition of fine and idiomorphic olivine by EPMA. The samples subjected to the analysis were taken from the lava of Paranapanema-Ribeira of Intermediate-Ti type and from the lava of Gramado of low-Ti type as well as from the feeder dyke and sill of Gramado. A list of these samples is given in Table II-3-3-2 and microscopic photos and results of analysis are shown at the Appendix.

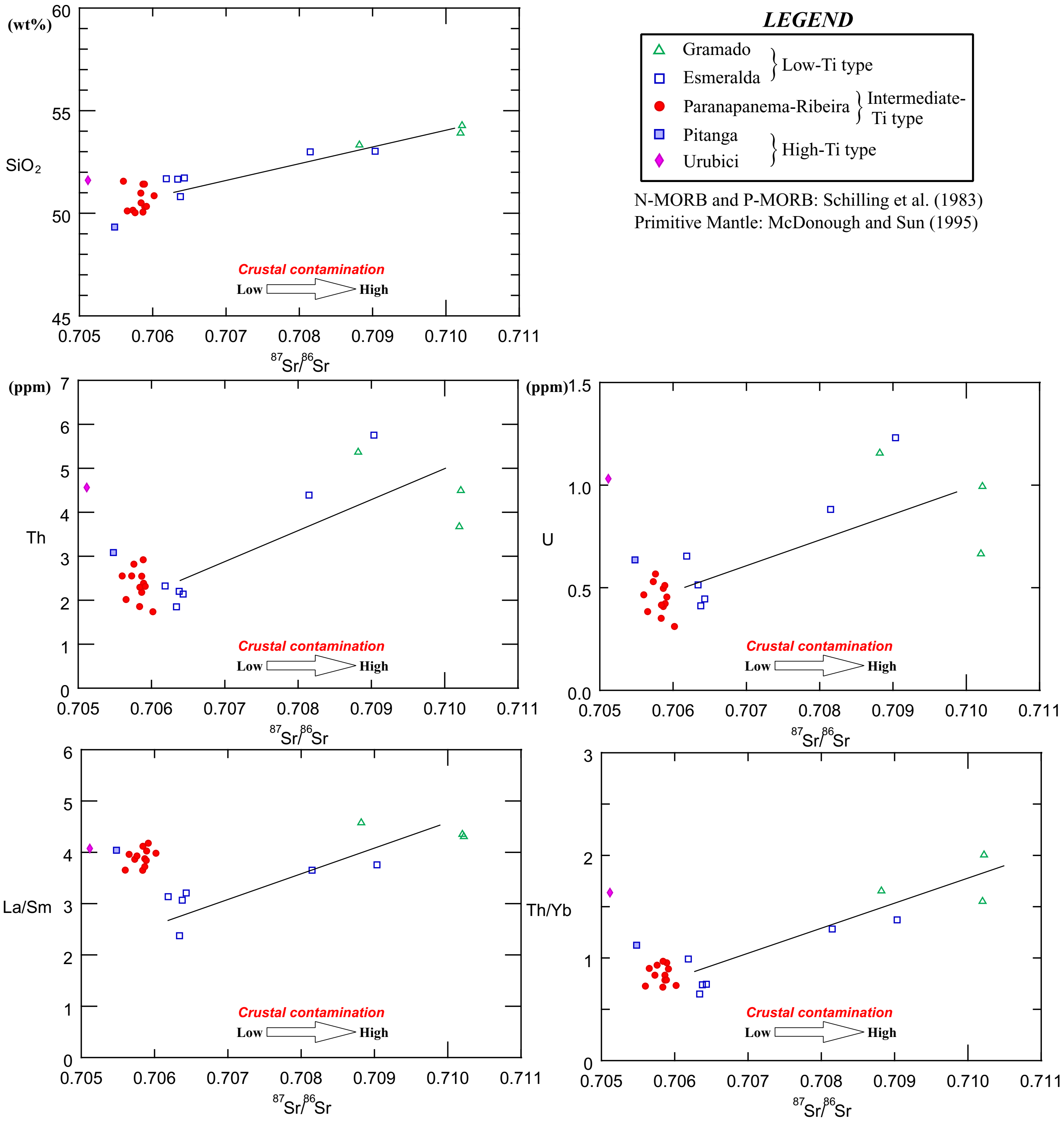

Fig. II-3-3-37 Variation of selected elements and ratios by crustal contamination for lava samples

Table II-3-3-2 Samples for EPMA

Sample No.	Description	Magma Type	Mg#	FeO/MgO (whole rock)	Ni (olivine)	Ni (whole rock)	Cr (whole rock)	KD
					wt%	ppm	ppm	
	primitive basalt		≒ 70	≦1	≒ 0.4	200～450	500～1000	≒ 0.3
AS004A	lava, fine grained basalt	Paranapanema	61.43	2.5	0.04	51	88	0.43
AS021	lava, fine grained basalt with native copper	Gramado	66	2	0.02	48	25	0.4
KN003	feeder dyke, fine grained olivine basalt	Gramado	81.5	0.9	0.19	21	601	0.31
TG62-226.3	sill, olivine dolerite (drill core)	?	90.2	0.4	0.18	894	3370	0.85
TG114-289.9	sill, olivine dolerite (drill core)	Gramado?	88.6	0.5	0.15	705	2020	1.03

It is known that undifferentiated basalt possess the following features in common (Green et al., 1974; Sato, 1977).

- FeO_{total} (wt%)/MgO (wt%) ≦ 1
- Mg number around 70
- High Ni and Cr content
  (Ni: 200 ~ 450 ppm, Cr: 500 ~ 1000 ppm)
- High content of Ni contained in olivine phenocryst
  (Ni: approx. 0.4%)

Besides, undifferentiated basalt magma and olivine contained in it are thought to have reached equilibrium until a melt was isolated from the mantle to start erupting. The distribution coefficient is then the same between FeO and MgO, as expressed by the following equation. Any material satisfying this equation may be said to be basalt formed from primary magma.

KD = (FeO/MgO) mol olivine / (FeO/MgO) mol whole rock ≒ 0.3

Results of the above judgment are given in Table II-3-3-2. Fig. II-3-3-39 is shows the diagram with Fo (Forsterite) component of olivine as abscissa and quantity of Ni as ordinate.

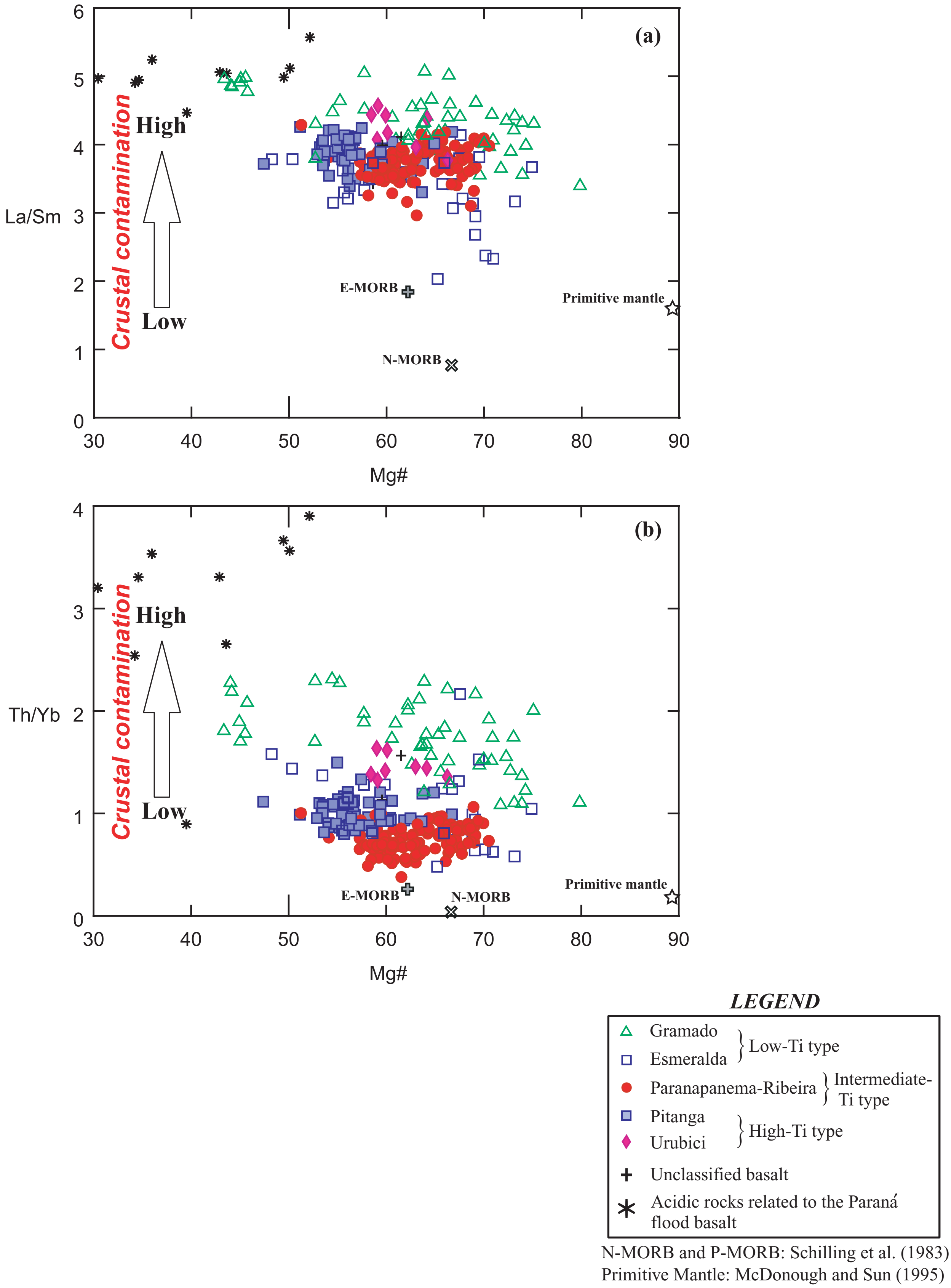

Fig. II-3-3-38 Mg number vs. La/Sm and Th/Yb diagrams for lava samples

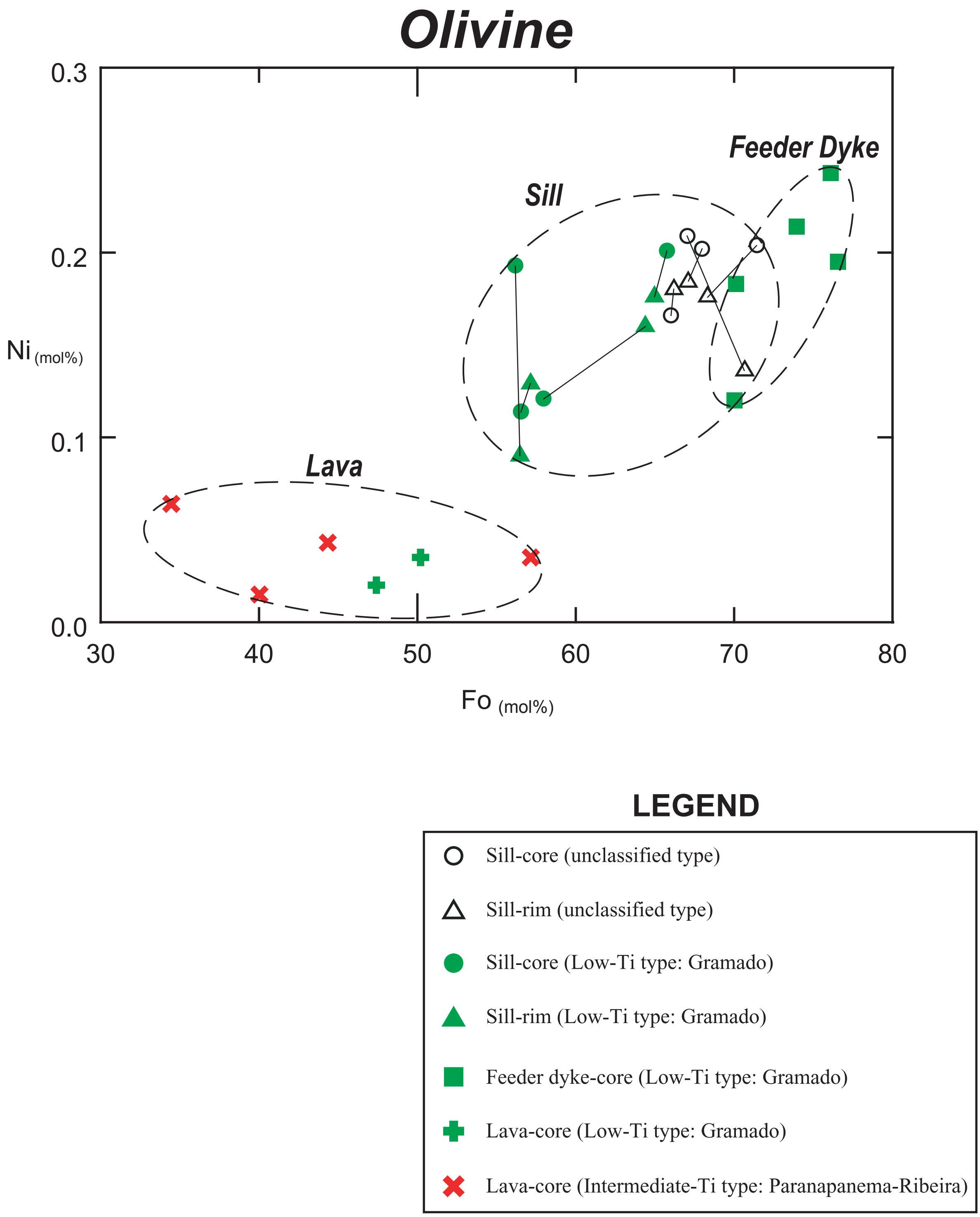

Fig.II-3-3-39 Variation of Ni with forsterite in olivines from intrusion lava and intrusion

No clear indication of features of primary basalt was found in the samples collected. Hence it is thought that even samples containing olivine and indicating a high value of Mg# had undergone a certain degree of differentiation or assimilation by another magma or crust material before it erupted or intruded in a magma chamber. The more primitive sample is a feeder dyke sample collected from Lomba Grande region (KN003).

A comparison between the lava and the intrusive rock fell out with the result that the olivine contained in the intrusive rock were enrich in Ni and Mg than that of contained in the lava. Therefore, features of something undifferentiated yet are left over in the intrusive rock than in the lava. This may be because some magma in an undifferentiated condition flew out of a magma chamber and intruded into its surroundings to stay there as sill and dyke rather than erupting as lava.

3-3-3 Ar-Ar Age of the Paraná Flood Basalts

The Paraná flood basalt reveals a limited spacial distribution of magma types, which suggests changes produced in the horizontal igneous activities. ^{40}Ar-^{39}Ar dating, which makes accurate measurement possible and takes the effect of alteration into account rather than K-Ar dating, was used to analyze the samples collected in this survey, and also studied the erupting age of each magma types by using existing age data.

(1) ^{40}Ar-^{39}Ar Dating

The locations where the samples were collected are shown in Fig.II-3-3-40, a list of samples in Table II-3-3-3 and the plateau age in Fig. II-3-3-41 (a) ~ (c). Analysis was conducted with step heating by laser.

Samples were collected by moving from the center to the south of Paraná Basin in the NW-SE direction, which is in harmony with the direction of magma distribution, with care to collect samples which are not altered yet.

To acknowledge plateau age, heating age of more than three continuous steps in high temperature zone must be consistent within 95 % confidence limit, and contain more than 50 % of ^{39}Ar of all (Uto and Ishizuka, 1999). In genreal, concerning the plateau consisting age determination value, all of its weighted averge is considered to the plateau age. The highly reliable ^{40}Ar-^{39}Ar step heating age (Lanphere and Dalrymple 1978) is defined as follows:

- Plateau age is obtained
- An isochron can be drawn by plotting data of a plateau part.
- The ages of both plateau and isochron are in agreement with each other within a range of 95 % confidence limit.

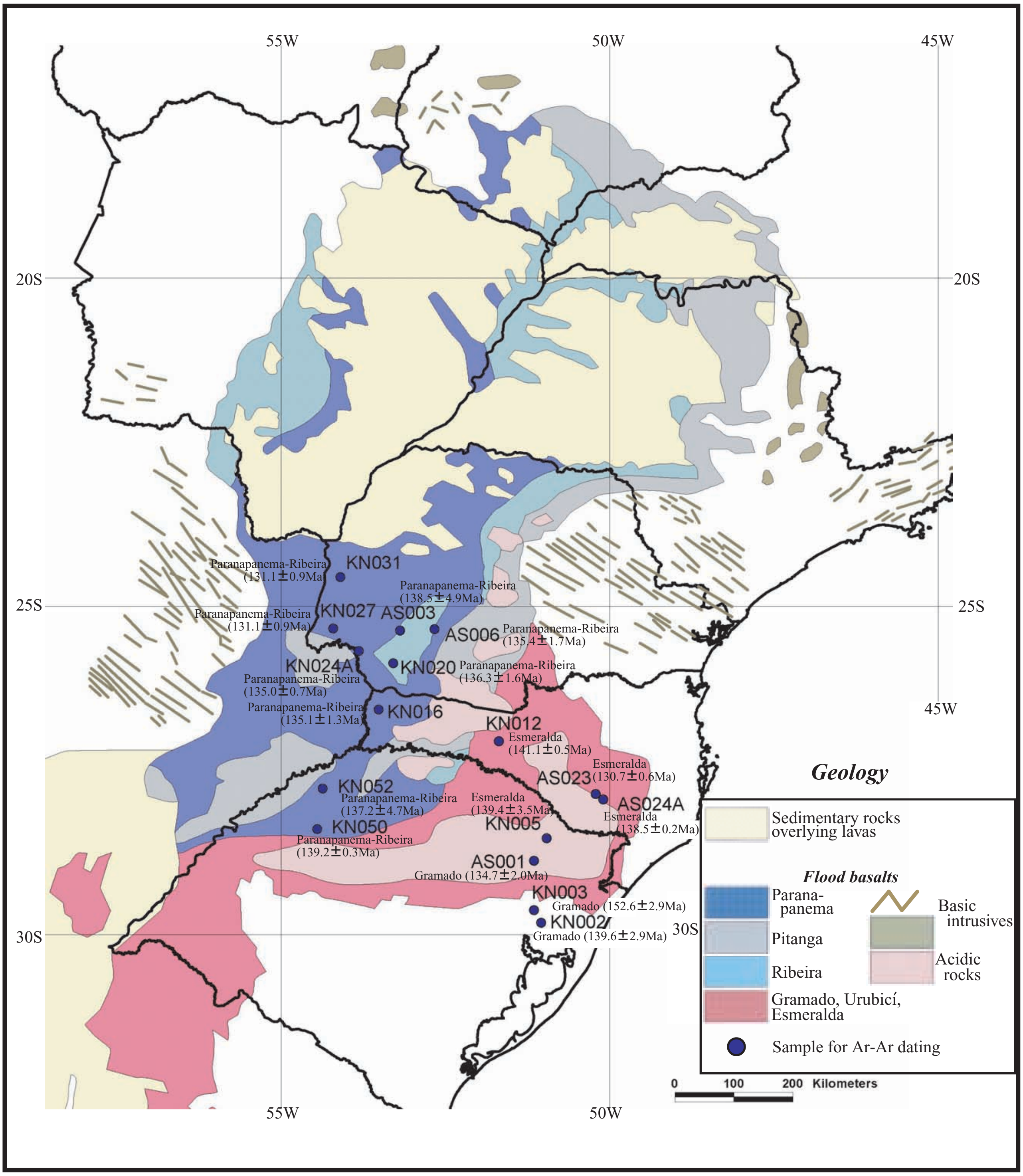

Fig. II-3-3-40 Location of collected samples for Ar-Ar dating in the Paraná flood basalts

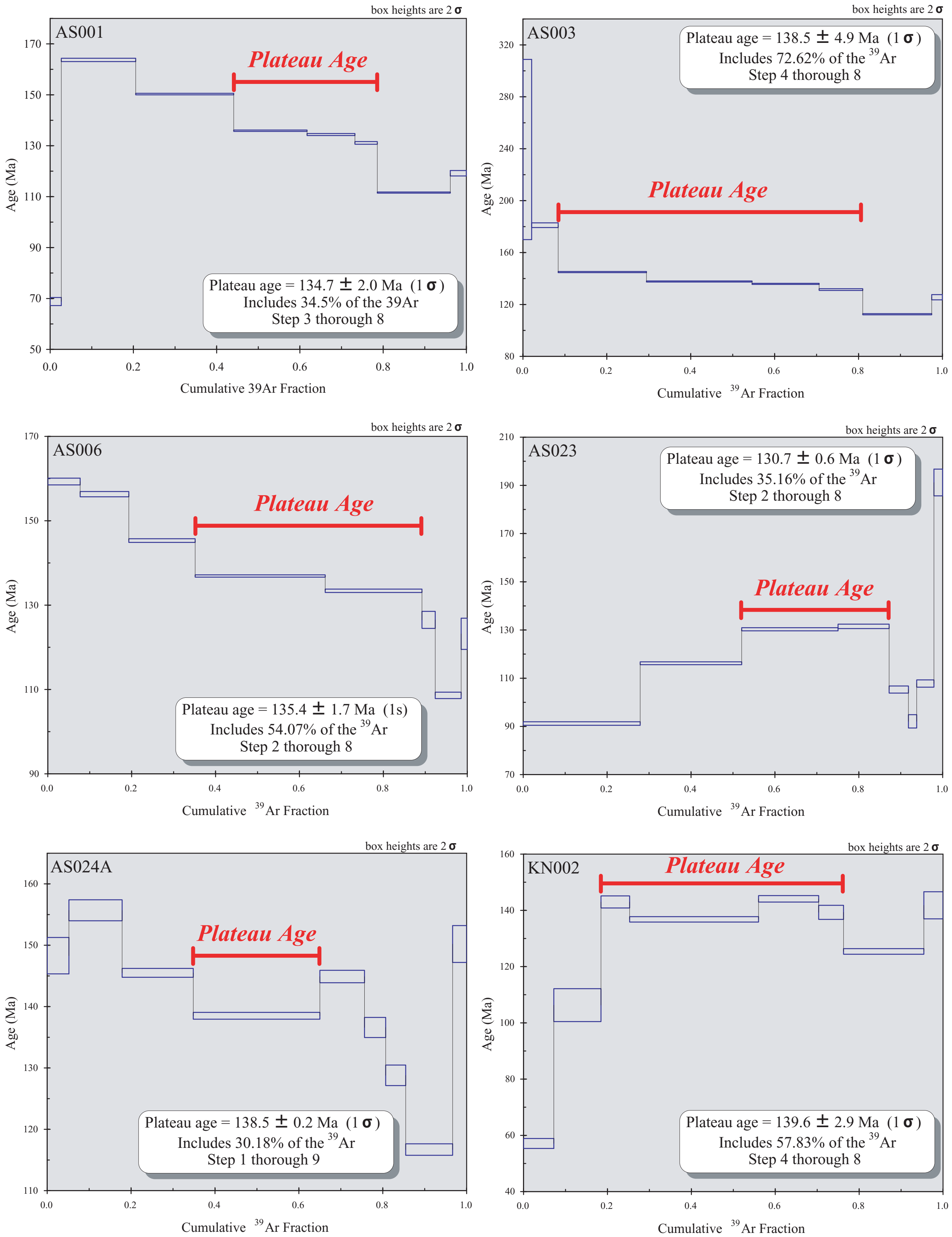

Fig. II-3-3-41 (a) Laser step-heating results and plateau age for the Paraná flood basalts

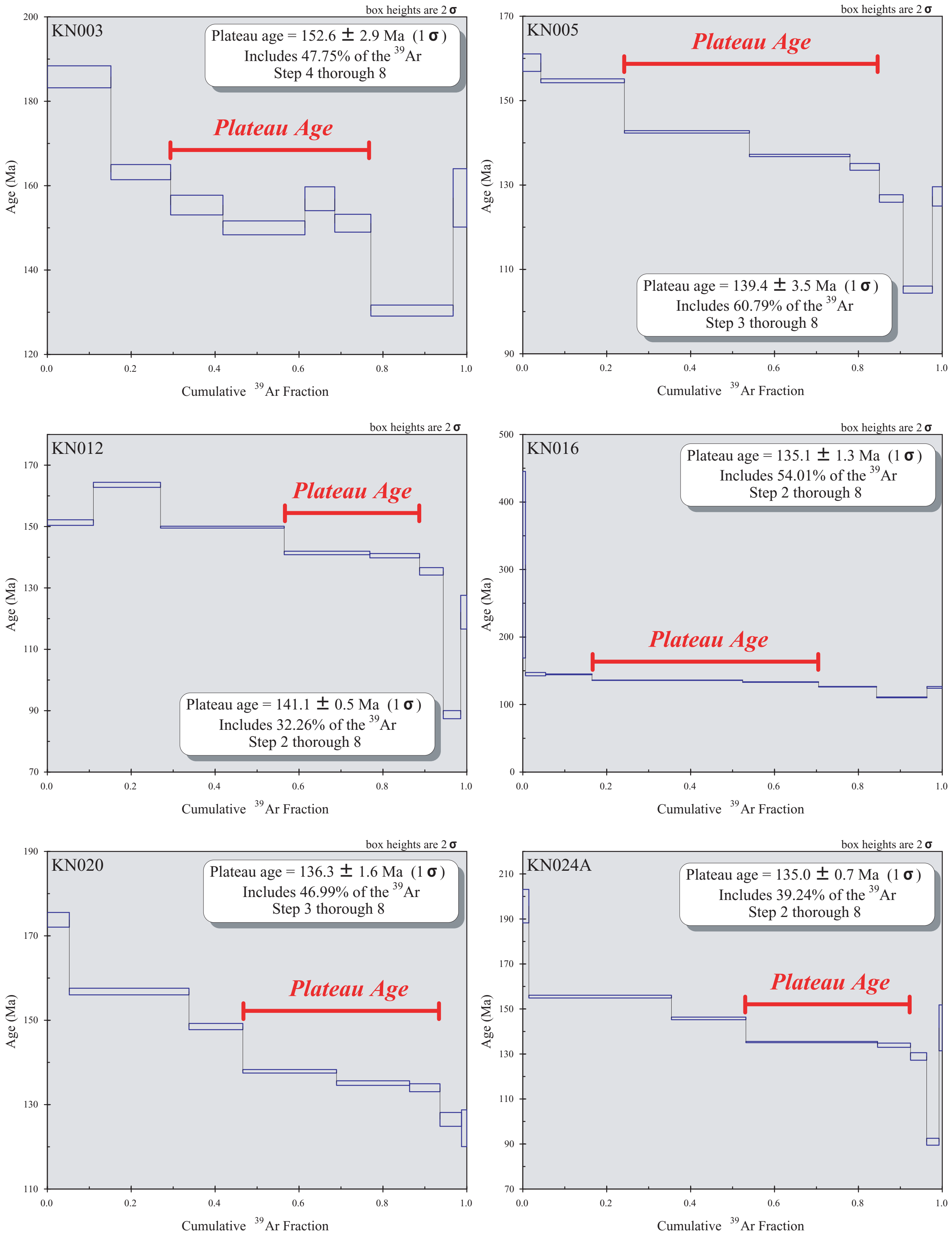

Fig. II-3-3-41 (b) Laser step-heating results and plateau age for the Paraná flood basalts

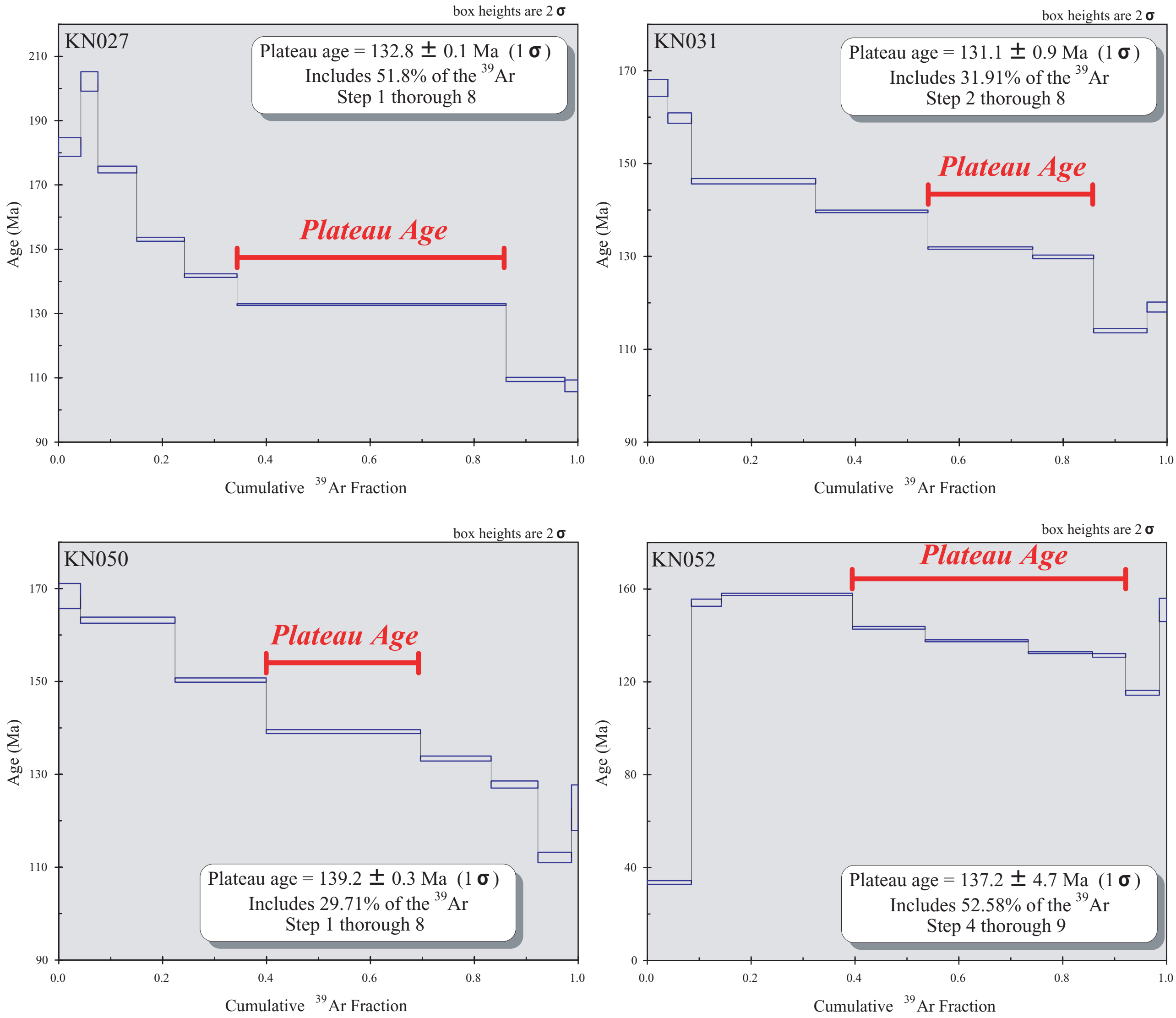

Fig. II-3-3-41 (c) Laser step-heating results and plateau age for the Parana flood basalts

- Primary ^{40}Ar-^{39}Ar ratio of isochron not remarkably deviating from 295.5

Table II-3-3-3 Samples for Ar-Ar dating

Sample No.	Locality	Type	Rock Name	Description	Alteration (amount of alteration minerals)	Magma Type
AS001	Rio das Antas near S. Bemardo, RG.	Lava	basalt	lava, dark gray, fine, massive, native copper included	rare (celadonite)	Gramado
AS003	Road cut near Tr騒s Barras do Paran	Lava	basalt	lava, gray, fine, massive.	minor (celadonite)	Ribeira
AS006	Quarry on the way from Quedas do Igua輹 to Nova Laranjeiras	Lava	basalt	lava, dark gray, fine, massive, rarely greenish celadonite included	minor (celadonite)	Parana-panema
AS023	Lages, basalt fall	Lava	basalt?	dark gray fine-grained basalt or intrusion, fine-grainrd sulfide (pyrite?) included.	unaltered	Esmeralda
AS024A	Quarry at Painel, 25 km southeast from Lages	Lava	basalt?	black aphanitic rock, conpact and very homogenious, columner joint(10-30cm) well developed	unaltered	Esmeralda
KN002	Lomba Grande Quarry	Intrusion (sill)	gabbro	sill, dark greenish grey and redish dots, coarse grain, picritic, pyroxene+plagioclase+olivine.	unaltered	Gramado?
KN003	First Flow of basalt eruption	Intrusion (Dyke)	basalt	feeder dyke, dark greenish grey, fine grain(glassy), phenocryst: pyroxene+plagioclase.	rare (celadonite)	Gramado?
KN005	Quarry of basalt near Vacaria	Lava	basalt	lava, dark greenish grey, fine grain, phenocryst: plagioclase(+pyroxene).	rare (celadonite)	Esmeralda
KN012	Near Catanduvas	Lava	basalt	lava, greenish grey, medium grain, phenocryst: plagioclase+pyroxene, native copper.	common (celadonite)	Esmeralda?
KN016	Road cut near S. Miguel d'Oeste, Santa Catarina	Lava	basalt	lava, greenish grey, fine grain, massive, phenocryst: plagioclase+pyroxene, magnetite, native copper.	rare (celadonite)	Parana-panema
KN020	Abandoned quarry near Novo Esperan軋, Same location as Otavio's OL2179	Lava	basalt	lava, dark greenish grey, fine grain, massive, glassy, phenocryst: plagioclase(+pyroxene).	rare (celadonite)	Parana-panema
KN024A	Quarry in Capanema	Lava	basalt	lava, grey, fine grain, glassy, phenocryst: plagioclase, magnetite.	common (celadonite)	Parana-panema
KN027	Road cut near S縊 Miguel do Igua輹	Lava	basalt	lava, greenish grey, fine grain, massive, glassy, phenocryst: plagioclase, magnetite.	rare (celadonite)	Parana-panema
KN031	Quarry near Mal C緘dido Rondom	Lava	basalt	lava, grey, fine grain, massive, native copper along joint.	unaltered	Parana-panema
KN050	Road cut, the southeast of Santo ツngelo	Lava	basalt	lava or sill?, dark grey, medium-coarse grain, massive, phenocryst: plagioclase+pyroxene, sulfide dissemination.	minor (celadonite)	Parana-panema
KN052	Road cut, between of Santa Rosa and Tr鷽 de Maio	Lava	basalt	lava, grey, fine-medium grain, massive, phenocryst: plagioclase+pyroxene, native copper in.	minor (celadonite)	Ribeira

Since in this survey the age heating values of all the samples determined after more than three steps of heating were not all in concordant with one another within a range of 95% confidence limit, the age was calculated by weighted averaging relatively continuous values of the plateau (Fig.II-3-3-41 (a) ~ (c)). It is therefore necessary to treat all the values as those intended for reference only. The cause of the phenomenon is unknown, but a possible cause one can think of is an insufficient number of steps of heating.

(2) Results of ^{40}Ar-^{39}Ar Age According to this Survey

According to the results of the analysis done in the present survey, a value of 131.1 ~ 138.5 Ma was obtained from the measurement of Paranapanema-Ribeira lava distributed near the center of Paraná Basin while a value of 137.2 ~ 139.2 Ma is obtained from the measurement of the same distributed in the central and south part of the said Paraná Basin. The measurement of Gramado lava to the southeast of the area investigated fell out with a value of 130.7 ~ 139.4 Ma while the one of the intrusive rock to the southeast of the area investigated fell out with a value of 139.6 ~ 152.6 Ma. All the age values thus obtained trended to vary widely than the publicized values, which suggests that there are many errors.

(3) Horizontal Transition of Igneous Activities Based on Publicized Ar-Ar Age

Fig.II-3-3-42 is a diagram drawn by plotting the publicized age values quoted from Turner et al. (1994), Stewart et al. (1996) and from Renne et al. (1992; 1996).

The age during which Paraná flood basalt was formed shows a geographical trend. Values are obtained for relatively old ages from Pitanga lava of high-Ti type in the north and southwest of Paraná Basin as well as from Paranapanema-Ribeira lava of Intermediate-Ti type. The age value is 136.9 ± 1.3 Ma in the north part and 138.4 ± 1.3 ~ 136.5 ± 0.8 Ma in the west part of Paraná Basin. A group of dykes of Ponta Grossa Arch shows more recent ages than the above by 2 ~ 8 Ma, namely 134.1 ± 1.3 ~ 130.4 ± 2.9 Ma. The most recent age is obtained from the Gramado of low-Ti type distributed in the southeast part to the southwest part of Paraná Basin. Gramado lava in the southwest part of Paraná Basin shows an age of 132.8 ± 1.8 ~ 126.8 ± 2.0 Ma while that in the southwest of the same shows an age of 133.3 ± 0.8 ~ 127.7 ± 4.6 Ma.

As can be seen from the above, as the horizontal erupting age of Paraná Flood Basalts lava, the age of ParanáFlood Basalts tend to process from northern part to southeastern part of Paraná Flood Basalts.

(4) Transition of the Vertical Igneous Activities Based on Publicized Ar-Ar Age

Fig. II-3-3-43 shows the stratigraphy of each lava types obtained by eight drillings in Paraná Basin, based on the data of Peate et al. (1992) (Table II-3-3-4; For locations of drilling sites, see Fig. II-3-3-42). In this drawing it should be noted that the vertical axis is nearly 1.5 km long while the horizontal axis expressing the distance of lines connecting the eight drilling sites is about 700 km. That is to say, on the south side with a shallow basement representing the south end of the Basin, Gramado and Esmeralda lavas, each of low-Ti type, flow toward the north of the Basin for a distance of 400 ~ 500 km. Located above it are Pitanga and Paranapanema traced over a distance of more than 600 km, which fall under high-Ti type and which occupy the center of the Paraná Basin, a part of which presenting a distribution, which is, so to say, a tribute branching off southward.

Fig.II-3-3-43 shows all the age determination values of the drilling samples by Stewart et al. (1996), superimposed on the stratigraphic classification by Peate et al. (1992). Stewart et al. (1996) publicized the Ar-Ar age determination of the four drilling samples and of some surface samples collected in Paraná Basin and maintained that the period of activities of Paraná Flood Basalts was 10 Ma. Besides, from a three-dimensional distribution of the age determination values they concluded that the igneous activities moved from the northwest to the southeast,

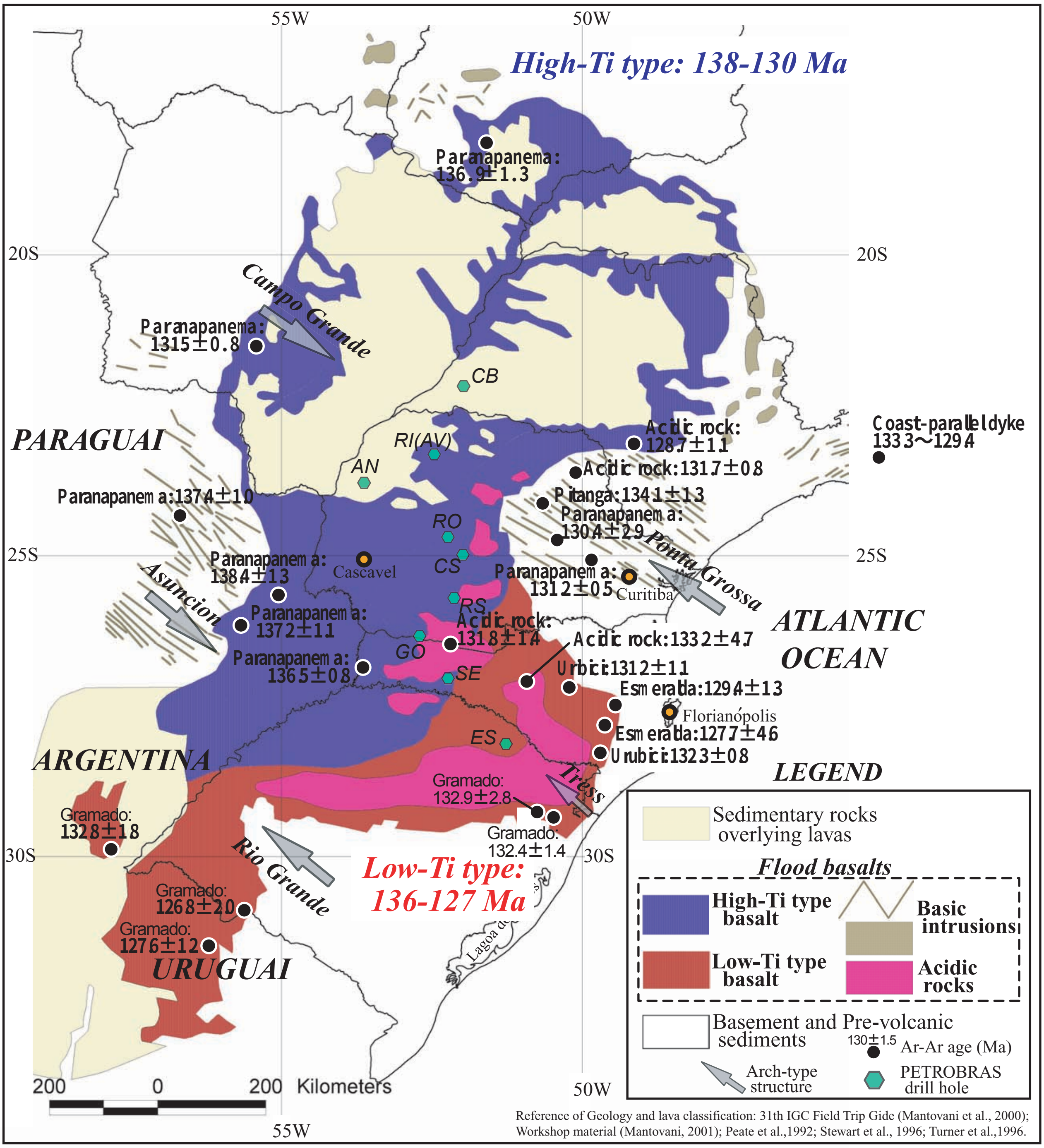

Fig. II-3-3-42 Magma types and Ar-Ar data in the Paraná flood basalts (after Turner et al., 1994 ; Stewart et al., 1996)

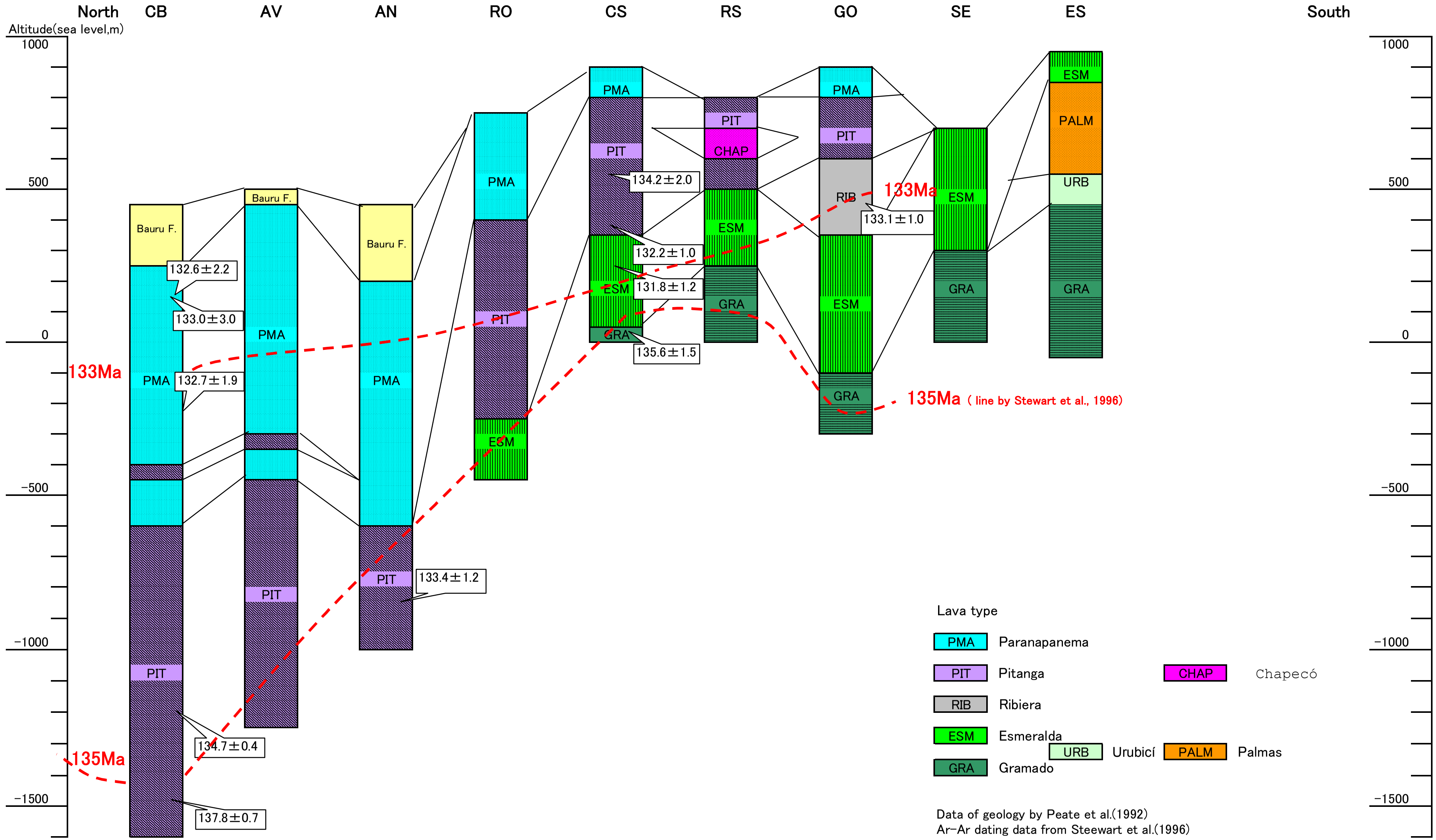

Fig.II-3-3-43 Chemical stratigraphy and Ar-Ar dating data by drill samples along North-South direction in Paraná basin

thus leading to genesis of the Atlantic Ocean.

Table II-3-3-4 Nomenclature scheme for the Paraná magma types, and their relationship to previous groups from the Paraná and Etendeka literature (Peate et al., 1992)

Basalt magma types	
"Low-Ti" ***Gramado***	LTiB[1], LTi(S)[2], LPT[3], sector II[5], Tafelberg[9], Albin[9]
Esmeralda	LTiB[1], LTP upper[4], sector I[5]
Ribeira	LTiB[1], LTi(N)[2], group A[6]
"High-Ti" ***Urubicí***	HTiB[1], HTi(S)[2], HPT[3], Khumib[10]
Pitanga	HTiB[1], HTi(N)[2], HPT[3]
Pranapanema	HTiB[1], IPT[3], ITi[7], sector III[5]
Rhyolite magma types	
Palmas	PAV[8], LPT rhyolite[3], Taferberg and Springbok quartz latite[9]
new subgrouops:	Santa Maria, Caxias do Sul
Chapecó	CAV[8], HPT ryolite[3], Sarusas quartz latite[10]
new subgrouops:	Guarapuava, Ourihos (Paraná); Sarusas (Etendeka)

Sources: [1] Bellieni et al. (1984a), [2] Marques et al. (1988), [3] Hawkesworth et al. (1988), [4] Peate et al. (1988b), [5] Fodor et al. (1985), [6] Petrini et al. (1987), [7] Mantovani et al. (1988), [8] Bellieni et al. (1986), [9] Erlank et al. (1984), [10] Duncan et al. (1988)

3-3-4 Geochemical Features and Magmatism of the Paraná Flood Basalts

Table II-3-3-5 shows geochemical features of each magma type for the Paraná flood basalts.

Paraná Flood Basalts are roughly divided into three groups, namely high-Ti type, Intermediate-Ti type and low-Ti type magma. This fact is thought to reflect the difference of degree of partial melting. The spacial distribution of the each magma type trend to be different and limited area in the Basin. The order of distribution is from high-Ti type (northern part) to low-Ti type (Southern Part), and Intermediate-Ti type distribute around center part of the Basin. low-Ti type magma Gramado and a part of Esmeralda are affected by the crustal contamination. Esmeralda, in particular, shows the similer composition of oceanic basalts surmised to have suffered an action of an exhausted mantle source.

Such geochemical features of the magma types are thought to reflect the thinning of the lithosphere of the continent resulting from the Tristan plume activities, the relative shift of Tristan plume, the source mantle produced by the separation of the continent as well as the difference in the degree of partial melting, of crystallization-differentiation and of contamination of the materials in the upper part of the crust. That is, a change in the relation between the mantle plume and the lithosphere accompanied by tension of lithosphere might have brought about regional difference of the magma.

Table II-3-3-5 Comparison of magmatisms of each magma type for the Paraná flood basalt

Magma type	High-Ti		Intermediate-Ti	Low-Ti	
	Pitanga	Urubicí	Paranapanema-Ribeira	Gramado	Esmeralda
Duration time of volcanism	137.8 - 132.2 Ma	132.3, 131.2 Ma	138.4 - 130.4 Ma	135.6 - 126.8 Ma	129.4, 127.7 Ma
Tectonic setting	Intraplate →				Ocean ridge
Degree of partial melting (Depth of magma generation)	Low (deeper) →				High (shallower)
Amount of incompatible elements (source mantle)	Enrichment (Fertile mantle? or plume?) →				Depletion (mantle upwelling?)
Degree of crustal contamination	Low			High	Low
Depletion of Pt and Pd for crustal contamination	no	no	no	yes	?
Depletion of Pt and Pd for fractionation	yes	?	rarely	?	?

The explanation given to date was that the mode of activities of Paraná flood basalt was such that the eruption of the low-Ti type magma Gramado shifted northward with the rift zone expanding from the south. It is unusual, however, to assume that the low-Ti type magma formed at a relatively shallow place becomes active earlier than the high-Ti type magma, which was formed, it is believed, at a relatively deep place. Therefore, we thought that magmatic activity had shifted from high-Ti type to low-Ti type.

Fig. II-3-3-44 shows a model of the formation of Paraná flood basalt that might have taken place mostly with plume activities under the following premises:

The magma types distributed from the south of Brazil, Uruguay, to Argentine are exclusively low Ti type. From this fact it may even be gathered that the igneous activities occurring along the rift simultaneously with the initial rift formation are one thing and those occurring in Paraná Basin is another. On such assumption, it is thought that activity of mantle plume was the main power to generate magma in Paraná basin, and right above the plume was

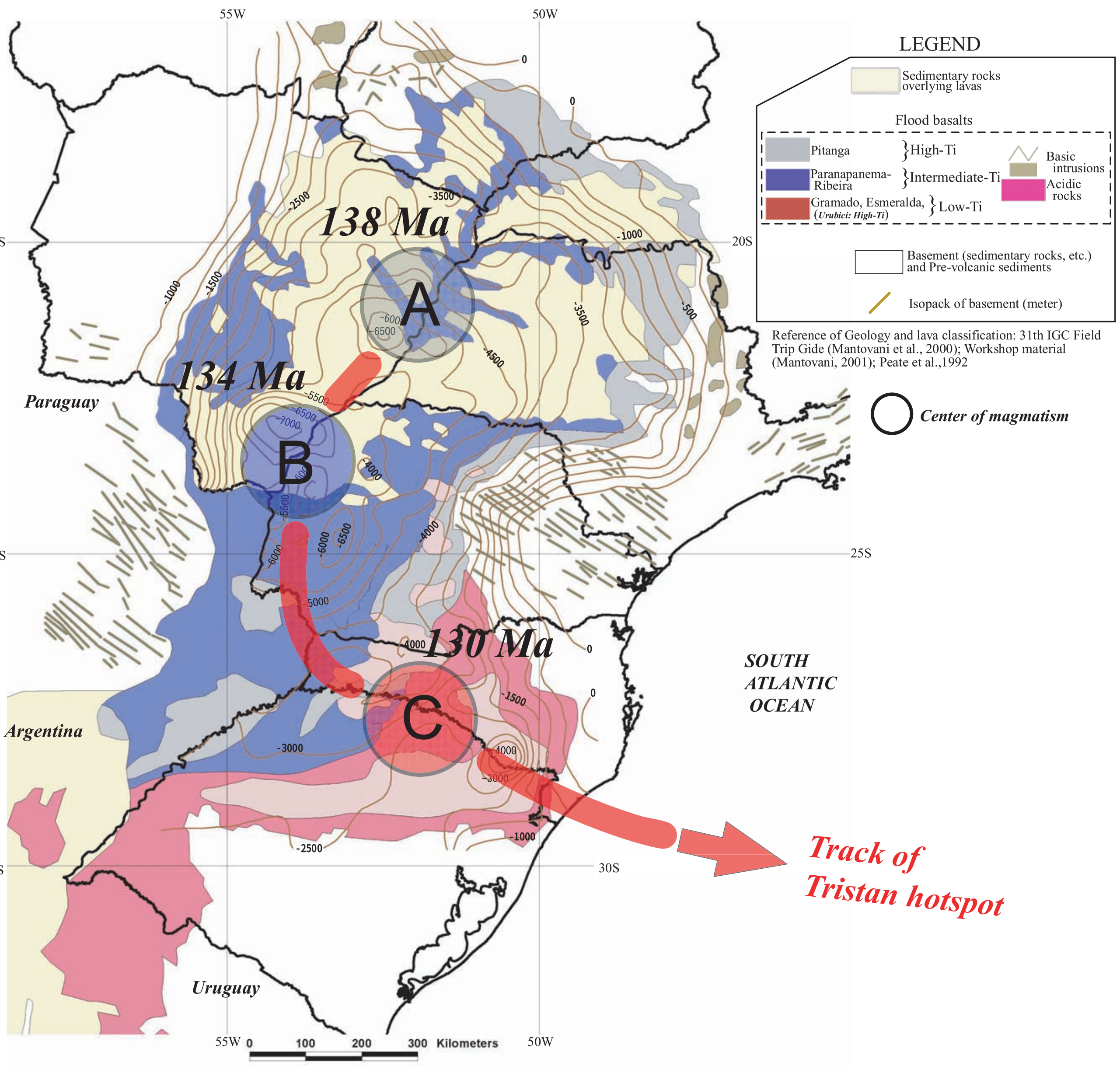

A <approximately 138 Ma>

- Mantle plume arrived at lower lithospheric mantle, and flood basalts magmatism started.
- Magma generated at deeper level with relatively smaller degree of partial melting.
- Pitanga (High-Ti type) erupted.
- Low-Ti type magma might have erupted on the initial stage of magmatism?

B <approximately 134 Ma>

- Magma generation depth become shallower level according to the thinning crust. Degree of partial melting becomes larger.
- Activity of Pitanga was weakened, and Paranapanema-Ribeira (Intermediate-Ti type) peaked.
- The most voluminous magma erupted in this period.

C <approximately 130 Ma>

- Magma genaration depth became shallower, and degree of partial melting became larger.
- The generated magma was contaminated by upper crustal materials. Acidic magma and highly contaminated Gramado (Low-Titype) erupted.
- Breaking up of Gondwana (opening of Atlantic sea) started.
- Mantle plume arrived shallower level with accompanying thinning of crust, and Esmeralda (Low-Ti type) magma generated with largest degree of partial melting. This magma probably was formed by mixed crustal assimilated Gramado magma with asthenospheric origin magma. Urubici (High-Ti type) was formed with a similar event, too.

Fig. II-3-3-44 Schematic transitional model of magmatism for the Paraná flood basalts

the center of igneous activity. This means that the places which have the thickest lava pile were the volcanic center. The continuum of volcanic center may indicate traces of the plume that passed through it.

The plume model is explained in the following.

At approximately 138 Ma the mantle plume reached the bottom of the lithosphere and commenced the igneous activities of Paraná flood basalt. Due to the thick lithosphere of the continent, the formation of magma took place at a deep part, so that partial melting is believed to have taken place only to a small degree. It was during this period that Pitanga of high Ti type erupted. In terms of the geochemical stratigraphy, it is known that at the lowest bottom of lava in the north of Paraná Basin there exists a distribution of lava of low-Ti type. This can be explained by the assumption fact the low-Ti type magma might have been formed either due to igneous activities eventually existing during the formation of the rift before the Tristan plume activities or due to the crustal contamination occurring eventually on a relatively large scale at the initial stage of activities before the formation of a permanent feeder.

At approximately 134 Ma, due to the progress of the thinning of the lithosphere, is thought that magma began to generate at shallow part and degree of partial melting progressed. During this period the activities of Pitanga of high-Ti type diminished whereas those of Paranapanema-Ribeira of Intermediate-Ti type became full-fledged. It is assumed that the largest volume of lava erupted during this period.

It is assumed that at 130 Ma or so, magma generation took place in shallow part and degree of partial melting became very large. Since magma formation took place in shallow part, it began to assimilate a large mass of crust materials. During this period the activities shifted from the Intermediate-Ti type magma Paranapanema-Ribeira to the low-Ti type magma Gramado. In addition, the magma contaminated with a large mass of crust materials was mixed, thus causing acidic rocks to be formed locally. Similarly, as local magma activities, activities of low-Ti type Esmeralda, which was generated by mixing of asthenosphere-origin melt ascended through separated Atlantic Rift and Gramado magma, and high-Ti type Urubicí which was generated by contamination of crust material and remarkable crystallization-differentiation took place.

Later, with the expansion of the Atlantic Ocean, the Tristan Plume moved away relatively from the land, forming seamounts. The Tristan plume is now located around Mid-Atlantic Ridge.

3-4 Intrusions Distributed in the Eastern Margin of the Paraná Basin

3-4-1 Overview of the Cooperative Survey Program of Canada and Brazil

Canada and Brazil in their cooperative survey program studied geochemical characteristics of the intrusive rocks distributed in the eastern margin of the Paraná basin. Fig. II-3-4-1 shows the survey area. Their survey can be summarized as follows:

1) The petrochemical survey focused on the intrusive rocks distributed in the eastern margin of the Paraná basin from São Paulo in the northern part to Porto Alegre in the southern part of the basin. The survey aimed to evaluate probable mineralization of the Noril'sk style nickel-copper-PGE ore associated with intrusive rocks relating to the flood basalts.
2) Except for some depleted rocks, the flood basalts (lavas and intrusions) in the Paraná basin indicate high background values of Pt and Pd as the flood basalts in the other regions.
3) Like the lavas, the intrusions are classified into "High-Ti" type and "Low-Ti" type, which are respectively distributed in the northern part and in the southern part of the basin. The ratios of trace elements reveal that the "High-Ti" type magma and the "Low-Ti" type magma were generated from mantle materials of similar compositions in their different degrees of partial melting.
4) The most primitive rocks (MgO = 18.26 wt%) were found in the Lomba Grande Complex of the southern part and from the Porto Alegre metropolitan region to the Iruí-Leão area, whereas the most fractionated and MgO poor rocks were found in the Ponta Grossa Arch of the northern part.
5) Regarding the olivine rich intrusions in the southern part of the Paraná basin, cumulative olivine fractionation presumably played the important process in the early to middle stages of crystallization history, forming similar association found in the Noril'sk region. However, as a group these olivine rich intrusions reveal no combination of trace elements suggesting the depletion of chalcophile elements and the crustal contamination. No regional fissure/lineament, which acted as a major magma conduit, were observed.
6) Meanwhile, most of the rocks were found depleted in chalcophile elements in the sills of the Ponta Grossa Arch in the northern part of the Paraná basin. These rocks also suggest crustal contamination. Although chalcophile elements were observed depleted in the sills, no depletion of the elements was recognized in the dikes, which might have acted as conduit of the flood basalts. Depletion of chalcophile elements was also observed in some limited rocks of the intrusions in the southern part of the basin.
7) An existence of the intrusive rocks depleted in chalcophile elements and the active volcanic activity controlled by the fractures indicates that the Ponta Grossa Arch is the target most

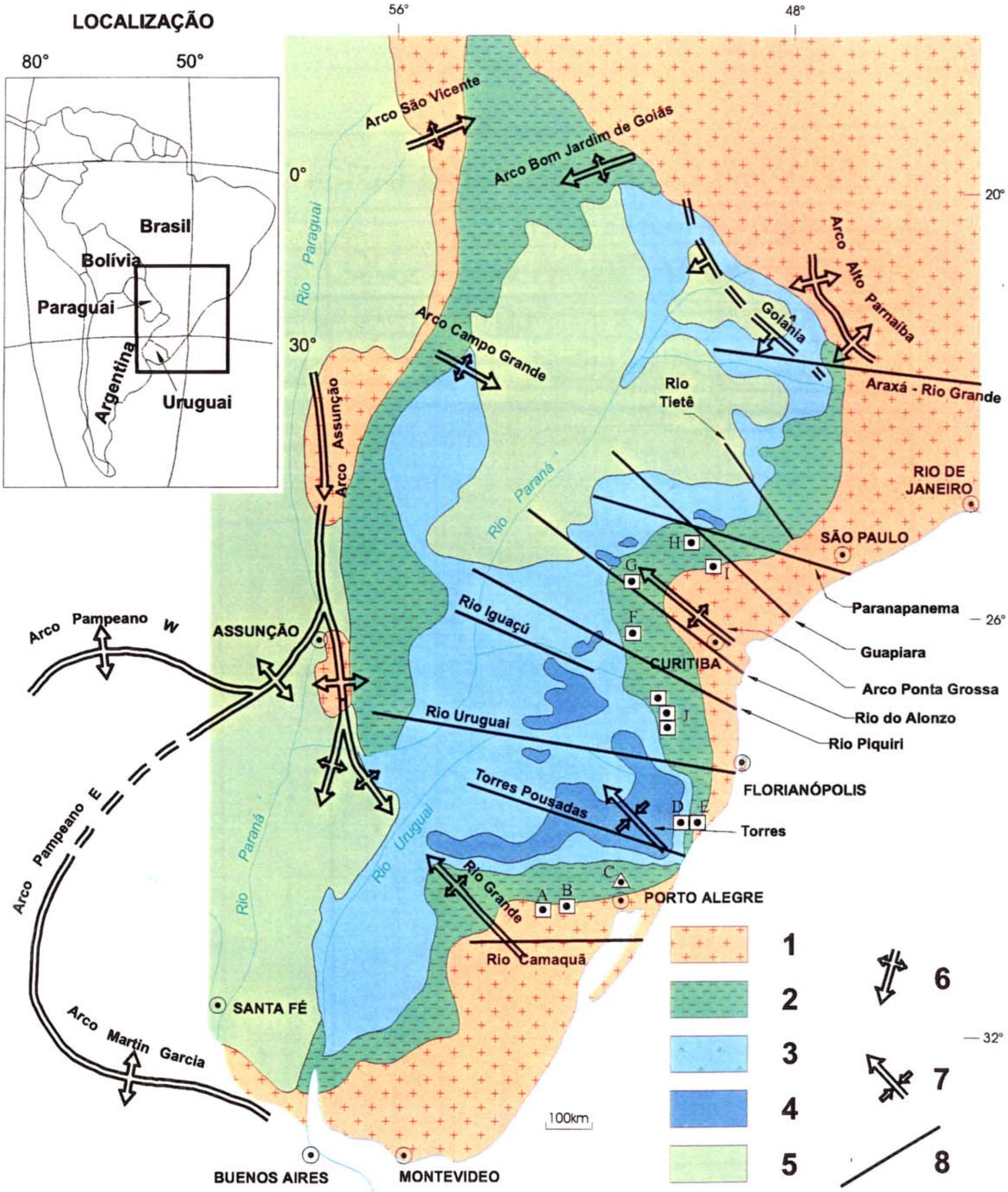

Esboço Geológico da Bacia do Paraná (modificado de Melfi et al, 1988): 1 Embasamento cristalino pré-devoniano; 2 Sedimentos pré-vulcânicos-dominantemente paleozóicos; 3 Lavas vulcânicas intermediárias e básicas; 4 - Derrames estratificados de lavas ácidas; 5 Sedimentos pós-vulcânicos (principalmente do Cretáceo Superior); 6 Estrutura tipo arco; 7 Estrutura tipo sinclinal; 8 Lineamento tectônico e/ou magnético. Sills ▣ ; intrusão hipoabissal ▲ ; A: região de Iruí- Leão-PA; B: região de Rio Pardo-PA; C: Lomba Grande-LG; D: Sill de Maracajá/Barro Branco-MB; E: Corpo Básico de Rio Urussanga-RU; F: Sill de Irati-PGA; G: Sill de Reserva-PGA; H: Sills de Siqueira Campos-PGA; I: Sill de Fartura-PGA; J: Corpo Básico de Pouso Redondo/Rio do Campo-PRR.

Fig.II-3-4-1 Intrusions studied by the Canada-Brazil cooperative project

potential for Noril'sk style mineralization. The fracture zone of the Ponta Grossa Arch presumably acted as conduits through which large volume of the magma ascended, like the Noril'sk - Kharaelakh fault in the Noril'sk region. These magma conduits probably provide suitable environments for the precipitation of sulfide melt containing nickel, copper, and PGE.

3-4-2 Distribution of Intrusions in the Eastern Rim of the Paraná Basin

CPRM/DNPM carried out large-scale drilling surveys in the distribution area of the Paleozoic strata in the eastern rim of the Paraná Basin from the 1970s to the 1980s. The drilling surveys aimed to explore coal deposits. The number of CPRM/DNPM's drillings amounted to over 2,400 holes. The drilling data, prepared by CPRM, indicated that many drillings identified presences of intrusions (sills). This survey tried unveiling the horizontal and vertical distributions of the sills in the aforementioned areas after transforming their data into database with the help of a mine development support system (MINEX).

Fig.II-3-4-2 shows a chart of the drilling sites; Fig.II-3-4-3 shows an isopach map of sill of the entire areas; and Fig.II-3-4-4 to Fig.II-3-4-6 respectively show isopach maps of sill of the Lomba Grande block, Santa Catarina block, and Ponga Grossa Arch block. In addition, Fig.II-3-4-7 to Fig.II-3-4-17 indicate typical geological profiles of the individual blocks mentioned above. Many sills have intruded into the Irati formation of the Permian and deeper. The maximum thickness of sill identified in these area stands at 217m, which was identified at the FP-02 hole of the Ponta Grossa Arch block (Fig.II-3-4-14, Fig.II-3-4-16). In the Ponta Grossa Arch block, sills of more than 100 meters in thickness have been also identified at several drillings (for example, FP-09 hole: 148m, SP-66 hole: 180m, SP-17 hole: 174m). Although the Ponta Grossa Arch has extensive dyke swarm, intrusive activity of sills was estimated to have been most active in the eastern rim of the Paraná Basin. In the Romba Grande block, the sill identified at neighboring TG-95 hole, TG-97 hole, and TG228 hole is distributed in an area some 100 km in ENE direction to the Porto Alegre. The sill is estimated to have an extension of some $80km^2$ and a thickness of more than 130m. Most of other sills identified have a thickness of less than 100m. The average thickness of the entire sills identified stood at approx. 20m.

3-4-3 Collecting Samples

We collected samples of intrusions (sills and dykes) at outcrops and CPRM/DNPM drillings for petrochemical analysis. Fig.II-3-2-1 shows the sites of the outcrop samples. Fig.II-3-4-18 shows the sites of the drillings that we collected samples. We could collect

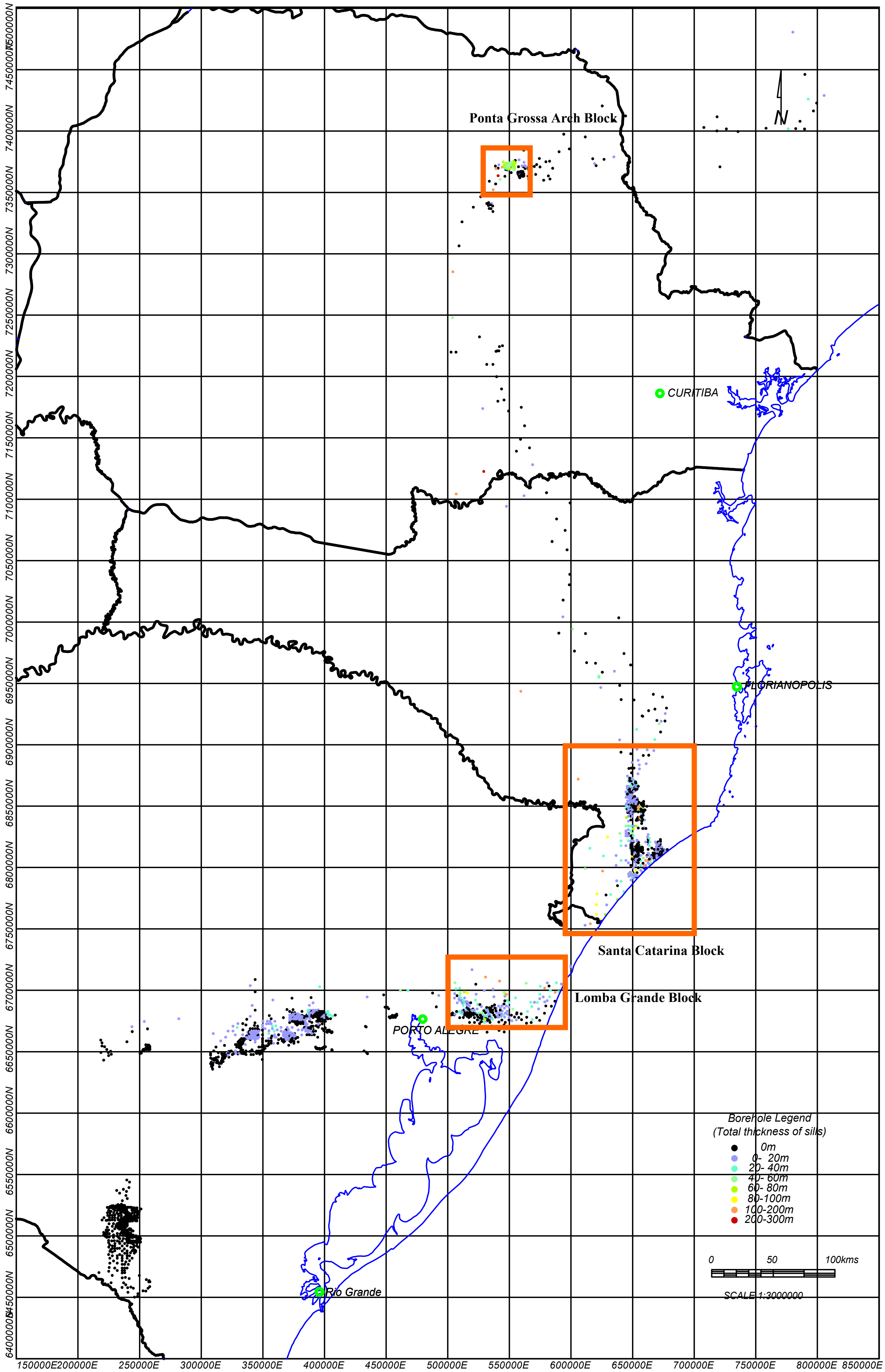

Fig.II-3-4-2 Borehole locations for the coal prospecting in the eastern margin of the Paraná basin

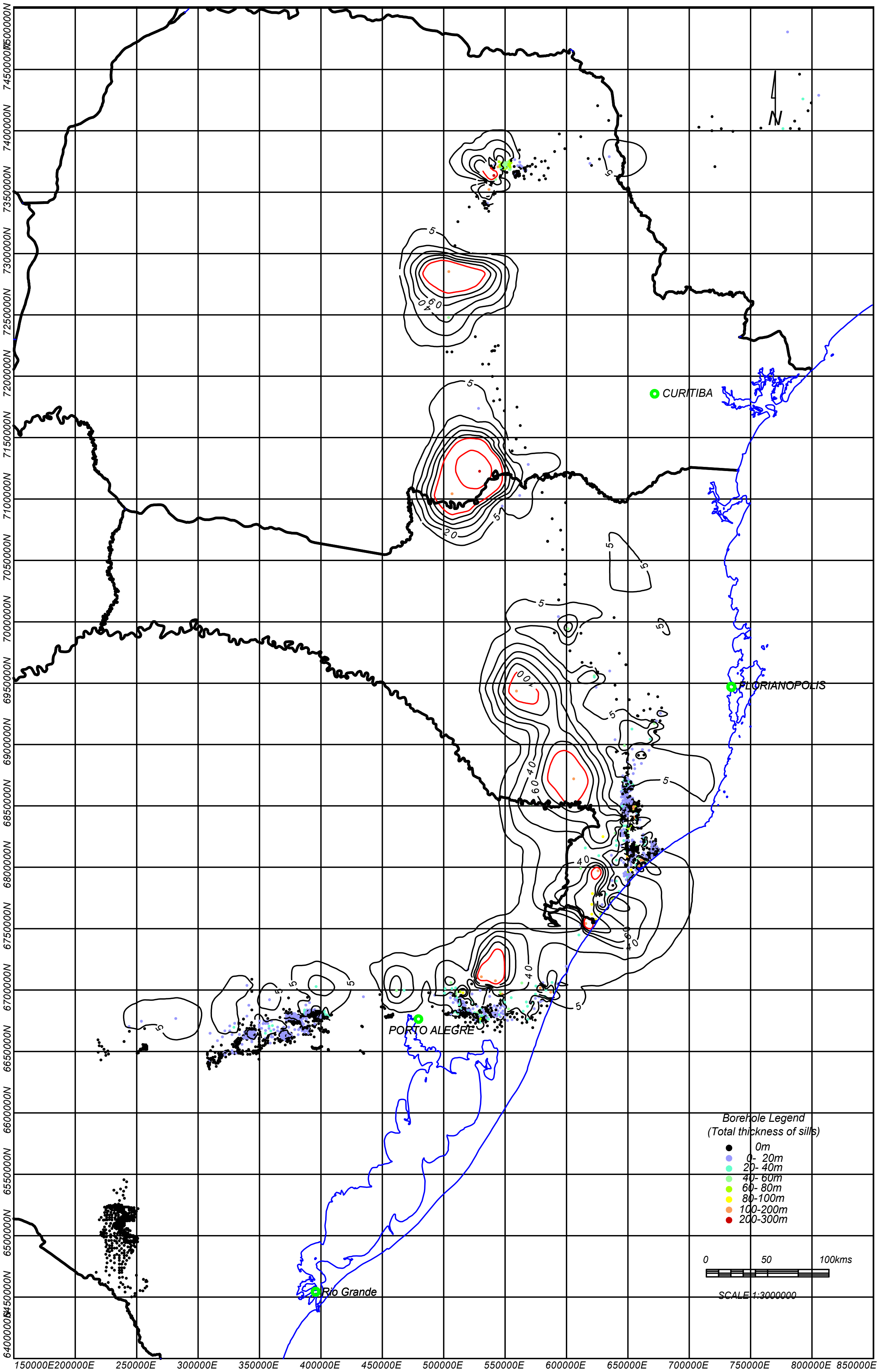

Fig.II-3-4-3 Isopach map of the total thickness of sills in the eastern margin of the Paraná basin

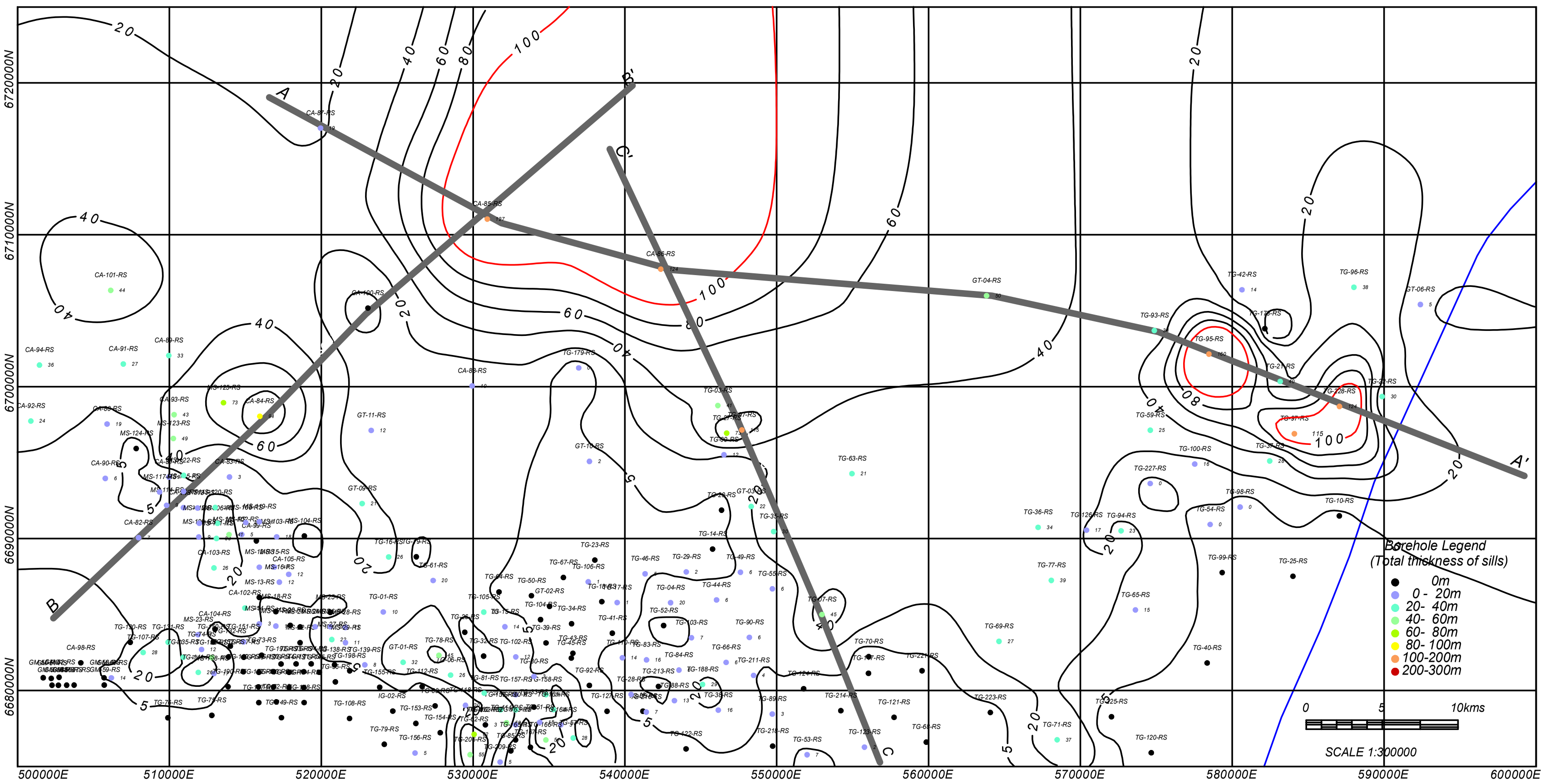

Fig.II-3-4-4 Isopach map of the total thickness of sills in the Lomba Grande Block

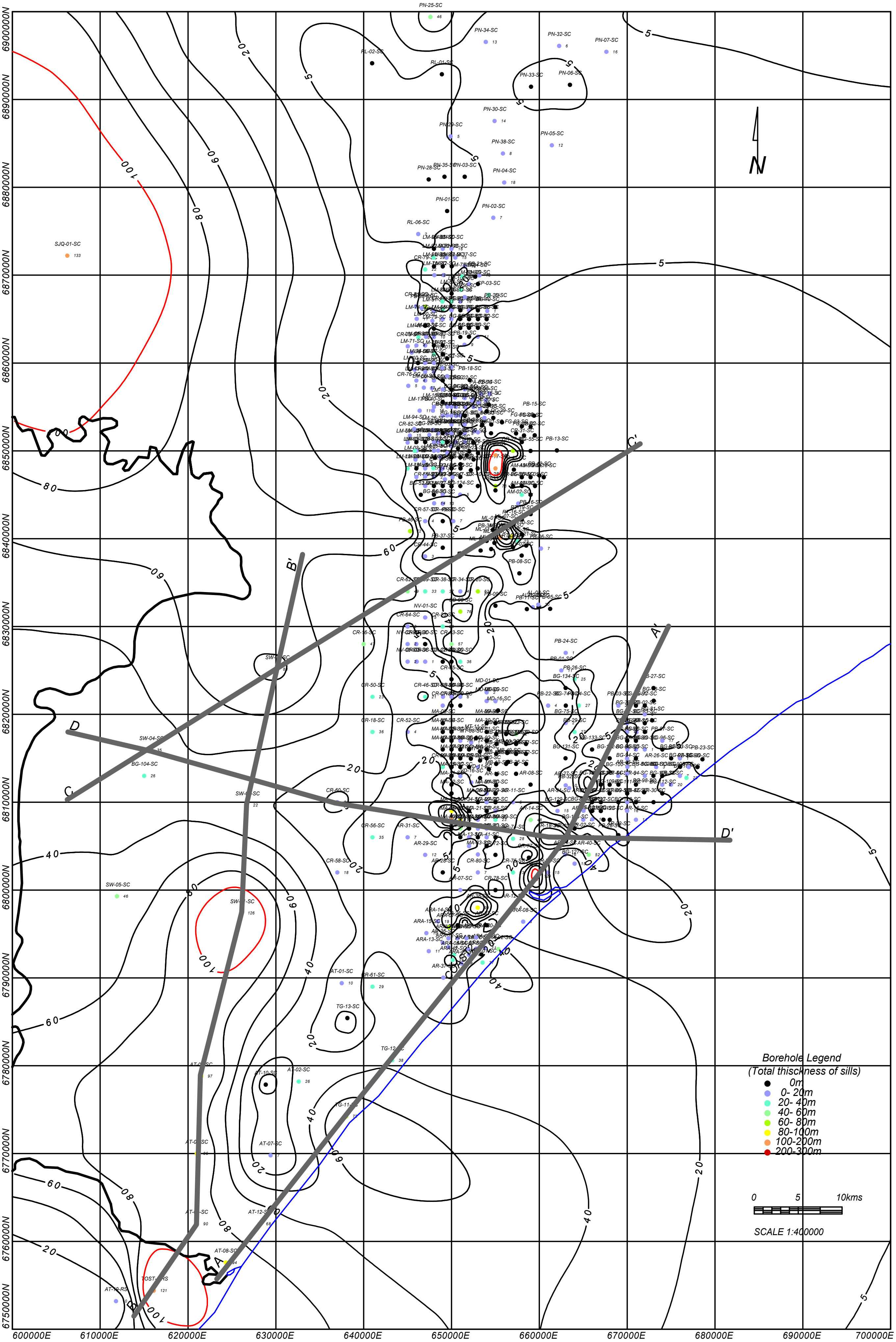

Fig.II-3-4-5 Isopach map of the total thickness of sills in the Santa Catarina Block

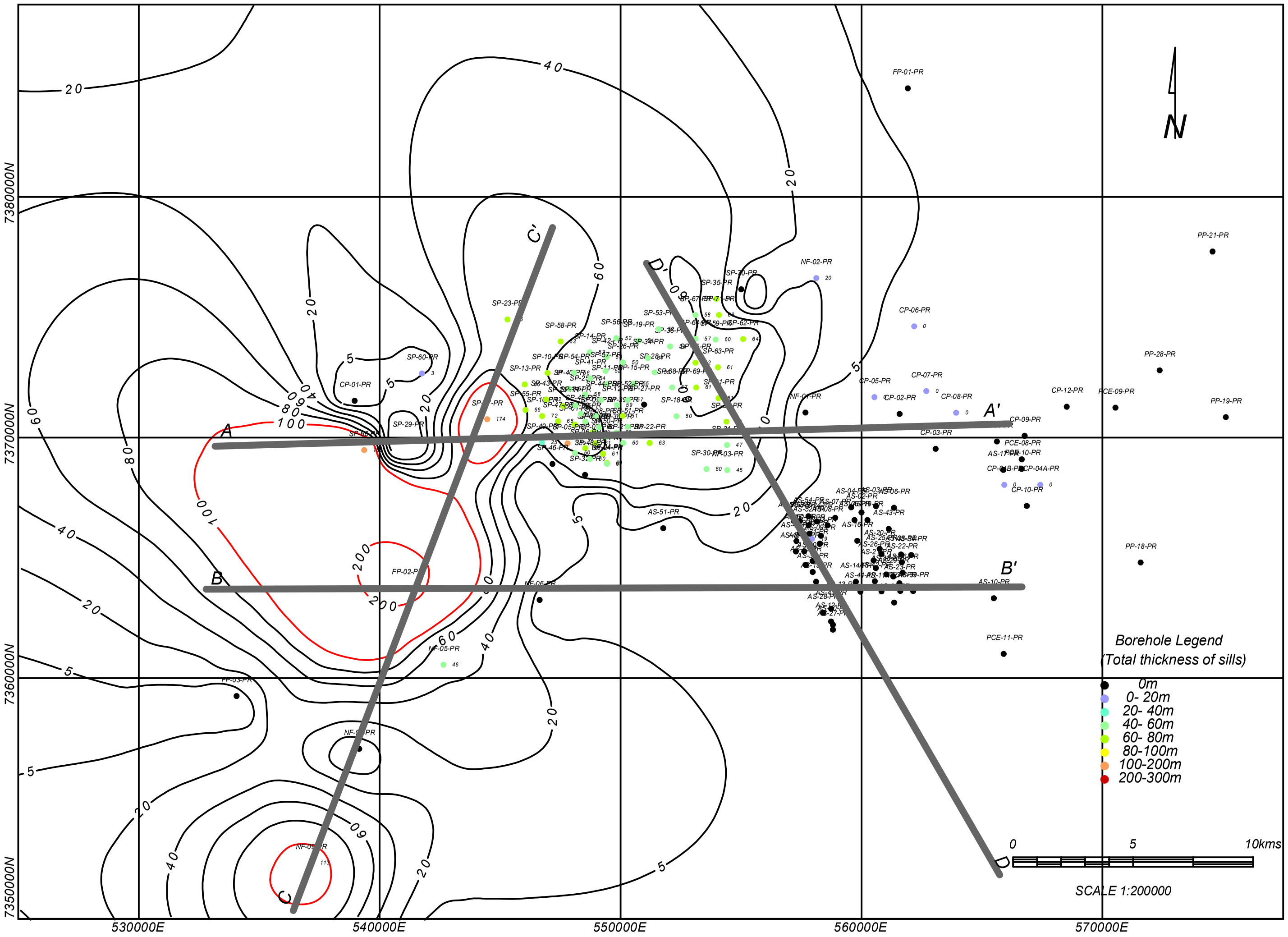

Fig.II-3-4-6 Isopach map of the total thicknessb of sills in the Ponta Grossa Arch Block

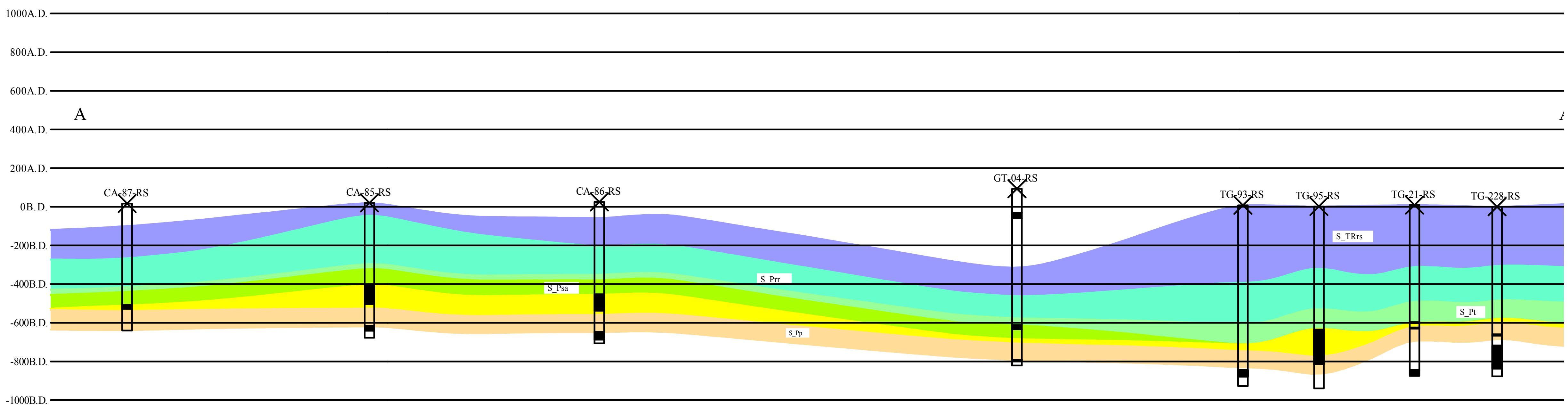

Fig.II-3-4-7 Lomba Grande Block A-A' Section (Scale; 1:250,000, H/V;1:10)

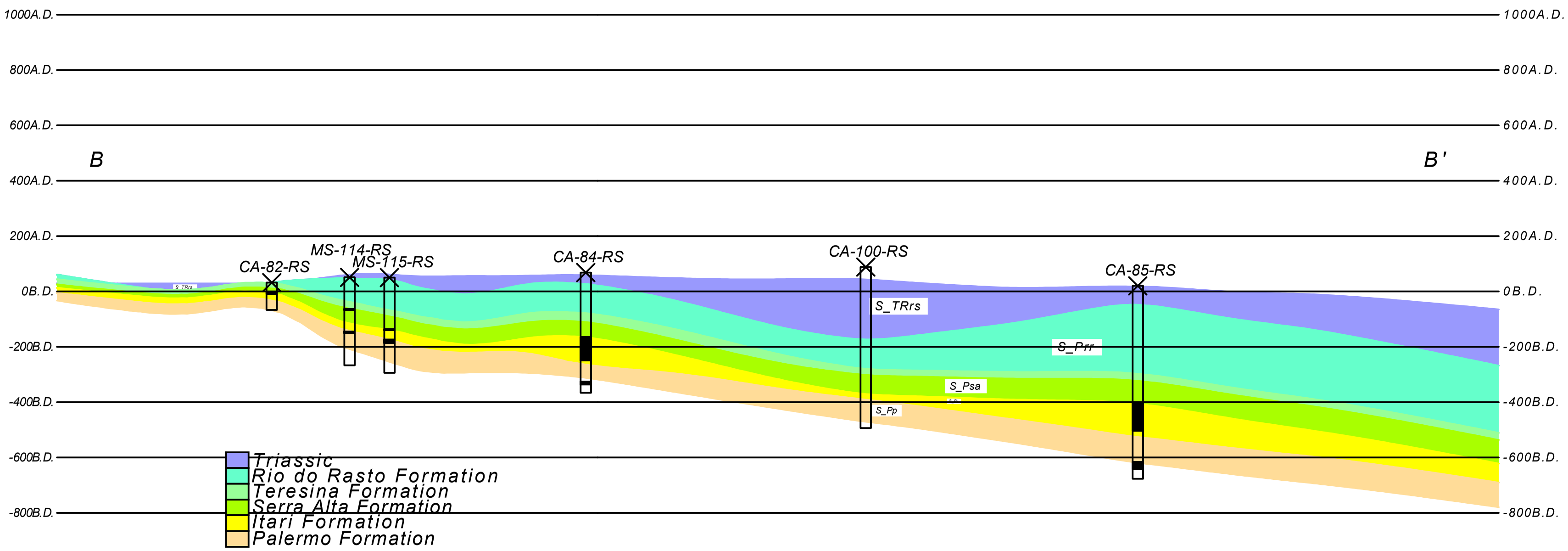

Fig.II-3-4-8 Lomba Grande Block B-B' Section (Scale; 1:250,000, H/V;1:10)

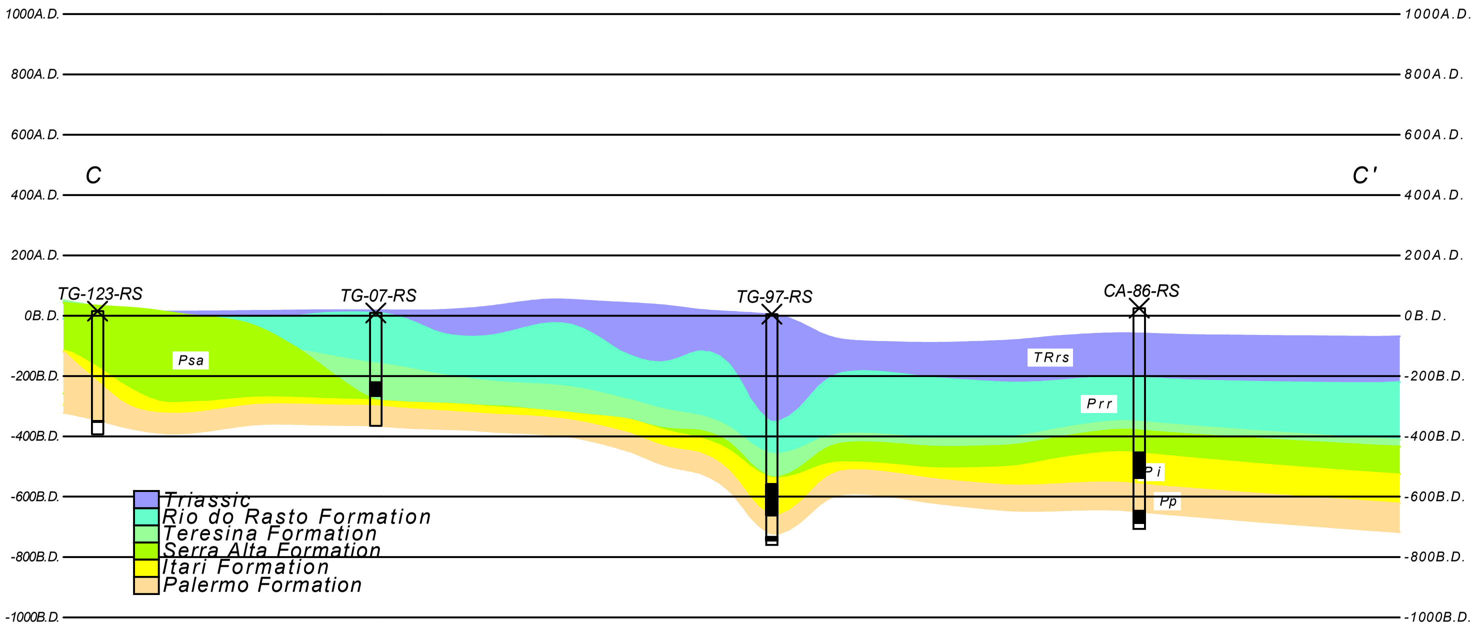

Fig.II-3-4-9 Lomba Grande Block C-C' Section (Scale; 1:250,000, H/V;1:10)

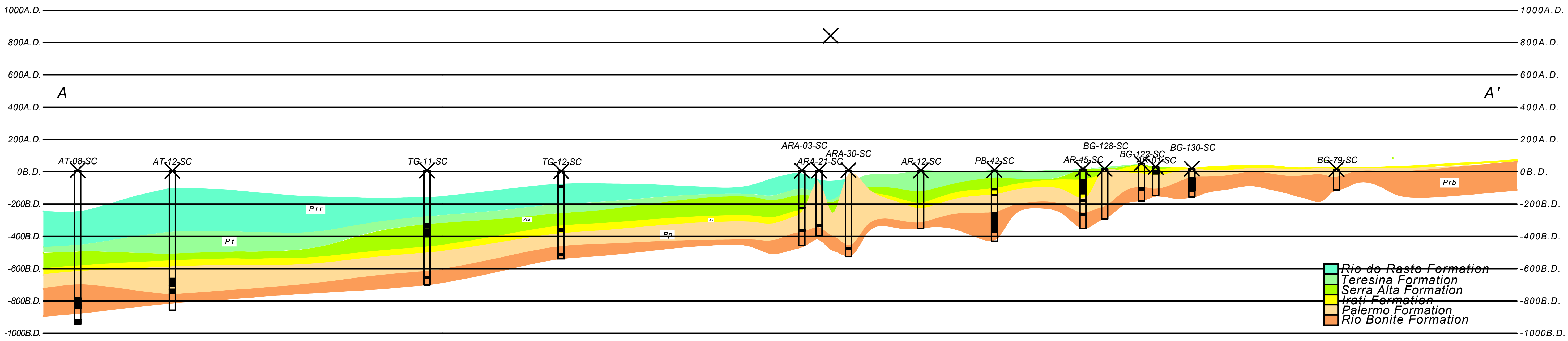

Fig.II-3-4-10 Santa Catarina Block A-A' Section (Scale; 1:250,000, H/V;1:10)

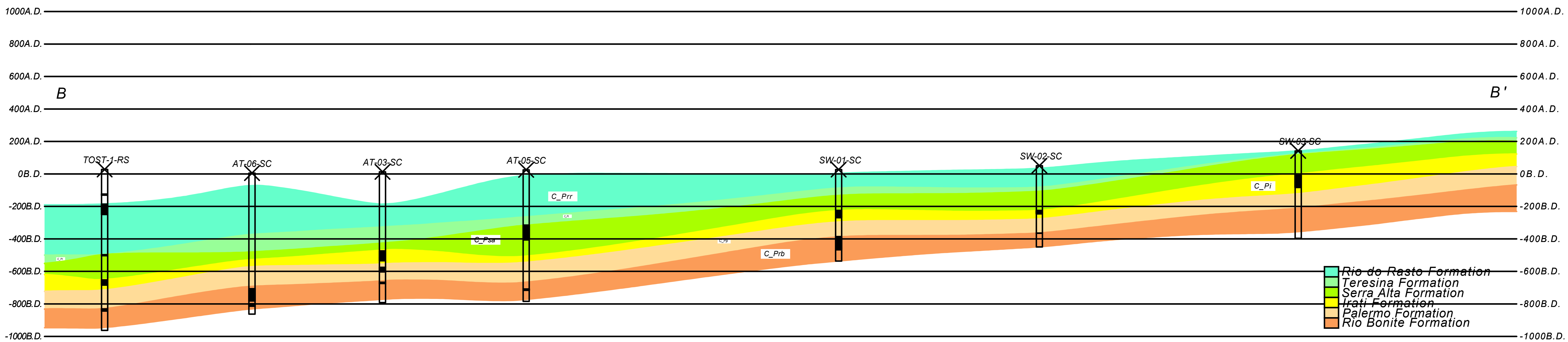

Fig.II-3-4-11 Santa Catarina Block B-B' Section (Scale; 1:250,000, H/V;1:10)

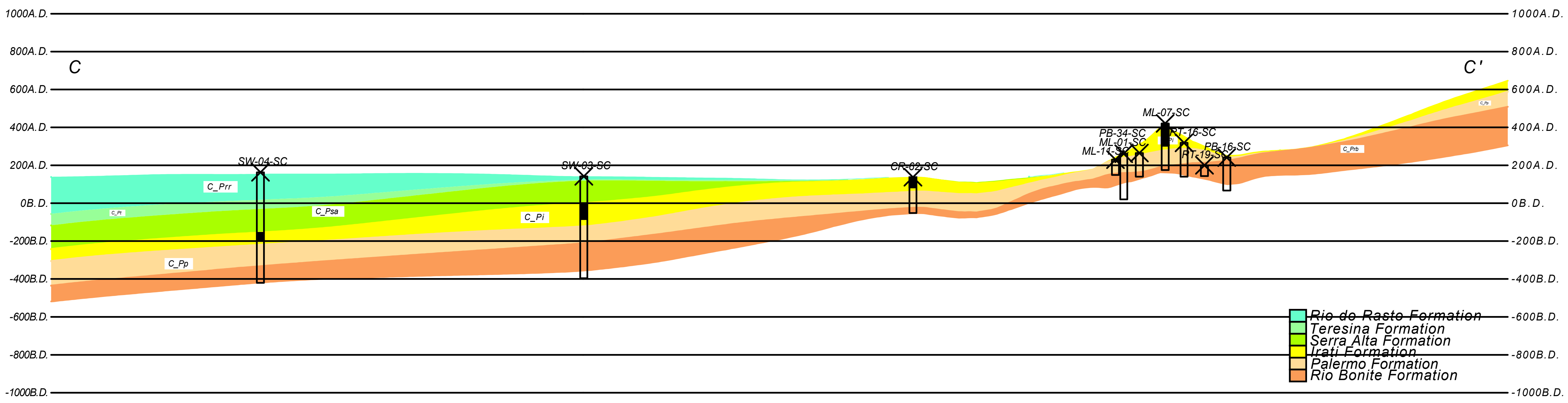

Fig.II-3-4-12 Santa Catarina Block C-C' Section (Scale; 1:250,000, H/V;1:10)

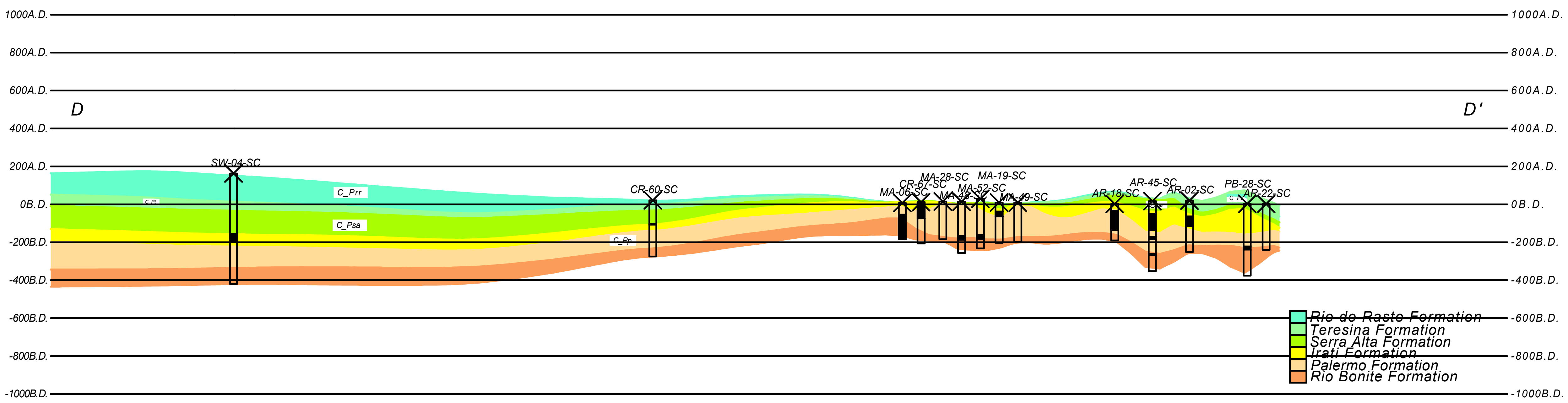

Fig.II-3-4-13 Santa Catarina Block D-D' Section (Scale; 1:250,000, H/V;1:10)

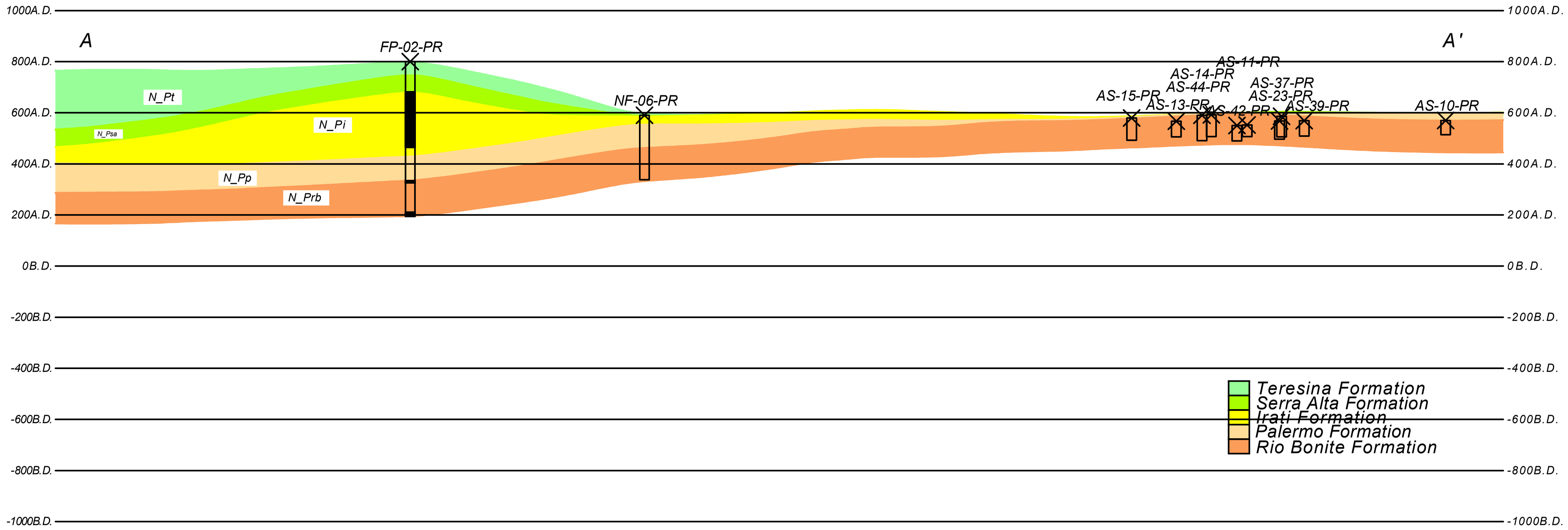

Fig.II-3-4-14　Ponta Grossa Arch Block A-A' Section (Scale;1:150,000, H/V;1:6)

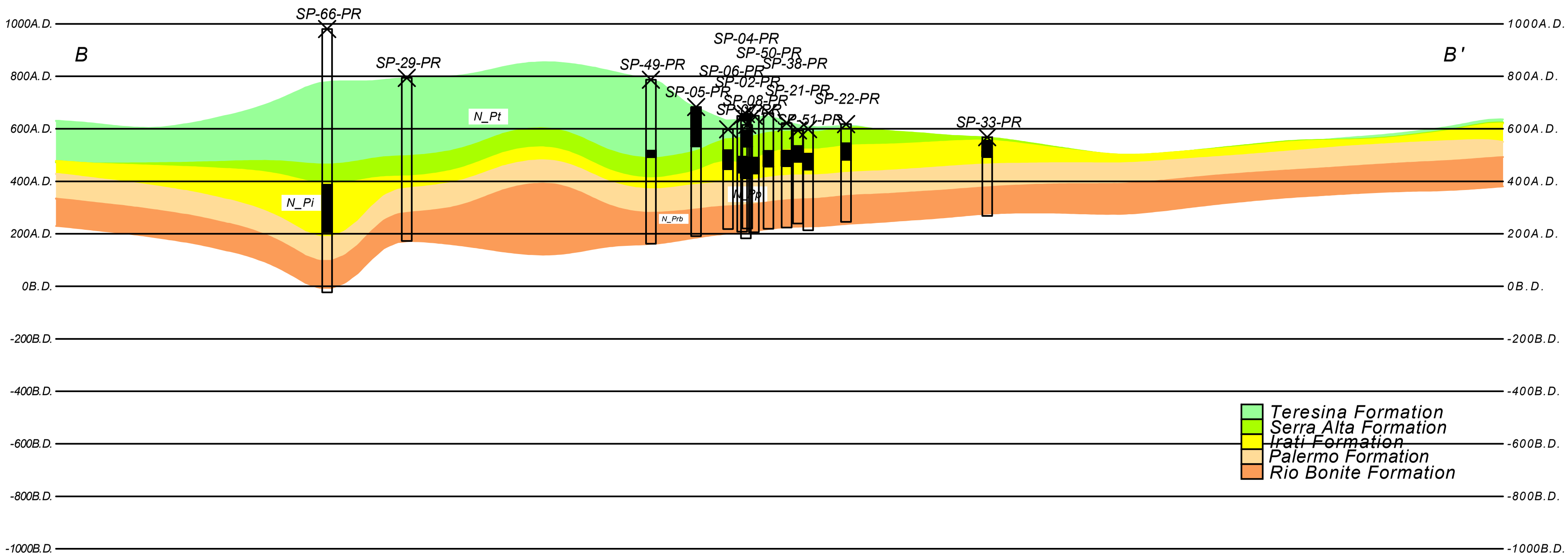

Fig.II-3-4-15 Ponta Grossa Arch Block B-B' Section (Scale;1:150,000, H/V;1:6)

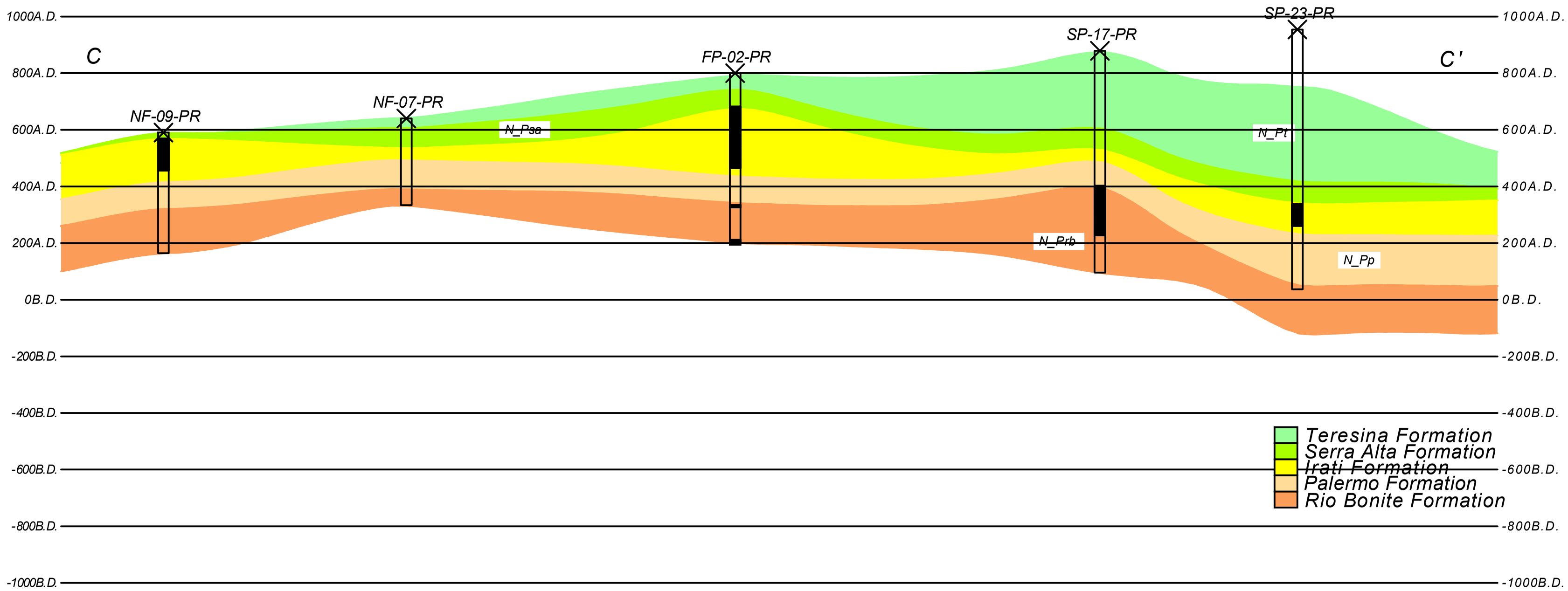

Fig.II-3-4-16 Ponta Grossa Arch Block C-C' Section (Scale;1:150,000, H/V;1:6)

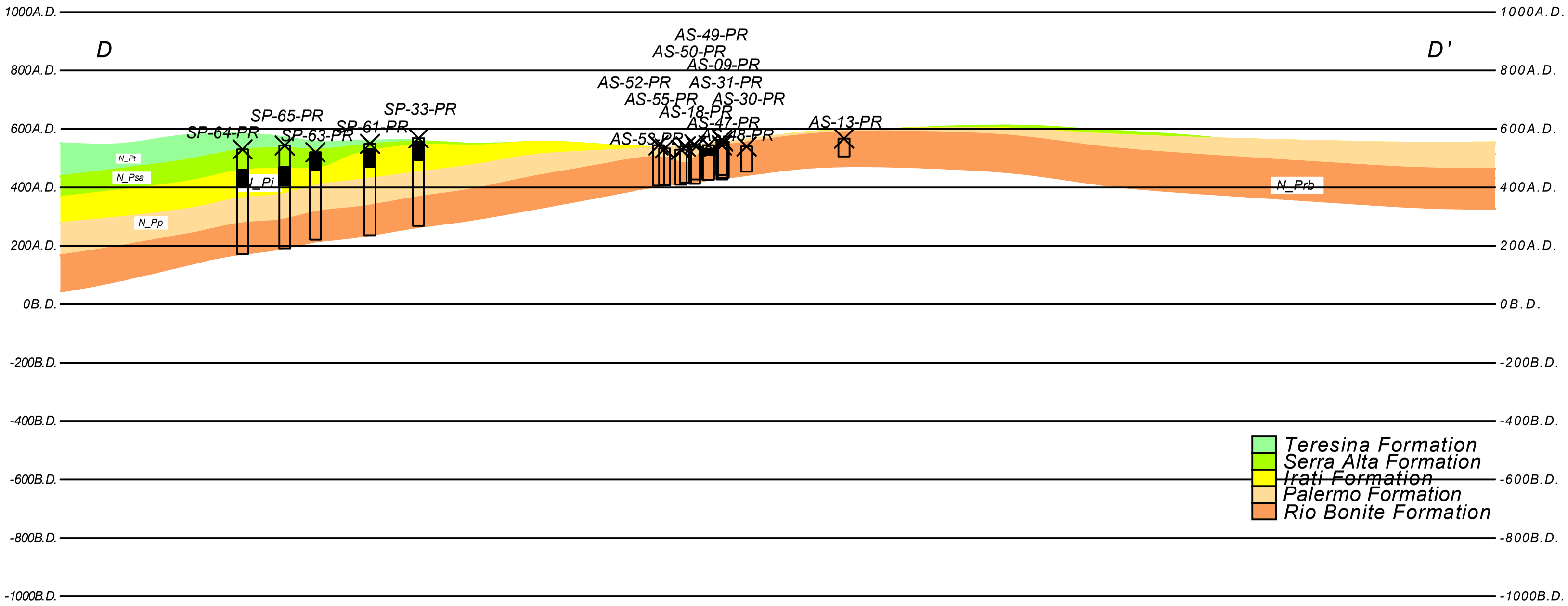

Fig.II-3-4-17 Ponta Grossa Arch Block D-D' Section (Scale;1:150,000, H/V;1:6)

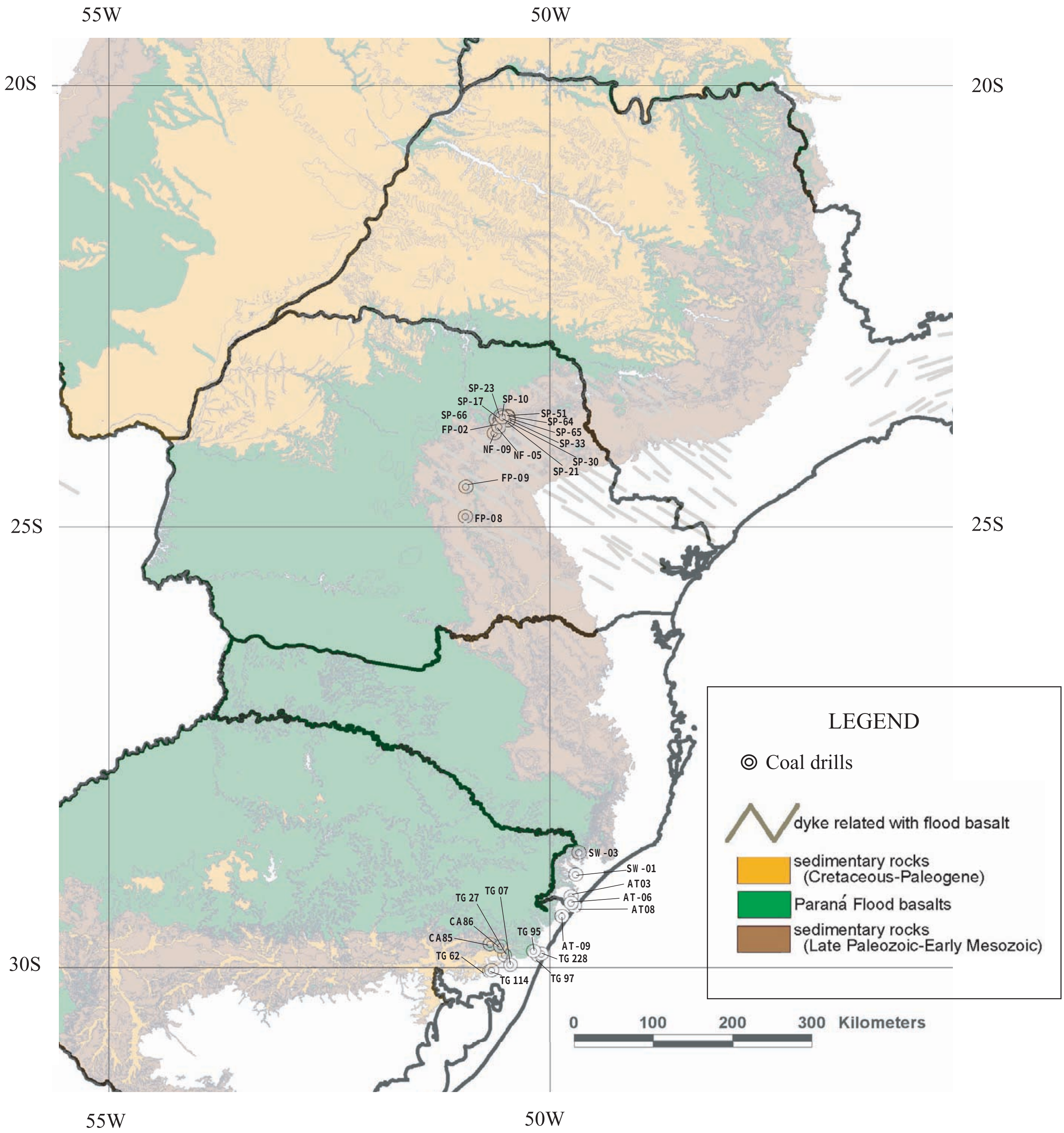

Fig.II-3-4-18 Location of the coal drills for sampling

samples at the outcrops evenly in the north to south directions along the eastern rim of the Paraná Basin. We also collected samples at drillings, namely 15 holes in the Ponta Grossa Arch block, 5 holes in the Santa Catarina block, and 10 holes in the Romba Grande block.

Most of the sills and dykes identified at outcrops were doleritic, and some were close to coarse gabbro. We also identified a number of weak disseminations of sulfides (pyrite or pyrrhotite). We identified scaly secondary pyrite (or pyrrhotite) along most cracks in the Ponta Grossa Arch, and seldom identified apparently fine primary pyrite in the matrix. All of the sills and dykes appeared to be very even and poor in changes of lithofacies. In other words, they appeared to be in a narrow range of differentiation. In case that we identified different kinds of lithofacies with samples collected at an outcrop, we collected samples by different kinds of lithofacies for analysis. However, in case of our petrochemical analysis, we used samples of lithofacies most typical of the outcrop. That is, we used more even doleritic parts as a typical of the outcrops for petrochemical analysis although coarse gabbro was partly identified in fine dolerite and medium-granular dolerite in many outcrops.

We collected doleritic (partly gabbro) samples from drilling cores. According to the drilling samples, we recognized an aphyric chilled margin in the part that contact with a country rock, where the dissemination of pyrite was rather marked. In particular, a strong dissemination of sulfides was observed in the drilling samples of the Ponta Grossa Arch, and in AT-03, AT-08, and SW-01 holes in the Santa Catarina block. Meanwhile, drillings in the Romba Grande block indicated a weak dissemination of sulfides. The drilling samples of the Ponta Grossa Arch block and the Santa Catarina block indicated a very small amount of fine chalcopyrite. We also identified coarse native copper in pore-space at the contact between a sill and its upper shale in the Santa Catarina block AT-03 hole.

We performed petrochemical analysis of these outcrop samples and drilling core samples. We also collected samples in 10- to 20-meter intervals from the AT-03, AT-08, TG-95, TG-97, TG-228, TG-62, and TG-114 drilling cores to examine vertical element fluctuations in sills. The specification of chemical analysis is the same as that of lava.

3-4-4 Petrochemistry of Intrusions

(1) Compositional Variations with Differentiation

Fig.II-3-4-19 to Fig.II-3-4-21 show variations in major element compositions while Fig.II-3-4-22 to Fig.II-3-4-24 show variations in trace element compositions. Fig.II-3-4-25 to Fig.II-3-4-26 show variations in metal element compositions. Using the classification standard similar to that of lava samples, we also classified all of the samples into the Low-Ti type (Gramado, Esmeralda), Intermediate-Ti type (Paranapanema-Ribeira), and High-Ti type (Pitanga, Urubici). When compared with lava samples, the intrusion samples had a low

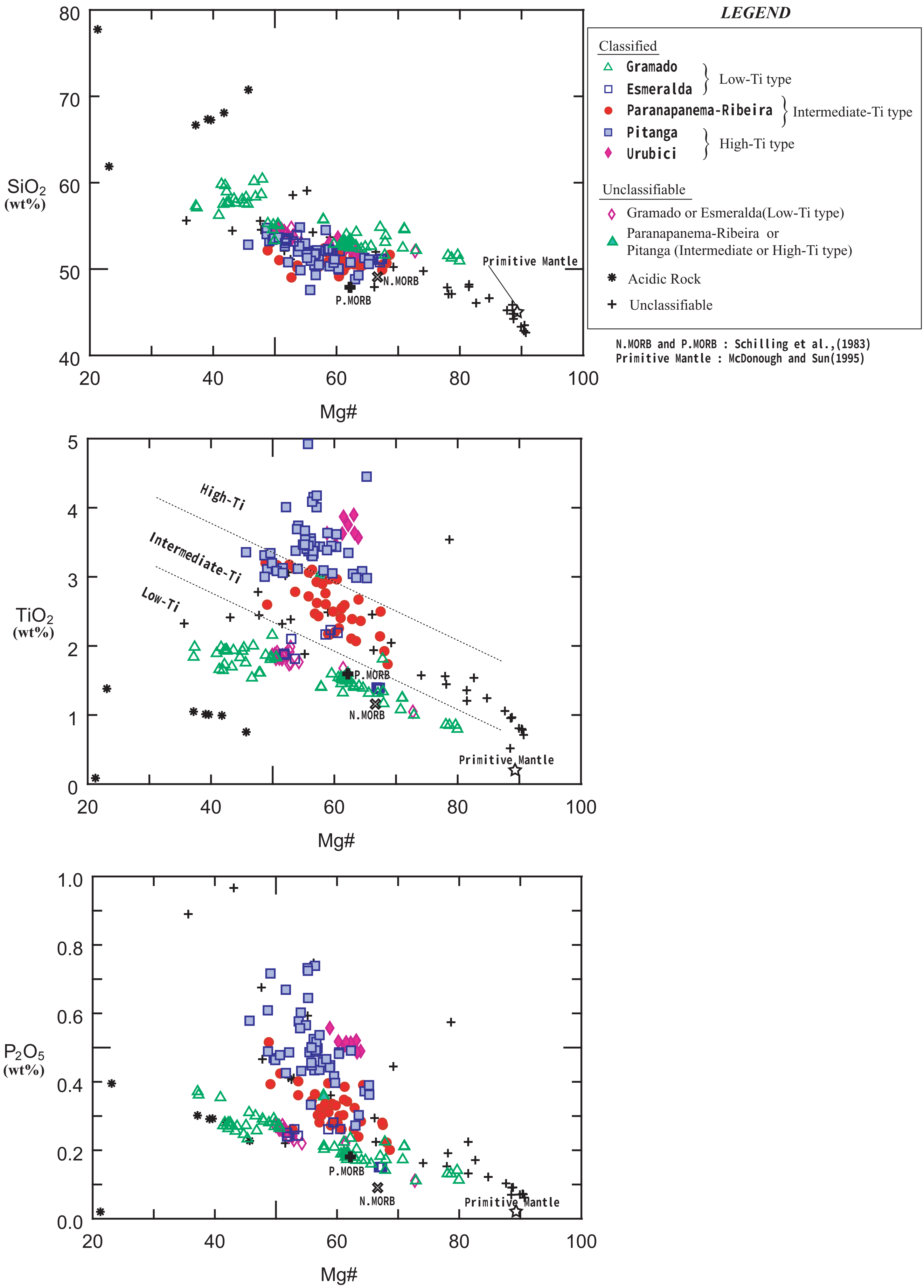

Fig.II-3-4-19 Mg# vs. major element diagrams(SiO_2, TiO_2, P_2O_5) for intrusive rocks

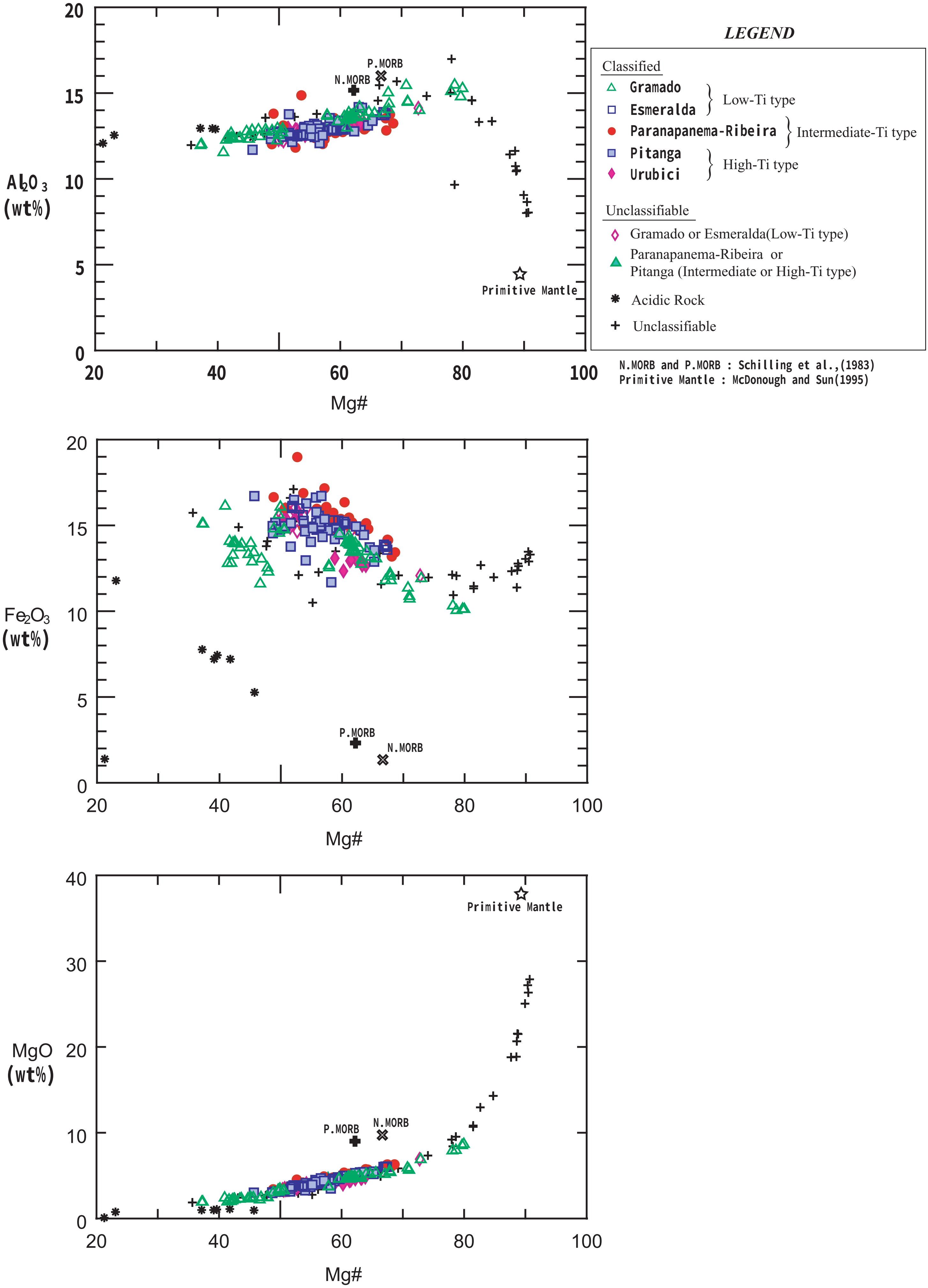

Fig.II-3-4-20 Mg# vs. major element diagrams(Al_2O_3, Fe_2O_3, MgO) for intrusive rocks

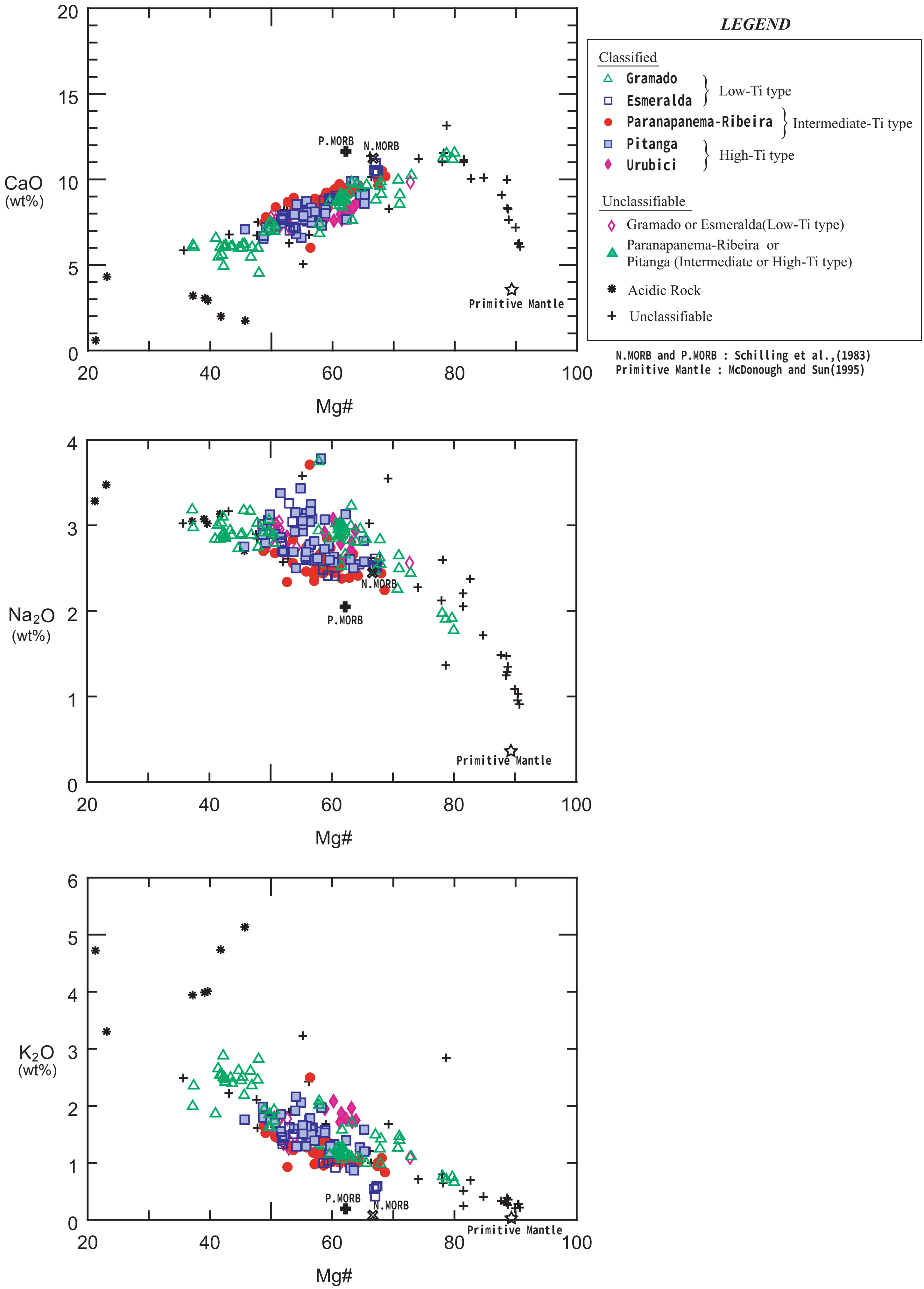

Fig.II-3-4-21 Mg# vs. major element diagrams(CaO, Na_2O, K_2O) for intrusive rocks

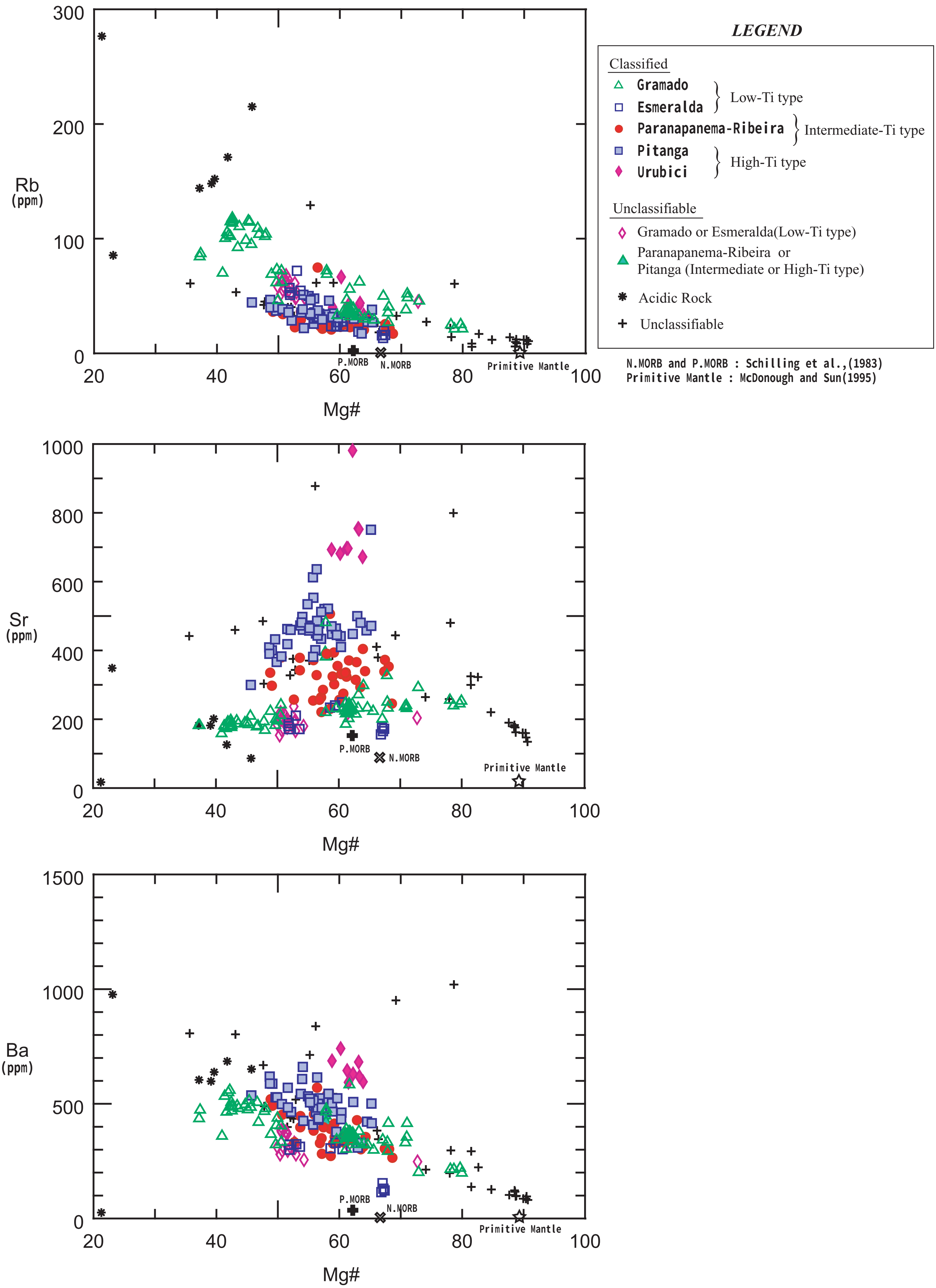

Fig.II-3-4-22 Mg# vs. trace element diagrams(Rb, Sr, Ba) for intrusive rocks

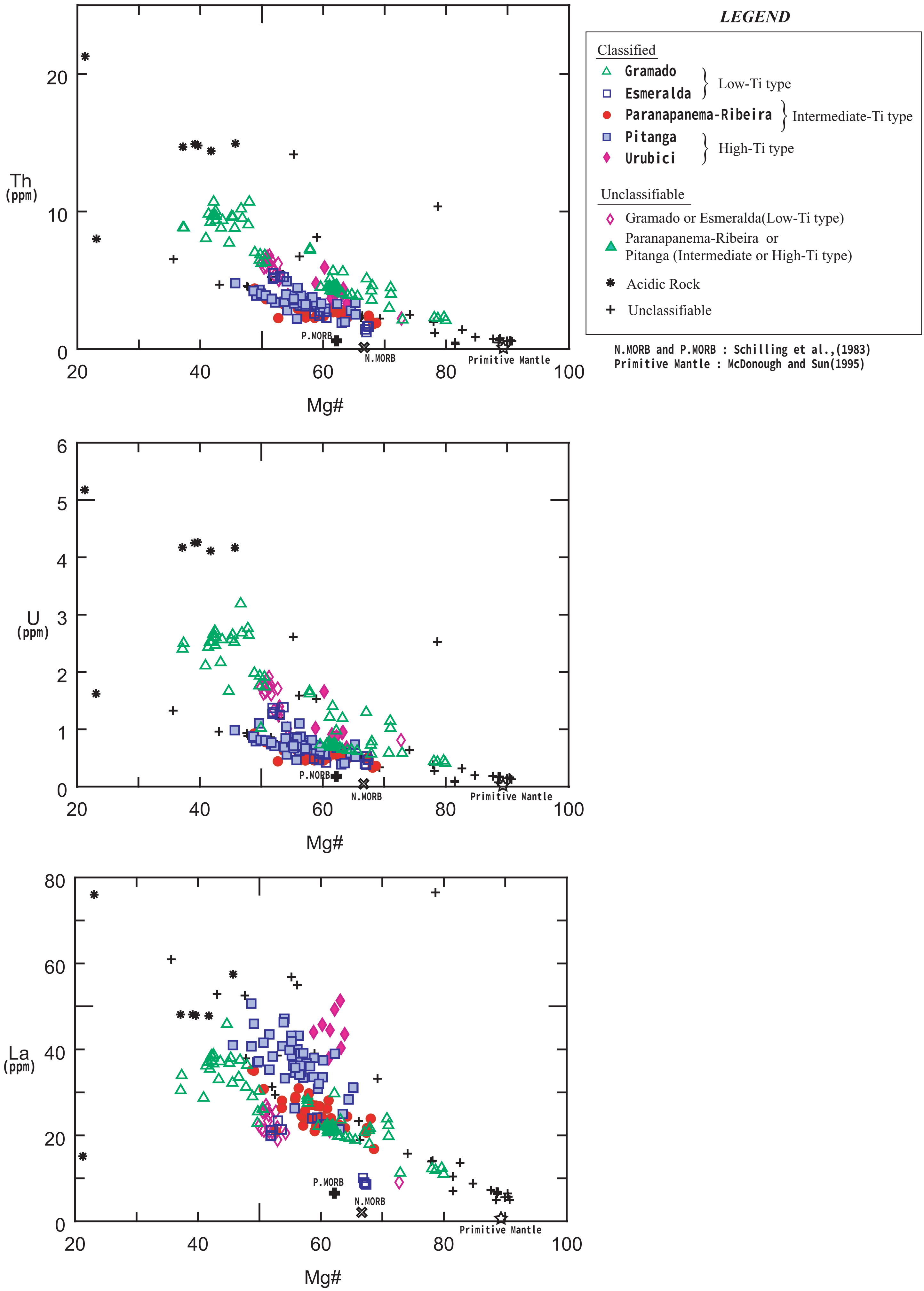

Fig.II-3-4-23 Mg# vs. trace element diagrams(Th, U, La) for intrusive rocks

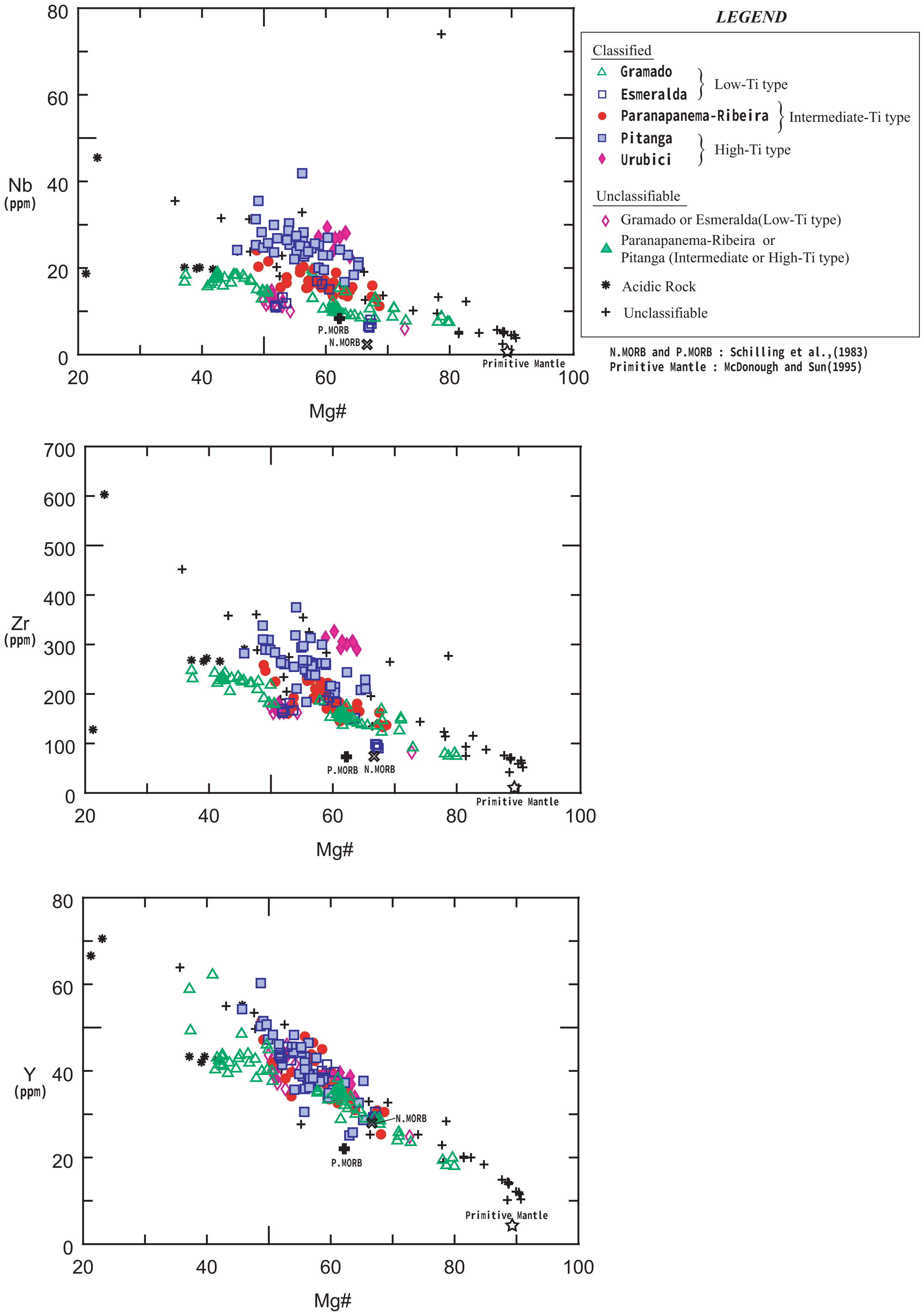

Fig.II-3-4-24 Mg# vs. trace element diagrams(Nb, Zr, Y) for intrusive rocks

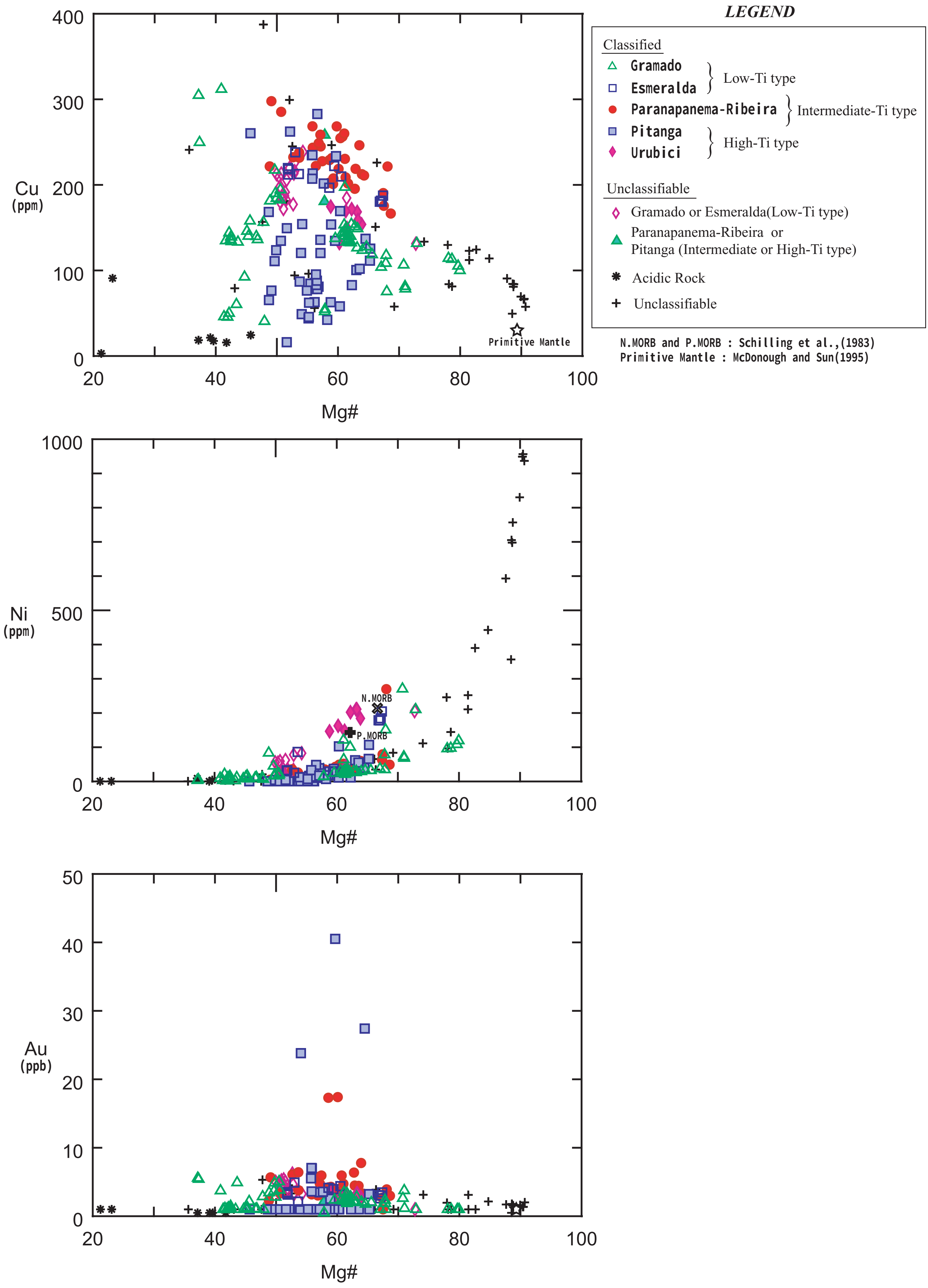

Fig.II-3-4-25 Mg# vs. chalcophile element diagrams(Cu, Ni, Au) for intrusive rocks

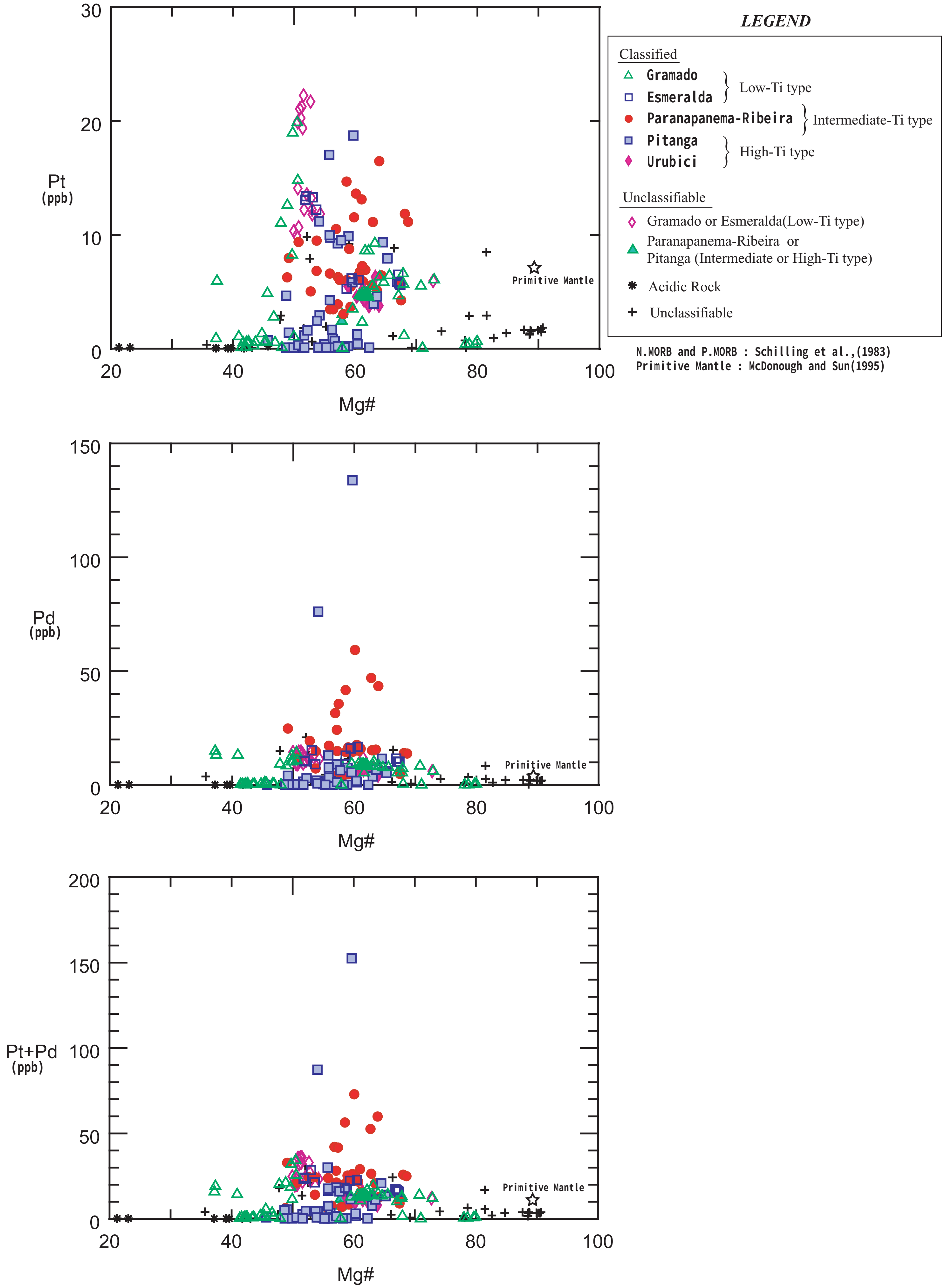

Fig.II-3-4-26 Mg# vs. chalcophile element diagrams(Pt, Pd, Pt+Pd) for intrusive rocks

identification rate. We often found it impossible to classify the samples into the types mentioned above. In particular, we often found the case that it is impossible to distinguish Low-Ti type Gramado from Esmeralda of the same type, and Intermediate-Ti type Paranapanema-Ribeira from High-Ti type Pitanga. This is because the phenocryst of the intrusion samples was coarse compared with that of lava samples, crystal accumulation after the intrusion was estimated to have influenced the compositions of the magma.

We could recognize the distribution of Pitanga in the north area surveyed, Gramado, Esmeralda, and Urubici in the southern area surveyed, and Pitanga and Paranapanema-Ribeira in the Ponta Grossa Arch of the central area surveyed (see Fig.II-3-3-3). Such distribution pattern observed in the magma types of intrusion samples is the same as that of lava samples.

Concerning the magma compositions, we identified that all the sills distributed in the northern to central areas surveyed are basaltic and narrow in magma composition range. Meanwhile, the compositions of the sills distributed in the southern area surveyed varied, from picritic to andesitic. They have similar association with that observed in the Noril'sk region. Regarding picritic rocks, we found it impossible to classify these rocks (for example, the Romba Grande intrusion in a vicinity of Porto Alegre) into any type of the magmas defined in the classification criteria of Peate et al.(1992).

Concerning the major element compositions (Fig.II-3-4-19 to Fig.II-3-4-21), as indicated in the Canada-Brazil cooperative survey report, the fractionation of olivine played the major role in the initial stage of crystallization differentiation (up to around 80 of Mg number) according to changes in compositions of Al_2O_3, CaO, and MgO before clinopyroxene and plagioclase played the major role of fractionation. When compared with the same Mg number, Gramado contains much SiO_2 and K_2O. P_2O_5 and TiO_2 indicated the similar behavior. Their unique composition range was identified in each of the Low-Ti, Intermediate-Ti, and High-Ti magma types.

Concerning trace element compositions (Fig.II-3-4-22 to Fig.II-3-4-24), LIL (Large Ion Lithophile) elements, including Th, U, and Rb, were found much in Low-Ti type Gramado. On the other hand, HFS (High Field Strength) elements, including Nb and Zr, were concentrated in High-Ti type Pitanga. It seems that Intermediate-Ti type Paranapanema-Ribeira was characterized as middle between these types.

Concerning compositions of metal elements (Fig.II-3-4-25 to Fig.II-3-4-26), as indicated in the Canada-Brazil cooperative survey report, gaps were observed between the compositions of Pt and Pd; it seemed some samples depleted in these elements while other samples included these elements. Samples depleted in these elements were found much in Gramado and Pitanga. Paranapanema-Ribeira had a lot of contents of Pt, Pd, and Au, and hardly had depleted samples. Urubici was characterized as having samples with much Ni content even they were relatively differentiated (Mg number 60 or so).

(2) Degree of Partial Melting and Crustal Contamination

Fig.II-3-4-27 shows relationships between Th/Nb, Th/Ta and Gd/Yb. Although Th/Nb and Th/Ta hardly indicate changes in crystallization differentiation, these ratios seem to have a sharp increase due to contaminations of granitic materials in the upper part of the continental crust. The Gd/Yb also indicates an index value of degree of partial melting of mantle materials under a presence of residual garnet.

Based on these diagrams, we estimate that degree of partial melting becomes smaller in the following order; Low-Ti type(Esmeralda(largest)), Gramado), Intermediate-Ti (Paranapanema - Ribeira), High-Ti type(Pitanga, Urubici(smallest)). This is the same as the result of our lava examinations.

Concerning Gramado and Esmeralda of Low-Ti type, we recognized some crustal contamination, especially in Gramado. The fact is consistent with the fact that Gramado is rich in SiO_2, K_2O, Rb, U, and Th. A presence of acidic rock in the southern Paraná Basin is likely to have some relation in the formation of Gramado. Our examination of the compositions of the acidic rock revealed that the Gd/Yb is almost the same as Gramado and that the Th/Nb and Th/Ta are plotted onto the extension line of the Gramado trend. Accordingly, the possible contaminant of Gramado is estimated to be the source material of the acidic rock. On the other hand, the magmas of High-Ti type(Pitanga, and Urubici) and Intermediate-Ti type(Paranapanema - Ribeira) had a minor influence of crustal contamination.

For typical samples, we measured the Sr isotopic ratio ($^{87}Sr/^{86}Sr$) and the Nd isotopic ratio ($^{143}Nd/^{144}Nd$). After adjusting all of the isotopic ratios measured to the initial ratios (130Ma), we plotted them into Fig.II-3-8-28. Gramado indicated high Sr isotopic ratios and a low Nd isotopic ratios, suggesting some contamination of crustal materials. Meanwhile, we estimated that the degrees of contamination of Paranapanema-Ribeira and Pitanga are weak. In this way, our examinations of the Sr isotopic ratio and the Nd isotopic ratio indicated a consistent result with the result of trace element examination.

(3) Vertical Compositional Variations of Sills

We examined vertical variations of element concentrations within the sills identified in the At-03, AT-08, TG-95, TG-97, TG-228, TG-62, and TG-114 holes (Fig.II-3-4-18) in the southern areas surveyed. Fig. II-3-4-29 to Fig.II-3-4-35 indicate vertical variations of element concentrations with individual drillings.

・AT-03 Hole and AT-08 Hole

The AT-03 hole and the AT-08 hole are located at the southernmost part of the Santa Catarina block in the border with Rio Grande do Sul Province. We estimate that these drillings

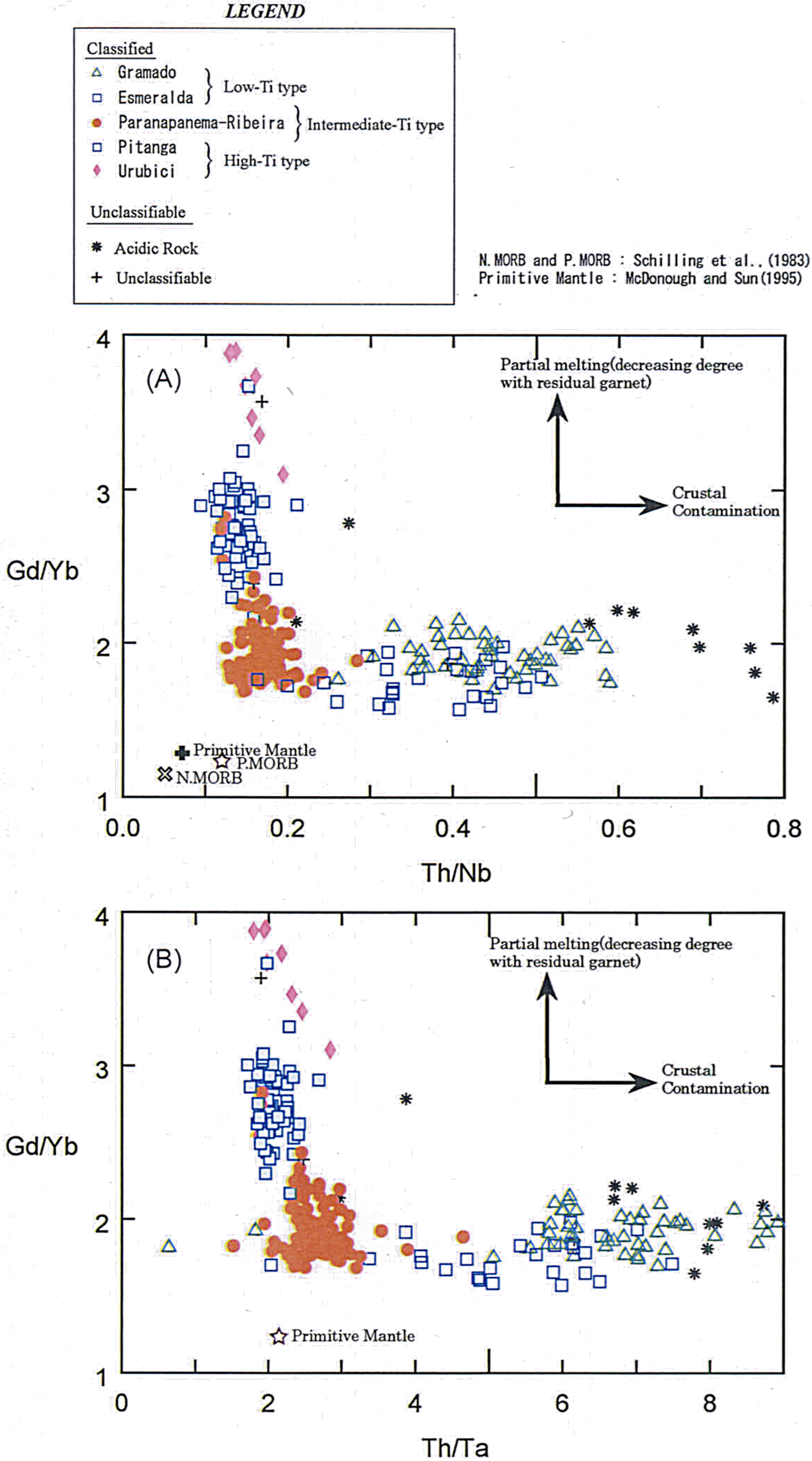

Fig. II-3-4-27 (A) Th/Nb - Gd/Yb diagram for intrusive rocks;
(B) Th/Ta - Gd/Yb diagram for intrusive rocks

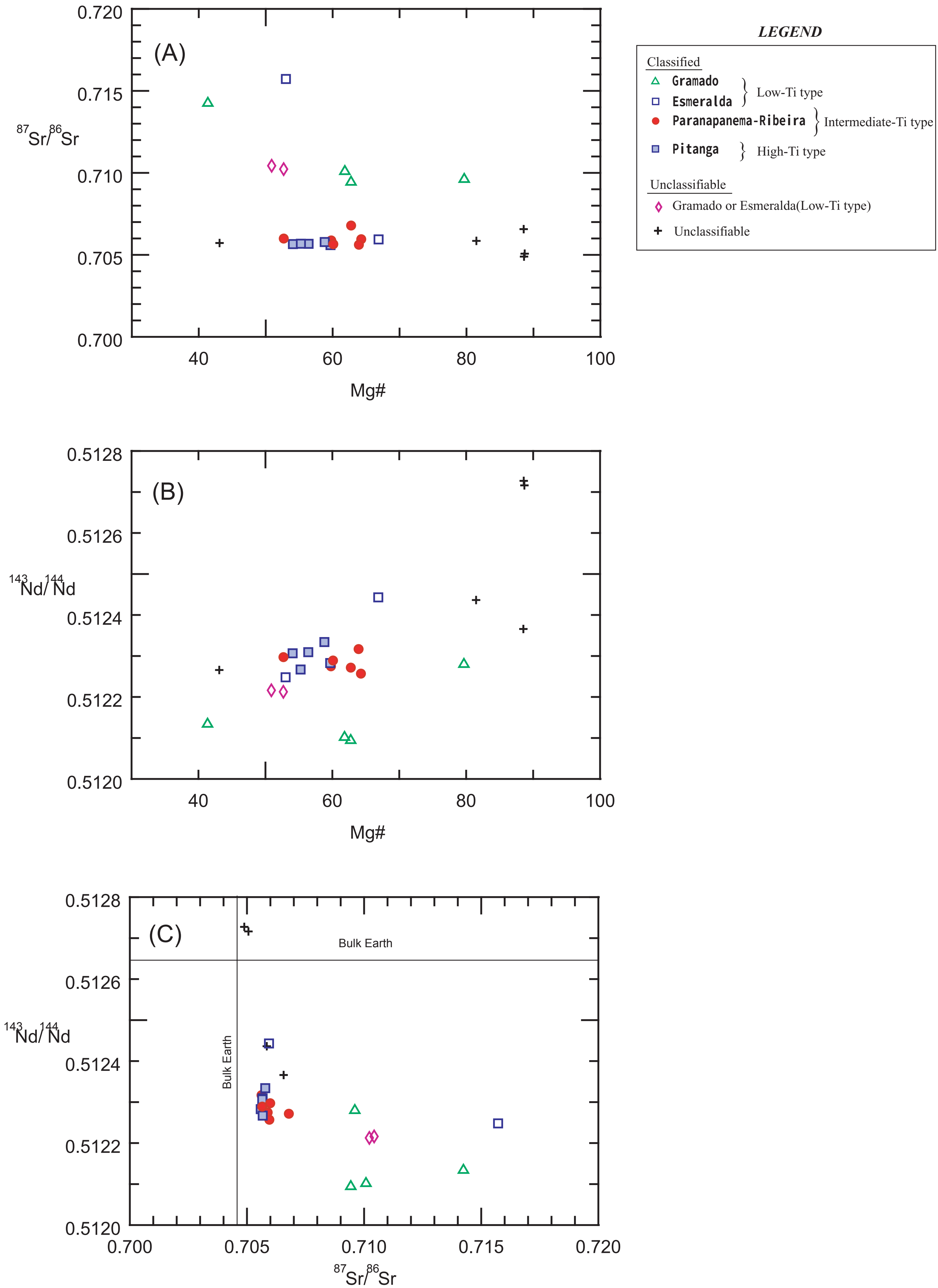

Fig.II-3-4-28 (A) Mg-number - Sr-isotope initial ratio diagram; (B) Mg-number - Nd-isotope initial ratio diagram; (C) Sr-isotope initial ratio - Nd-isotope initial ratio diagram

intruded into the same sill. The thickness of the sill intruded by the AT-03 hole stood at 131m, while that of the AT-08 stood at 155m. The both drillings indicated that a sedimentary rock is sandwiched between sills and that the thickness of a continuous sill was short of 100m. The drillings indicated rich in sulfides.

The sill had SiO_2 at 53 to 55wt%, and low MgO and high Fe_2O_3 in content, compared with the sills identified at the Romba Grande block TG-95, TG-97, and TG-228 holes. Although the Ni content is almost the same with the sill of Romba Grande block, this sill is characterized as rich in Cu, Pt, and Pd. In particular, some samples had a high contents of Pt at 20ppb or higher. The both drillings indicated an increase in SiO_2, and La/Sm and depletion in Pt and Pd in the top part of the sill. An assimilation of the country rock might induce segregation of immiscible sulfide melts.

・TG-95 Hole, TG-97 Hole, and TG-228 Hole

We estimate that the TG-95, TG-97, and TG-228 holes in the Romba Grande block intruded the same sill. These three holes are poor in sulfides. The thickness of the sill intruded stood at 134 m for the TG-95 hole; 95m for the TG-97 hole; and 105m for the TG-228 hole. The sill indicated relatively homogeneous composition of around SiO_2 53wt%. TG-97 hole and TG-228 hole indicated approx. 5 ppb of Pt and approx. 9 ppb of Pd, indicating almost even contents of PGE. Two samples of the upper part of TG-95 hole indicated a rather high content of SiO_2 and depletion in Pt and Pd. An assimilation of the country rock had possibly segregated immiscible sulfide melts.

・TG-62 Hole and TG-114 Hole

The TG-62 hole and TG-114 hole in the Romba Grande block intruded a 65-meter sill and a 23-meter sill, respectively, both of which contain picritic rocks. Both drillings are poor in sulfides.

The 45-meter thick upper part of TG-62 hole is andesitic while the 20-meter thick lower part is basaltic to picritic. This indicates a marked gap of compositions, suggesting that two different types of sills may have intruded into the same location. Most of the upper andesitic part contains no Pt and Pd and has depleted completely. On the other hand, the lower basaltic to picritic part contains less than 3 ppb of Pt and Pd. The basaltic to picritic part shows a regular increase in Cu according to the progress of crystallization differentiation shown in the decrease in Ni. However, Pt and Pd remain almost the same.

Most of the samples collected at the TG-114 hole are undifferentiated basaltic to picritic ones. The top part of the drilling indicates a composition differentiated up to SiO_2 54wt%. Trends of chalcophile elements are same as those of the TG-62 hole. The basalts of differentiated composition of the top part of the drilling have depleted in Pt and Pd. An

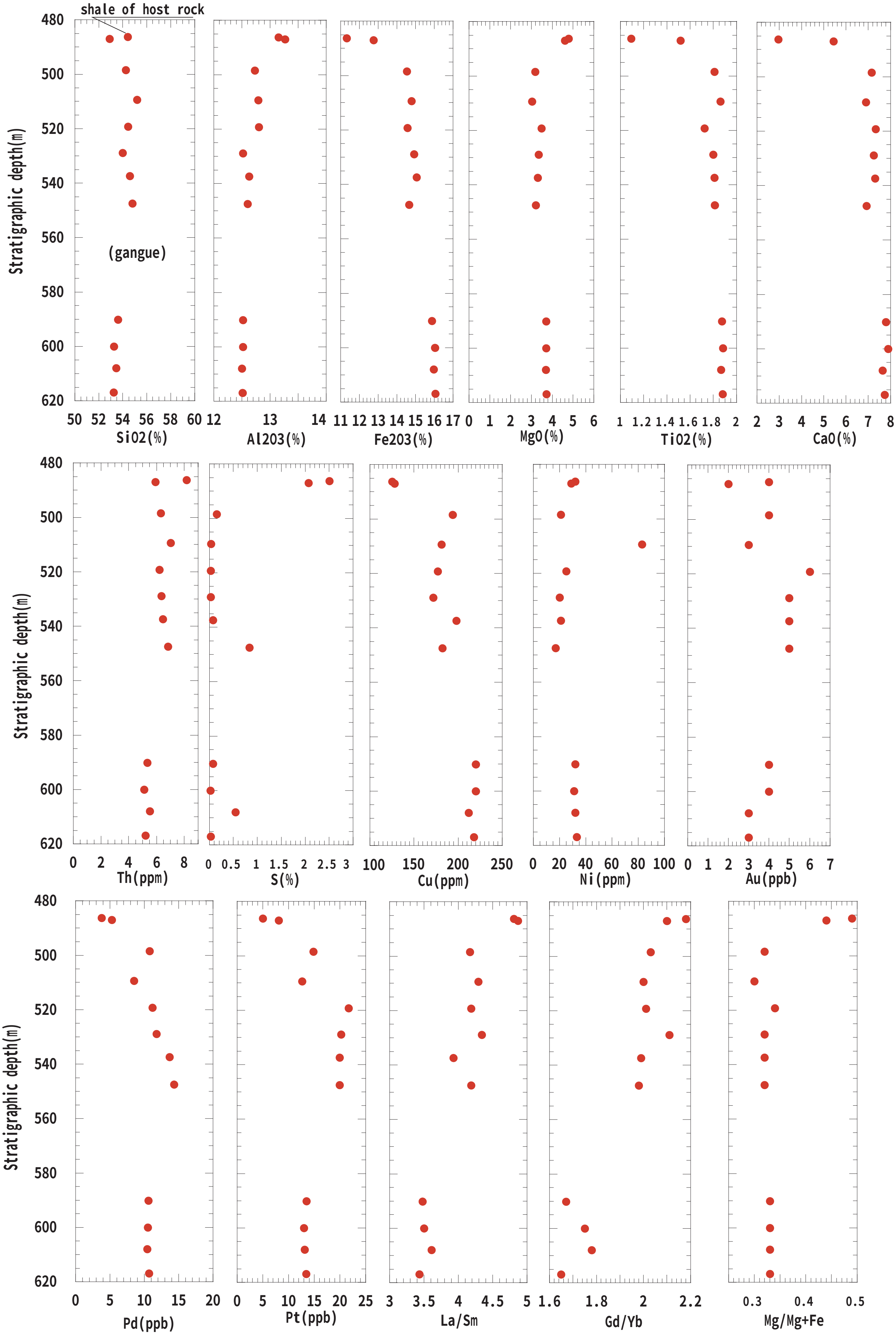

Fig.II-3-4-29 Vertical variations in major and trace-element in sill intersected by drill(AT03)

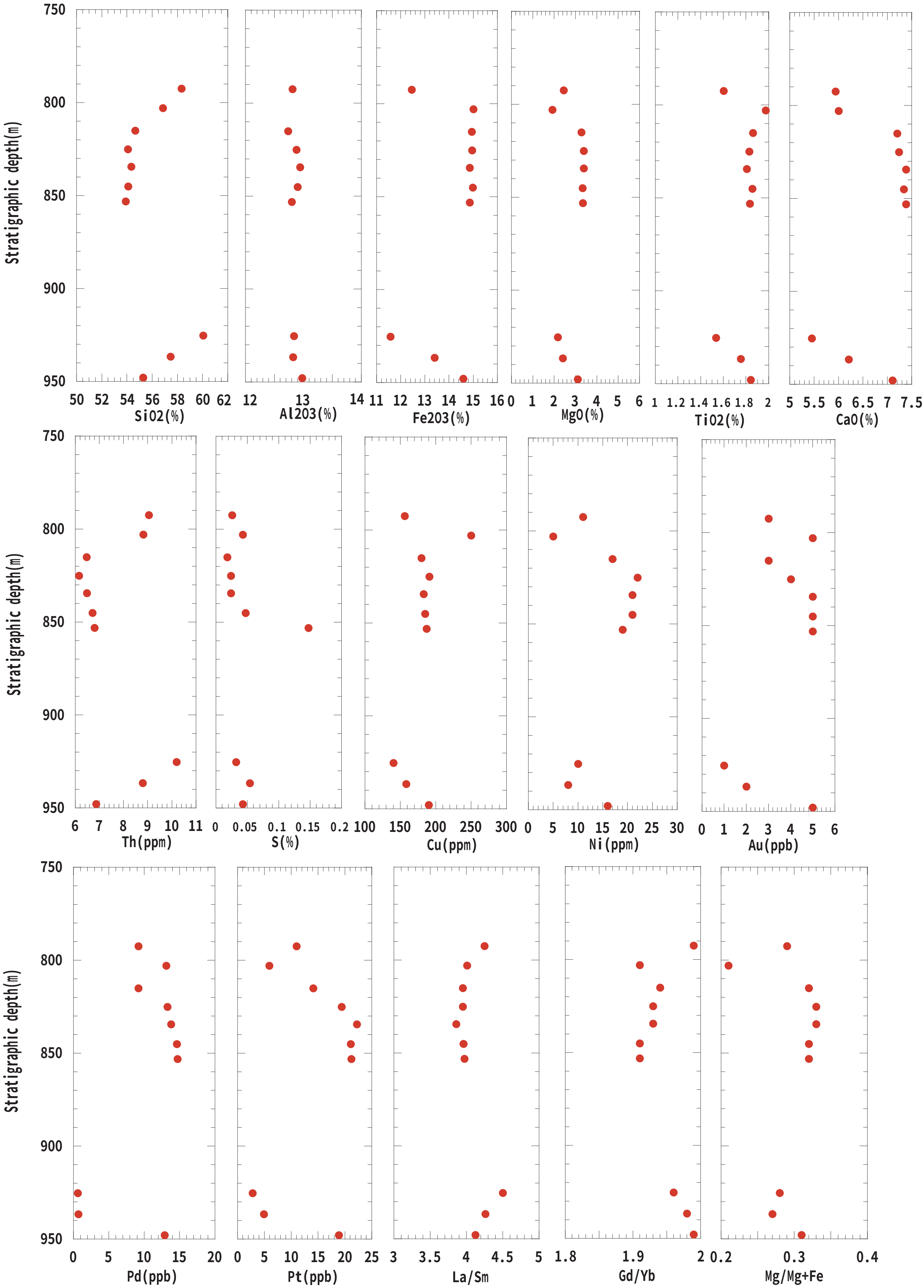

Fig.II-3-4-30 Vertical variations in major and trace-element in sill intersected by drill(AT08)

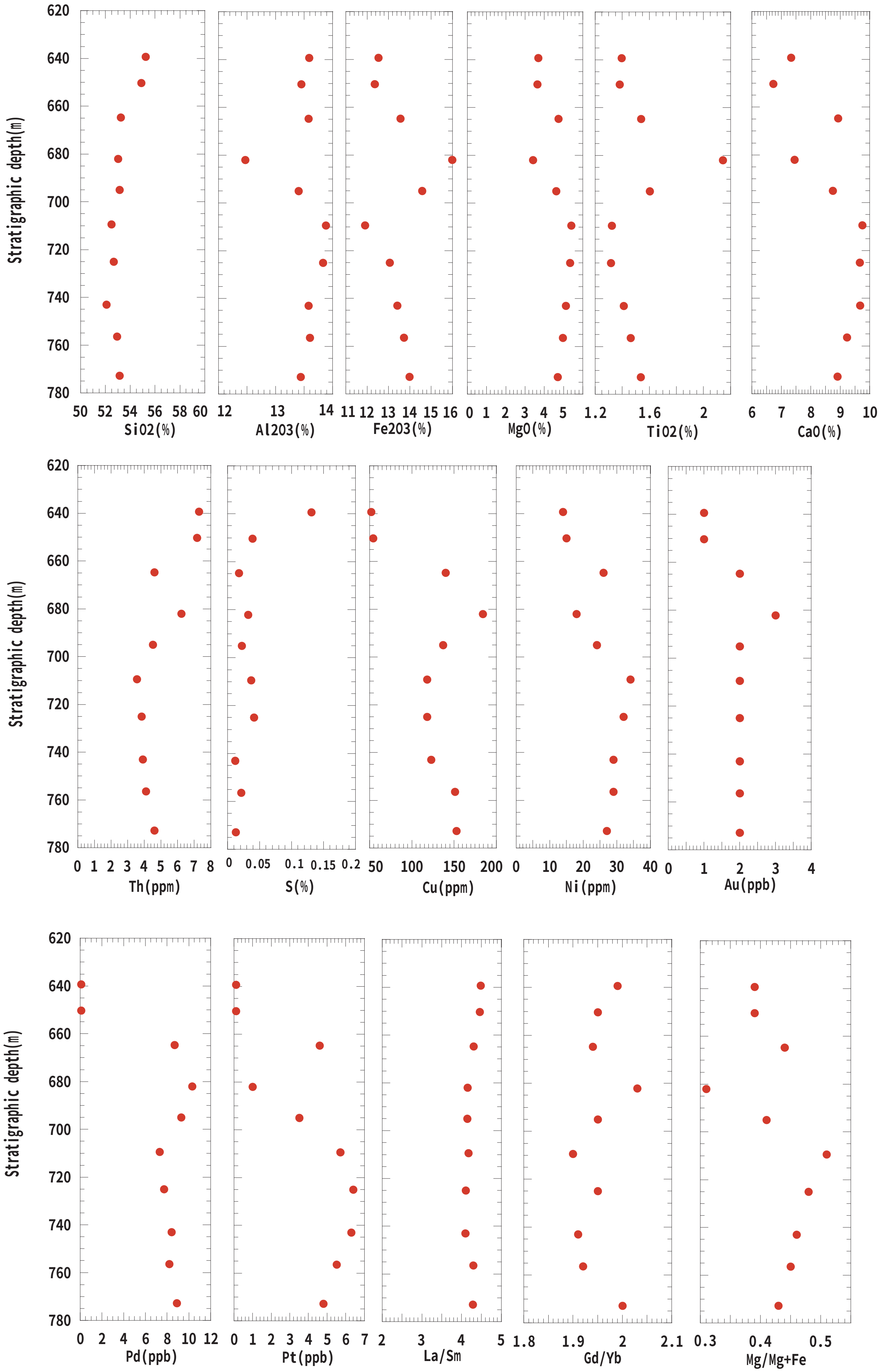

Fig.II-3-4-31 Vertical variations in major and trace-element in sill intersected by drill(TG95)

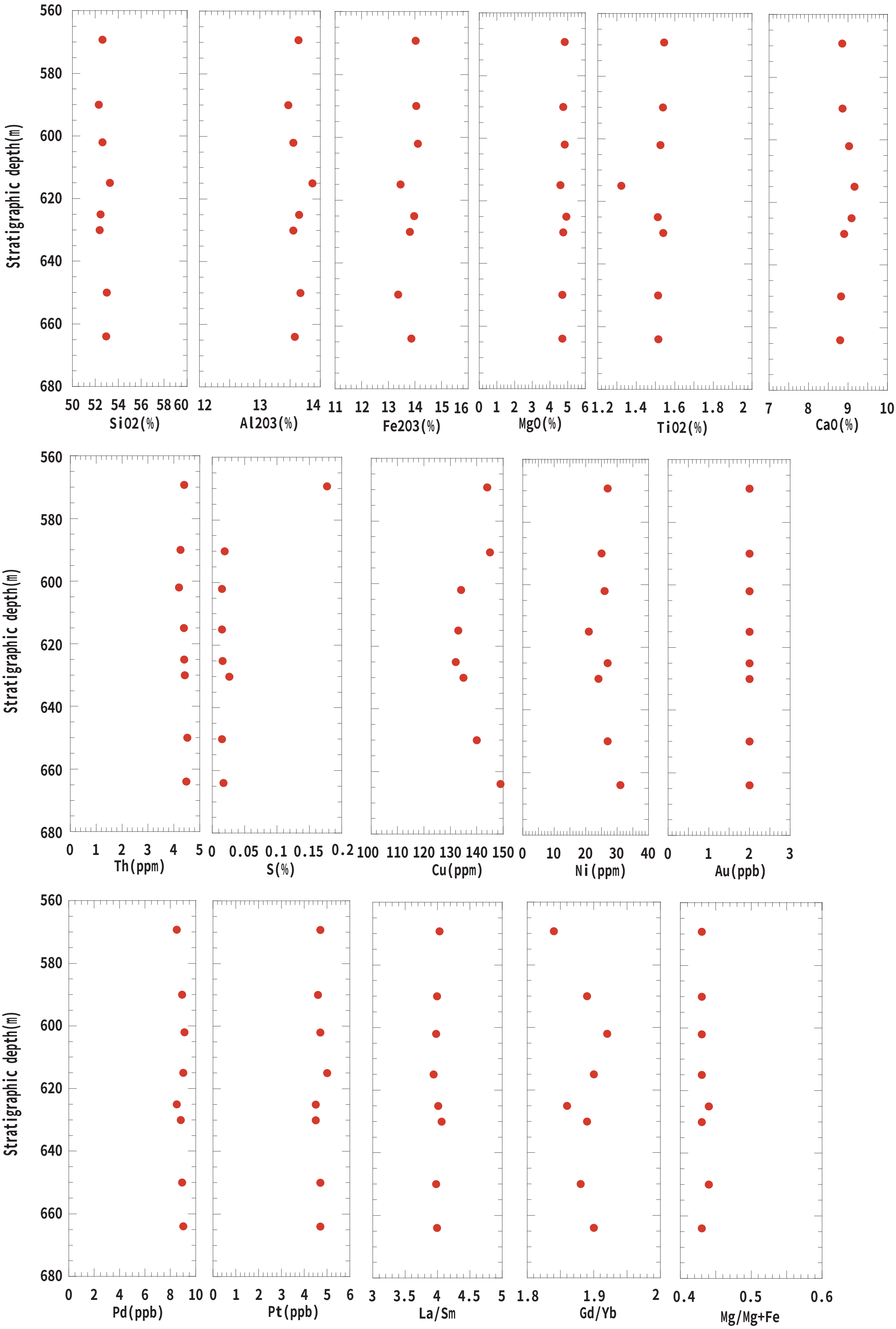

Fig.II-3-4-32 Vertical variations in major and trace-element in sill intersected by drill(TG97)

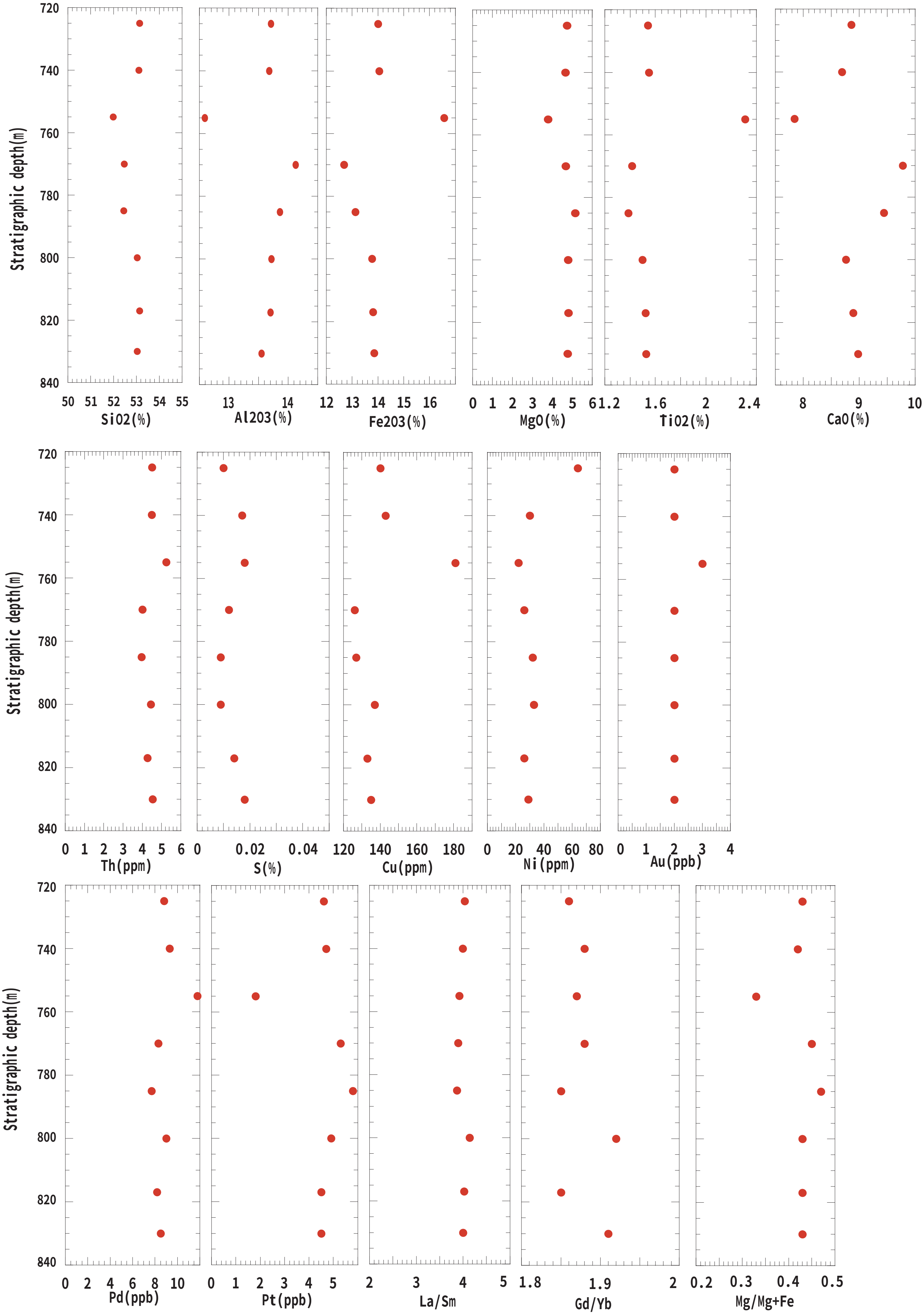

Fig.II-3-4-33 Vertical variations in major and trace-element in sill intersected by drill(TG228)

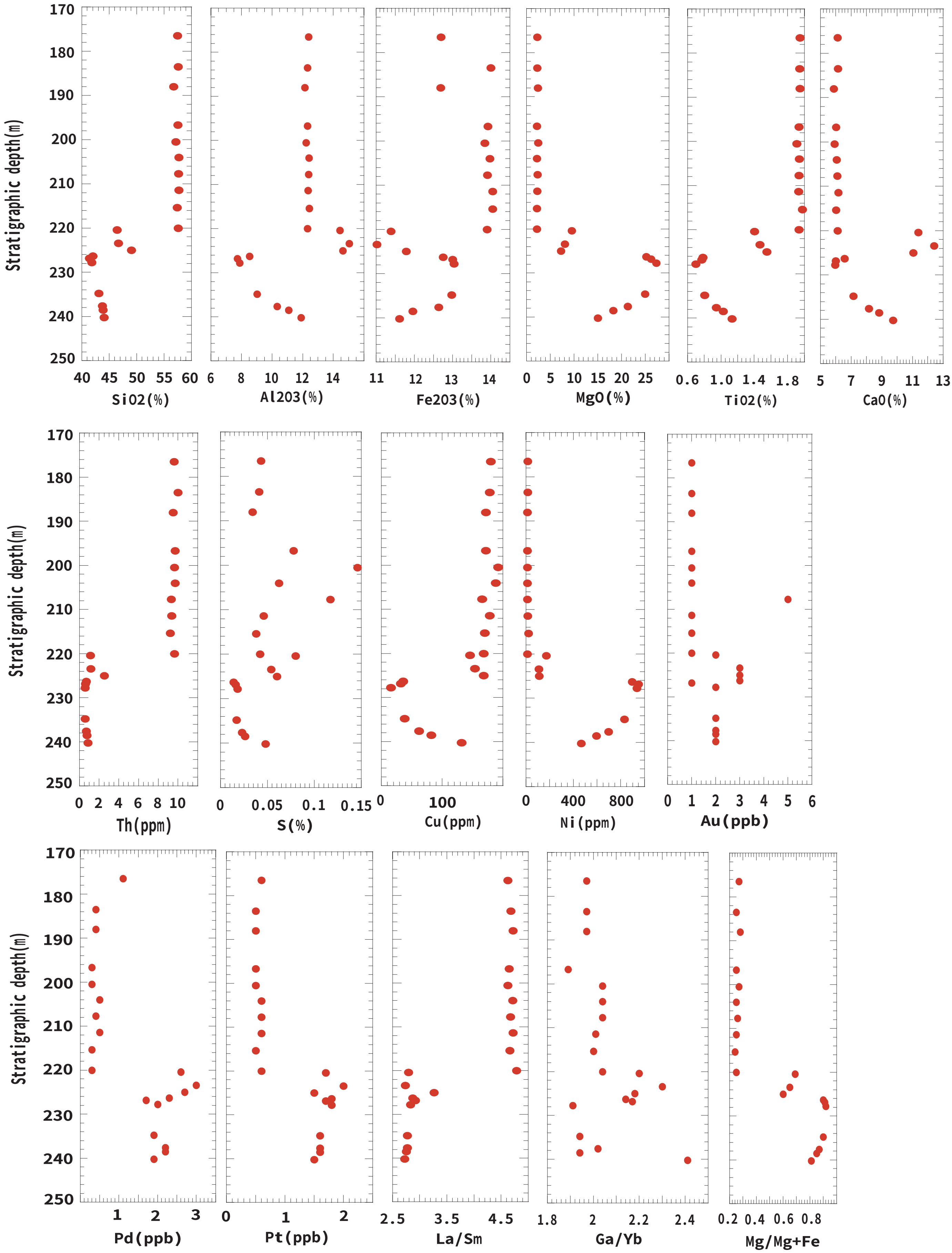

Fig.II-3-4-34 Vertical variations in major and trace-element in sill intersected by drill(TG62)

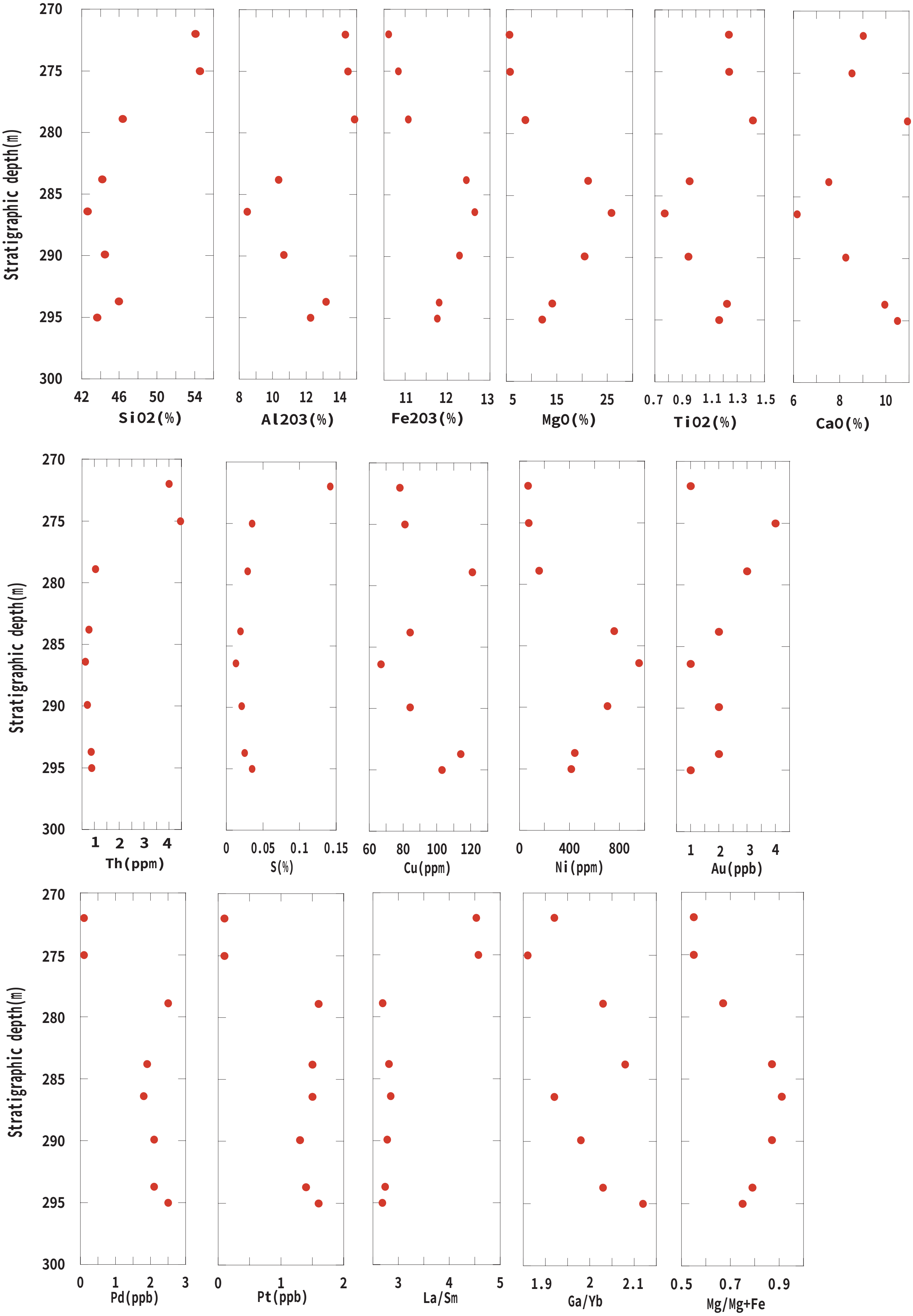

Fig.II-3-4-35 Vertical variations in major and trace-element in sill intersected by drill(TG114)

assimilation of hanging wall country rock possibly segregated immiscible sulfide melts.

3-4-5 Sulfur Isotopic Ratio

In order to consider the origin of sulfur in the intrusions, we carried out measurements of sulfur isotopic ratios of sulfides (mostly pyrite) separated from intrusions and sedimentary rocks, which might be the source of the sulfur in the intrusions. Table.II-3-4-2 lists the result of our measurements.

The range of $\delta^{34}S$ of five intrusion samples stood at +9.6 to +16.2‰, relatively high values. The values are almost same as those of mineralized sills of the Noril'sk region(+6‰ to +16‰). It is estimated that the high sulfur isotopic ratios in the Noril'sk region could be attributable to supplies of sulfur from anhydrite in the basement sedimentary rocks.

Meanwhile, $\delta^{34}S$ of six samples of sedimentary rocks indicate a range of from -22.6 to +19.2‰. The sample (SW-01 547.10-547.30) that showed the highest +19.2‰ and the sample that showed the lowest -22.6‰(SP-17 734.40-734.55) are from hornfelsed or silicified sedimentary rocks of Rio Bonito formation, in the vicinity of sill.

The values of intrusive rocks ranging from +9.6 to +16.2‰ are high for igneous rocks. This may suggest supplies of sulfur from an external source. However, since the sulfur isotopic ratios in sulfides of the country rock are dispersed into broad range, we can’t identify external source of sulfur at this stage.

Of intrusion samples, TM110 is classified into the Urubici type while KN040B and AS010 are classified into the Paranapanema-Ribeira type. These magma types are influenced less from contamination. The fact that sulfides contained in these magma types indicate consistently high $\delta^{34}S$ may suggest that source materials of Paraná flood basalts itself had a high sulfur isotopic ratio.

Table.II-3-4-1 Sulfur isotopic ratios of intrusive rocks and sediments

No.	Sample No.	Descriptions		$\delta^{34}S$ (‰)
1	TM110	Pyrite film in dyke or sill (northern rim of Paraná flood basalt), Urubici type	Outcrop	16.2
2	KN040B	Pyrite in sill(Ponta Grossa Arch), Paranapanema-Ribeira type	Outcrop	10.1
3	AS010	Pyrite in dike(Ponta Grossa Arch), Paranapanema-Ribeira type	Outcrop	9.6
4	5AT-03-SC 486.90	Pyrite in sill(Southernmost Santa Catarina), Gramado type	Drill core	10.5
5	SW-03 234.00-234.20	Dissemination of pyrite in sill(Southernmost Santa Catarina), Esmeralda type	Drill core	10.6
6	TM108	Pyrite dissemination in calcalious rock (northern rim of Paraná flood basalt)	Outcrop	3.7
7	SP-51 171.40-172.05	Irati Pyrite-conc. (Ponta Grossa Arch)	Drill core	-3.8
8	SP-64 138.15-138.30	Irati Pyrite-conc. (Ponta Grossa Arch)	Drill core	6.2
9	AS020	Pyrite rich coal ore of Rio Bonito F.; (Lomba Grande)	Outcrop	-0.6
10	SW-01 547.10-547.30	Pyrite veinlet in hornfelsed sediment(Southernmost Santa Catarina)	Drill core	19.2
11	SP-17 734.40-734.55	Dissemination of pyrite in weak silicified footwall mudstone (Ponta Grossa Arch)	Drill core	-22.6

1～4 : Pyrite in intrusions(sill/dike)

5～11 : Pyrite in sedimentary rocks

3-5 PGE Geochemistry of the Paraná Flood Basalts

3-5-1 PGE Contents of the Paraná Flood Basalts

For the formation of economic orthomagmatic sulfide ore deposit, it is necessary to generate sulfur undersaturated magma and to intrude it to the shallow part of the crust. This kind of magma should show high contents of the platinum and palladium.

Table II-3-5-1 Platinum and Palladium concentrations of lava and intrusion samples

Magma Type		Lava				N	Intrusion				N
		Pt (ppb)		Pd (ppb)			Pt (ppb)		Pd (ppb)		
		Range	Average	Range	Average		Range	Average	Range	Average	
Paraná flood basalt											
Acidic rocks		<0.1-2.7	0.9	0.1-9.8	1.9	10	<0.1-0.7	0.2	<0.1-0.4	0.1	8
Ulubici	High-Ti	<0.1-7.3	4.7	<0.1-8.6	6.0	8	<0.2-11.0	4.7	0.3-8.6	5.8	11
Pitanga	High-Ti	<0.2-11.2	2.2	<0.2-28.4	4.5	61	<0.2-18.7	2.9	<0.2-133.8	5.9	65
Paranapanema-Ribeira	Intermediate-Ti	<0.2-22.8	7.9	<0.2-41.1	14.3	111	<0.2-16.5	7.4	<0.2-59.3	15.2	48
Esmeralda	Low-Ti	2.3-15.2	7.1	1.0-18.8	10.1	30	3.8-22.2	11.1	6.0-16.7	11.6	30
Gramado	Low-Ti	0.4-14.7	5.5	0.2-33.4	6.5	38	<0.1-21.7	4.4	<0.1-14.9	5.4	89
Siberian Trap											
Tuklonsky	Low-Ti	9-13	11.2	9.0-13.0	10.7	5					

D.L: Detection Limit(Pt:0.1 or 0.2ppb, Pd:0.2ppb; Tuklonsky: The least PGE depleted magma of the Siberian Trap

The contents of Pt and Pd of the lava and intrusion samples collected during this survey are shown in Table II-3-5-2, and the frequency diagram of Pt and Pd contents are shown in Figs. II-3-5-1 and II-3-5-2. Both lava and intrusion samples show comparatively high Pt and Pd contents. This suggests that the Paraná flood basalts were generally derived from PGE rich fertile magmas. Comparing lava samples and intrusion samples for each magma type, the average Pt and Pd contents are almost equal, but the contents of the intrusion samples vary widely in the analyses results. The characteristics of Pt and Pd contents in each magma type are as follows;

<u>Paranapanema-Ribeira (Intermediate-Ti Type)</u>

The characteristics of this type are the richest in Pt and Pd of all magma types, and are particularly rich in Pd. And there are very few samples that are depleted in Pt and Pd in this type. The maximum value of Pd contents is 41.1 ppb in lava samples, and 59.3 ppb in

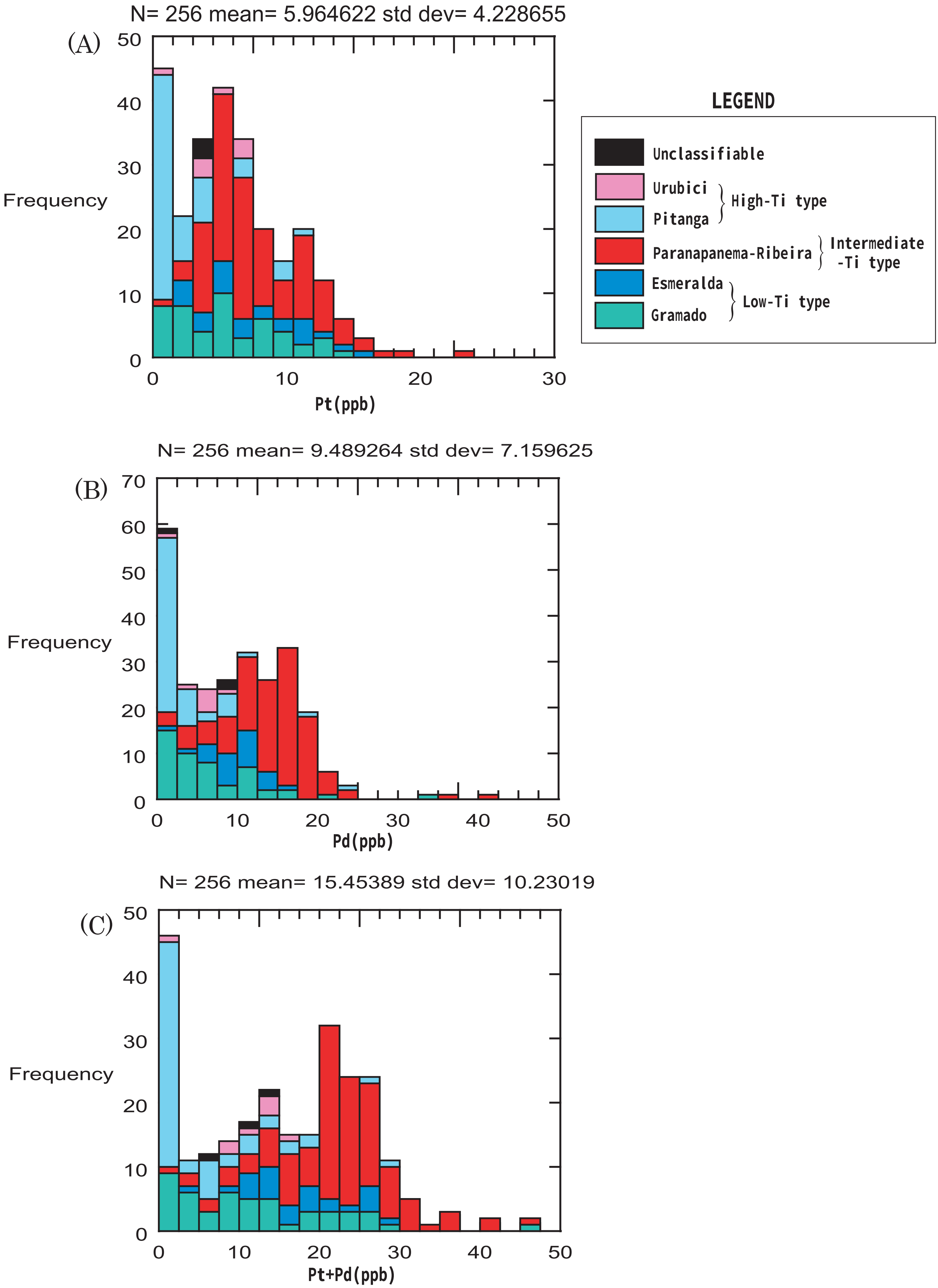

Fig. II-3-5-1 Frequency diagrams of assay data of Pt(A), Pd(B), and Pt+Pd(C) for lava samples

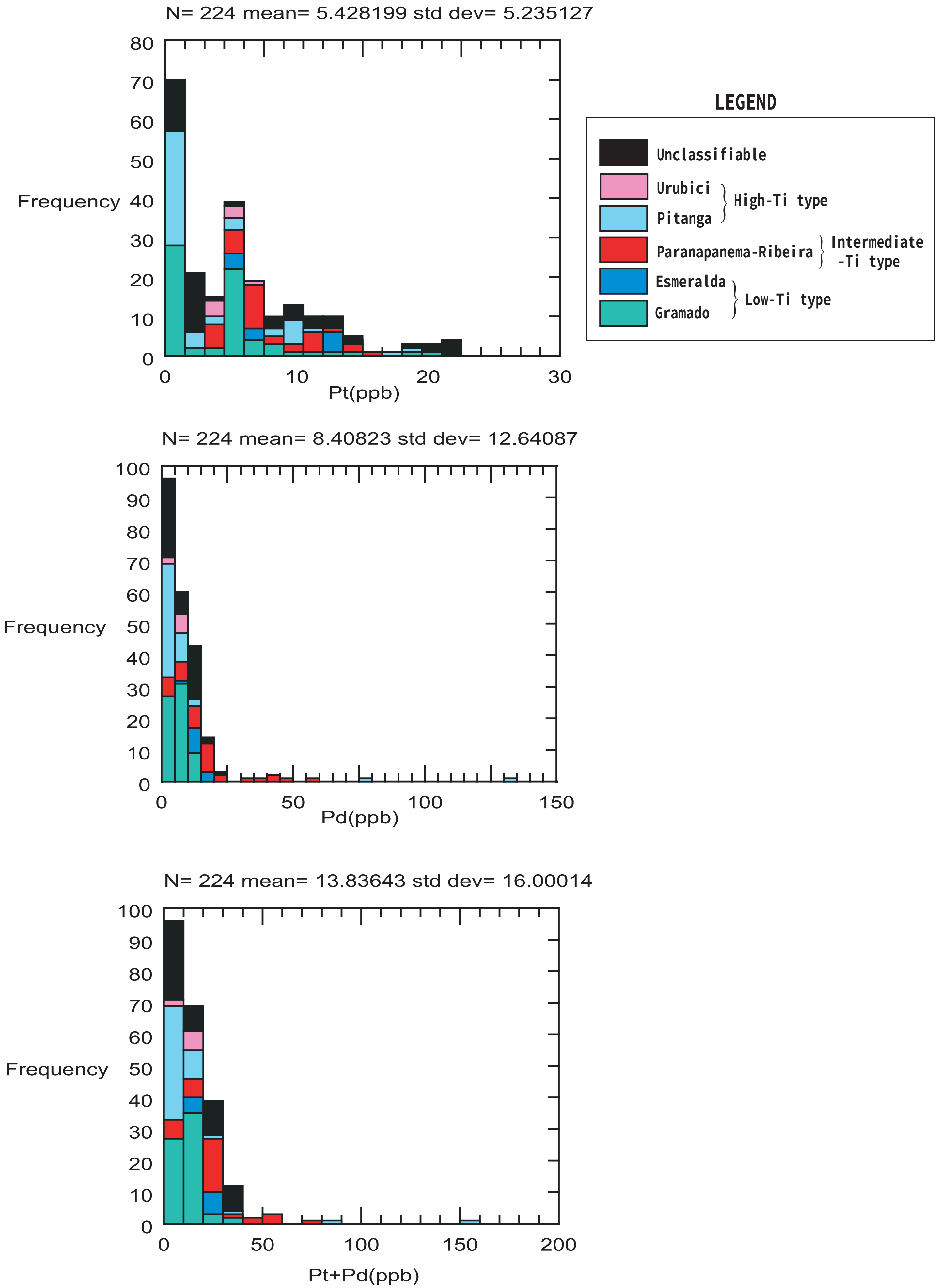

Fig. II-3-5-2 Frequency diagrams of assay data of Pt(A), Pd(B), and Pt+Pd(C) for intrusion samples

intrusion samples. The average value of Pd contents is 14.3 ppb in lava samples, and 15.2 ppb in intrusion samples. The average total content of Pt and Pd is 22.2 ppb in lava samples. This is almost equal to the 21.9 ppb of the Tuklonsky lava samples that are the richest in PGE in the Noril'sk region.

Esmeralda (Low-Ti Type)

The Pt and Pd contents of the Esmeralda type show the highest value after those of Paranapanama-Ribeira. There are very few samples that are depleted in Pt and Pd in this type as well as in the Paranapanema-Ribeira.

Gramado (Low-Ti Type)

The average contents of Pt and Pd are almost equal to those of Pitanga (High-Ti Type) and Urubici (High-Ti Type). One characteristic of this type is that there are many samples that are depleted in Pt and Pd.

Pitanga (High-Ti Type)

The average contents of Pt and Pd are almost equal to those of Gramado (Low-Ti Type) and Urubici (High-Ti Type). Still, one characteristic of this type, as well as the Gramado type, is that there are many samples that are depleted in Pt and Pd. A few samples of intrusions, however, that were collected from Ponta Grossa Arch show extremely high Pt and Pd contents, for example, KN104 shows the highest Pt and Pd contents of 28.4 ppb and 133.8 ppb, respectively.

Urubici (High-Ti Type)

The average contents of Pt and Pd are almost equal to those of Gramado (Low-Ti Type) and Pitanga (High-Ti Type). As we have few samples of this type, distinct characteristics of this type are unknown.

The relationship between Pt and Pd is shown in Figs. II-3-5-3 and II-3-5-4. Pt and Pd contents show good correlations in the flood basalt of the Noril'sk region. The Pt/Pd ratio is approximately 1. This value is smaller than the Pt/Pd ratio (1.9) of the primitive mantle. This means that the magma of the Noril'sk was more depleted in Pt than in Pd. Such a non-primitive mantle-like Pt/Pd ratio is believed to reflect the characteristics of the source material. The source material is probably the subcontinental lithosphere mantle or plumes originating in the lower mantle(Brugmann et al., 1993). On the other hand, the Pt/Pd ratios of almost all the samples of Paraná Flood Basalts are smaller than 1, and the ratios are plotted varying in the wide area. Therefore magma of the Paraná Flood Basalts is more depleted in Pt than the

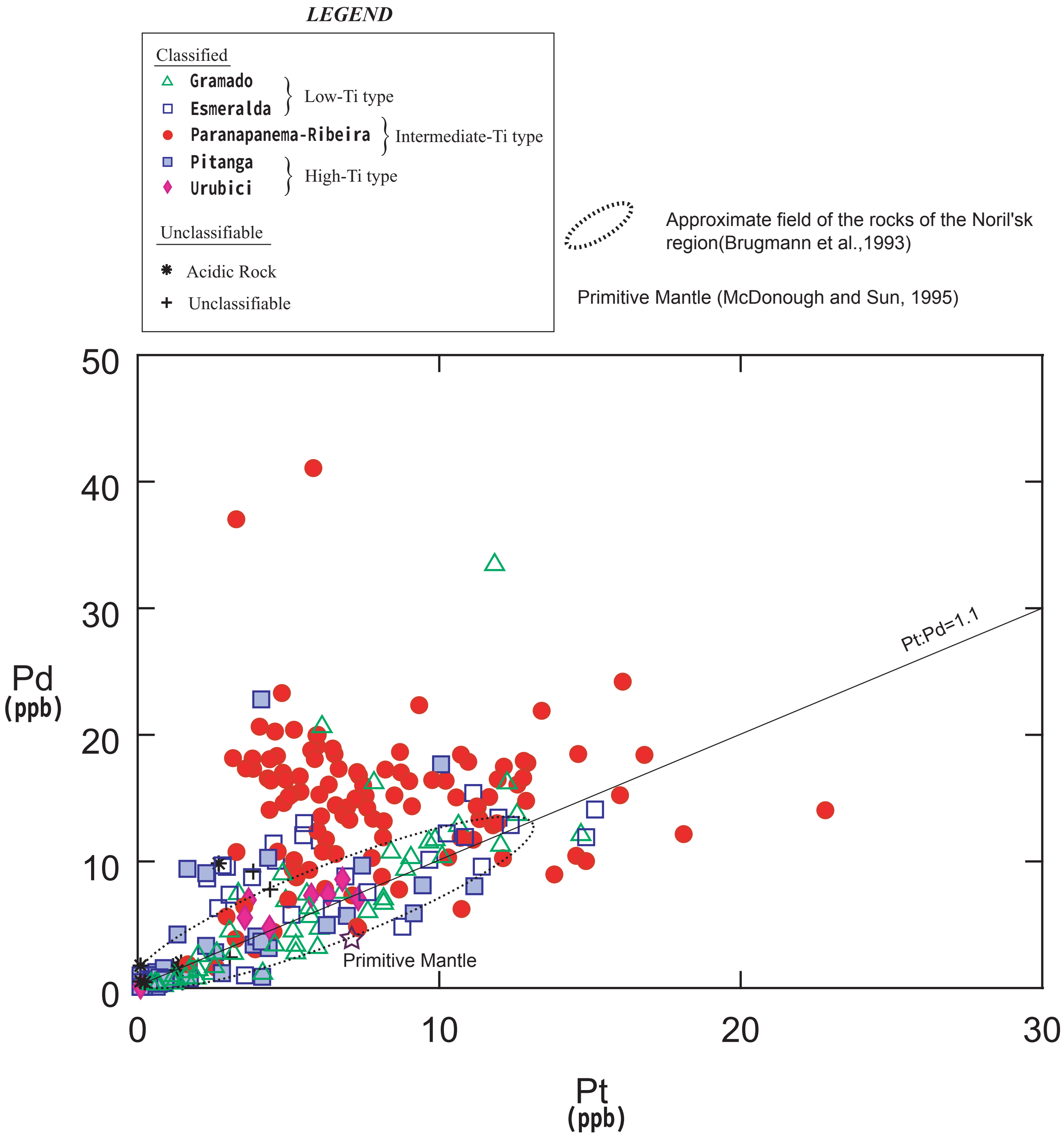

Fig.II-3-5-3 Pt - Pd correlation diagram for lava samples

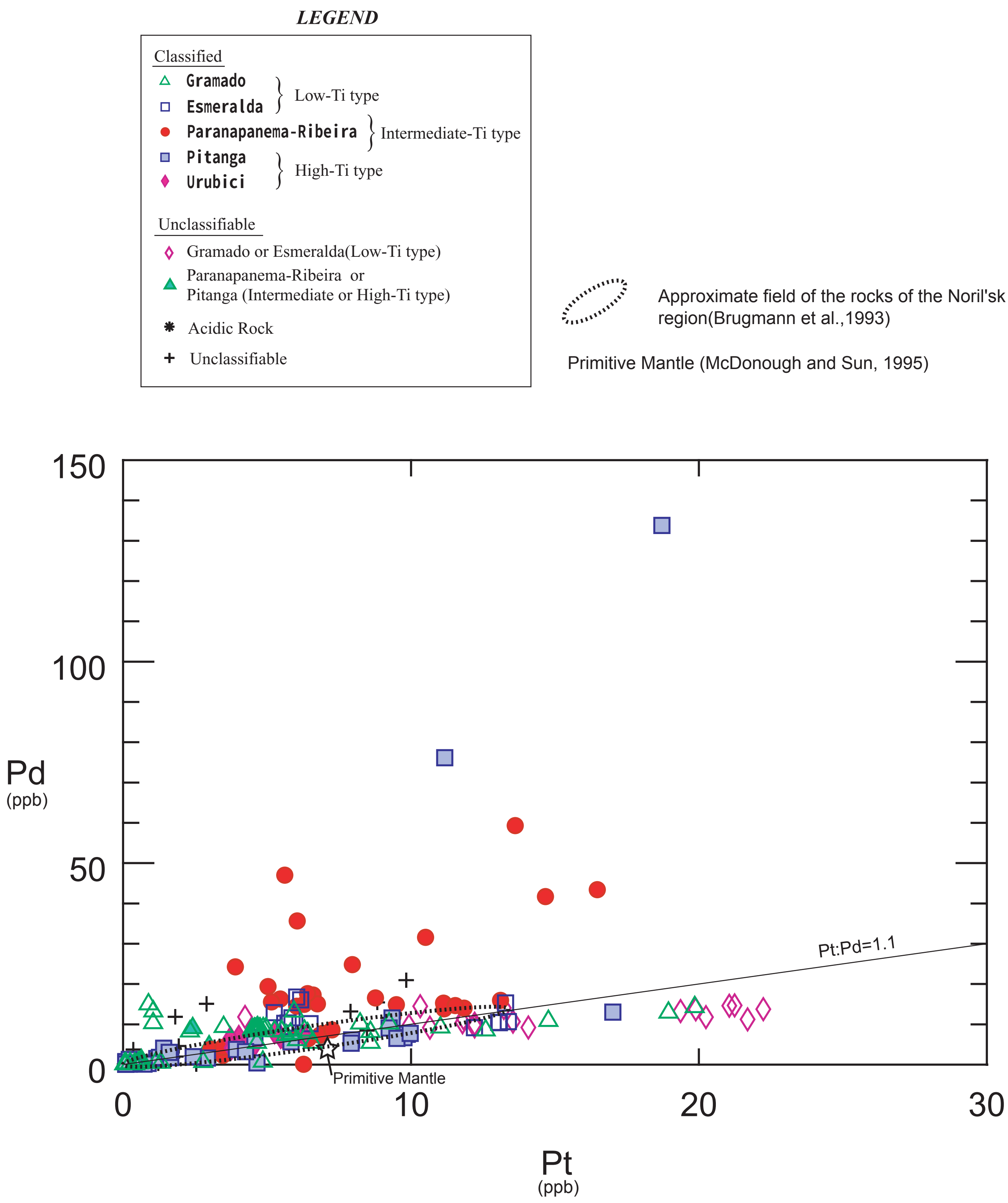

Fig.II-3-5-4 Pt - Pd correlation diagram for intrusive samples

Table II-3-5-2 Metal elements concentrations for selected samples

Sample No.	Magma_Type	Sample Type	Ni(ppm)	Ir(ppb)	Rh(ppb)	Pt(ppb)	Pd(ppb)	Au(ppb)	Cu(ppm)
WW134	Gramado	Lava	40	0.2	1	12.6	13.7	3.3	88
WW175	Gramado	Lava	261	<0.1	<0.2	11.8	33.4	1.0	172
WW184	Gramado	Lava	118	0.3	0.8	6.1	20.6	7.0	142
YM108	Gramado	Lava	25	0.1	0.2	7.8	16.2	5.2	100
YM168	Gramado	Lava	118	0.6	0.8	12.3	16.2	4.1	163
YM146	Esmeralda	Lava	34	0.1	0.3	5.5	13.0	5.6	170
KM104	Esmeralda	Lava	28	0.2	1	11.1	15.4	17.5	141
YM114	Esmeralda	Lava	49	<0.1	0.6	3.8	8.8	1.0	144
YM115	Esmeralda	Lava	9	0.1	0.7	12.4	12.9	3.5	200
KM116	Paranapanema	Lava	21	0.5	0.7	3.3	37.0	21.6	151
KM120	Paranapanema	Lava	23	0.1	1	5.1	15.3	8.3	279
TM153	Paranapanema	Lava	53	0.1	0.3	12.1	10.3	3.0	228
YM119	Paranapanema-Ribeira	Lava	42	0.5	0.8	5.8	41.1	4.0	182
YM125	Paranapanema	Lava	22	<0.1	0.5	4.8	23.3	3.7	192
YM130	Paranapanema-Ribeira	Lava	61	0.2	0.4	16.1	24.2	6.9	209
TM126	Pitanga	Lava	8	0.2	<0.2	4.1	22.8	7.5	116
TM129	Pitanga	Lava	25	0.3	0.7	10.1	17.7	2.3	143
TM130	Pitanga	Lava	33	1.8	0.7	9.5	8.1	3.8	142
TM164	Pitanga	Lava	1	<0.1	0.5	1.7	9.4	2.5	157
YM208	Pitanga	Lava	225	0.3	0.7	4.3	10.3	2.2	138
YM182	Urubici	Lava	130	0.2	0.6	6.8	8.6	3.8	172
YM184	Urubici	Lava	225	0.3	1	5.8	7.3	3.2	152
YM210	Urubici	Lava	214	0.2	0.5	6.3	7.4	1.0	130
YM223	Urubici	Lava	175	0.2	0.7	7.3	7.1	3.3	128
KN110A	Paranapanema-Ribeira	Dyke	60	0.2	0.8	16.5	43.4	7.8	212
KN112	Paranapanema-Ribeira	Dyke	33	<0.1	0.7	5.6	47.0	6.4	195
KN173	Paranapanema-Ribeira	Dyke	34	<0.1	0.6	13.6	59.3	17.4	219
KN150	Pitanga	Sill	<1	<0.1	<0.2	11.2	76.1	23.8	49
KN104	Pitanga	Dyke	30	<0.1	<0.2	18.7	133.8	40.5	234
KN001	Unclassifiable	Sill	246	<0.1	0.3	0.7	0.8	1.9	130
KN002	Unclassifiable	Sill	356	<0.1	0.3	1.2	0.3	0.5	49
Primitive Mantle*			1960	3.2	0.9	7.1	3.9	1	30

*McDonough and Sun(1995)

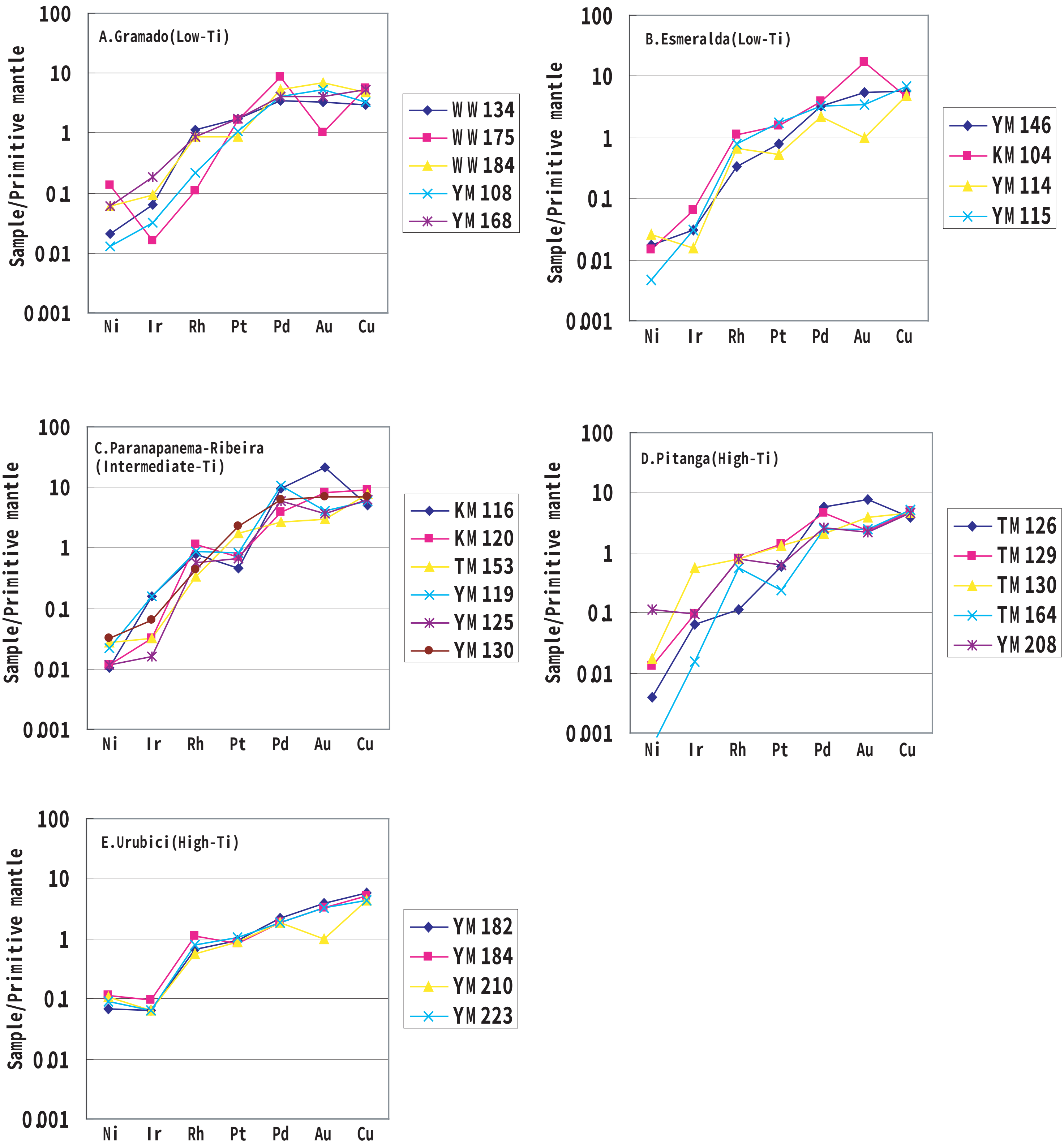

Fig.II-3-5-5 (A, B, C, D, and E)   Mantle-normalised metal patterns for selected lava samples

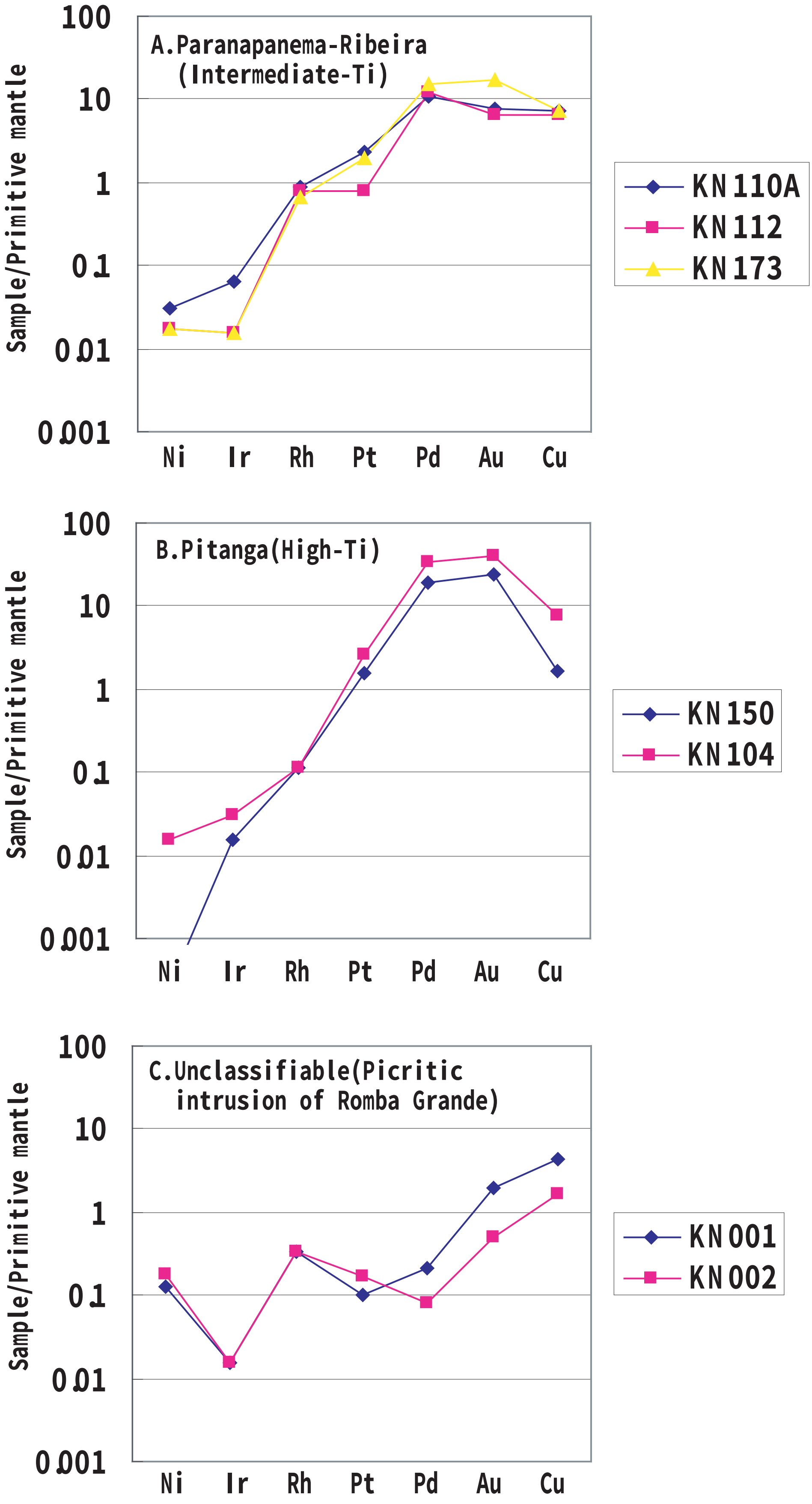

Fig.II-3-5-6 (A, B, and C) Mantle-normalised metal elemento patterns for selected intrusion samples

magma of the Noril'sk region, and considered as more non-primitive mantle like. This tendency is more distinct in Paranapanena-Ribeira that is richest in Pd. The characteristics of Pt depletion are similar to those of the PGE contents of the flood basalt in East Greenland (Momma et al., 2002).

The contents of metallic elements of the representative lava and intrusion samples are shown in Table II-3-5-1, and the primitive mantle normalized patterns are shown in Figs. II-3-5-5 and II-3-5-6. Ir acts as a compatible element during crystallization differentiation of sulfur undersaturated magma, while Pd acts as an incompatible element. Therefore, the ascending inclination in Figs. II-3-5-5 and II-3-5-6 is believed to show the progress of crystallization differentiation. According to Fig. II-3-5-5, Paraná flood basalts which are comparatively differentiated show steep inclination from Ni to Pd, and flat pattern from Pd to Cu. Urubici shows an exceptional pattern that is a comparatively moderate ascending inclination to the right from Ni to Cu. Fig. II-3-5-6 shows the pattern of intrusions. The samples KN104 (Pd 133.8 ppb) and KN150 (Pd 76.1 ppb), the richest in Pd that were collected in this survey, show very steep ascending inclination to the right from Ir to Pd, and as descending inclination to the right from Au to Cu. No ascending inclination to the right from Ni to Pd is shown for the two samples of the Romba Grande intrusion in the southern part of the Paraná Basin, the only picritic intrusion in the survey area. This is probably due to the accumulation of olivine.

3-5-2 Relationship between Degree of Partial Melting and PGE Content

As mentioned in Chapter 3-3, the degree of partial melting of each type differs. The degree of partial melting becomes smaller in the following order; Low-Ti(Esmeralda, Gramado), Intermediate-Ti(Paranapanema-Ribeira), High-Ti(Pitanga and Urubici). With decreasing degree of partial melting, the depth of magma generation is estimated to be deeper, and the source material becomes more enriched from depleted. The difference between Paranapanema-Ribeira and Pitanga distributed from the central area to the north in the Paraná Basin is thought to have been generated by the difference of degree of partial melting of comparatively similar sources (Mantvani et al., 2000).

The relationship between the degree of partial melting and concentration of Pt and Pd is shown in Fig. II-3-5-7. Since many samples from Pitanga are depleted in Pt and Pd, the comparison between Paranapanema-Ribeira and Pitanga was carried out without these depleted samples. As the result, Paranapanema-Ribeira that was generated with larger degree of partial melting is richer in Pt and Pd than Pitanga. Therefore, even though the original materials are the same, more Pt and Pd were obtained in the magma according to increasing degree of the partial melting. Therefore, in the case of the same sources, magma with a larger degree of

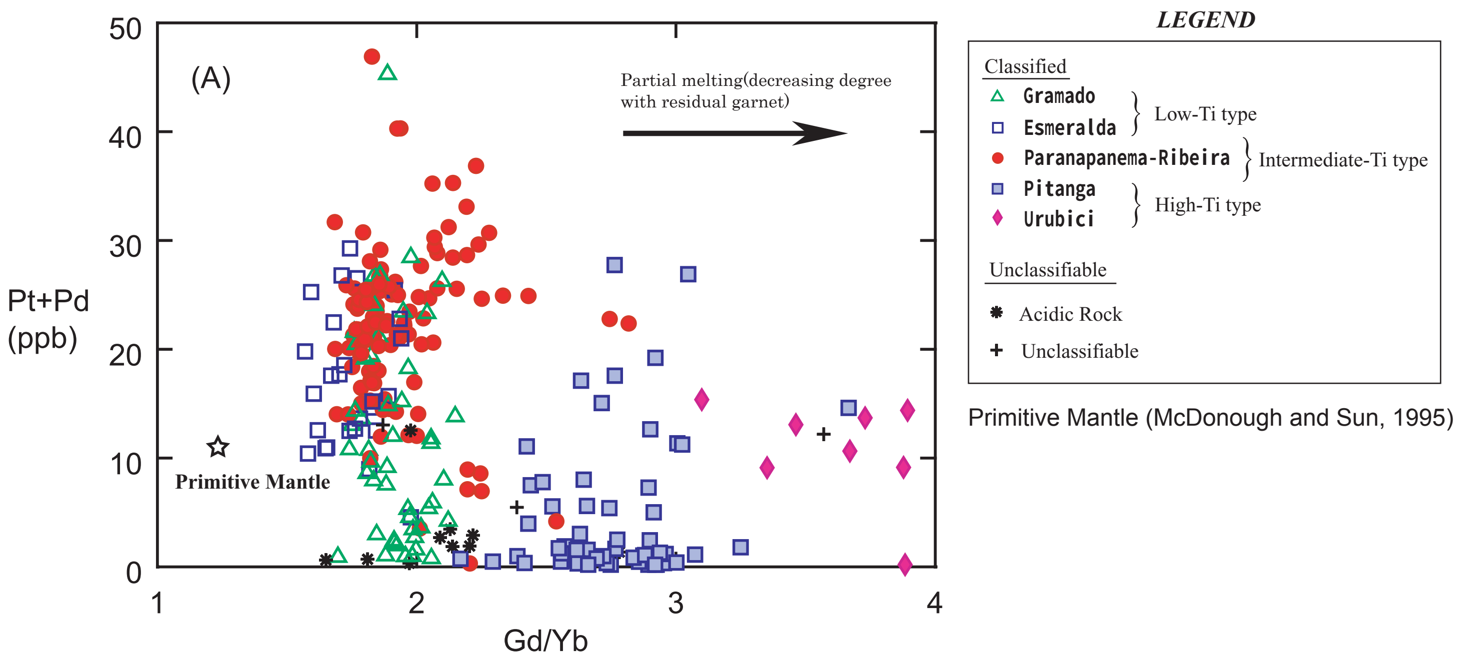

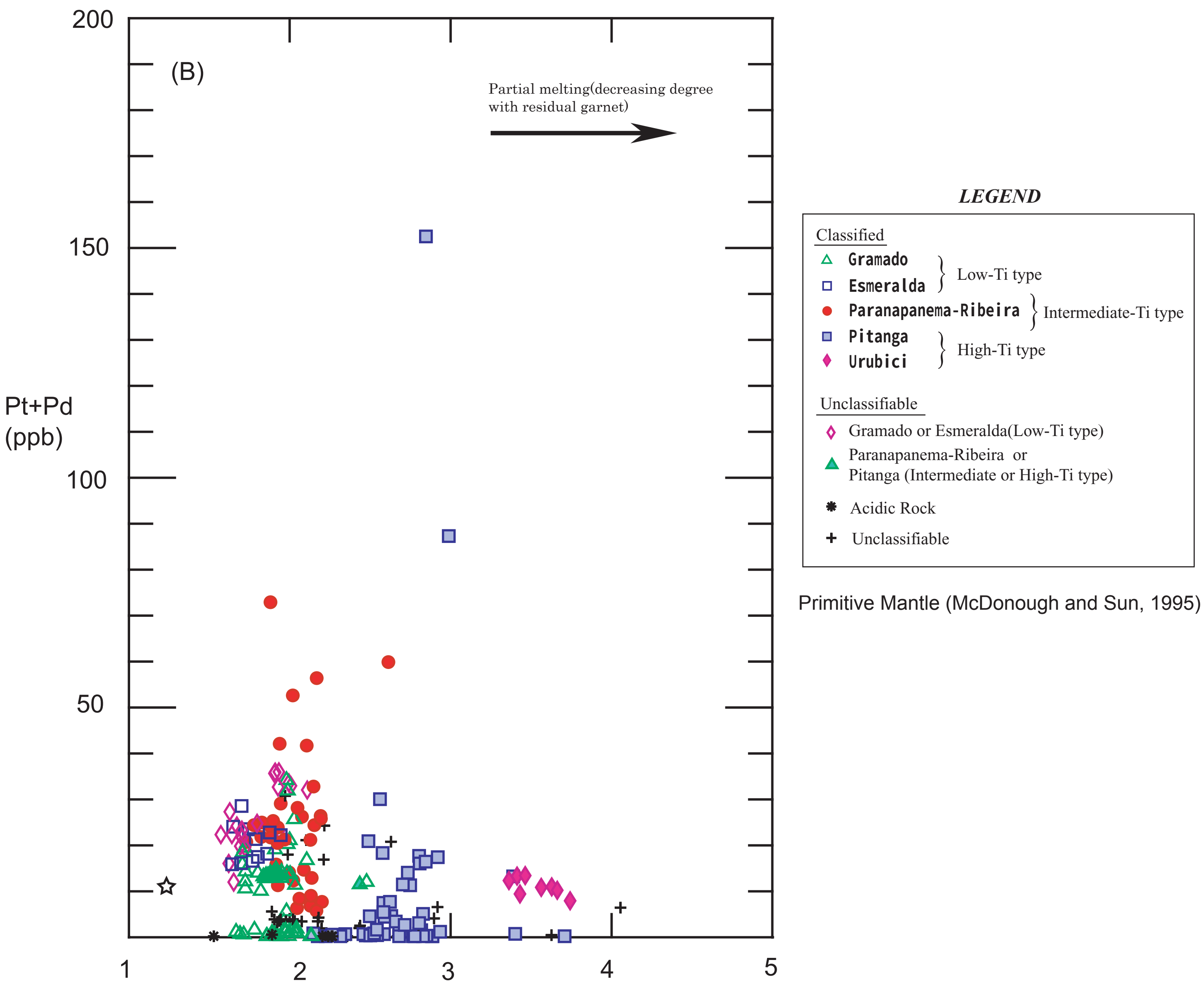

Fig.II-3-5-7 (A) Gd/Yb - Pt+Pd concentrations for lava samples;
(B) Gd/Yb - Pt+Pd concentrations for intrusion samples

partial melting contributes more effectively to the genesis of sulfide ore deposit.

3-5-3 Relationship between Sulfur Saturation and PGE Content

Although PGE contents vary according to the difference of the magma types, the Paraná flood basalts, as a whole, were generated from initially PGE rich magma. The orthomagmatic process is necessary to form sulfide ore deposit from such magma. The orthomagmatic process means the segregation of immiscible sulfide melt from silicate melt saturated in sulfur.

Figs. II-3-5-8 and II-3-5-9 show the relationship between Cu and Pd of the lava and intrusion samples respectively. These two elements have the properties to concentrate within sulfide melt, and the property of Pd is more marked than that of Cu. The distribution coefficient of Cu between sulfide melt and silicate magma is 600 to 1,000, while the coefficient of Pd is 10,000 to 100,000. Therefore, Pd concentrates 15 to 100 times as much as Cu within sulfide melt. For this reason, when silicate magma saturates in sulfur and separates immiscible sulfide melt, both Pd and Cu are depleted in the silicate magma. At that time, the Pd depletion progresses markedly. Therefore, according to the progress of segregation of immiscible sulfide melt, the Pd/Cu ratio in the silicate magma must rapidly decrease.

Each lava type of Paraná Basin is plotted in the specific region as shown in Figs. II-3-5-8 and II-3-5-9. Almost all the samples of Paranapanena-Ribeira that are Intermediate-Ti type and Esmeralda that are Low-Ti type are plotted in the sulfur undersaturated region, and their Pd contents are high. Particularly, both the Pd and Cu of Paranapanea-Ribeira are plotted in the highest region. The Pd in Gramado (Low-Ti Type) and Pitanga (High-Ti type) is plotted stretching over the regions saturated and undersaturated in sulfur. Particularly many Pitanga samples are depleted in Pd and are plotted in sulfur saturated regions. Although the numbers of samples were limited, almost all the Urubici samples are plotted in the regions of sulfur undersaturated. The result is that all the original magmas of these five lava types is thought to have been initially undersaturated in sulfur and rich in Pd. Nonetheless, part of the original magma of Gramado and Pitanga became saturated in sulfur for some reason, and separated the immiscible sulfide. The highest Pd content of 133.8 ppb observed in an intrusion sample (KN104) of Pitanga is obviously too great for initial magma content. It is thought to suggest the existence of sulfide melt with Pd.

Why have Gramado and Pitanga reached saturation in sulfur? For Gramado and Esmeralda, the Low-Ti types in the five types, from the compositions of trace elements and isotopes, the influence of upper crustal contamination is observed. Especially, for Gramado, the influence is remarkable. The relationship between the crustal contamination and sulfur saturation is shown in Fig. II-3-5-10. According to this figure, as regards Gramado, samples with progressed contamination show the depletion tendency of Pd.

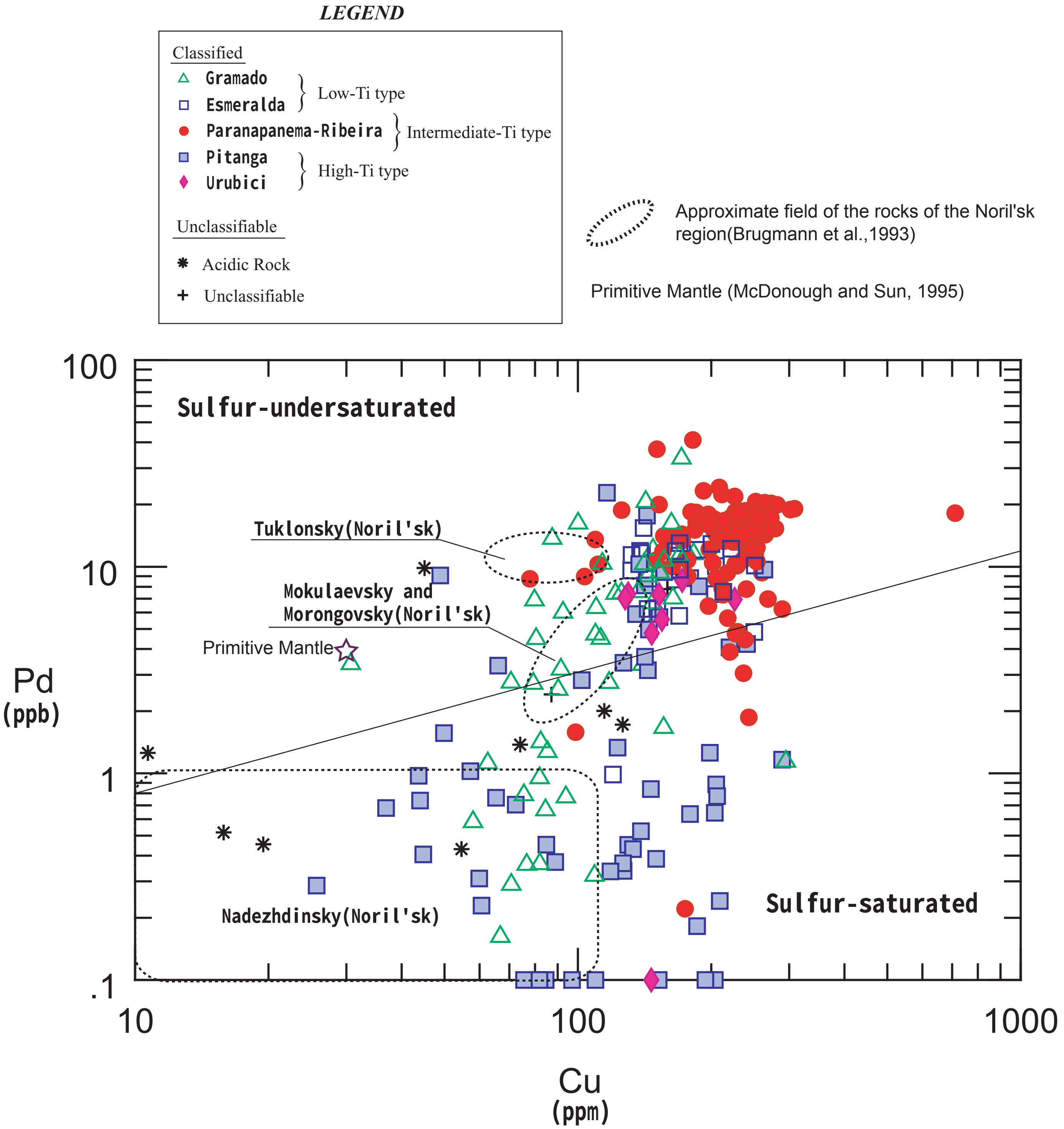

Fig.II-3-5-8 Cu vs. Pd discriminant diagram between the field of rocks formed by Sulfur-saturated magmas and the field of rocks formed by Sulfur-undersaturated magmas(Brooks et al., 1999) for lava samples.

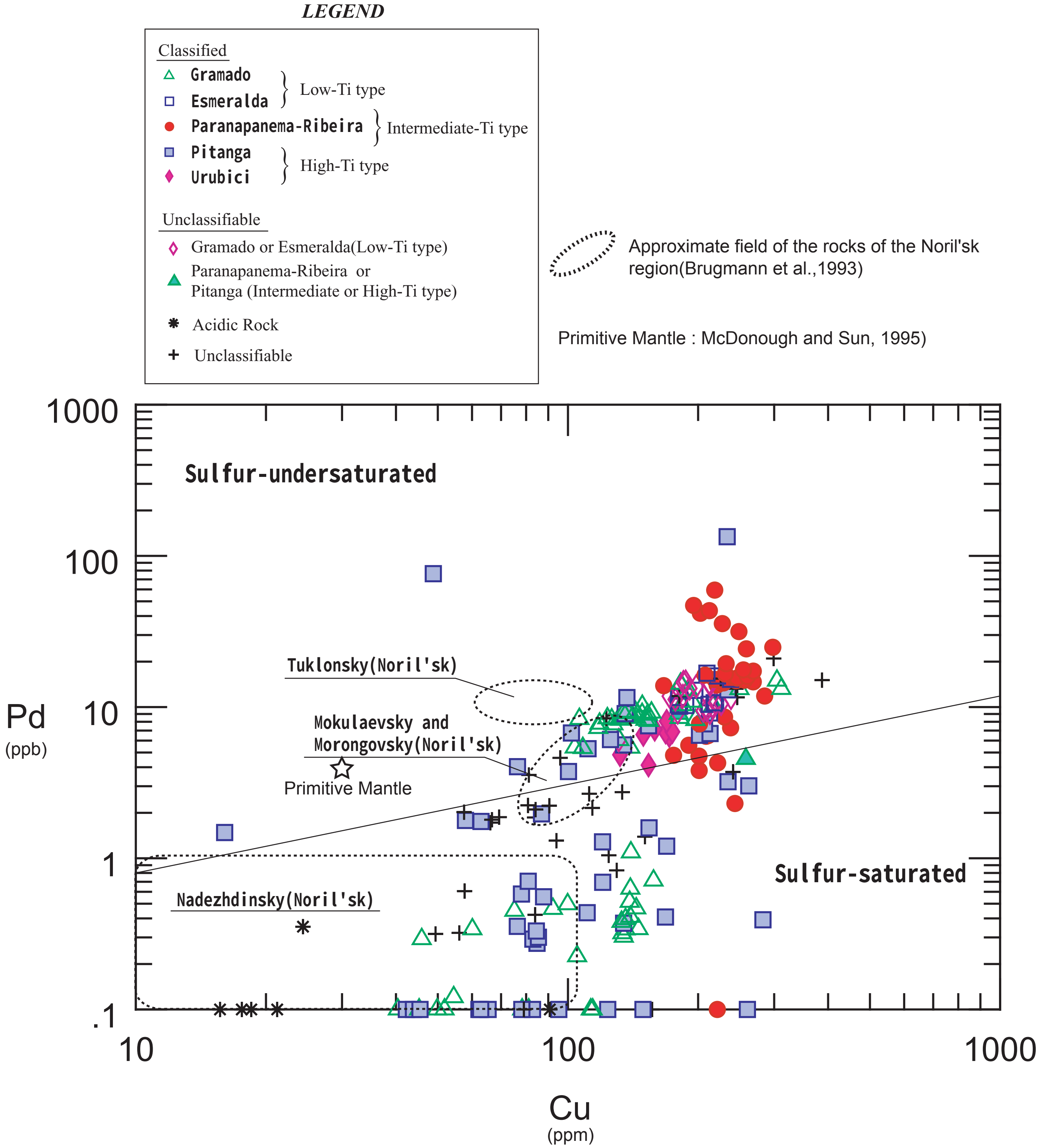

Fig.II-3-5-9 Cu vs. Pd discriminant diagram between the field of rocks formed by Sulfur-saturated magmas and the field of rocks formed by Sulfur-undersaturated magmas(Brooks et al., 1999) for intrusive rocks.

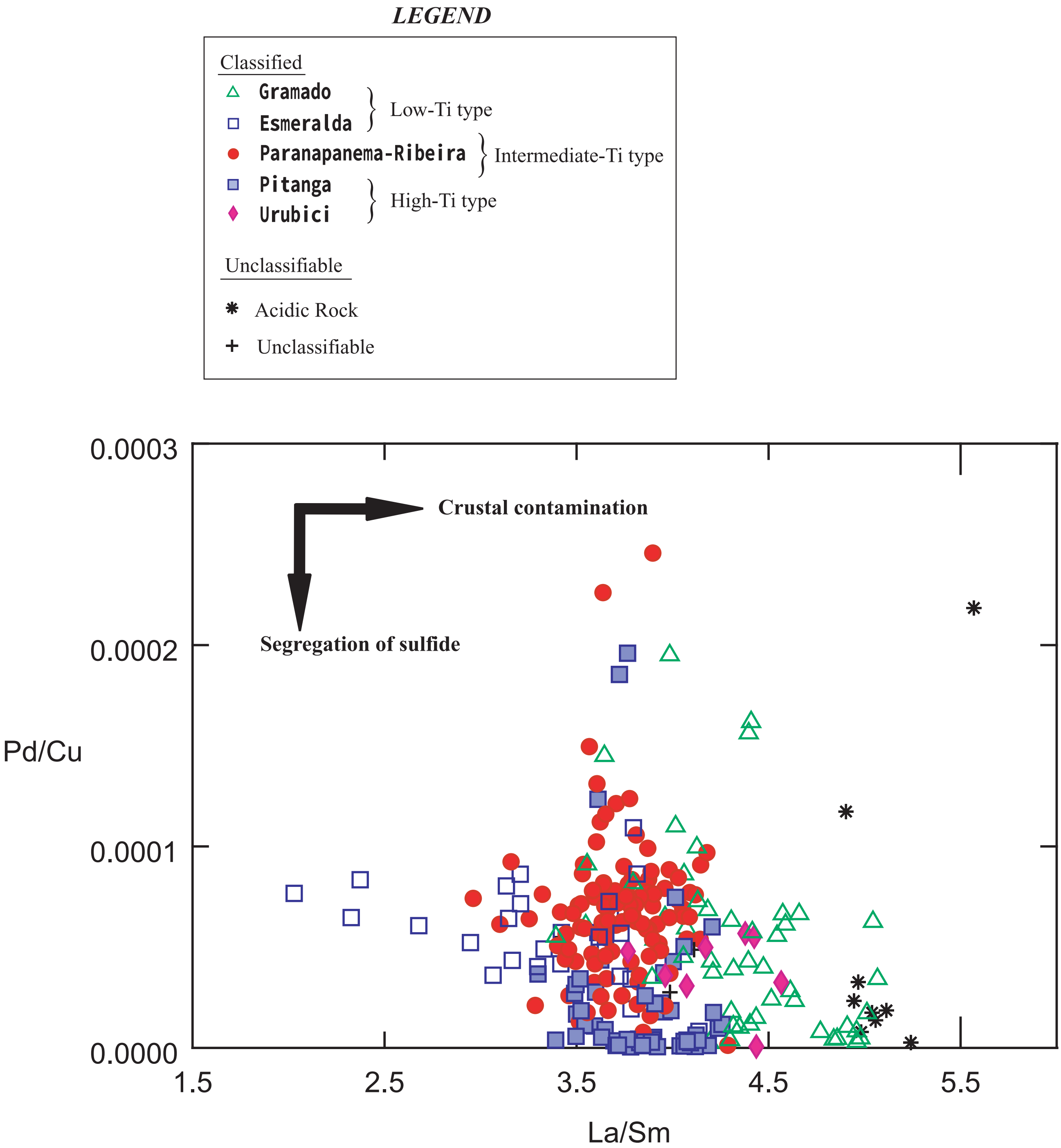

Fig.II-3-5-10 La/Sm - Pd/Cu correlation diagram for lava samples

The relationship between the progress of crystallization differentiation and sulfur saturation is shown in Fig. II-3-5-11. Although both Paranapanema-Ribeira and Pintanga are viewed as the magma less affected by the contamination, the saturation tendency in sulfur is observed on the more differentiated side of the border of Mg number 60. Many Pitanga samples that are more differentiated show low Pd/Cu ratios. Some differentiated samples of Paranapanema-Ribeira show decreasing Pd/Cu ratios. Given this, the saturation factor in Pitanga is considered the crystallization differentiation.

3-5-4 Potential of Cu-Ni-PGE Sulfide Deposit Accompanied with Paraná Flood Basalts

Comparing Paraná Flood Basalts and flood basalt of Noril'sk, the former is generally richer in Cu (Figs. II-3-5-8 and II-3-5-9). This tendency is particularly remarkable in Paranapanema-Ribeira. As regards Pd, although the average value in Paranapanema-Ribeira is the same as the average value in the Tuklonsky lava of Noril’sk, the former includes more samples with high Pd contents. The high Cu and Pd contents of Paraná Flood Basalts are assumed to exist because Paraná Flood Basalts were more differentiated than the flood basalts of Noril’sk, and because Cu and Pd concentrated densely in the magma acted as incompatible elements in sulfur undersaturated conditions.

As mentioned above, concerning the richness of PGE and metallic elements, Paraná Flood Basalts slightly exceeds the magma of the Noril’sk area. Therefore, Paraná Flood Basalts satisfies the first requirement to form orthomagmatic sulfide ore deposit, as mentioned in Chapter 1-3; “the generation of sulfur undersaturated magma and its intrusion into shallow crustal level”. Yet, the temperature of Paraná Flood Basalts is presumed to be lower than that of the magma of the Noril’sk region judging from their slightly differentiated compositions. Considering the above assumption, the ability to assimilate the country rock is thought to be low. Although almost all the magma in the Noril’sk region is basaltic, picritic magma is existed in the sill that embeds ore deposits. In such sill, picritic magma assimilating the country rock is observed on a large scale while picritic magma is rarely observed in Paraná Flood Basalts. The Paraná Flood basalts is more differentiated than the basalts in the Noril’sk region, and the temperature of the former is lower than that of the latter. It is possible that the large scale segregation of undersaturated sulfide was obstructed by the above process in the Paraná.

However, as presumed for Pitanga, it is possible that the segregation of immiscible sulfide occurred due to the simple progress of crystallization differentiation. The phenomenon of gradual reduction of PGE according to magma differentiation is observed from 240 m to 570 m in the drilling core of Paranapanema-Ribeira type lava in the groundwater drill(PP-02 hole). In this drilling core, Pt almost regularly decreases from 8.3 ppb to 3 ppb corresponding to the decreasing Mg number at advance from 570 m to 240 m. As regards Pd, the same decreasing

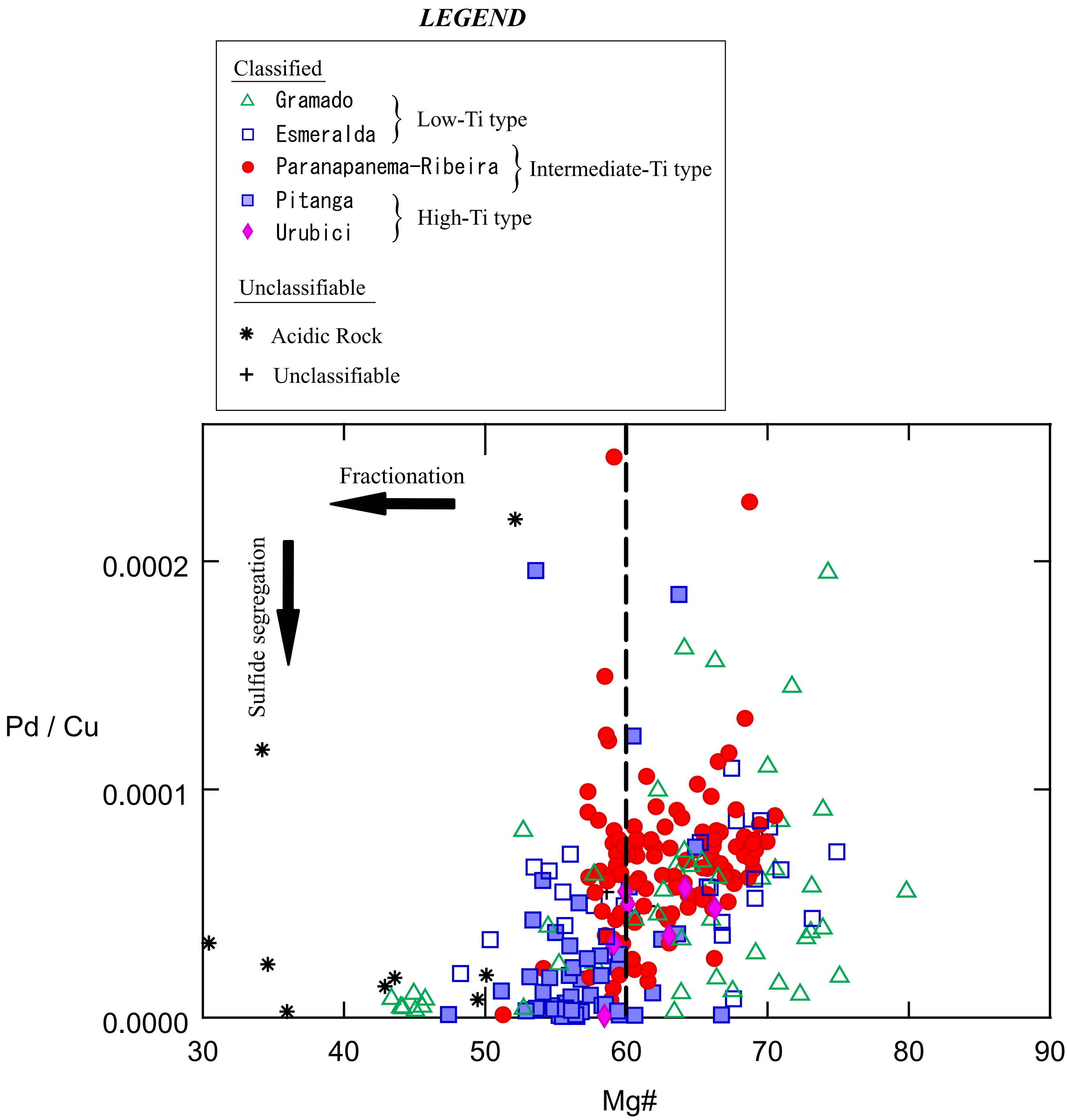

Fig.II-3-5-11 Mg# - Pd/Cu diagram for lava samples

pattern with decreasing Mg number is observed (Fig.II-3-3-27). This sulfur saturation mechanism is the similar one considered for the Skaergaad intrusion in East Greenland (Anderson et al., 1998) and for the Sonju Lake intrusion, Minnesota, USA (refer to APPENDIX.2) that are composed of tholeiitic magmas, as well as Paraná Flood basalts.

All the samples of intrusion including Ponta Grossa Arch sill that could be collected in this survey were distributed in the marginal area of the Basin, the edge area away from the center of magmaic activity. The sills are mostly poor in sulfide, and the maximum thickness is approximately 200 m, which is comparatively thin. The rock compositions show basaltic, and although show high PGE contents, the magma temperature is lower than that of the magma of Noril'sk. The contamination effect of country rock in such intrusions is weak. This weak effect is considered to be the cause only for generating the faint dissemination of sulfide. To generate sulfide ore deposit from such PGE rich basaltic magma, the segregation of sulfide within a large scale magma chamber like Skaergaard intrusion under high R factor is necessary. The most probable location for the above phenomenon in the Paraná Basin is thought to be the center of the eruption of Paranapanema- Ribeira and Pitanga type magmas.

3-6 Study of the Stream Sediment Geochemical Anomaly by MINEROPAR

3-6-1 Review of the Stream Sediment Geochemical Survey by MINEROPAR

The MINEROPAR, the provincial agency for mining, carried out a reconnaissance multi-elements geochemical survey, using stream sediment and water samples, in the Paraná Province with IPARDES, IAPAER, EMATER and CPRM during 1994 to 1998.

The survey area was approximately 170,000 km^2, which covers 85 % of the whole Paraná Province. The sampling density was 26 km^2/sample to 238 km^2/sample, and the average was 225 km^2/sample. Totally 696 samples (696 drainages) were collected. Besides these samples, 40 samples, integrating 696 drainages to 40 drainages, were produced. The analysis was carried out in accordance with the Global Geochemical Reference Network, which is the world standard of UNESCO/IUGS.

As a result of this program, covering the area of 40,000 km^2 in the southwestern part of the Paraná Province, the high anomalies of Cu, Zn, Co, Ni, V, Ti, Cr, MgO, Pt, and Pd, and the low anomalies of SiO_2, Ba, Be, Sn, and W were extracted by the stream sediments. These multi-elements anomalies were thought to have related to the flood basalts activities (Fig. II-3-6-1). The geochemical anomaly zone that consists of chromium, nickel, copper, titan, vanadium, platinum, and palladium of NE-SW direction was delineated from Capanema to Mambore in the south- western part of the Paraná Province. This anomaly zone suggested the existence of mafic to ultramafic rocks, and led to the conclusion that the PGE such as platinum and palladium concentrate within those rocks. To follow the survey, MINEROPAR carried out a field survey, and found out a sixteen outcrops of gabbros (the thickness is several to 80 cm) within the basalt flows. Some of these gabbros show high concentrations of PGE, for example 46-48 ppb Pd and 15-20 ppb Pt.

3-6-2 Origin of the Geochemical Anomaly

The above anomaly zone of NE-SW direction is coincident with the NE-SW orientated horst and graben structure in the basement inferred by Milani (1997) (Fig. II-3-6-2). Licht (2000) discussed the relation between this deep structure and the geochemical anomaly.

The geochemical characteristics of six lava types of the Paraná basin are defined in the present survey. Within these six types, the "Intermediate-Ti" Paranapanema-Ribeira is most enriched in Cu, Pt, and Pd. As shown in Fig. II-3-3-2, Paranapanema-Ribeira is distributed in NE-SW direction in the west of the Paraná Province, and its distribution is well coincident with the anomaly zone by MINEROPAR (Fig. II-3-6-1). Surrounding Paranapanema-Ribeira, the sedimentary rocks overlying the flood basalts and “High-Ti” Pitanga, both of which are poor in

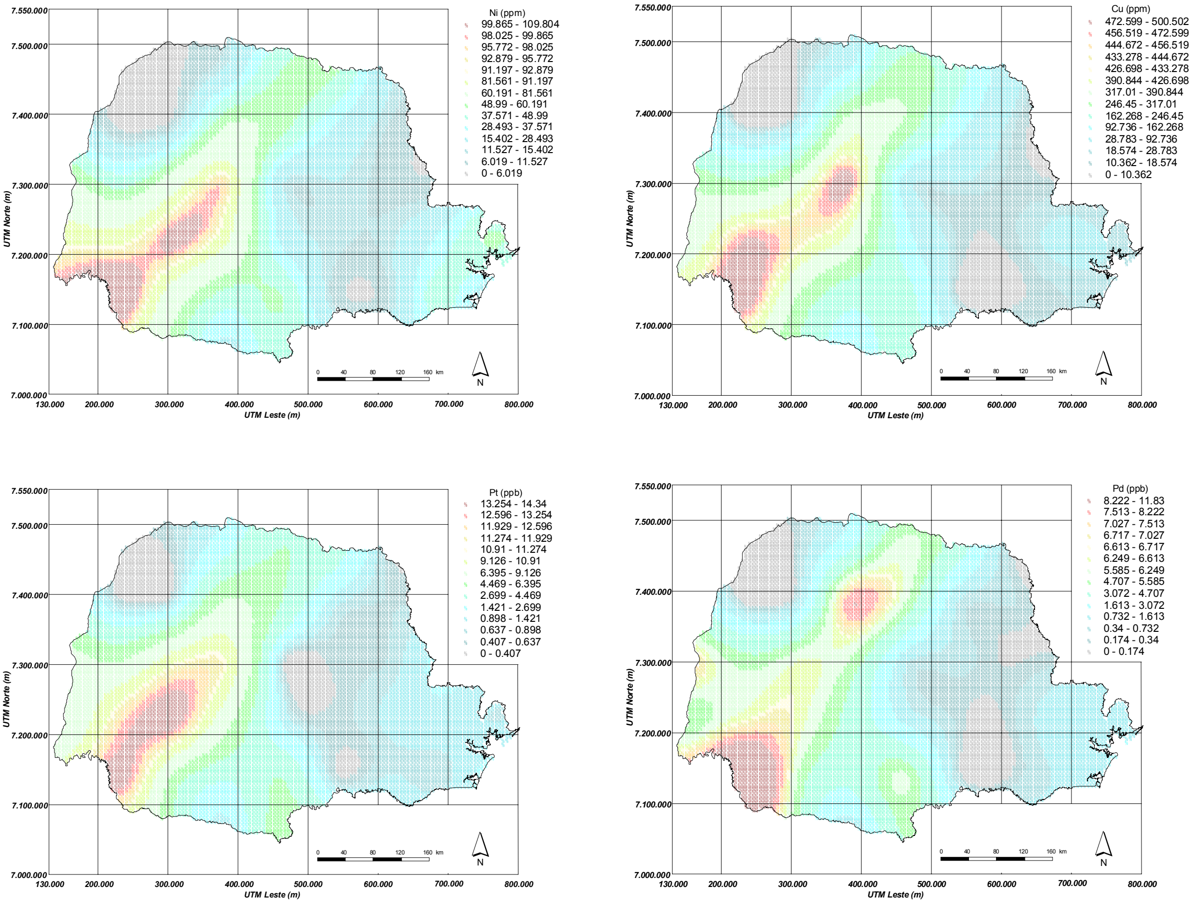

Fig.II-3-6-1 Stream sediment geochemical maps of Ni, Cu, Pt and Pd by MINEROPAR(Licht, 2000)

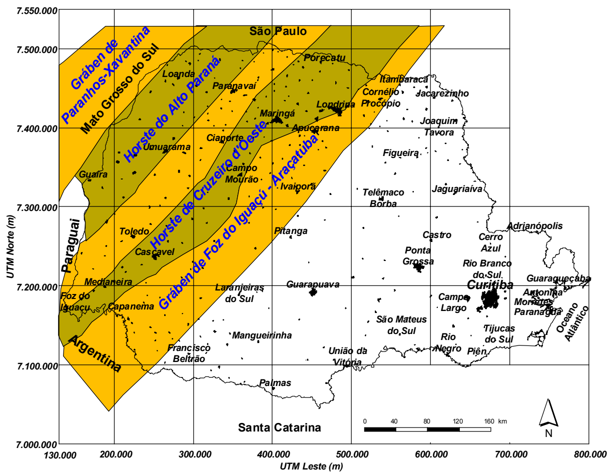

Fig.II-3-6-2 NE-SW trending horst and graben structure by Milani(1997) (Licht, 2000)

Cu, Pt, and Pd compared with Paranapanema-Ribeira, are distributed.

Therefore, the geochemical anomaly zone by MINEROPAR that suggested the existence of mafic to ultramafic rocks possibly indicates the distribution of Paranapanema-Ribeira itself, which is rich in these elements. Moreover the weak anomaly, which extends from the southern extremity of the Paraná Province to the north, indicates possibly the distribution of the "Low-Ti" type basalts (Gramado or Esmeralda) (see Fig.II-3-3-2). Therefore, it would be concluded that the anomalies extracted by the stream sediment geochemical survey by MINEROPAR have reflected surface geology very sensitively. However, the stream sediment geochemical pattern, which shows the higher concentrations toward the center of the anomaly (Fig.II-3-6-1), is not described in lavas(Fig.II-3-3-15～Fig.II-3-3-18).

Regarding the relationship between the basement structure and the distribution of Paranapanema-Ribeira, the horst and graben structure implies the existence of the fracture zone by tensional stress, therefore the structure might have acted as feeder of Paranapanema-Ribeira.

3-7 Metallic mineral in the Paraná Flood Basalts

A trace of native copper is often found in the Paraná basin flood basalts, and flaky native copper often exists in pore-space and fracture. Native copper is considered to be a secondary mineral because of its shape. Native copper is distributed from central west side to south side of Paraná basin, as a result of the surface geological survey for two years of 2001 and 2002.

The native copper is often present in Paranapanema type of lava on a central west side, and is present in Gramado Ulubici and Esmeralda type of low-Ti lava on the south side (Fig.II-3-7-1).

Moreover, the distribution of the sulfide minerals, which is dominated by pyrite, is apparent in sill and intrusive rocks though sulfide minerals is rare visible in lava. Especially, sulfide minerals are found in sill and dyke, which appears border of intrusive rock zone from central east side to the southeast side of Paraná basin (Fig.II-3-7-1).

Furthermore, we examined some representative samples that contained pyrite under a microscope test in order to identify sulfide minerals. Examination of all samples with microscope has found that the metallic minerals contained were pyrite, loellingite, pyrrhotite, chalcopyrite and sphalerite (Table II-3-7-1). By means of microscopic observation polished section, pyrite occupy interspaces of a groundmass and its feature are disseminated or specks of cluster with minor amounts of chalcopyrite. And in the sample of KN104, disseminated chalcopyrite is found in the vesicle of the groundmass (Fig.II-3-7-2).

And then, we made chemical analysis on pyrite and loellingite identified under the microscope. The instruments used for the measurement were an electron microscope, JEOL5400, and Link System model, QX2000 (energy dispersion system). The acceleration voltage was 15kV and the electrical current for irradiation was 1nA. The diameter of the beam was 3-4 nm, and the duration of the measurement was 80 seconds. We conducted a quantitative analysis on pyrite and loellingite for the following 8 elements: Cu, Fe, As, Bi, S, Se, Co and Ni. The analytical value thus derived was revised using ZAF correction. The result of the analysis is shown in Table II-3-7-2.

The results of a quantitative analysis on pyrite, a minor of As(max 1.29wt%) and a trace of Co(max 0.32wt%) were found. Also for KN104, a trace of Ni(0.30wt%) was found(chemical analysis : 234ppm Cu, 30ppm Ni, 18.7ppb Pt,134ppb Pd, 41ppb Au).

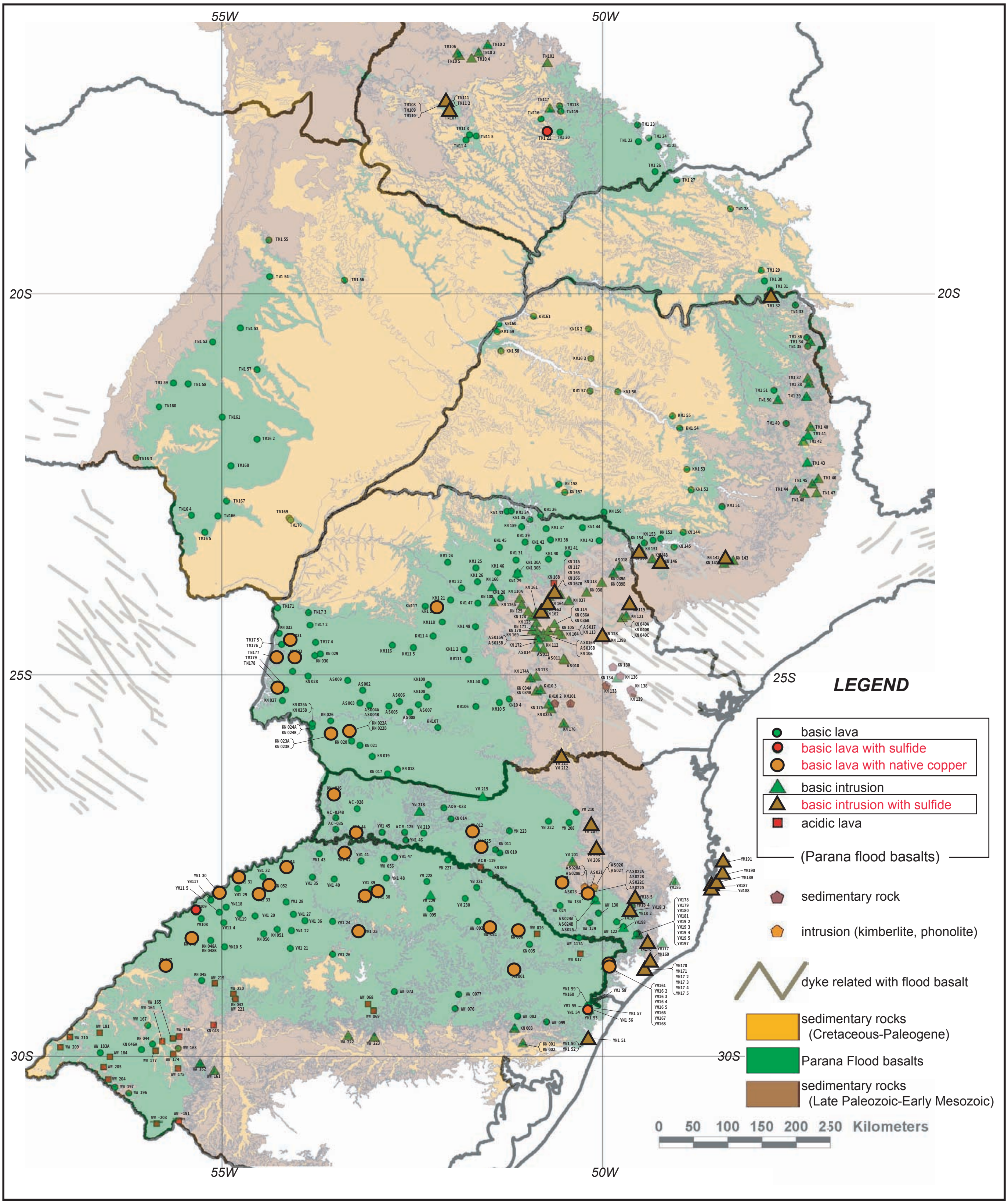

Fig. II-3-7-1 Distribution of the native copper in the Paraná basin flood basalts

Table II-3-7-1 Microscopic Observation of Polished Section

Sample No.	Type	Minerals				
		Lo	Po	Cp	Py	Sp
SW01 553.15-.35m	sill			△	○	
SP17 731.00-.20m	sill	△		△	○	
SP17 735.45-.50m	mudstone			△	◎	△
SP02 580.15-.40m	sill			△	○	
FP02 586.15-35m	sill		○		○	
SP66 776.50-.70m	sill				○	
NF09 70.70-.90m	sill		○		◎	
KN104-1	sill			△	△	
KN104-2	sill			△	△	
KN104-3	sill			△	△	
KN104-4	sill		△	△	△	
KN104-5	sill		△	△	△	

Lo : Loellingite Po : Pyrrhotite Cp : Chalcopyrite Py : Pyrite Sp : Sphalerite

△ : rare ○ : minor ◎ : common ● : abundant

SW01 553.15-.35m

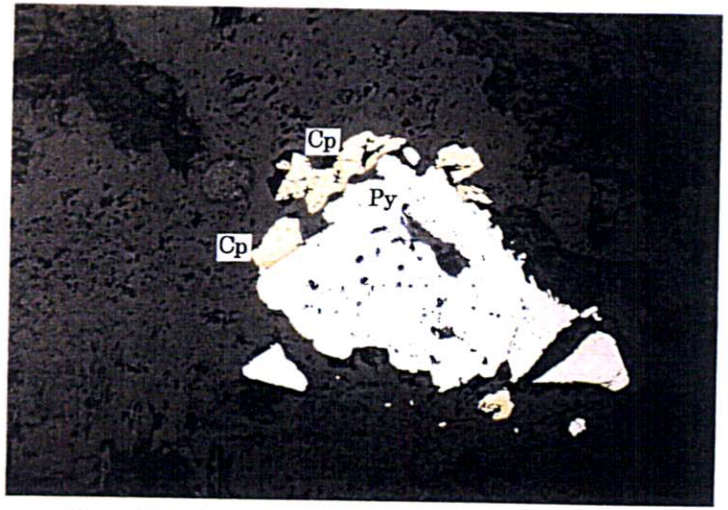

Py : Pyrite　Cp : Chalcopyrite　100 μ m

FP02 586.15-35m

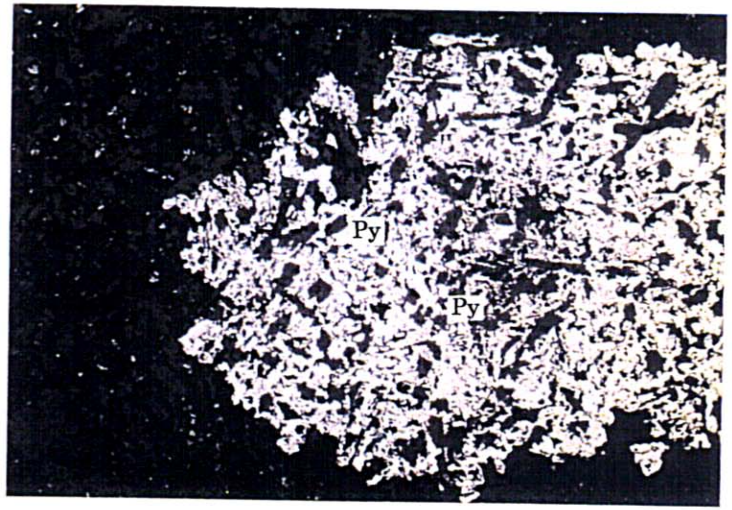

Py : Pyrite　100 μ m

SP17 731.00-.20m

Lo : Loellingite　Py : Pyrite　100 μ m

KN104-4

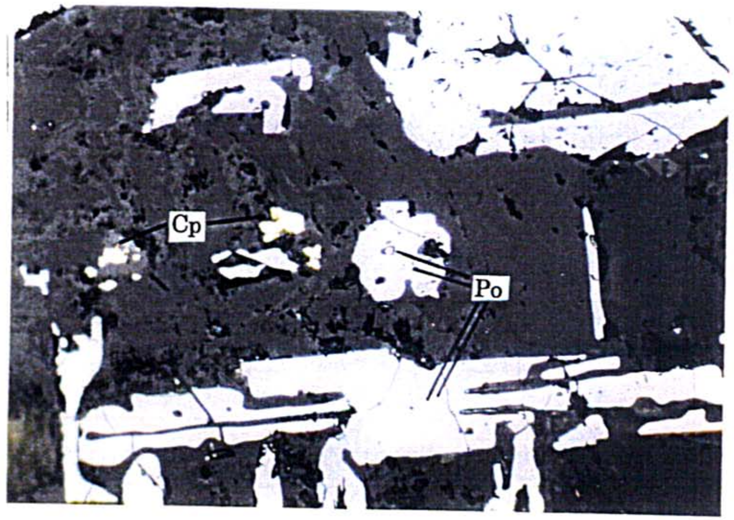

Po : Pyrrhotite　Cp : Chalcopyrite　100 μ m

Fig. II-3-7-2　Microscopic image

Table II-3-7-2 Metal mineral analysis

Sample	SW01	SW01	SP17 731m	SP17 731m	SP17 731m	SP17 731m	SP17 731m	SP17 731m	SP17 731m	SP17 735m
Mineral	pyrite	pyrite	pyrite	pyrite	lollingite	lollingite	pyrite	pyrite	pyrite	pyrite
Cu (wt%)	0.16	0.07	0.01	0	0	0.02	0.02	0.01	0.02	0.05
Fe	46.9	46.71	46.97	46.9	28.81	29.05	46.94	46.96	46.56	46.12
As	0.11	0.16	0.65	0.12	72.48	72.51	0.31	0	1.18	1.29
Bi	0	0.05	0	0.02	0	0	0	0.09	0.04	0.03
S	53.51	53.14	53.53	53.29	0.71	0.6	53.33	53.24	52.74	52.42
Se	0	0.05	0.07	0.02	0.02	0	0.03	0.06	0.12	0
Co	0.04	0.04	0.05	0.07	0.03	0.04	0.05	0.16	0.11	0.32
Ni	0	0	0.01	0	0.04	0.02	0	0.01	0.01	0.06
total	100.72	100.23	101.27	100.42	102.09	102.23	100.68	100.51	100.8	100.28

Sample	SP17 735m	SP02	SP02	FP02	FP02	SP66	SP66	NF09	NF09	KN104-4
Mineral	pyrite	pyrite	pyrite	pyrite	pyrite	pyrite	pyrite	pyrite	pyrite	pyrite
Cu (wt%)	0	0.02	0.03	0	0	0	0	0	0	0.06
Fe	46.7	47.2	47.04	47.15	46.42	46.65	46.9	47.13	47.1	44.47
As	0	0.15	0.02	0.02	0	0	0.04	0	0.03	0
Bi	0	0	0.07	0	0.16	0.09	0	0	0	0.07
S	53.38	53.56	53.84	53.66	52.8	53.39	53.18	53.61	53.58	51.93
Se	0.04	0	0	0.02	0	0	0.03	0	0.06	0.04
Co	0.05	0.03	0.07	0.04	0.04	0.06	0.04	0	0.13	0.17
Ni	0	0	0.01	0	0	0.01	0	0.01	0.01	0.3
total	100.17	100.94	101.09	100.88	99.42	100.21	100.2	100.75	100.89	97.04

3-8 Geochemical Survey with Stream Sediments

3-8-1 Introduction

The stream sediment survey carried out during 2002, took place in two distinct geological contexts, in Rio Grande do Sul and Paraná states. In Paraná almost all samples were collected from sedimentary sequences, on the edge of Paraná Basin, which are characterizeby by intrusions of sills and dikes. The feeder dike system is composed of hundreds of dikes that generated the Ponta Grossa Arc standing alongside of a deep fault system, like Rio Alonzo structure.

Concerning Rio Grande do Sul state, the samples were collected in the western/northwestern side of it, near the border with Argentina and Uruguay, at the top of a volcanic sequence, where the geology is strongly controlled by the São Gabriel Arc, Torres-Posadas Lineament, and Uruguai, Ibicuí, Camaquã and Piratini rivers lineaments. Geologically this area may be divided into two blocks roughly delimited by the Piratini river. In the southern portion, there is a thin volcanic sequence, no thicker than 200 meters, interfingered by some sedimentary layers of the predominantly acid Botucatu Formation. Some sill intrusions were detected during the field survey and confirmed by drill holes made during groundwater and oil prospection.

The northern block is marked by an abrupt subsidence of the sedimentary substratum that makes a graben structure whose volcanic thickness varies from ~200 to >1000 m, detected during drillings for groundwater and oil prospection. On the geological sketch (Fig.II-3-8-1) we can see between São Luiz Gonzaga and Santa Rosa towns (~62km) a change from 200 m to 1115 m in the volcanic sequence. This structure was probably generated during the magma extraction through a deep fault system that crosscuts the whole sedimentary basin and the craton area, probably during the Gondwana breakdown and the Atlantic opening.

The stream sediment samples were collected in Rio Grande do Sul in stream basins larger than 100 km^2 (generally between 100 and 300 km^2). In Paraná the samples were collected in smaller basins, normally in sediments in the Paraná Basin connected with mafic intrusions like sills and dikes.

The samples were collected during August and September in 2002. 64 samples were collected in Paraná and 217 samples in the area of São Gabriel, Rio Grande do Sul state. The samples from São Gabriel were added to the geochemical data bank of 135 samples collected during field survey in 2001, making up a set of 352 samples that were interpreted together.

The collected material weighed 1 - 2 kg and was dried at 80^o and sieved at 120 mesh in CPRM's laboratory. The samples were sent to Activation Laboratories Ltd - ACTLABS, in Canada where they were submitted to analytical procedures. They were chemically analyzed to 31 elements by plasma with optic emission spectrometry (ICP-OES).

3-8-2 Geochemical interpretation

The analytical database was submitted to a statistical interpretation, aiming the detection of the most important geochemical aspects of the two areas (Paraná and Rio Grande do Sul) (Table II-3-8-1). The following elements were selected to be interpreted during the evaluation of sulfide potentiality: Cu, Mn, Ni, Pb, Zn, Ba, Co, Cr, Fe, Mg,V and S. Other elements as Cd, Bi and Sb have very low detection values.

To make the geochemical maps, the anomalous values where selected from the statistical interpretation. The values higher than 95 % where selected as a first order anomaly, or as a high concentration on the selected element, and the values between 95 and 85 % as second order anomaly. All maps where constructed with these values and can be seen on Table II-3-8-1.

The empiric adoption of ample anomalous values was focused on the possibility of not detecting, some potential anomaly in those large sampled areas, especially working on stream sediments basins as large as 300 km^2 , with a particular geological context.

3-8-3 Survey Results

(1) Ponta Grossa Arc - Paraná state

Concerning the Ponta Grossa Arch, the selected targets were concentrated on mafic feeder dikes_related to the fault zones of Rio Alonzo lineament, especially near the structure limit, as well as to(?) some sills, feeded by dikes, like Jaguariaiva and Reserva areas. As a general view, the Cu, Ni, Co, Fe, Zn, Mg, S and Ba values are low, with some exceptions to local values of Cu, Zn and S. A broad geochemical view can be seen on Fig. II-3-8-2, as well as the position of those three areas at the bottom right of this figure.

Among the selected samples of Jagariaiva (ES-104, ES-112) three only (ES-107, ES-108 and ES-10) have a second order Cu anomaly, with Cu ranging from 67 to 73 ppm, associated with Ni values from 13 to 18 ppm and with Zn from 70 to 89 ppm. The sample ES-108 contains S at 0.016 %(Fig.II-3-8-3).

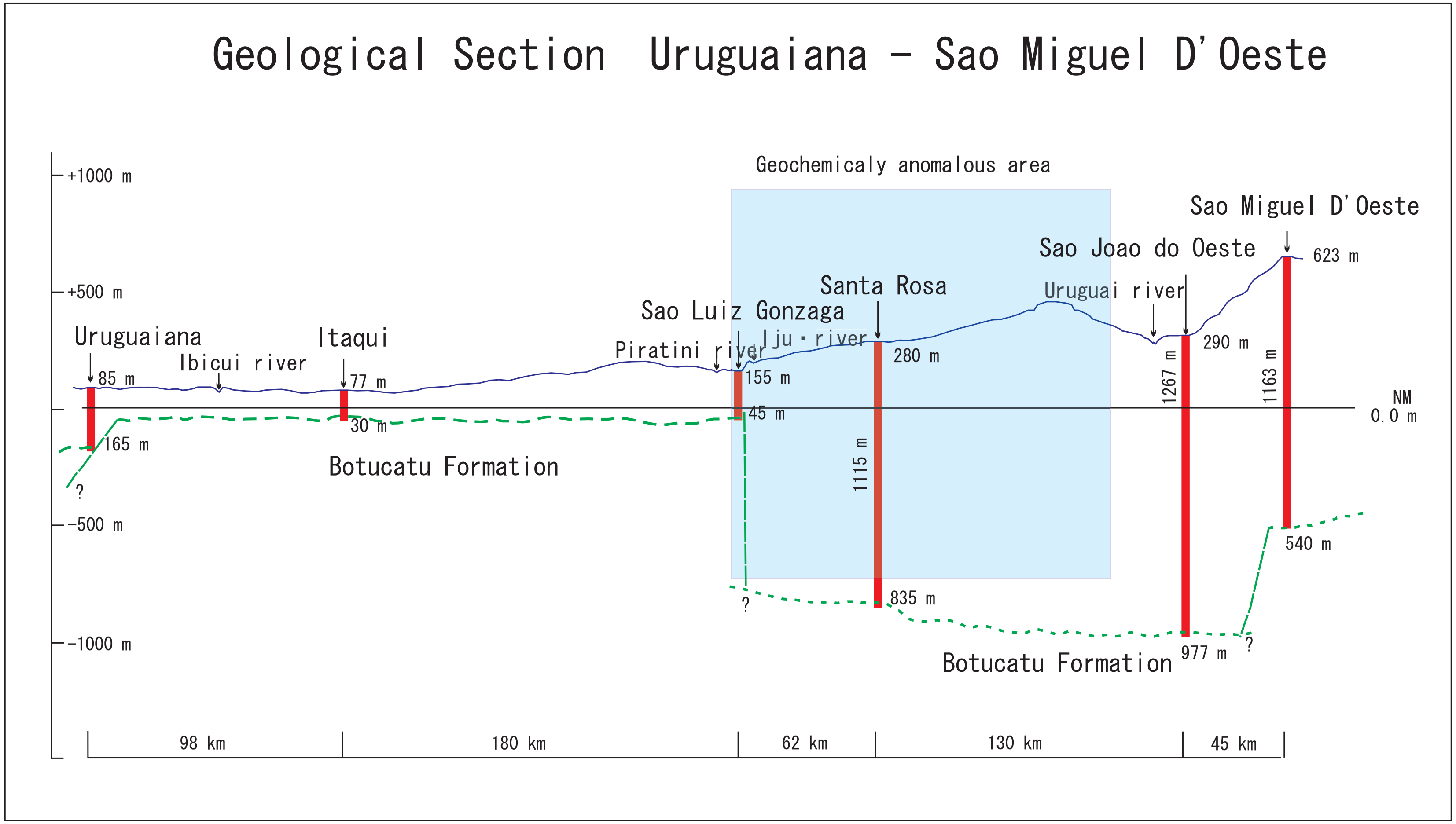

Fig.II-3-8-1 Geological section (Uruguaiana - São Miguel d'Oeste)

Table II-3-8-1 General interpretation

AREA	Variable	ELEMENTS											
		Cu (ppm)	Mn (ppm)	Ni (ppm)	Pb (ppm)	Zn (ppm)	Ba (ppm)	Co (ppm)	Cr (ppm)	Fe (%)	Mg (%)	V (ppm)	S (%)
Ponta Grossa Arc	Average	34,81	510,60	12,85	10,55	52,82	122,51	12,72	13,92	3,34	0,11	182,50	0,010
	Intercession	22,36	445,77	11,64	10,00	51,83	111,51	10,62	11,72	2,61	0,10	132,40	0,010
	Deflection	30,39	349,23	7,48	5,93	25,12	54,47	9,00	11,21	2,22	0,08	159,64	0,010
	Assimetry	1,97	2,17	2,37	0,06	0,48	0,27	1,93	3,04	0,99	0,70	1,07	3,94
	Minimum	5	35	2	2	8	22	1	2	0,34	0,01	8	0,002
	Maxim	135	2.178	48	21	113	247	52	66	10,28	0,35	617	0,051
	samples	64	64	64	64	64	64	64	64	64,00	64	64	64
	Percèntil 98	133	1.400	35	21	111	225	36	48	8,00	0,29	550	0,021
	Percentil 95	103	1.200	27	20	100	200	29	27	7,00	0,27	500	0,019
	Percentil 85	67	740	18	18	78	184	20	19	6,00	0,22	360	0,016
	Percentil 75	46	635	16	15	72	170	15	16	5,00	0,17	260	0,014
	Percentil 65	30	565	14	13	64	144	13	13	4,00	0,13	210	0,012
	Percentil 50	23	446	12	10	52	111	11	12	3,00	0,10	132	0,010
São Gabriel Arc	Average	89,24	1.266,25	20,91	15,39	65,39	240,35	32,13	26,35	6,19	0,16	322,55	0,010
	Intercession	67,15	1.151,98	18,16	13,96	64,36	226,48	30,76	14,61	5,72	0,13	250,74	0,010
	Deflection	83,05	1.055,14	18,17	9,18	42,84	214,20	27,74	26,61	4,39	0,12	286,52	0,010
	Assimetry	1,26	3,11	1,01	0,93	0,63	4,47	3,01	1,34	0,53	0,89	1,20	2,97
	Minimum	1	22	1	2	1	9	1	1	0,11	0,01	3	0,002
	Maxim	430	11.209	87	60	270	2495	299	126	19,89	0,72	1.660	0,072
	samples	352	352	352	352	352	352	352	352	352	352	352	352
	Percentil 98	306	4.680	67	36	150	750	90	93	16,00	0,45	970	0,029
	Percentil 95	260	2.940	57	32	136	532	70	78	14,00	0,35	858	0,023
	Percentil 85	177	1.920	41	25	105	361	55	60	11,00	0,25	637	0,017
	Percentil 75	122	1.730	30	21	90	305	48	40	10,00	0,21	495	0,015
	Percentil 65	99	1.550	24	18	80	271	40	27	8,00	0,17	388	0,013
	Percentil 50	67	1.150	19	14	64	227	31	15	6,00	0,13	250	0,010

Estatistic briefing about stream sediments samples from Ponta Grossa and São Gabriel Arc areas.

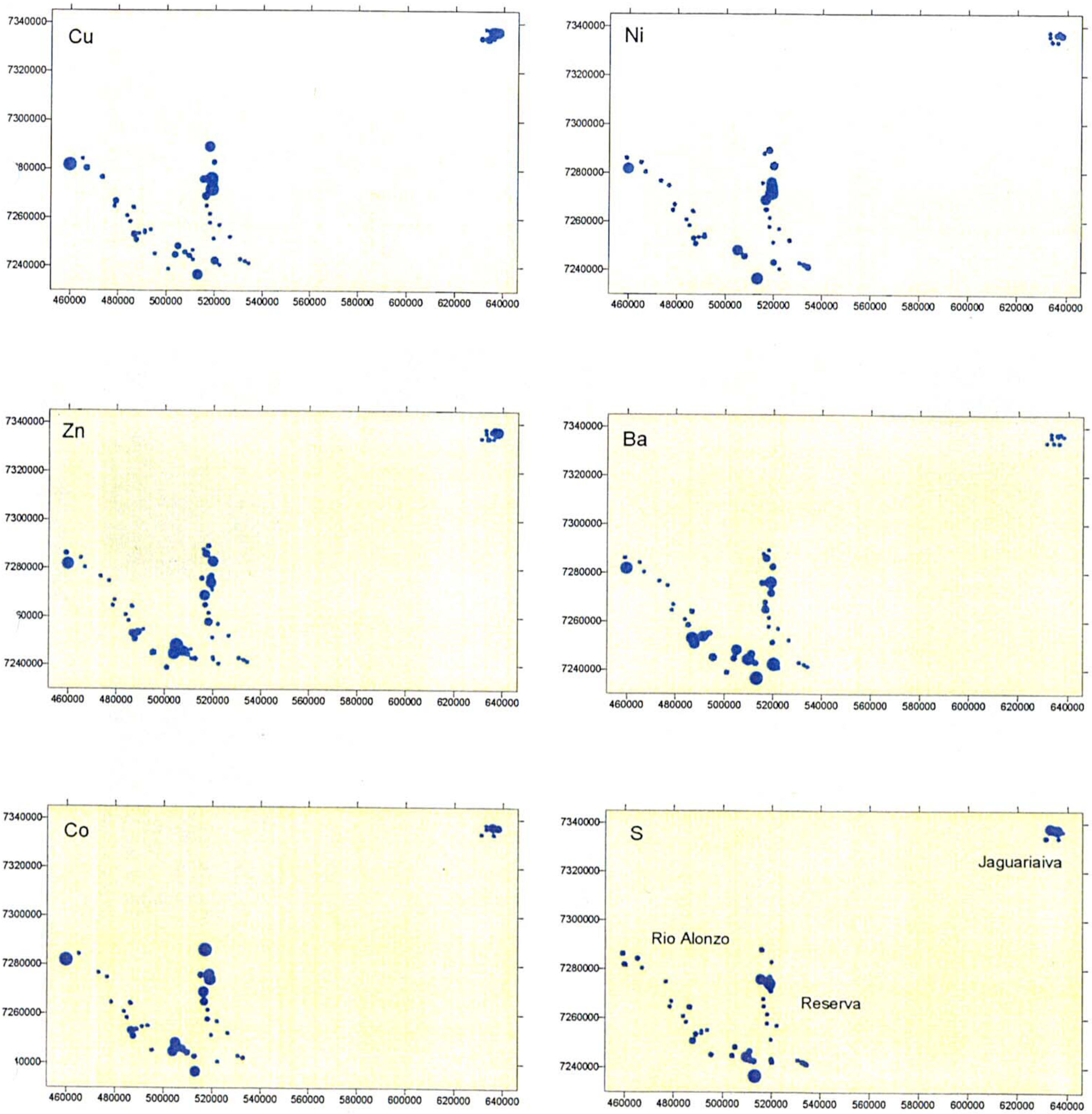

Fig. II-3-8-2 Map of Cu, Ni, Zn, Ba, Co, S for stream sediments in Paraná (Ponta Grossa arch)

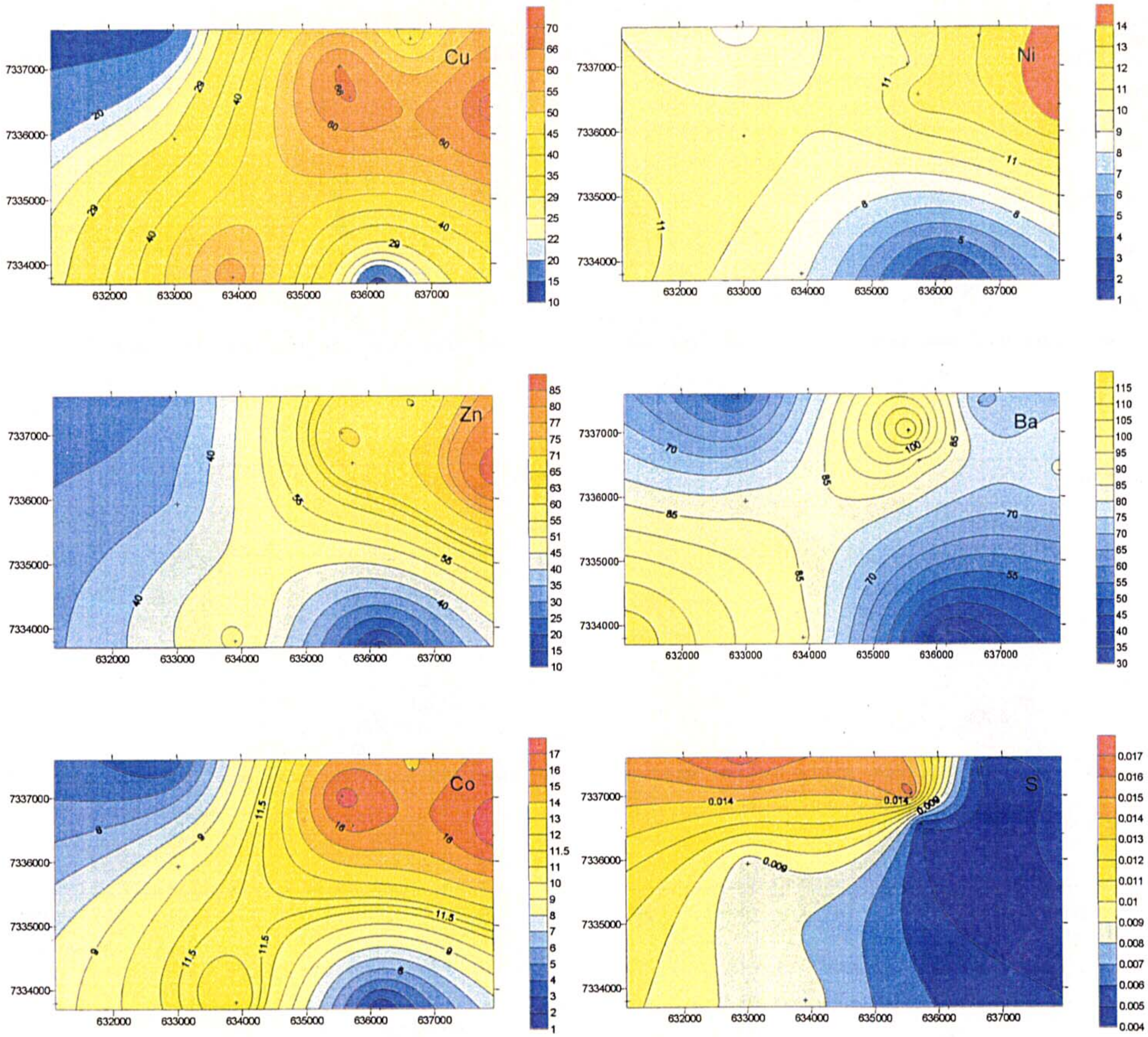

Fig. II-3-8-3 Contour map of Cu, Ni, Zn, Ba, Co, S for stream sediments in Paraná (Jaguariaiva)

Almost all of Rio Alonzo target area samples, from ES-85 to 103 have low values of Cu, Ni, Co, Zn and S, with exception of sample ES-86 with 135ppm Cu, 25 ppm Ni 108 ppm Zn and 52 ppm Co (Fig.II-3-8-4).

Reserva sill in Paraná area, holds the best results (samples ES-49, 50, 54, 58 and 84) with Cu>100 ppm, Ni 17 to 42 ppm associated to first or second order anomalous values, S 0.013 to 0.019 % (ES-71 with 0.051 %), Co with values higher than 26 ppm, and Zn ranging from 74 to 111 ppm(Fig.II-3-8-5)

(2) São Gabriel Arc - western / northwestern Rio Grande do Sul state

The geochemical view of this area reflects the lithostratigraphic division presented above in the Introduction. As one can seen in the geochemical maps (Figs.II-3-8-6, II-3-8-7, II-3-8-8) almost all of the elements show higher values north of Piratini river (28^o750 S), and flat or with low values at south.

The São Gabriel area contour maps show a very good correlation between Cu, Ni, Zn and Fe, that matches very well with the tectonic control and shear zones representing the graben margin, as one can see in Fig.II-3-8-1. Some specific zones make good correlation with S(Fe), (Zn), (Cu), Ba and Co, especially in southern block.

The differences between both blocks are geological as much as geochemical, and the geochemical scenario reflects these differences. In the north block almost all samples have higher values than in the south**:** Cu 160-430 ppm, Ni 40-87 ppm, Zn 100-270 ppm, and Co 45-127 ppm, while in the south the same elements range from Cu 100-204 ppm, Ni 35-65 ppm and Zn 80-137 ppm. Some Co values may reach 299 ppm as well as Ba and S, with higher values than those of the north.

Table II-3-8-1 shows all anomalous values, first and second order anomalies, concerning this interpretation. In this investigation apprenticeship, comprising vast sampling areas, some larger than 300 km^2, even so seems obvious that the north block of São Gabriel Arc, especially north of Piratini river, presents the best chance for sulfide deposits prospecting, and as the second(?) the lineament NW-SE where we have the Cu, Co, Ba and S anomalies.

It is interesting to point out that among the selected anomalous values, those that make associations like Ni-Cu, Co-Cr and Cu-Zn are more intriguing, for they may have a connection with ortomagmatic sulfide deposits, related to mafic - ultramafic rock association or to hydrotermal deposit. On the other hand we may detect isolated high values that may have no metallogenetic significance as sample OC-109 which contains Co-299 ppm, Ni-65 ppm, Cu-84 ppm, but with

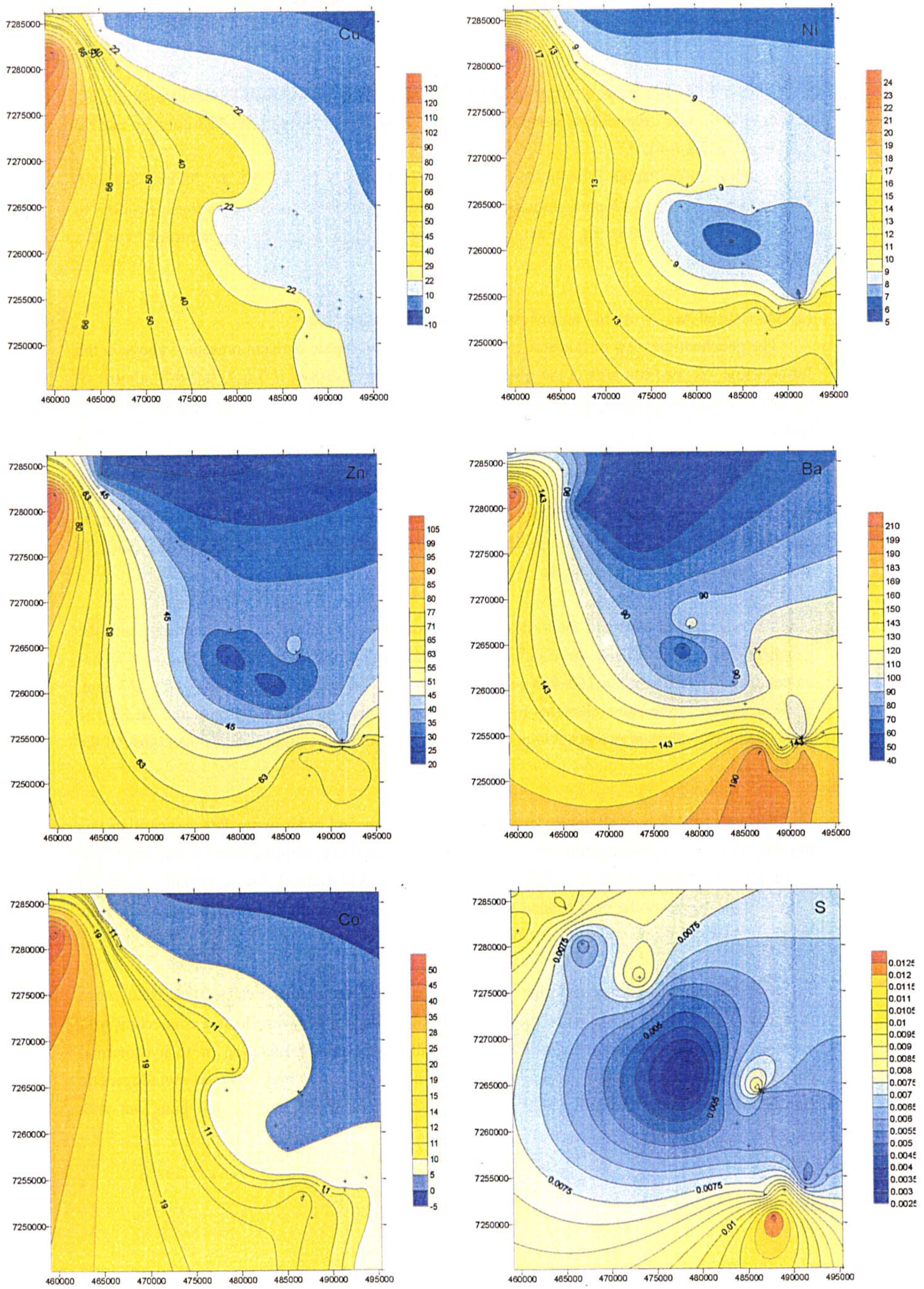

Fig. II-3-8-4 Contour map of Cu, Ni, Zn, Ba, Co, S for stream sediments in Paraná (Rio Alohzo)

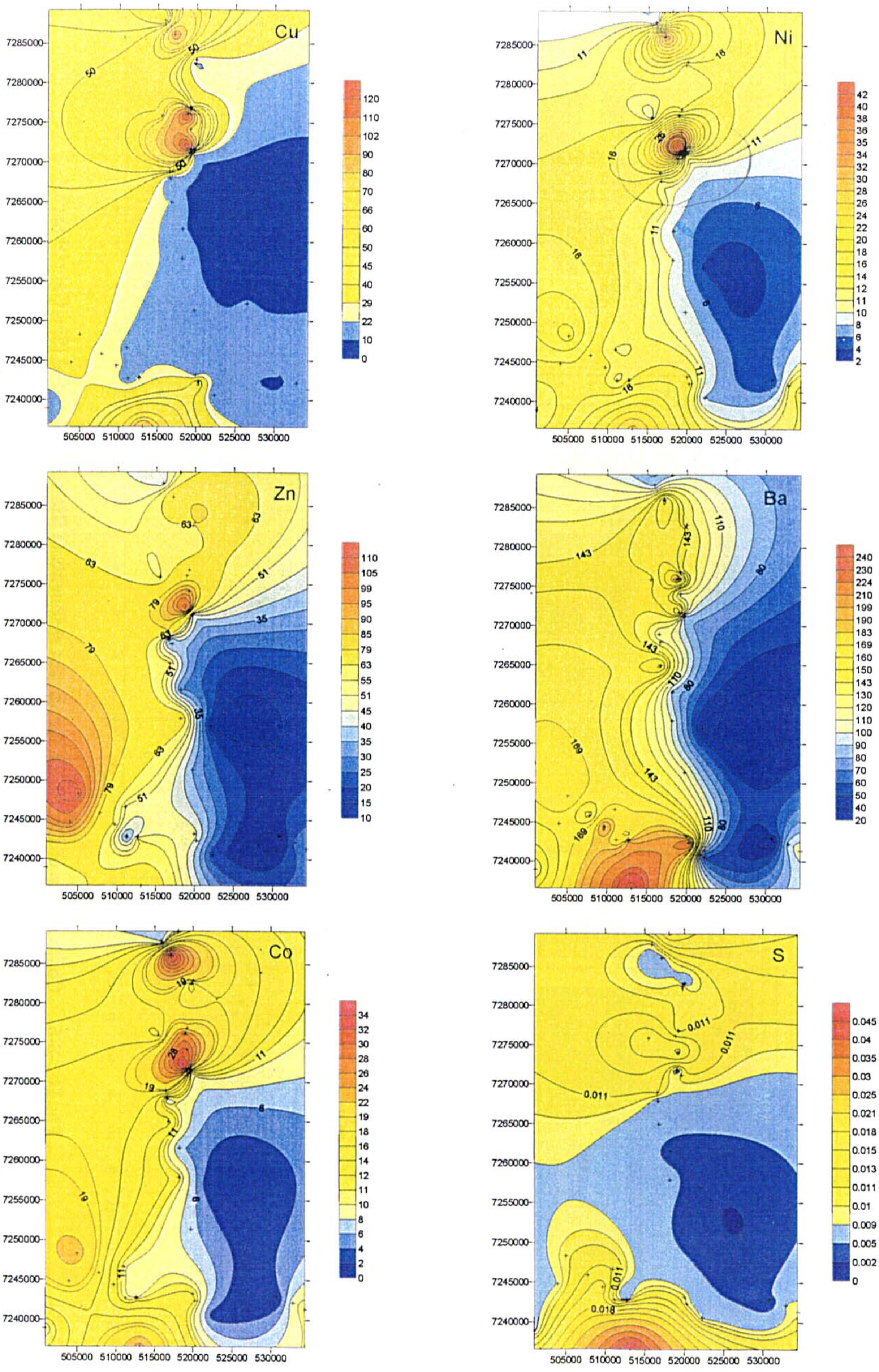

Fig. II-3-8-5 Contour map of Cu, Ni, Zn, Ba, Co, S for stream sediments in Paraná (Reserva)

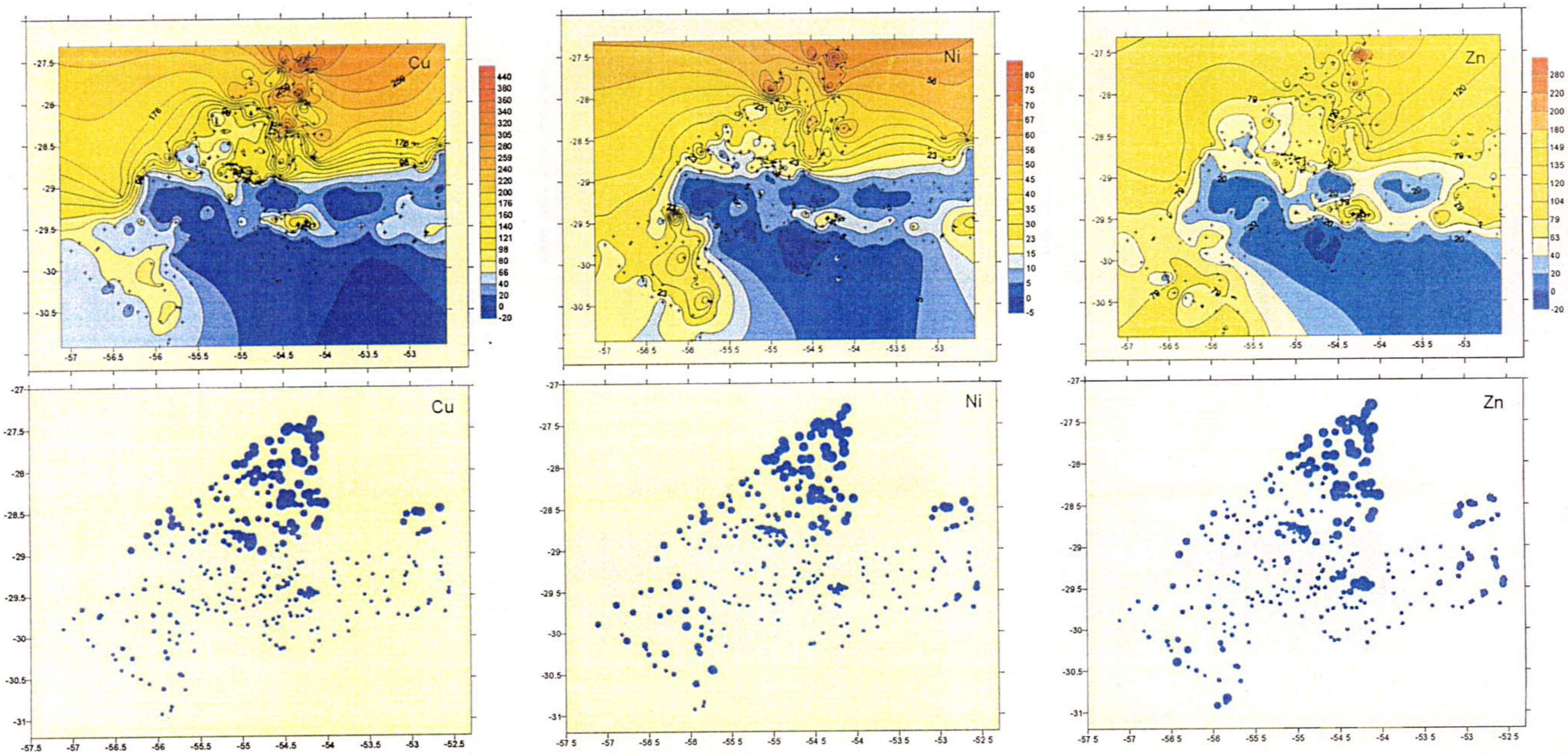

Fig. II-3-8-6 Contour map of Cu, Ni, Zn for stream sediments in Rio Grande do Sul (São Gabriel arch)

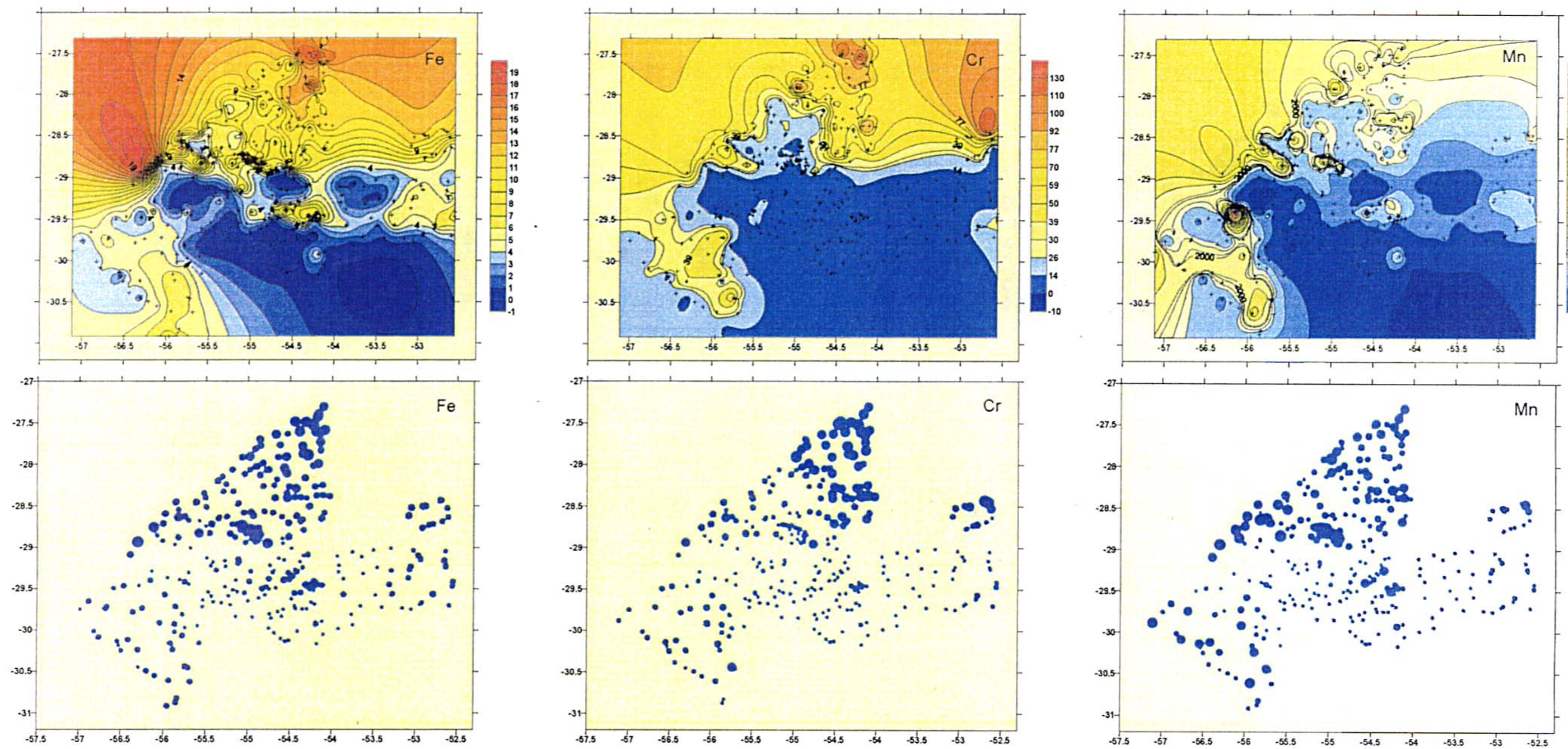

Fig. II-3-8-7 Contour map of Fe, Cr, Mn for stream sediments in Rio Grande do Sul (São Gabriel arch)

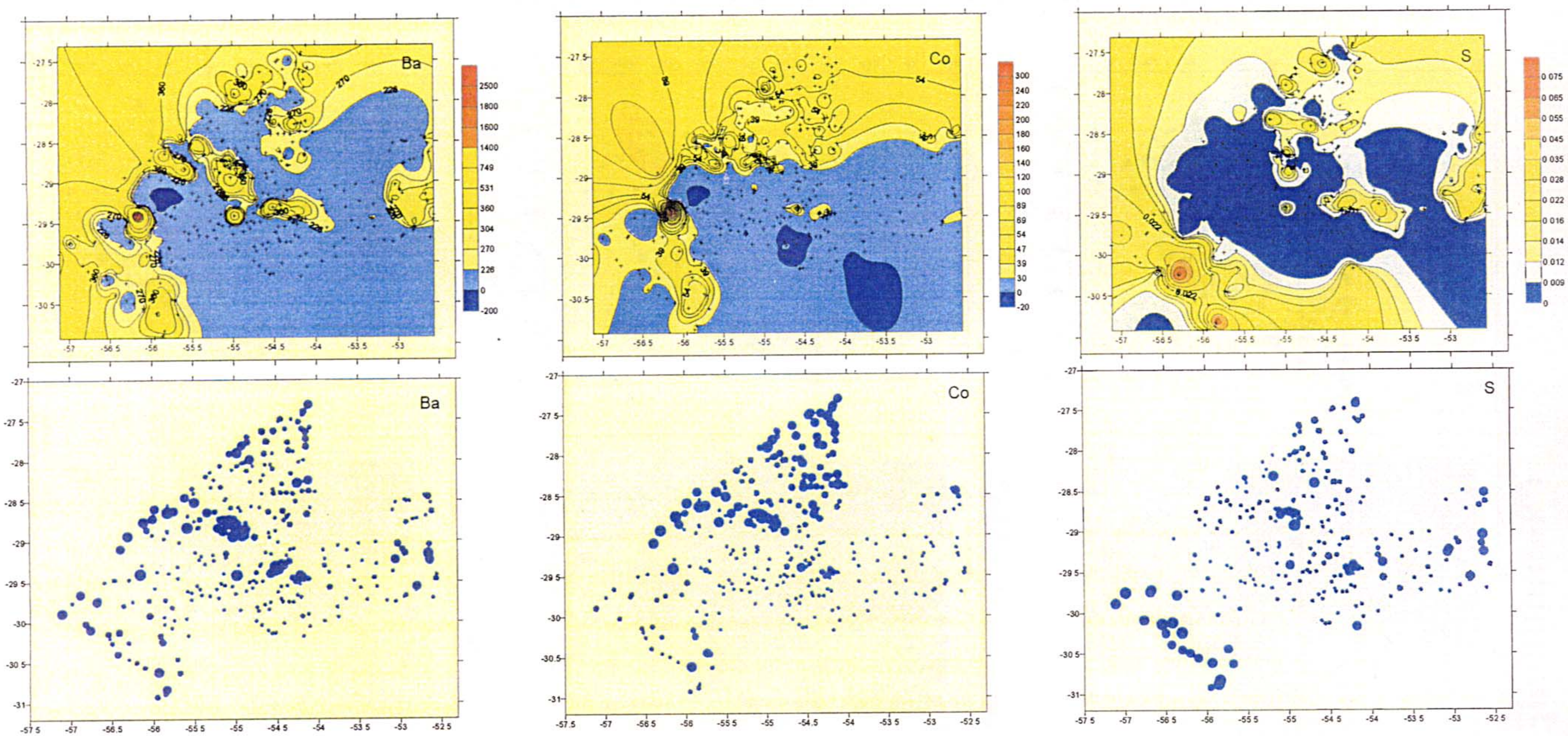

Fig. II-3-8-8 Contour map of Ba, Co, S for stream sediments in Rio Grande do Sul (São Gabriel arch)

respect to manganese, that have a high absorption potential by metallic elements, shows significant 11209 ppm.

With respect to high Cu, Ni, Zn and Co values related to low S content, it may be a consequence of the sulfur's high geochemical mobility in acid environment. On the other hand, the high sulfide values may be connected to some sedimentary layers, as Irati formation that outcrops near São Gabriel area.

3-8-4 Summary of the Survey

In Ponta Grossa Arch, and alongside the Serra Geral flows and in the sediments, there are a few hundred intrusions, and a huge area to be prospected. Our knowledge nowadays is almost nothing, and some deep intrusions were detected by the geophysical maps. So, the selected targets must be resurveyed with a more thickset samples program, spreading the sampling area to the whole basin bourder.

The São Gabriel Arch, especially its areas placed at the north of the Piratini river, seems to be one of the best target where carry on this prospecting survey, considering the local favorable geological environment with a deep fault system that probably reached the upper mantel level, the magmatic intrusions like the sills detected by Petrobras's drillings during oil prospection, the existing contaminants in the sedimentary layers, and the geochemical anomalous values, or with a high background, like Cu, Ni, Zn and Co. A complementary field survey, followed by geophysical information, namely ground gravimetry and magnetometry, all over the north of Rio Grande do Sul and west of Santa Catarina states, shall make this area one of the best targets for the next survey phase.

Chapter 4: Considering the Survey Results

This project started in anticipation of whether we can find Noril'sk style copper-nickel-PGE sulfide ore deposits in the Paraná flood basalts. Studies on LIPs (Large Igneous Provinces), including the flood basalt that formed ore deposit of this type, have just made rapid development since 1995. Because discussions are still on the progress on the characteristics and origin of LIP, researchers have naturally different opinions.

Given this situation, this survey began, based on existing literature, by reviewing the characteristics and genesis of flood basalts around the world, chemical stratigraphy and geological structure of the Noril'sk ore deposits and Siberian trap, and considering the exploration criteria of the Noril'sk style ore deposits. According to the exploration criteria studied, the approaches from analyzing both the geological structure and the geochemistry of the basalts were conducted in order to extract an area with similar geological environment to the Noril'sk region in the Paraná Basin. That is, the geological structure analysis of the entire basin was carried out using the existing documents, satellite images, and gravity/geomagnetic data. At the same time, the analysis of the major chemical compositions and trace elements, such as Pt, Pd, Au, and REE, and isotope analysis for rock samples collected during the survey were also carried out. This resulted in defining the geochemical characteristics of the Paraná flood basalts. Based on comprehension of these results, we carried out study for the area that has a potential for existence of ore deposits.

4-1 Genesis of Flood Basalt and PGE Sulfide Ore Deposit

A number of theories exist concerning the genesis of flood basalt, including a theory that supports active involvement of the mantle plume and a theory that emphasizes ascensions of the asthenosphere in continent breaking up. However, there has been no established theory yet concerning the genesis of flood basalt. Since 1995, a new theoretical model has been attracting researchers. According to this model, vast amounts of oceanic crust (slab) that subducted from continental margins deposited at the deep of the mantle, and ascended as heterogeneous mantle plume. The flood basalt magma characteristically erupted huge amounts of lava in a short period generally within 1 Ma or less. The heterogeneous plume that consists of basalt constituent having low melting temperature and peridotite constituent. In addition to such variety of the theory, magma activities of flood basalt vary depending on the location, so the theory of flood basalt formation does not necessarily lead to direct linkage to the existence of PGE ore deposits.

Most PGE concentrate in the earth's core and are rarely included in the continental crust that is markedly differentiated. Therefore, it is reasonable to think that the original magma of PGE deposit was brought from the deep part of the earth. The source materials of flood basalt that yielded the PGE mineralization may have been brought from mantle plume that ascended from the core and mantle boundary zone. The magma is also expected to be generated with large scale melting of plume and surrounding mantle. During the formation of flood basalt, large magma quantities are generated compared to periods of ordinary igneous activity. At this stage, PGE that ordinarily concentrates in solid phases is considered to have a high possibility to be caught in the melt with relatively large quantity. Since PGE concentration is affected by factors of the supplies of SiO_2 and sulfur by crustal contamination, and the local tectonic setting, such factors that influence to PGE concentration are important for forming PGE ore deposits from the magmas generated by the above process.

4-2 Exploration criteria of the Noril'sk style deposit

Assuming that the Noril'sk ore deposits in Russia belong to a type of orthomagmatic sulfide ore deposit, we considered the geological environment that satisfies the common requirements for the genesis of orthomagmatic sulfide has been formed connected to the flood basalt magmatism in the Noril'sk region. Based on such standpoint, a document survey regarding the world orthomagmatic sulfide deposits and the Noril'sk ore deposits was carried out.

The magmas related to the genesis of the Noril'sk ore deposits were initially sulfur undersaturated and rich in PGE, and were also picritic to basaltic compositions of high temperature. The Noril'sk ore deposits were formed in an area with large quantities of such magmas, that is the center of plume related magmatic activity. Considering the forming environment of the Noril'sk ore deposits from the view point of the condition of orthomagmatic sulfide ore deposit forming, the follows are presented as the exploration criteria for orthomagmatic ore deposit accompanied with flood basalt:

(1) The existence of sulfur undersaturated PGE rich magmas as lavas or intrusions.
(2) The existence of magmas showing the signatures of crustal contamination and sulfide segregation associated with above PGE rich magmas as lavas or intrusions.
(3) It is desirable that the magmas are high temperature picritic to basaltic composition that easily contaminates the crust materials.
(4) The center of the magmatic activity where the large volume of silicate magmas are supplied through crustal suture zone

4-3 Geology and Geological Structure of the Paraná Basin

After Paleozoic in age, intracratonic basins such as Paraná Basin, etc. were formed in the Gondwana continent. M. S. M. Mantovani et al. (2001) calculated the thickness of lithosphere of South-American plates using the tidal gravity anomalies. According to the results, the thickness of lithosphere of Paraná Basin is 10 to 20 km or more thinner than that of surrounding basement rocks. At this kind of portion with thin lithosphere, intracratonic basins are formed by changes of regional stress field and mantle plume (Bott, 1971; Makenzie et al., 1978). The Noril'sk ore deposit was formed in Gydansk-Omsk rift (Zonnenshain et al., 1990) and Duluth ore deposit in Midcontinent Rift (MCR) of North America.

From Paleozoic to Mesozoic in age, the Paraná Basin was repeatedly deposited and eroded due to dilation and constriction of mantle plume. The present total thickness of the sedimentary rocks attains a maximum of more than 4,000 meters. In Early Cretaceous in age, tholeiite basaltic magma was active in rift and subsequently Gondwana continent was ruptured (Rezende, 1972). The sedimentary rocks and volcanic rocks of Paraná Basin can be divided into the following six Supersequences (SS) according to geologic ages (Milani et al., 1998; Fig. II-1-4-9). They are the Rio Ivai SS (Ordovician to Silurian), the Paraná SS (Devonian), Gondwana I SS (Late Carboniferous to Early Triassic), the Gondwana II SS (Early to Middle Triassic), the Gondwana III SS (Early Cretaceous) which mostly comprises thoreiitic flood basalt (maximum thickness 1,723 m) and the Bauru SS (Late Cretaceous).

As the flood basalt lava is distributed thickly in the NE-SW direction along the Paraná River, the area is estimated to have been a rift. Drillings for oil exploration revealed that a large amount of sills and dykes associated with flood basalt magmatism intruded into the rift. There are two zones which accumulated thickness of sills and dykes are larger. The one is an area where extends in the NW-SE direction from the east of Paraná River to Ponta Grossa Arch and the other an area where are located in the boundaries between Matto Grosso do Sul Province and Sao Paulo province in the northern area of the Basin and extends in the N-S direction. In the TM false color image (RGB=234), they are expressed as geographyic features uplifted in the form of thin strings and sometimes continue over 100 kilometers.

Based on the residual gravity anomaly map (M. C. L. Quintas, 1995), A large and high anomaly is present along Paraná River in the NE-SW direction of the central area of Basin. The high gravity anomaly of the rift may be due to the density difference between asthenosphere (3.33 g/cm^3) and lithosphere (2.80 g/cm^3). Other large high anomalies and large low anomalies are considered to indicate basement structures blocked by faults in the N-S direction, NE-SE direction, and NW-SE direction.

With respect to the basement structure of the cetral region of the Basin based on aeromagnetic anomalies, large and high pseudogravity anomalies are recognized in the N-S direction in the eastern part and the western part, while a large and low pseudogravity anomaly is recognized in the N-S direction at the central part of the central region. The former are inferred to be regions with basement rocks in comparatively shallow depth and the latter a region where basement rocks collapsed due to flood basalt magmatism. The high pseudogravity anomaly in the western part may be possibly a part of Paraguay-Araguay belt and the high pseudogravity anomaly in the eastern part a part of Sao Francisco craton under the flood basalt lava pile. In the large low anomaly of the central part, high anomalies and low anomalies are recognized in the NE-SW direction, which run nearly in the same direction as Paraná River. The low anomaly along the right side of Paraná River coincides with high residual gravity anomaly and thick part of flood basalt lava.

Many magnetic lineaments which indicate faults are present on the pseudogravity anomaly map and so on. Principal directions of faults are NW-SE direction, NE-SW direction, and E-W direction. The magnetic lineaments in the NW-SE direction are continuous faults which have sharp boundaries. The magnetic lineaments in the E-W direction are poorly continuous. Most of faults in the E-W direction seem to be secondary shear faults derived from sinstral wrench faults in the NW-SE direction. The unclockwise rotations of them coincide with those mentioned by Turner et al. (1994) and W.M. de Rezende (1972). A large amount of sills and dykes are recognized in the areas where Rio Alonzo fault in the NW-SE direction and rift along Paraná River in the NE-SW direction intersect.

4-4 Promising Areas of Emplacements of Ni-Cu-PGE Ore Deposits Estimated from Geological structure

We will present a comprehensive explanation of Precambrian basement rocks, sedimentary rocks and flood basalts in Post- Early Paleozoic, and faults in the Paraná Basin and consider the relation among the rift zone and the regional stress field, and promising areas of emplacement of Noril'sk-type Cu-Ni-PGE ore deposit (Fig.II-1-5-25).

A large low anomaly zone in the central part of the pseudogravity anomaly map overlaps with a zone where sedimentary sequence and flood basalt lava are thicker, with a zone where a large quantity of sills and dykes intruded, with a high residual gravity anomaly zone, and with a high attenuation factor zone. Based on these facts, it is concluded that the large low anomaly zone was rift zone associated with flood basalt magmatism.

The direction of the rift zone extends in the N-S directions in the northern Basin; in the NE-SW directions the central Basin, and branches into the NE-SW and NW-SE directions in the southern Rio Alfonzo fault. The inside of the rift zone has repetitions of high anomaly zones and low anomaly zones in the NE-SW direction. These anomaly zones in the NE-SW directions were formed by stair-step normal faults (vertical direction: maximum compressive principal stress axis σ_1) in the extensional stress in the NW-SE directions field (minimum compressive principal stress axis σ_3).

Many magnetic lineaments which represent faults in the NW-SE direction are recognized on the pseudogravity anomaly map. For example, Rio Alfonzo fault on the geological map are represented by several magnetic lineaments on the pseudogravity aomaly map. The faults in the NW-SE directions are estimated to be sinistral transcurrent faults because they have sharp boundaries and are accompanied with many secondary shear faults in E-W directions. In the Duluth ore deposit, many secondary shear fractures occurred in the form of Cymoid Loop-like tensional fractures in areas where the rift zone and transcurrent faults cross. The Duluth Complex intruded there and formed the ore deposit. The Noril'sk ore deposit was also formed in the volcano-center where magma extruded most instensely in the Gydansk-Omsk rift zone (Tamrazyan, 1962).

As the results mentioned above, we propose the following four promising areas, which rift zone and transcurrent faults cross, of emplacements of Ni-Cu-PGE ore deposits.

(1) The area where the Tiete structural line in the NW-SE direction crosses through Paran River
(2) The area where the Guapiara fault in the NW-SE direction crosses through Paraná River.
(3) The area where Rio Alfonzo fault in the NW-SE direction crosses through Paraná River.
(4) The western part of Torres - Posadas fault in the southern region of Paraná Basin

All of these areas are estimated to have been the volcano-center of flood basalt magmas. The largest volcano-center is found in the area (3) where the Rio Alfonzo fault crosses through Paraná River. Among four areas, it is concluded that areas where the Guapiara fault and the Rio Alfonzo fault in the NW-SE directions cross through Paraná River are the most promising area of emplacements of Ni-Cu-PGE ore deposits.

4-5 Geochemical Characteristics of Paraná Flood Basalts

(1) Classification of Magma Type

Six types of lava units of Paraná flood basalts are divided into Low-Ti type and High-Ti type by Peate et al. (1992). Since the Ti contents of Paranápanema and Ribeira are intermediate in this survey, the two above were geochemically judged not to be classified into

Low-Ti type nor High-Ti type. Therefore, the two above were newly classified as the Intermediate-Ti type, and the magma types of Paraná flood basalts were classified as follows. The difference of Ti contents among the three types is obvious, and each type shows different trends of fractionation in Mg#-TiO_2 diagram.

	Peate et al. (1992)	This survey
Low-Ti type	Gramado	Gramado
	Esmeralda	Esmeralda
	Ribeira	
Intermediate-Ti Type	—	Paranápanema-Ribeira
High-Ti Type	Paranápanema	Pitanga
	Pitanga	Urubicí
	Urubicí	

Ggeochemical examinations were carried out for both lava samples and intrusion samples in this survey. Both samples show entirely the same geochemical trend. Therefore, both lava and intrusion samples were classified into the above five magma types. As for distribution, Pitanga is distributed in the northern part of the Paraná Basin, Pitanga and Paranápanema-Ribeira are distributed in the central part, and Gramado, Esmeralda and Urubici are distributed in the southern part. Pitanga and Paranápanema-Ribeira are intermingled in the intrusions of the Ponta Grossa Arch in the central part. The results of the geochemical examinations are summarized in Table II-4-5-1.

(2) Partial Melting and Crustal Contamination

Pitanga, High-Ti type, is distributed from the northern to the central part of the Paraná Basin. This magma type shows the smallest degree of partial melting. It is thought to have been generated in relatively deeper portion in the upper mantle. Paranápanera-Ribeira, the Iintermediate type, is distributed in the central area of the Paraná Basin. The degree of partial melting of this type is shown larger than that of Pitanga. This means that it has been generated in a shallower portion than Pitanga was generated. The effect of the crustal contamination is considered limited in these two types of magma because of poor contents of U and Th that concentrate in the crust. Mantovani et al. (2000) described that the two types above were generated from a similar magma source with different degrees of partial melting. The large quantities of the two magma types above erupted and were piled with a thickness of approximately 1,800 meters along the Paraná River in the central part of the Paraná Basin, which is thought to be the center of the magmatic activity.

The Low-Ti type magmas (Gramado and Esmeralda) show relatively large degree of partial melting. They are thought to have been generated in relatively shallower portions compared to the other magma types. The increases of LIL elements such as Th, U and the likes that concentrate in crust, and Sr isotopic ratio are observed in both magma types. It is thought to be the effect of crustal contamination. The effect is particularly marked in Gramado. Esmeralda is considered to be the most primitive magma among all the magma types because of its low contents of light rare earth elements and a relatively high Nd isotopic ratio.

As regards the Low-Ti types of magma, the following three points are thought to have a close relationship. The first is that the magma was generated in a shallow portion. The second is that the magma was highly affected by crustal contamination, and the third is the existence of acidic rocks, which are considered to be the products of lower crust melting, in the southern part of the Paraná Basin. More specifically, the following process is thought to have occured. That is, the acidic magma was generated from the melt of the lower crust by the mantle plume heating. After generating the acidic magma, this magma and the magma generated by the melting of the mantle plume itself mixed and yielded Gramado type magma. Finally, just after the commencement of expanding the Atlantic, Esmeralda type magma is thought to have been generated that is less influenced by crustal contamination although the origin is the same as Gramado.

(3) PGE Contents of the Paraná Flood Basalts

The original magmas of the Paraná flood basalts are thougth to be PGE rich as a whole, particularly Pd rich (Refer to Table II-3-5-1) although there are some differences among the magma types. The most PGE enriched magma is Paranápanema-Ribeira. The average content of Pt and Pd summing is approximately the same as that of the Tuklonsky lava, the most PGE enriched lava in the Noril'sk region. Paranápanema-Ribeira is also rich in Cu. The magma of this type as lavas is distributed along the Paraná River in the central part of the Paraná Basin, and much native copper is observed in the cavities. The geochemical anomaly in PGE, Ni, Cu, and other elements that is observed in the western part of the state of Paraná (by the stream sediment geochemical survey carried out by MINEROPAR) possibly shows the distribution of Paranápanema-Ribeira that has high PGE contents. Paranápanema-Riberia as intrusions is distributed in the Ponta Grossa Arch intermingled with Pitanga of High-Ti type. The magma type of the higher PGE content next to Pitanga is Esmeralda that has the most primitive chemical composition. The PGE depletion by sulfur saturation is rarely observed in Paranápanema-Ribeira and Esmeralda.

Regarding Gramado and Pitanga, there are two populations of samples, PGE enriched and depleted. These two types are thought to have been initially PGE enriched. The depletion of PGE, however, is thought to have occurred due to sulfur saturation in a part of the magma. As the cause of sulfur saturation, the crustal contamination in Gramado, and the crystallization differentiation in Pitanga are both thought to have occurred. Pd contents of 133.8 ppb were obtained by analyses of the intrusion sample (KN104) of Pitanga type that was collected in the Ponta Grossa Arch. This value exceeds the Pd content of ordinary basaltic magma, and suggests the existence of sulfide that includes Pd.

According to the facts above, all magma types of Paraná basalts are considered to be initially sulfur undersaturated and rich in PGE. They have the potential to form the ore deposits if satisfy other requirements demonstrated above.

4-6 Mineralization Potential of the Paraná Flood Basalts

In the Noril'sk region, the majority of the lava and intrusion is basaltic, however, the sills which embed ore deposits contain picritic parts and the assimilation of country rock on a large scale in the picritic sill is observed. Picritic magma, however, is rarely observed in the Paraná flood basalts, and the basalts are more differentiated than in the Noril'sk region. The magma temperature of the Paraná flood basalts is thought to be lower than that of the Noril'sk region. It is thought to be possible that this low temperature obstruct the assimilation of country rock and the large scale segregation of immiscible sulfides. As assumed in Pitanga, though, there is a possibility of segregating immiscible sulfides by the progress of the simple crystallization differentiation without the influence of contamination. The saturation mechanism on sulfur mentioned above is the same process considered in the Skaergaard intrusion in East Greenland (Anderson et. al., 1998) and the Sonju Lake intrusion in Minnesota, USA (Refer to APPENDIX.2)

All the samples of intrusion including the Ponta Grossa Arch sill that could be collected in this survey were distributed in the marginal area of the Basin, the edge area away from the center of magmaic activity. The sills are mostly poor in sulfide, and the maximum thickness is approximately 200 m, which is comparatively thin. The rock compositions show basaltic, and although show high PGE contents, the magma temperature is lower than that of the magma of Noril'sk. The contamination effect of country rock in such intrusions is weak. This is considered to be the reason why only a faint dissemination of sulfides is observed (pyrite/pyrrhotite/chalcopyrite/sphalerite). The segregation of sulfides in a large scale magma chamber like the Skaergaard intrusion under the high R factor is necessary to generate sulfide ore deposit from basaltic magma with high PGE contents.

The location with the highest possibility of generating sulfide ore deposit is thought to be the eruption center of Paranápanema-Ribeira and Pitanga types, which have the largest quantities of magmas among the Patana flood basalts. The eruption center is thought to be located in the central area of the Paraná Basin along the Paraná River where the lava piles are the thickest. Based on the existing data analysis, the strong shrinkage of lithosphere by the ascension of the asthenosphere is observed in this area, and magma intrusion is estimated to be the most active in this area.

4-7 Subjects and Survey methods in the Future

From analyses of existing geological papers, geological survey on the ground surface, geophysical anomaly maps, drilling data of coal exploration and so on resulted in identifying geotectonic characteristics of the Paraná Basin and geochemical characteristics of flood basalt magmas and possibility of emplacements of Ni-Cu-PGE ore deposits such as the Noril'sk, Duluth and Skaergaard ore deposits.

According to the dykes and sills in the basement rocks, although the drilling cores of coal exploration and the outcrops were investigated, no Ni-Cu-PGE mineralization was almost identified.

Hereafter, diamond drillings are proposed for identifying mineralization of dykes and sills in the basement rocks in the promising area where have been located at volcano-centers of flood basalt magmas. But, as most of volcano-centers are located at more than 1,000 meters below the ground surface, it is difficult for ore deposits to be economic.